Physiology of *Pseudovibrio* sp. FO-BEG1 – a facultatively oligotrophic and metabolically versatile bacterium

Dissertation

zur Erlangung des Doktorgrades
der Naturwissenschaften
- Dr. rer. nat. -

dem Fachbereich Biologie/Chemie
der Universität Bremen

vorgelegt von

Vladimir Bondarev

Bremen, Februar 2012

Die vorliegende Arbeit wurde in der Zeit von Januar 2008 bis Februar 2012 am Max-Planck-Institut für Marine Mikrobiologie in Bremen angefertigt.

1. Gutachterin: Prof. Dr. Heide Schulz-Vogt
2. Gutachter: Prof. Dr. Ulrich Fischer

3. Prüfer: Prof. Dr. Rudolf Amann
4. Prüfer: PD Dr. Jens Harder

Table of contents

Summary

Bacteria belonging to the genus *Pseudovibrio* are frequently found in marine habitats, mainly in association with sponges, corals and tunicates. Particularly sponges harbor populations of *Pseudovibrio* spp.-related bacteria, which led to the proposal that this genus contains sponge symbionts. However, the physiology of the genus *Pseudovibrio* is insufficiently studied and hardly anything is known about its relevance in the environment. In the course of this thesis, the *Pseudovibrio* strain FO-BEG1 was investigated. It had previously been enriched together with the sulfide oxidizing *Beggiatoa* sp. 35Flor from a black band diseased coral and was eventually cultured axenically, permitting sequencing of the genome as well as metabolic studies and investigations of physiological changes under different growth conditions.

The results of the genomic and physiological analyses of *Pseudovibrio* strain FO-BEG1 are described in **Chapter II**. Strain FO-BEG1 was shown to be a generalistic bacterium with a versatile metabolism, capable of importing and oxidizing a wide range of organic and inorganic compounds to meet its carbon, nitrogen, phosphorous and energy requirements under oxic and anoxic conditions. Furthermore, the genomic analysis of strain FO-BEG1 revealed adaptations to a eukaryote-associated life style. Genes that could promote bacteria-host interactions and facilitate attachment or invasion of host cells were identified in the genome of *Pseudovibrio* sp. FO-BEG1. Interestingly, comparative genomics with *Pseudovibrio* strain JE062, a strain that has been isolated from a sponge, demonstrated the presence of almost identical physiological and symbiosis-related features in the genome of the sponge-associated isolate, indicating a close relationship of both strains. Additionally, strain FO-BEG1 was shown to grow under extreme nutrient limitation, which has been studied along with the isolation of other bacteria capable to grow in nutrient-rich and -depleted environments, as shown in **Chapter III**.

In **Chapter IV**, the phylogenetic affiliation of *Pseudovibrio* sp. FO-BEG1 is discussed. This question is resolved by using a polyphasic approach and comparing the genotypic and phenotypic data with the *Pseudovibrio denitrificans* type strain. It is suggested that *Pseudovibrio* sp. FO-BEG1 represents a new strain within the *P. denitrificans* species and not a new species within the genus *Pseudovibrio*, because the two strains are physiologically very

similar and the genotypic analysis revealed values which are only at the border of justifying the description of a new species.

Growth under phosphate limited conditions, as described in **Chapter V,** induces an adaptive response in *Pseudovibrio* sp. FO-BEG1, characterized by the secretion of a yellow component into the medium. Detailed chemical, physiological and proteomic analysis were performed to characterize changes in the metabolism of *Pseudovibrio* sp. FO-BEG1 cells grown under phosphate limitation and phosphate surplus. Along with secretion of yet unidentified metabolites, FO-BEG1 cells regulate the expression of proteins involved in many different cellular processes like cell envelope modification and oxidative stress response and induce the expression of enzymes required for degradation of phosphorus-containing molecules as well as high-affinity transporters for phosphates and phosphonates. Furthermore, initial analysis of secreted metabolites was performed using a Fourier transform ion cyclotron resonance mass spectrometer, which will help to chemically and structurally characterize the extracellular compounds.

Zusammenfassung

Bakterien, die zur Gattung *Pseudovibrio* gehören, findet man in marinen Habitaten, hauptsächlich assoziiert mit Schwämmen, Korallen und Tunikaten. Insbesondere werden Schwämme von *Pseudovibrio* spp.-verwandten Bakterien besiedelt, was zu der Vermutung führte, dass die Gattung *Pseudovibrio* auch Symbionten von Schwämmen einschließt. Allerdings ist die Physiologie dieser Bakterien noch unzureichend untersucht. Auch die Auswirkungen des Metabolismus und die daraus resultierende Relevanz für den marinen Lebensraum sind ungeklärt. In der vorliegenden Dissertation wurde der Stamm *Pseudovibrio* sp. FO-BEG1 untersucht. Wurde der Stamm FO-BEG1 anfänglich zusammen mit dem sulfidoxidierenden Bakterium *Beggiatoa* sp. 35Flor aus einer von der Schwarzband-Krankheiten befallenen Koralle angereichert, so wird er derzeit axenisch kultiviert. Das Vorhandensein dieser Reinkultur ermöglichte die Sequenzierung des Genoms von *Pseudovibrio* sp. FO-BEG1, sowie Untersuchungen über den Metabolismus und den physiologischen Veränderungen bei unterschiedlichen Wachstumsbedingungen.

Die Ergebnisse der genomischen und physiologischen Analyse von *Pseudovibrio* sp. FO-BEG1 sind in **Kapitel II** dargestellt. Es wurde gezeigt, dass Stamm FO-BEG1 ein generalistisches Bakterium mit einem vielfältigen Metabolismus ist. Es hat die Fähigkeit, viele unterschiedliche organische und anorganische Substanzen aufzunehmen und zu oxidieren, um seine Kohlenstoff-, Stickstoff-, Phosphor- und Energieversorgung unter oxischen und anoxischen Bedingungen zu gewährleisten. Weiterhin wurde bei der genomischen Untersuchung festgestellt, dass Stamm FO-BEG1 Anpassungen an eine Eukaryoten-assozierte Lebensweise aufweist. Es wurden Gene identifiziert, die für Interaktionen zwischen Bakterien und dem Wirt sowie die Anhaftung oder das Eindringen in die Wirtszellen notwendig sein können. Zusätzlich wurde das Genom eines zweiten Stammes, *Pseudovibrio* sp. JE062, der direkt aus einem Schwamm isoliert wurde, für vergleichende Genomik verwendet. Es wurde festgestellt, dass die untersuchten physiologischen und symbiotischen Eigenschaften, die bei *Pseudovibrio* sp. FO-BEG1 identifiziert wurden, auf genetischer Ebene fast identisch im Stamm JE062 vorliegen, was darauf hinweist, dass die Stämme FO-BEG1 und JE062 miteinander nah verwandt sind. Zusätzlich konnte gezeigt werden, dass *Pseudovibrio* sp. FO-BEG1 unter extremer Nährstofflimitierung wachsen kann. Dieser Aspekt wurde, im Vergleich mit anderen Bakterien, die unter Nährstoffmangel sowie Nährstoffüberfluss leben können, genauer in **Kapitel III** untersucht.

In **Kapitel IV** wird auf genotypischer und phänotypscher Ebene die phylogenetische Zugehörigkeit von *Pseudovibrio* sp. FO-BEG1 in einer vergleichenden, polyphasischen Untersuchung mit dem *Pseudovibrio denitrificans* Typstamm diskutiert. Die Resultate deuten darauf hin, dass *Pseudovibrio* sp. FO-BEG1 einen neuen Stamm innerhalb der *P. denitrificans* Spezies darstellt. Für die Beschreibung einer neuen *Pseudovibrio* Spezies konnten nicht genügend physiologische und genotypische Unterschiede zwischen *P. denitrificans*^{T} und dem Stamm FO-BEG1 festgestellt werden.

In **Kapitel V** wird die adaptive Antwort von *Pseudovibrio* sp. FO-BEG1 auf Phosphatlimitierung, die durch die Ausscheidung einer gelben Substanz ins Medium charakterisiert ist, diskutiert. Chemische, physiologische und proteomische Untersuchungen wurden durchgeführt, um die Unterschiede zwischen *Pseudovibrio* sp. FO-BEG1 Zellen, die unter Phosphatlimitierung bzw. -überfluss gewachsen sind, zu charakterisieren. Neben der Sekretion von bisher unidentifizierten Metaboliten verändern FO-BEG1 Zellen unter Phosphatlimitierung die Expression von Proteinen, die an verschiedenen zellulären Prozessen beteiligt sind. Zum Beispiel führt Phosphatlimitierung zur Modifikation der Zellmembran, zur Induktion von Proteinen zum Schutz vor oxidativem Stress und auch zur Induktion von Enzymen für den Abbau phosphorhaltiger Verbindungen. Außerdem ist die Expression hochaffiner Transporter für Phosphate und Phosphonate hochreguliert. Darüber hinaus wurden erste Analysen der ausgeschiedenen Metabolite mittels Fouriertransformations-Ionenzyklotronresonanz-Massenspektrometrie durchgeführt, um die chemische und strukturelle Charakterisierung der extrazellulären Metabolite zu unterstützen.

Chapter I

General introduction

The genus *Pseudovibrio*

Pseudovibrio denitrificans has been isolated from shallow coastal waters off Taiwan in 2004 and was described as the type species of the genus *Pseudovibrio*. It is a heterotrophic, gram-negative bacterium of the family *Rhodobacteriaceae* within the class *α-Proteobacteria* (Shieh *et al.*, 2004). Main characteristics of this species are motility by the means of one to several flagella, straight or curved rod morphology with occasionally Y- and V-shaped cells and a facultatively anaerobic metabolism. Under anoxic conditions, *P. denitrificans* grows by fermenting sugars as substrates in a mixed acid fermentation or by reducing NO_3^- and NO_2^- to N_2. Growth requirements include a temperature range from 20 to 35 °C and salinity of the medium between 2 to 6% (Shieh *et al.*, 2004). Comparative sequence analysis of 16S rRNA genes showed that *P. denitrificans* clustered together with the sequences MBIC3368, NW001 and SB89 with an identity between 98.3% and 99.9%, all of which belong to bacteria that have been isolated from sponges (Hentschel *et al.*, 2001; Webster and Hill, 2001).

Two years later, a second *Pseudovibrio* species, *P. ascidiaceicola*, was isolated from two sea squirts (*Polycitor proliferus* and *Botryllidae* sp. from the subphylum Tunicata, class Ascidiacea) off Japan. This species was also capable of fermentation and denitrification and was mobile by the means of flagella (Fukunaga *et al.*, 2006). In contrast to *P. denitrificans*, cells of the new isolate were pleomorphic, resembling straight or curved rods during the exponential growth phase and exhibiting a coccoid shape in the late stationary phase. Additionally, formation of star-shaped aggregates could be observed during the early exponential growth phase. Fatty acid analysis showed that the profiles of *P. denitrificans* and *P. ascidiaceicola* were quite similar, but with differences in the relative proportions of several fatty acids. Furthermore, several differences in enzyme activities and carbon source utilization were demonstrated together with a DNA-DNA hybridization (DDH) value of less than 30%, which required the description of this isolate as a new species (Fukunaga *et al.*, 2006).

The third and so far latest *Pseudovibrio* species, *P. japonicus*, was isolated from surface coastal waters off Japan (Hosoya and Yokota, 2007). The new strain featured the main physiologic and morphologic characteristics known for the genus *Pseudovibrio*, including heterotrophic, facultatively anaerobic growth with the ability to ferment and denitrify as well as rod-shaped, motile cells. However, differences in terms of substrate usage, enzyme

functionality and DDH values between *P. japonicus*, *P. denitrificans* and *P. ascidiaceicola* of less than 40% led to the classification into a new species.

Figure 1.1. Global map showing the locations where *Pseudovibrio* spp.-related bacteria were found by either detection of respective 16S rRNA gene sequences in clone libraries or by isolation of the respective strains. Different star colors illustrate the habitat where the bacteria originate from. The data were compiled from following publications: Hentschel *et al.* (2001), Webster and Hill (2001), Olson *et al.* (2002), Thakur *et al.* (2003), Thiel and Imhoff (2003), Thoms *et al.* (2003), Shieh *et al.* (2004), Agogué *et al.* (2005), Lafi *et al.* (2005), Enticknap *et al.* (2006), Fukunaga *et al.* (2006), Koren and Rosenberg (2006), Hosoya and Yokota (2007), Muscholl-Silberhorn *et al.* (2007), Sertan-de Guzman *et al.* (2007), Riesenfeld *et al.* (2008), Kennedy *et al.* (2009), Rypien *et al.* (2010), Santos *et al.* (2010), O'Halloran *et al*. (2011), Penesyan *et al.* (2011), and Vizcaino (2011).

Intriguingly, besides *P. denitrificans* and *P. japonicus*, only one more *Pseudovibrio* spp.-related bacterium has been detected in open coastal marine waters (Agogué *et al.*, 2005). In all other surveys, *Pseudovibrio* spp.-related bacteria have been isolated or identified by comparative sequence analysis of 16S rRNA genes only in association with marine eukaryotes. Currently, there exist 22 publications, in which *Pseudovibrio* spp.-related strains have been identified and which include the descriptions of the three type strains. In twelve of these, *Pseudovibrio* spp. were associated with sponges (Hentschel *et al.*, 2001; Webster and Hill, 2001; Olson *et al.*, 2002; Thakur *et al.*, 2003; Thiel and Imhoff, 2003; Thoms *et al.*,

2003; Lafi *et al.*, 2005; Enticknap *et al.*, 2006; Muscholl-Silberhorn *et al.*, 2007; Kennedy *et al.*, 2009; Santos *et al.*, 2010; O'Halloran *et al.*, 2011); in three they were detected in tunicates (Fukunaga *et al.*, 2006; Sertan-de Guzman *et al.*, 2007; Riesenfeld *et al.*, 2008); in three they originated from corals (Koren and Rosenberg, 2006; Rypien *et al.*, 2010; Vizcaino, 2011); in another three they were found in open coastal waters (Shieh *et al.*, 2004; Agogué *et al.*, 2005; Hosoya and Yokota, 2007); and in one they were detected as an epiphyte of algae (Penesyan *et al.*, 2011). In summary, *Pseudovibrio* spp.-related bacteria are ubiquitous, often associated with eukaryotes and even occur in antarctic tunicates (Riesenfeld *et al.*, 2008), indicating the existence of psychrophilic *Pseudovibrio* strains (**Figure 1.1**).

The association between sponges and *Pseudovibrio* spp.-related bacteria was investigated in several studies. First indications for the symbiotic character of this genus were published by Webster and Hill (2001), which found a *Pseudovibrio* sp. (at that time, the genus *Pseudovibrio* did not exist yet) as the dominating culturable α-proteobacterium associated with the sponge *Rhopaloeides odorabile*. Strain NW001, as it was designated in that study, was localized in the mesohyl region of the sponge surrounding the choanocyte chambers, as shown by fluorescence *in situ* hybridization (FISH). Indicative for a symbiotic life style, the *Pseudovibrio* spp.-related strain was neither found in water sampled adjacent to the sponge, nor in diseased sponges sampled in the same region. As a conclusion, this bacterium, and hence the modern *Pseudovibrio* spp., were considered as true, commensalistic/mutualistic symbionts of the sponge *Rhopaloeides odorabile*. In contrast to that study, Hentschel *et al.* (2001) isolated *Pseudovibrio* sp. strain SB89 from the sponges *Aplysina aerophoba* and *A. cavernicola*, but could not localize the bacterial cells in the sponge tissue. However, the hypothesis of Webster and Hill (2001) was supported by Enticknap *et al.* (2006), showing the presence of a *Pseudovibrio* sp. in larvae of the sponge *Mycale laxissima*, comprising about 50% of the total bacteria observed by FISH (**Figure 1.2**). Consequently, the authors confirmed the symbiont status of *Pseudovibrio* and proposed its vertical transmission in sponges. Even though *Pseudovibrio* spp.-related bacteria have been isolated from seawater as well as from corals and tunicates, and therefore do not belong to the sponge-specific cluster that is composed of bacteria isolated exclusively from sponges, the previously mentioned facts supply strong evidence for *Pseudovibrio* spp. being true symbionts of sponges (Taylor *et al.*, 2007). The fact that *Pseudovibrio* strains have so far never been identified in diseased sponges argues for a commensalistic/mutualistic type of symbiosis, however, a parasitic or even pathogenic relationship cannot be excluded.

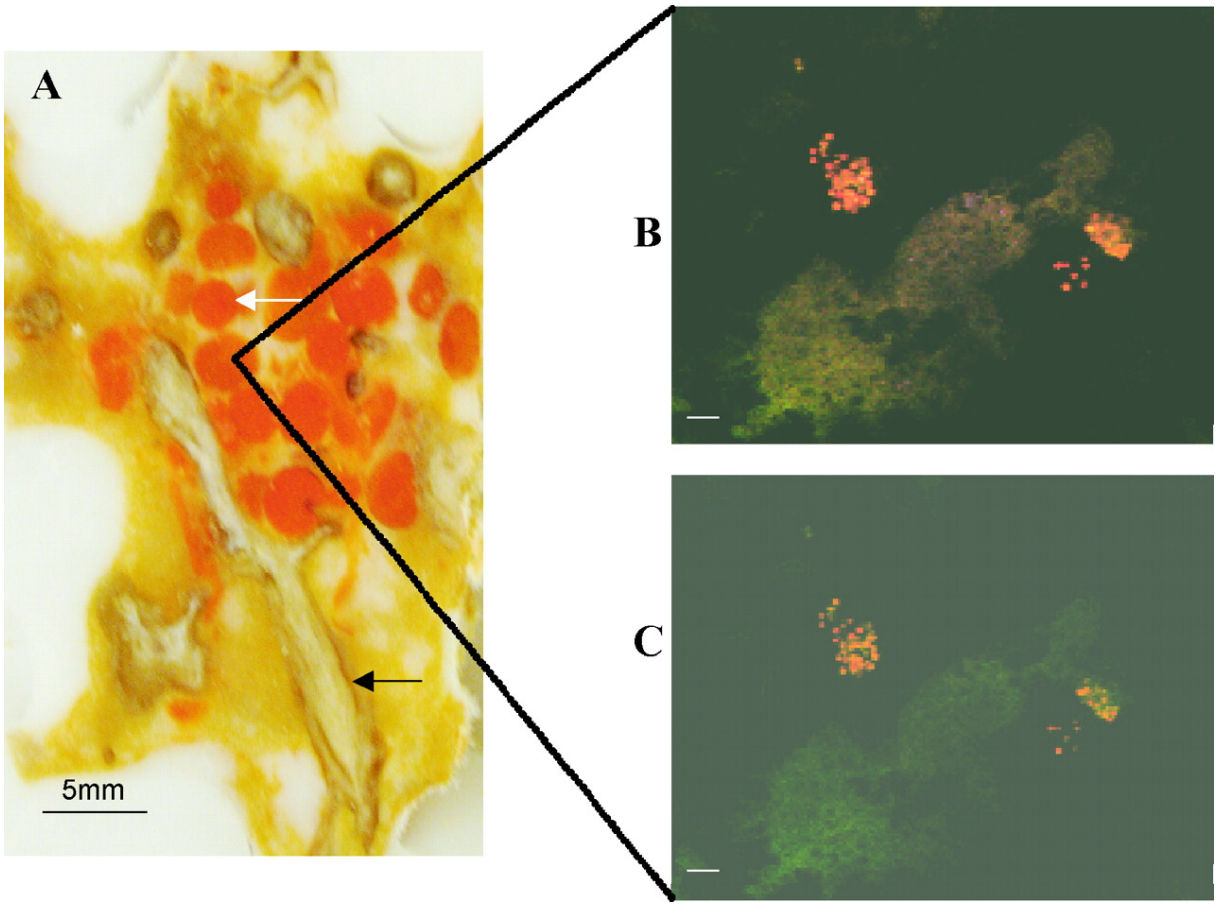

Figure 1.2. Occurrence of *Pseudovibrio* sp. in sponge larvae. (A) Cross-section of the mesohyl of a sponge, in which the larvae are indicated by the white arrow and are bright orange in color. The black arrow indicates sponge fibers. (B and C) FISH images from inside of the larvae with the universal EUB338 probe (B) and the *Pseudovibrio* spp. specific NW442 probe (C). Scale bars 10 µm. Image is adapted from Enticknap *et al.* (2006).

More than 90 isolates of *Pseudovibrio* spp.-related bacteria have been shown to produce bioactive compounds (Hentschel *et al.*, 2001; Thiel and Imhoff, 2003; Muscholl-Silberhorn *et al.*, 2007; Sertan-de Guzman *et al.*, 2007; Kennedy *et al.*, 2009; Rypien *et al.*, 2010; Santos *et al.*, 2010; O'Halloran *et al.*, 2011; Penesyan *et al.*, 2011; Vizcaino, 2011), however, only few of these compounds were so far isolated and characterized. As an example, Sertan-de Guzman *et al.* (2007) identified a heptylprodigiosin-producing *Pseudovibrio* strain. Heptylprodigiosin is a tripyrrole compound with a wide range of activities that e.g. acts against gram-positive bacteria and protozoa in general and may even have potential antimalaria effects (Kaur *et al.*, 2009). Penesyan *et al.* (2011) detected a *Pseudovibrio* sp. producing tropodithietic acid (TDA), which is a compound with antimicrobial activity. Furthermore, Vizcaino (2011) identified the bile acid glycocholic acid (GCA) and a novel

polypeptide termed Pseudovibrocin, which are both substances exhibiting antimicrobial activities.

Sponges and sponge-bacteria associations

The term symbiosis is used in this work according to the definition of Anton de Bary in 1879: a symbiosis describes all types of associations between dissimilarly named organisms, which is also including all degrees of parasitism (de Bary, 1879). A symbiont is therefore a bacterium that interacts with the host in a commensalistic/mutualistic or parasitic/pathogenic way.

Sponges (phylum Porifera) belong to the oldest metazoan animals and originated 600 to 800 million years ago (Müller, 2001). They are filter-feeders and are capable of filtering many thousands of liters of seawater per day (Reiswig, 1974), retaining up to 96% of bacterial cells and other particles (Reiswig, 1971) and excreting nearly sterile water. Considering an average of $5 \cdot 10^5$ bacterial cells per milliliter seawater (Whitman *et al.*, 1998), the amount of microbes a sponge is retaining during a single day is enormous. For instance, a sponge filtering five thousand liter of water, would come into contact with around 10^{12} bacterial cells per day. Porifera consist of three classes, the Hexactinellida (glass sponges), Calcarea (calcareous sponges) and Demospongiae (demosponges). The majority of all known sponge species belong to the latter (Müller *et al.*, 2003). The overall organization of sponge tissue is remarkably simple (Taylor *et al.*, 2007), as illustrated in **Figure 1.3**. The outer surface consists of pinacocytes, epithelial cells forming the pinacoderm, which also revets the interior canals that begin at the surface of the sponge as pores (ostia) and continue penetrating the entire sponge. Then, these canals lead to chambers, which consist of choanocytes (the cell layer of choanocytes is called choanoderm) that are flagellated cells, generating a water flow by beating. Additionally, the choanocytes are responsible for the feeding by filtering out food particles. Once food particles are caught, they are transported to the mesohyl, which is a connective tissue made up of mainly a gelatinous matrix with a number of different wandering cells (Bonasoro *et al.*, 2001; Taylor *et al.*, 2007). In the mesohyl, the food particles are digested by archaeocytes, which represent the totipotent stem cells of sponges that are capable of differentiating into any other cell type (Müller, 2006). Once the water has been filtered in the choanocyte chambers, it is expelled through the exhalant opening, the osculum (Taylor *et al.*, 2007).

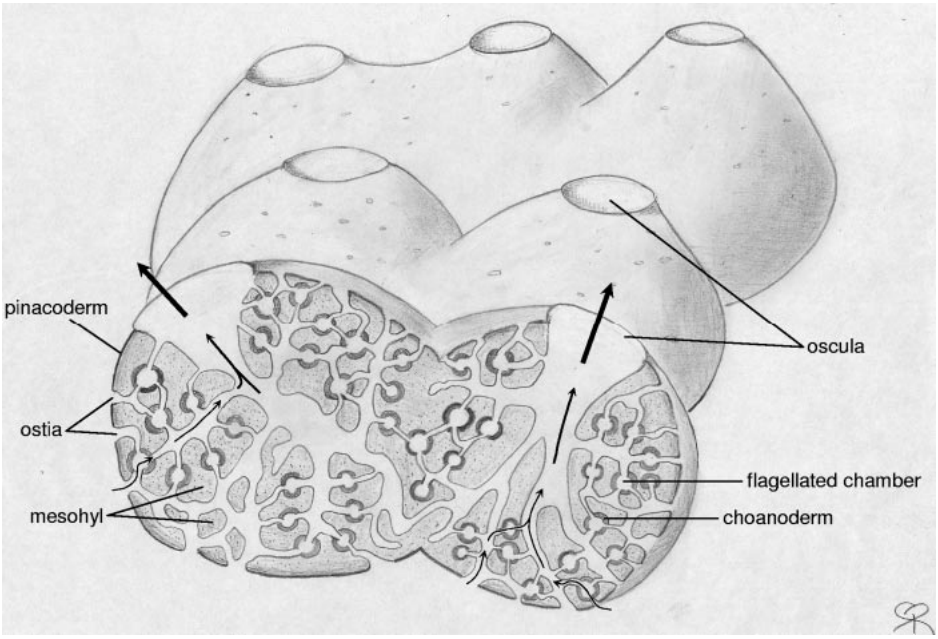

Figure 1.3. Schematic illustration of a sponge. The water flow is represented by arrows and is generated by the choanoderm – a cell layer of flagellated choanocytes in the chambers (depicted in dark grey). The water enters the sponge through the ostia, is filtered by the choanocytes which transport the particles into the mesohyl, and leaves the sponge through the oscula. Image taken from Taylor *et al.* (2007), adapted from Rupert and Barnes (1996).

Despite the simple body plan, sponges posses a very effective innate immune system and are capable of differentiation of self and non-self tissue by fusion of autografts (self tissue) and rejection of allografts (non-self tissue), as demonstrated by Müller *et al.* (1999). In 2001, the first report on the molecular response of a sponge to a bacterial infection has been published (Böhm *et al.*, 2001). It has been shown that after incubation of sponge tissue with lipopolysaccharide (LPS), an endotoxin of gram-negative bacteria, two mitogen-activated protein (MAP) kinases, p38 and c-Jun N-terminal kinase (JNK), were activated via phosphorylation within the first hour after LPS exposure. Subsequently, first evidence for a Toll-like receptor (TLR) system as well as LPS-interacting proteins has been identified in sponges (Wiens *et al.*, 2005). Both molecules are known to mediate detection of bacteria by concertedly binding to the bacterial lipopolysaccharides, thereby stimulating the activation of the MAP kinase pathway (Palsson-McDermott and O'Neill, 2004). In the case of gram-positive bacteria, a response to peptidoglycan was shown to include endocytosis and an increased release of lysozyme in order to degrade the bacterial cell wall (Thakur *et al.*, 2005). Associations of microbes and sponges were for the first time described in the late 70's by Vacelet and Donadey (1977) and Wilkinson and Fay (1979). In certain sponges, the amount

of extracellular bacteria populating the mesohyl is very high (between 10^8 to 10^{10} cells per gram of sponge wet weight). Thus, prokaryotes can account for up to 40% of the sponge mass (high-microbial-abundance sponges). On the other hand, there are also sponges that contain only very few bacteria (10^5 to 10^6 bacteria per gram of sponge wet weight; low-microbial-abundance sponges; Hentschel *et al.*, 2006; Taylor *et al.*, 2007). Until now, sponge-specific bacterial 16S rRNA gene sequences are distributed over 16 bacterial phyla and the archaeal lineages *Crenarchaeota* and *Euryarchaeota* (Taylor *et al.*, 2007). In order to establish a successful symbiosis with a sponge, these prokaryotes must avoid the defense mechanisms of the sponge and therefore need systems on their own to either repress or evade the immune answer of the host. In particular, the discrimination of symbiotic and "food bacteria" for the sponge is mediated by the functionality of the archaeocytes, however the mechanisms behind this selection are not yet understood (Wehrl *et al.*, 2007). It is assumed that the sponge-associated bacteria can avoid digestion by e.g. the production of specific slime layers or capsules (Friedrich *et al.*, 1999).

As already mentioned, the sessile life style and immense filtering capacity of a sponge expose it to an enormous amount of microorganisms, many of which harbor potential parasitic or pathogenic properties. It is therefore plausible that besides the innate immune system also other effective methods of defense against pathogenic microbes are required. Sponges rely on bioactive compounds, which are supposed to protect them from pathogens. Thus, it is not surprising that sponges seem attractive as a source for pharmaceutically relevant metabolites with anticancer, antibacterial, antifungal, antiviral, anti-inflammatory and antifouling properties (Taylor *et al.*, 2007 and references therein). In the year 2009 alone, 287 new compounds isolated from sponges were reported – a number similar to previous years (Blunt *et al.*, 2011). In fact, a yet unknown part of these bioactive compounds was assumed to be produced by symbiotic microorganisms within the sponges (Piel, 2009 and references therein). This assumption led to an increased interest to isolate and culture sponge-specific bacteria. Due to their relatively easy cultivation (if isolation approaches were successful), rapid growth rates, high amount of biomass and their possible biotechnological application they could outcompete the struggle for the establishment of sponge cultures, which is a challenging task (Sipkema *et al.*, 2005; Taylor *et al.*, 2007). However, also isolation of sponge-specific bacteria was successful only for a small part of the bacterial community, whereby the *Pseudovibrio* spp.-related strains were among the most prominent and easiest to cultivate (Hentschel *et al.*, 2006). Natural products synthesized by *Pseudovibrio* spp. are therefore of

current interest. First, there already exists a range of different isolated metabolites (Sertan-de Guzman *et al.*, 2007; Penesyan *et al.*, 2011; Vizcaino, 2011) and second, the bacteria are ubiquitous and simple to isolate from sponges all over the world.

Bacterial secretion systems and their role in symbiosis

Secretion of molecules into the environment or injection of proteins into host cells is a complex process in gram-negative bacteria due to the presence of two membranes. So far, six secretion systems have been identified that differ in complexity and the secretion mechanisms (Saier, 2006; Tseng *et al.*, 2009). Type I, III, IV and VI pathways export the secreted molecules in a single step across both membranes. Type II and V systems transport molecules into the periplasmic space from where they are then secreted across the outer membrane (Tseng *et al.*, 2009). Of particular interest are secretion systems III, IV and VI that have the ability – besides spanning the two membranes of the gram-negative bacterium – to translocate proteins, so called effectors, across a third membrane, which in most of the cases belongs to an eukaryotic organism. Thereby, they facilitate prokaryote-eukaryote interactions. In the following, the focus will be laid on type III and type VI secretion systems due to the importance of these systems for the present work (**Figure 1.4**).

Type III secretion system

Type III secretion systems (T3SS) are found in many pathogens of animals and plants and are among the best studied secretion systems. They are present in commensalistic/ mutualistic bacteria, but have been studied in particular in the pathogen *Yersinia* spp. (Mota and Cornelis, 2005), which will be used here as a model organism. For the synthesis of the type III secretion system, the injectisome, around 25 different proteins are required, most of which are structural components. Only 9 proteins (YscC, -J, -N, -Q, -R, -S, -T, -U and -V) constitute the core of the injectisome, and were found to be conserved in all strains examined until now (Cornelis, 2006). These components encode mainly for the basal body of the secretion system that spans the peptidoglycan and both membranes of the prokaryote. It includes an ATPase (YscN), which is necessary for the energy supply during the secretion process (Cornelis, 2002; Cornelis, 2006). Besides the basal body, the injectosome consists of a needle-like structure with an inner diameter of approximately 25 Å, which translocates the effector proteins. The needle structure consists of proteins that have a low sequence conservation, most likely due to the adaptations to specific host or environmental conditions, in which the respective secretion system needs to operate (Cornelis, 2006).

The physiological role of the T3SS is the injection of effector proteins into host cells. Inside the eukaryotic cell, the effectors modify cellular processes and enable host cell invasion, repression of the pro-inflammatory response or inhibition of phagocytosis (Mota and Cornelis, 2005; Cornelis, 2006). Even though type III secretion systems are best studied in animal and plant pathogens (Troisfontaines and Cornelis, 2005; Tseng *et al.*, 2009), they have been also described in commensalistic/mutualistic bacteria like rhizobia, the nodule-forming plant symbionts (Deakin and Broughton, 2009; Kambara *et al.*, 2009), the tse-tse fly symbiont *Sodalis glossinidius*, the nematode symbiont *Photorhabdus luminescens* as well as the human commensal *Pantoea agglomerans* (Cornelis, 2006). Therefore, type III secretion systems should be regarded as a mechanism facilitating prokaryote-eukaryote interaction rather than just as a virulence factor of pathogenic bacteria (Tseng *et al.*, 2009).

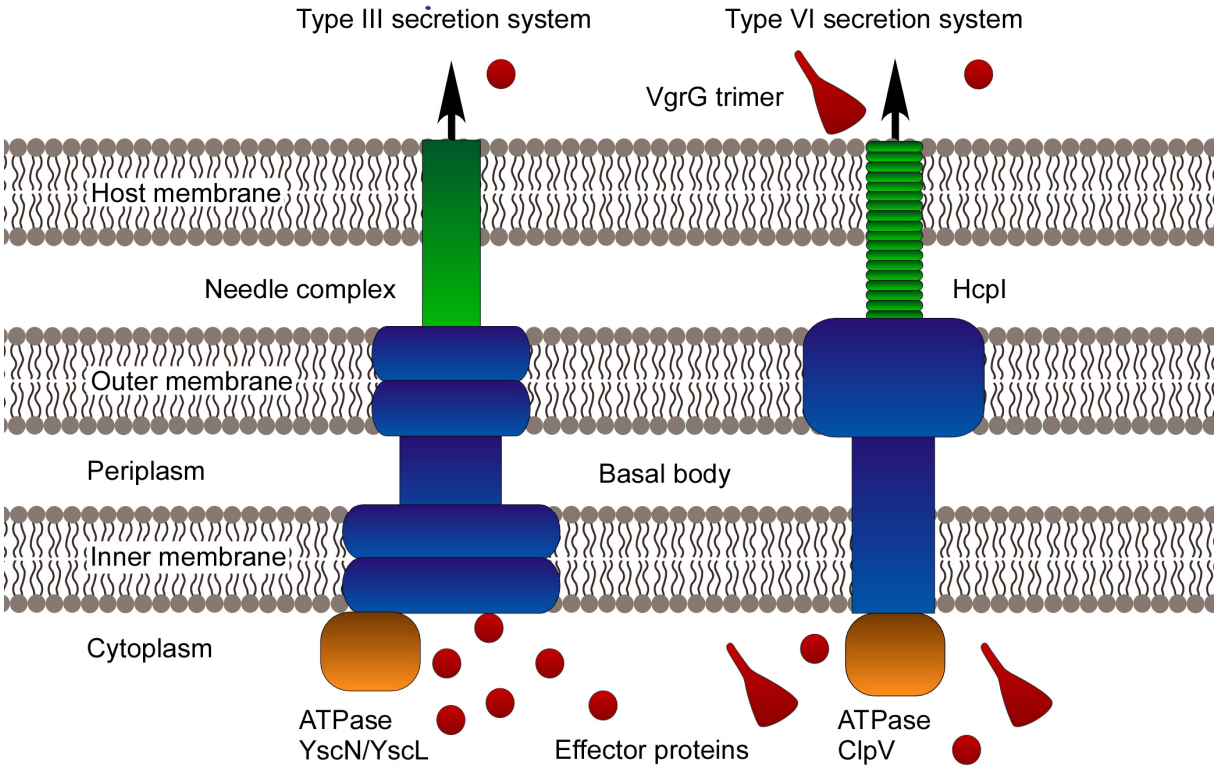

Figure 1.4. Schematic illustration of type III and type VI secretion systems. ATPases, which energize the translocation process, are represented in orange. The basal body of both systems spans the inner and the outer membranes and is shown in blue. The needle complex of type III secretion system is shown in green. A functioning type III secretion system can translocate effector proteins (red) across all three membranes into the host cell. The injection apparatus of the type VI secretion system is composed of HcpI rings (green) and the VgrG (red) trimer, which is the membrane-puncturing device. However, VgrG might also be involved in effector functions. Additionally, regular effector molecules could be translocated with the type VI secretion systems. Image based in parts on Tseng *et al.* (2009), Cornelis (2006) and Bönemann *et al.* (2010).

Type VI secretion system

Only recently, the type VI secretion system (T6SS) has been described as a widespread secretion system (Mougous *et al.*, 2006; Pukatzki *et al.*, 2006) as it was detected in about 25% of all sequenced gram-negative bacterial genomes. So far, it was mainly found in pathogenic proteobacteria, where it was encoded in a cluster of 15 to 20 genes (Boyer *et al.*, 2009; Bönemann *et al.*, 2010). The analysis of genomes containing a T6SS resulted in the identification of a set of 13 proteins – a core of conserved and essential subunits found in every type VI secretion system known until today (Boyer *et al.*, 2009). The knowledge on the T6SS structure is rather rudimental, but the current model suggests that a part of the secretion system is embedded in the inner and the outer membrane, spans the peptidoglycan and is provided with energy by the ClpV, which is the ATPase of the complex (Bönemann *et al.*, 2010). The injection apparatus forms a pilus-like structure and mainly consists of hexameric HcpI rings that form a tube with an inner diameter of 40 Å. On top it has a spike complex assembled by a VgrG trimer, which is required to puncture the membranes on its way to the targeted cytoplasm of the host cell (Pukatzki *et al.*, 2009; Bönemann *et al.*, 2010).

In general, T6SS is suggested to act as a protein translocating device between the prokaryote and the host, delivering the effector into the cytoplasm of the eukaryote. However, only a few putative effector molecules have been reported until today and their function has not yet been unambiguously proven (Pukatzki *et al.*, 2009). Actual effector characteristics have been proposed for the VgrG trimer, which forms the membrane piercing tip of the T6SS needle. Some of these VgrG proteins, termed “evolved” VgrGs (Pukatzki *et al.*, 2007), possess a C-terminal extension that contains functional domains and might therefore act as an effector with diverse functions, e.g. crosslinking of host actin, which results in the reorganization of the host cytoskeleton (Pukatzki *et al.*, 2009; Bönemann *et al.*, 2010). Interestingly, evolved VgrGs mostly do not belong to the T6SS-encoding cluster but are distributed throughout the bacterial genome together with the gene coding for HcpI (Pukatzki *et al.*, 2009). Typically, type VI secretion systems are described as virulence factors of pathogenic bacteria required for cytotoxicity, host-cell invasion and survival within the host (Cascales, 2008; Jani and Cotter, 2010). However, also functions not involved in virulence are proposed for T6SSs, including biofilm formation, quorum sensing, interactions between different bacterial species and even antipathogenesis factors (Jani and Cotter, 2010 and references therein).

Oligotrophy in the oceans and bacterial adaptations

Apart from eukaryote-associated growth, *Pseudovibrio* spp. are also capable of proliferation under oligotrophic conditions (Schwedt, 2011). Oligotrophic environments are characterized by low nutrient concentrations, and even more importantly, by a low carbon flux (Poindexter, 1981). The open ocean is mainly an oligotrophic environment, with concentrations of dissolved organic carbon (DOC) between 0.1 and 1 milligram carbon per liter (Schut *et al.*, 1997). It is widely accepted that only a small part of the DOC is amenable for biodegradation (Bada and Lee, 1977; Ammerman *et al.*, 1984). Nevertheless, not all prokaryotes are dormant in low nutrient environments, but might actively grow and multiply (Ammerman *et al.*, 1984 and references therein), reaching cell numbers of around $5 \cdot 10^5$ cells per milliliter (Whitman *et al.*, 1998), indicating that the amount of nutrients is enough to sustain their metabolism and cell division. However, the nutrient distribution should not be regarded as homogeneous but rather patchy due to the presence of marine snow. Thousands of these nutrient-rich particles are present in a cubic meter of seawater (Azam and Long, 2001), with several orders of magnitude higher concentrations of carbon and nitrogen than in the surrounding, nutrient-poor environment (Alldredge and Silver, 1988; Schut *et al.*, 1997). Consequentially, prokaryotes in the open ocean are mainly exposed to severe nutrient limitation. However, they occasionally also encounter times of increased availability of nutrients that are released by the activity of hydrolytic enzymes produced by bacteria attached to the marine snow particles (Smith *et al.*, 1992).

Therefore, two ecological types of planktonic bacteria can be differentiated in the marine environment. The first type is adapted to changing nutrient conditions and benefits from occasional increase in substrates released from marine snow, resulting in increased growth rates. The second type comprises slow growing bacteria, which are well adapted to long-term nutrient starvation, but cannot cope with highly increased substrate concentrations (Azam and Long, 2001; Giovannoni and Stingl, 2005). The first of these two ecological types represents per definition a facultative, the second an obligate oligotrophic bacterium (Ishida *et al.*, 1982; Ishida *et al.*, 1986; Schut *et al.*, 1997). Oligotrophic bacteria are capable of growth on media with a carbon content between 0.2 and 16.8 milligram carbon per liter (Schut *et al.*, 1997). It has been proposed that oligotrophs possess specific characteristics in order to efficiently adapt to environments with low nutrient concentrations (Poindexter, 1981; Schut *et al.*, 1997; Cavicchioli *et al.*, 2003). A high surface-to-volume ratio results in a larger area that

can be used for nutrient uptake, concluding that the best shape for an oligotroph would be a thin rod (Poindexter, 1981). Substrate specificity is an important factor for oligotrophic bacteria. Carbon catabolic repression has been shown to be relieved at low growth rates, allowing the bacteria to use several carbon sources at the same time (Egli, 2010). This supports the hypothesis that oligotrophic bacteria need a broad substrate spectrum, as well as the physiological capacity to simultaneously metabolize different substrates in order to survive in the marine environment (Schut *et al.*, 1997). Consequently, oligotrophic bacteria require high-affinity transporters that are capable to bind and transport traces of nutrients against a concentration gradient (Poindexter, 1981; Cavicchioli *et al.*, 2003). Bacteria with the described characteristics should therefore be well adapted to low nutrient environments.

Phosphorus in oceanic environments

Phosphorus (P) is an essential element for all forms of life. It is present in the backbone of DNA, RNA and in the hydrophilic head groups of phospholipids as phosphate diester (**Figure 1.5**). Furthermore, it plays a fundamental role in the energy metabolism of the cell in the form of energy-rich phosphoanhydride bonds in the adenosine triphosphate (ATP) molecule (Paytan and McLaughlin, 2007). Molecules containing organophosphorus compounds with the very stable carbon-phosphorus bond that is resistant to chemical hydrolysis, thermal decomposition and photolysis (Quinn *et al.*, 2007) are termed phosphonates. They are found in nature and are present in glycoproteins, glycolipids or phosphonolipids (Huang *et al.*, 2005). These kinds of bonds have been identified in a number of marine invertebrates (Quin, 1965; Kittredge and Roberts, 1969) and it has recently been shown that *Trichodesmium erythraeum* synthesizes phosphonates, which constitute on the average up to 10% of their cellular phosphorus pool (Dyhrman *et al.*, 2009). Additionally, the phosphorus storage polymer polyphosphate (poly P_i) consists of inorganic phosphate connected via the energy-rich phosphoanhydride bond in chains of tens to hundred residues and can be found in living organisms from prokaryotes to mammals (Kornberg, 1995). The function of this polymer is very diverse and ranges from a P storage compound, which can also be used to substitute ATP due to its energy-rich phosphoanhydrid bonds, over chelating of toxic metals to a regulator of stress and survival (Kornberg, 1995; Brown and Kornberg, 2004).

For bacteria, inorganic phosphate (P_i) is the preferred and most bioavailable phosphorus source (Karl, 2000; Dyhrman *et al.*, 2007), however, it represents only a fraction

of the dissolved phosphorus in the surface waters of the oceans (Dyhrman *et al.*, 2007) and can become severely depleted in the oceanic environment (e.g. Wu *et al.*, 2000). Dissolved organic phosphorus (DOP) constitutes the main fraction of the dissolved P pool (Young and Ingall, 2010 and references therein) and consists of proteins, carbohydrates and lipids but mainly of a molecularly uncharacterized fraction and is present in concentrations between 70 to 200 nmol per liter in the surface ocean, declining with depth (Paytan and McLaughlin, 2007). High molecular weight (HMW, >50 kDa) DOP, representing between 15 to 30% of the dissolved organic phosphorus (Paytan and McLaughlin, 2007), has been determined to consist to a major part of phosphate esters (75%) and phosphonates (25%) (Kolowith *et al.*, 2001). In contrast, low molecular weight (LMW, <10 kDa) DOP comprises between 50 and 80% of the DOP pool (Paytan and McLaughlin, 2007), but only little information about the composition of this pool is currently available (Dyhrman *et al.*, 2007). Recent studies, however, indicate that LMW DOP might, among P esters like phosphosugars as well as nucleotides and phosphonates, contain up to 13% polyphosphate (Young and Ingall, 2010).

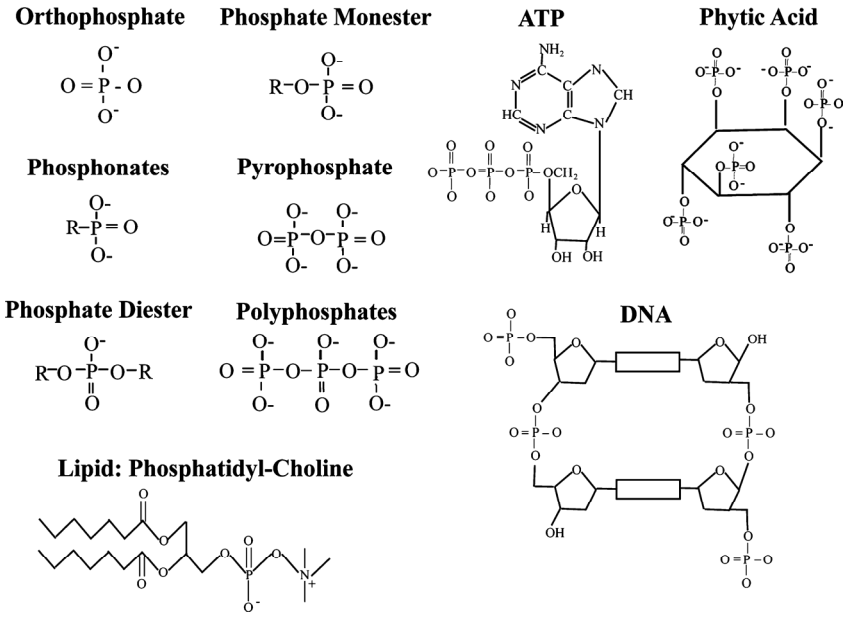

Figure 1.5. Illustration of important biological compounds containing phosphorus, indicating the respective P-involved bond types. –R represents a carbon moiety. Image adapted from Paytan and McLaughlin (2007).

Bacteria developed several mechanisms to access the diversity of phosphorus compounds available in their surroundings (**Figure 1.6**). P_i is imported via the high-affinity phosphate specific transporter (Pst), which can scavenge phosphate at very low concentrations (Wanner, 1993). Phosphate mono- and diester containing DOP is degraded via

phosphomonoesterases (e.g. alkaline phosphatases and 5-nucleotidases) and phospho-diesterases, respectively, both of which represent frequently found enzymes in aquatic environments and thus represent key-players for the P cycle (Karl and Yanagi, 1997 and references therein).

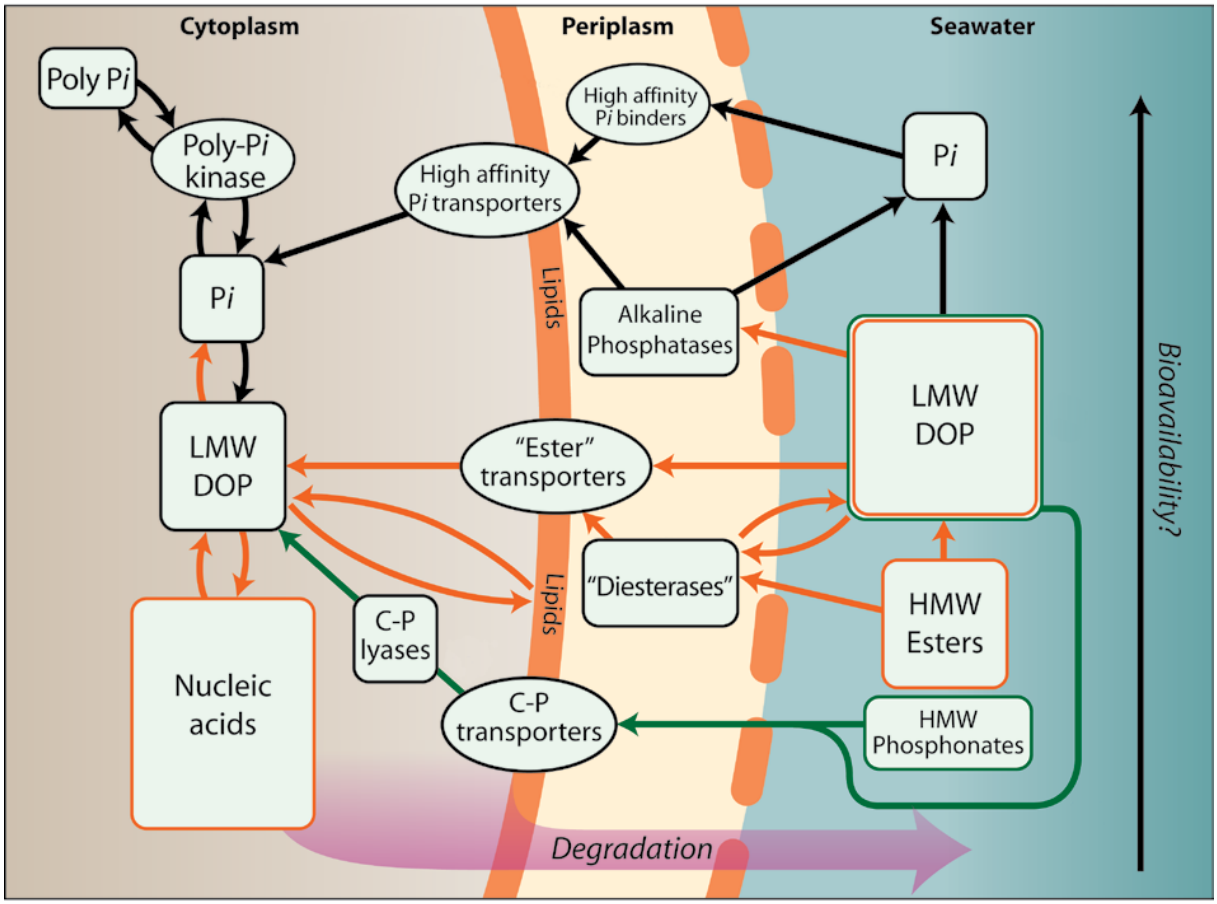

Figure 1.6. Schematic illustration of the dissolved organic phosphorus (DOP) in oceanic environments and the acquisition/transformation mechanisms of these DOP sources in marine bacteria. The phosphate (P_i) pool and respective reactions are depicted in black, phosphoesters in orange and phosphonates in green. The proposed bioavailability of different compounds is indicated by the arrow on the right hand side of the figure. Image adapted from Dyhrman *et al.* (2007).

Alkaline phosphatases (APases), which were initially considered to be mainly present either in the periplasm or being secreted in order to degrade DOP outside the cell, have now also been shown to remain in the cytoplasm (Luo *et al.*, 2009). This indicates that besides the extracellular degradation of phosphate esters, LMW DOP molecules are taken up by the cell before the phosphate is cleaved off, suggesting that marine bacteria might play an even more important role in the phosphorus cycle than previously recognized (Luo *et al.*, 2009; White, 2009). Phosphonates might be considered as a refractory P source due to their stable carbon-

phosphorus bond, which results in a low bioavailability. Nevertheless, the usage of phosphonates as the sole phosphorus source has been shown in 1963 for *Escherichia coli* (Zeleznick *et al.*, 1963) and since then for many other bacteria (Kononova and Nesmeyanova, 2002 and references therein). In *Trichodesmium erythraeum,* a phosphonate degradation pathway with broad substrate specificity (the C-P lyase pathway) was detected. As *T. erythraeum* represents an abundant N_2-fixing phototroph in the global oceans, it can be suggested that phosphonates might be an important source of phosphorus for the general marine bacterial community (Dyhrman *et al.*, 2006; White and Metcalf, 2007).

Phosphate limitation and the Pho regulon

In the oligotrophic parts of the open oceans, bacteria are regularly exposed to conditions of long-term phosphorus limitation and many have adapted to this type of starvation. For instance, *Prochlorococcus* and *Synechococcus* are ubiquitous and abundant picocyanobacteria that dominate photic oligotrophic environments. They substitute phospholipids in their membranes with non-phosphorus, sulfate/sugar- or sugar-based lipids, thereby decreasing their phosphorus demands by up to 43% (Van Mooy *et al.*, 2006; Van Mooy *et al.*, 2009). Furthermore, a reduction in genomic information would result in decreased P requirement for DNA synthesis. This phenomenon, termed genome streamlining, can be observed in *Prochlorococcus* sp. as well as in *Candidatus* Peligibacter ubique, a ubiquitous heterotroph dominating open ocean environments. Both have the smallest genomes reported for photosynthetic (<2.5 Mbp) and heterotrophic organisms (1.3 Mbp), respectively (Rocap *et al.*, 2003; Giovannoni *et al.*, 2005).

Aside from adaptations to long-term phosphorus starvation, bacteria developed an immediate response to P_i-limiting conditions. This mechanism is controlled by a two-component regulatory system, the PhoR-PhoB system (Wanner, 1993). PhoR is a sensory histidine kinase, responding to the concentration of phosphate in the periplasm. During phosphate surplus conditions, the histidine kinase is dephosphorylated, but under phosphate limiting conditions (<4 μmol l^{-1} for *Escherichia coli*) PhoR is auto-phosphorylated and in turn transfers the phosphoryl group to PhoB, the response regulator of this regulatory system. The phosphorylated PhoB now regulates a set of genes known as the Pho regulon by binding to so called Pho boxes in the promoter regions of those genes (Wanner, 1993; Lamarche *et al.*, 2008). The response to phosphorus deprivation has been extensively studied in *Escherichia coli* and *Bacillus subtilis* and numerous genes have been identified to be directly controlled by

the PhoR-PhoB regulatory system (Allenby *et al.*, 2005; Lamarche *et al.*, 2008). For example, in *E. coli*, the regulon induces the expression of the alkaline phosphatase (*phoA*), the glycerol phosphate uptake system (*ugpBAEC*), the phosphonate transport and degradation system (*phnCDEFGHIJKLMNOP*) as well as the high-affinity Pst (*pstSCAB-phoU*) system (Lamarche *et al.*, 2008; Hsieh and Wanner, 2010). The Pst system is composed of the integral membrane proteins PstC and PstA, the ATP cleaving permease PstB, the periplasmic binding protein PstS as well as the PhoU protein, which seems to have regulatory functions (Wanner, 1993). In fact, when the Pst system is deleted or mutated, the Pho regulon is expressed irrespective of the phosphate concentration (Lamarche *et al.*, 2008). Furthermore, even though not shown to be directly controlled by the PhoB response regulator, proteins involved in the import and degradation of phosphonates as well as enzymes responsible for synthesis and degradation of polyphosphate are induced during P starvation (Vershinina and Znamenskaya, 2002). Besides the control of direct phosphorus acquirement systems, the Pho operon also regulates modifications of the cell surface. As already described for long-term P-starvation, phosphorus-containing lipids can be exchanged for phosphorus-free lipids during induced phosphate limitation (Zavaleta-Pastor *et al.*, 2010). A similar response is found in gram-positive bacteria, as has been shown for *Bacillus subtilis*, which substitutes the phosphate-containing teichoic acid with the P-free teichuronic acid in its cell wall (Lamarche *et al.*, 2008).

Intriguingly, the Pho regulon is not only responsible for the upregulation of phosphorus-acquiring processes in the bacterial cell during P_i-limitation. It has been shown that phosphate deprivation stimulates the production of antibiotics like streptomycin, cephalosporin, cephamycin C, oxytetracycline and many other secondary metabolites, which could act as inhibitors for other microorganisms, competing for the same phosphorus source (see Martín, 2004 and references therein). On the other hand, recent studies demonstrated the involvement of the PhoR-PhoB regulatory system in bacterial virulence (reviewed in Lamarche *et al.*, 2008). The PhoR-PhoB system regulates biofilm formation and expression of the type III secretion system in *Pseudomonas aeruginosa*, and controls environmental and virulence genes as well as biofilm formation and stress response in *Vibrio cholerae*. In summary, the complex regulatory network that is active under phosphate limitation encompasses, aside from physiological adaptations to P homeostasis, pathogenic factors, secondary metabolite production as well as the general stress response (Haddad *et al.*, 2009; Pratt *et al.*, 2010; Sultan *et al.*, 2010; Zavaleta-Pastor *et al.*, 2010).

Aim of the thesis

In the present study, I investigated the strain *Pseudovibrio* sp. FO-BEG1. This strain has been isolated in the year 2007 by Anne Schwedt (2007; 2011) and represents the only accompanying organism from the *Beggiatoa* sp. 35Flor co-culture, growing in a lithotrophic sulfide-oxygen gradient medium. Initially, this co-culture was enriched from a black band diseased coral from Florida. Until today, *Pseudovibrio* spp.-related bacteria are encountered all over the world. They seem to exhibit an invertebrate-associated life style and feature the production of secondary metabolites, but are poorly investigated in all these aspects. Thus, the major interest in my thesis was the general and specific characterization of strain FO-BEG1. The complete genome of strain FO-BEG1 was sequenced and sequentially analyzed in respect to physiological properties of the strain, including the identification of genes indicative of prokaryote-eukaryote interactions. Additionally, the genome of strain FO-BEG1 was compared with the genome of *Pseudovibrio* sp. JE062, which had been isolated from a sponge. The results of this study are presented in **Chapter II** of this thesis. Further investigations of the metabolic capabilities of strain FO-BEG1 revealed insights into the ability of oligotrophic growth under extreme carbon limitation, also in comparison with other strains, which is described in **Chapter III**. The genus *Pseudovibrio* contains three species, and strain FO-BEG1 was most closely related to *Pseudovibrio denitrificans*^{T}. A polyphasic approach was performed to deduce the phylogenetic affiliation of strain FO-BEG1, which is presented in **Chapter IV** of this work. In **Chapter V** of my thesis, I investigated the response of *Pseudovibrio* sp. FO-BEG1 to phosphate limitation as another essential nutrient, which is rapidly exhausted in marine environments. Changes in the physiology and protein expression of strain FO-BEG1 as a reaction to phosphate depletion were analyzed. Additionally, a yet unidentified, colored compound was found to be secreted by the cells during phosphate-limited conditions. First analyses were therefore performed in order to identify the extracellular metabolome of *Pseudovibrio* sp. FO-BEG1.

References

Agogué H, Casamayor EO, Bourrain M, Obernosterer I, Joux F, Herndl GJ *et al.* (2005). A survey on bacteria inhabiting the sea surface microlayer of coastal ecosystems. *FEMS Microbiol Ecol* **54:** 269–280.

Alldredge AL, Silver MW. (1988). Characteristics, dynamics and significance of marine snow. *Prog Oceanogr* **20:** 41–82.

Allenby NEE, O'Connor N, Prágai Z, Ward AC, Wipat A, Harwood CR. (2005). Genome-wide transcriptional analysis of the phosphate starvation stimulon of *Bacillus subtilis*. *J Bacteriol* **187:** 8063–8080.

Ammerman JW, Fuhrman JA, Hagström A, Azam F. (1984). Bacterioplankton growth in seawater: I. Growth kinetics and cellular characteristics in seawater cultures. *Mar Ecol Prog Ser* **18:** 31–39.

Azam F, Long RA. (2001). Sea snow microcosms. *Nature* **414:** 495–498.

Bada JL, Lee C. (1977). Decomposition and alteration of organic compounds dissolved in seawater. *Mar Chem* **5:** 523–534.

Blunt JW, Copp BR, Munro MHG, Northcote PT, Prinsep MR. (2011). Marine natural products. *Nat Prod Rep* **28:** 196–268.

Böhm M, Hentschel U, Friedrich AB, Fieseler L, Steffen R, Gamulin V *et al.* (2001). Molecular response of the sponge *Suberites domuncula* to bacterial infection. *Mar Biol* **139:** 1037–1045.

Bonasoro F, Wilkie IC, Bavestrello G, Cerrano C, Carnevali MDC. (2001). Dynamic structure of the mesohyl in the sponge *Chondrosia reniformis* (Porifera, Demospongiae). *Zoomorphology* **121:** 109–121.

Bönemann G, Pietrosiuk A, Mogk A. (2010). Tubules and donuts: a type VI secretion story. *Mol Microbiol* **76:** 815–821.

Boyer F, Fichant G, Berthod J, Vandenbrouck Y, Attree I. (2009). Dissecting the bacterial type VI secretion system by a genome wide in silico analysis: what can be learned from available microbial genomic resources? *BMC Genomics* **10:** 104.

Brown MRW, Kornberg A. (2004). Inorganic polyphosphate in the origin and survival of species. *Proc Natl Acad Sci U S A* **101:** 16085–16087.

Cascales E. (2008). The type VI secretion toolkit. *EMBO Rep* **9:** 735–741.

Cavicchioli R, Ostrowski M, Fegatella F, Goodchild A, Guixa-Boixereu N. (2003). Life under nutrient limitation in oligotrophic marine environments: an eco/physiological perspective of *Sphingopyxis alaskensis* (formerly *Sphingomonas alaskensis*). *Microb Ecol* **45:** 203–217.

Cornelis GR. (2002). The *Yersinia* Ysc-Yop 'type III' weaponry. *Nat Rev Mol Cell Bio* **3:** 742–752.

Cornelis GR. (2006). The type III secretion injectisome. *Nat Rev Microbiol* **4:** 811–825.

de Bary A. (1879). Die Entstehung der Symbiose. Verlag von Karl, J. Trübner: Strassburg.

Deakin WJ, Broughton WJ. (2009). Symbiotic use of pathogenic strategies: rhizobial protein secretion systems. *Nat Rev Microbiol* **7:** 312–320.

Dyhrman ST, Ammerman JW, Van Mooy BAS. (2007). Microbes and the marine phosphorus cycle. *Oceanography* **20:** 110–116.

Dyhrman ST, Benitez-Nelson CR, Orchard ED, Haley ST, Pellechia PJ. (2009). A microbial source of phosphonates in oligotrophic marine systems. *Nat Geosci* **2:** 696–699.

Dyhrman ST, Chappell PD, Haley ST, Moffett JW, Orchard ED, Waterbury JB *et al.* (2006). Phosphonate utilization by the globally important marine diazotroph *Trichodesmium*. *Nature* **439:** 68–71.

Egli T. (2010). How to live at very low substrate concentration. *Water Res* **44:** 4826–4837.

Enticknap JJ, Kelly M, Peraud O, Hill RT. (2006). Characterization of a culturable alphaproteobacterial symbiont common to many marine sponges and evidence for vertical transmission via sponge larvae. *Appl Environ Microbiol* **72:** 3724–3732.

Friedrich AB, Merkert H, Fendert T, Hacker J, Proksch P, Hentschel U. (1999). Microbial diversity in the marine sponge *Aplysina cavernicola* (formerly *Verongia cavernicola*) analyzed by fluorescence in situ hybridization (FISH). *Mar Biol* **134:** 461–470.

Fukunaga Y, Kurahashi M, Tanaka K, Yanagi K, Yokota A, Harayama S. (2006). *Pseudovibrio ascidiaceicola* sp. nov., isolated from ascidians (sea squirts). *Int J Syst Evol Microbiol* **56:** 343–347.

Giovannoni SJ, Stingl U. (2005). Molecular diversity and ecology of microbial plankton. *Nature* **437:** 343–348.

Giovannoni SJ, Tripp HJ, Givan S, Podar M, Vergin KL, Baptista D *et al.* (2005). Genome streamlining in a cosmopolitan oceanic bacterium. *Science* **309:** 1242–1245.

Haddad A, Jensen V, Becker T, Häussler S. (2009). The Pho regulon influences biofilm formation and type three secretion in *Pseudomonas aeruginosa*. *Environ Microbiol Rep* **1:** 488–494.

Hentschel U, Usher KM, Taylor MW. (2006). Marine sponges as microbial fermenters. *FEMS Microbiol Ecol* **55:** 167–177.

Hentschel U, Schmid M, Wagner M, Fieseler L, Gernert C, Hacker J. (2001). Isolation and phylogenetic analysis of bacteria with antimicrobial activities from the mediterranean sponges *Aplysina aerophoba* and *Aplysina cavernicola*. *FEMS Microbiol Ecol* **35:** 305–312.

Hosoya S, Yokota A. (2007). *Pseudovibrio japonicus* sp. nov., isolated from coastal seawater in Japan. *Int J Syst Evol Microbiol* **57:** 1952–1955.

Hsieh YJ, Wanner BL. (2010). Global regulation by the seven-component Pi signaling system. *Curr Opin Microbiol* **13:** 198–203.

Huang JL, Su ZC, Xu Y. (2005). The evolution of microbial phosphonate degradative pathways. *J Mol Evol* **61:** 682–690.

Ishida Y, Eguchi M, Kadota H. (1986). Existence of obligately oligotrophic bacteria as a dominant population in the South China Sea and the West Pacific Ocean. *Mar Ecol Prog Ser* **30:** 197–203.

Ishida Y, Imai I, Miyagaki T, Kadota H. (1982). Growth and uptake kinetics of a facultatively oligotrophic bacterium at low nutrient concentrations. *Microb Ecol* **8:** 23–32.

Jani AJ, Cotter PA. (2010). Type VI secretion: not just for pathogenesis anymore. *Cell Host Microbe* **8:** 2–6.

Kambara K, Ardissone S, Kobayashi H, Saad MM, Schumpp O, Broughton WJ *et al.* (2009). Rhizobia utilize pathogen-like effector proteins during symbiosis. *Mol Microbiol* **71:** 92–106.

Karl DM. (2000). Phosphorus, the staff of life. *Nature* **406:** 31–33.

Karl DM, Yanagi K. (1997). Partial characterization of the dissolved organic phosphorus pool in the oligotrophic North Pacific Ocean. *Limnol Oceanogr* **42:** 1398–1405.

Kaur K, Jain M, Kaur T, Jain R. (2009). Antimalarials from nature. *Bioorgan Med Chem* **17:** 3229–3256.

Kennedy J, Baker P, Piper C, Cotter PD, Walsh M, Mooij MJ *et al.* (2009). Isolation and analysis of bacteria with antimicrobial activities from the marine sponge *Haliclona simulans* collected from irish waters. *Mar Biotechnol* **11:** 384–396.

Kittredge JS, Roberts E. (1969). A carbon-phosphorus bond in nature. *Science* **164:** 37–42.

Kolowith LC, Ingall ED, Benner R. (2001). Composition and cycling of marine organic phosphorus. *Limnology and Oceanography* **46:** 309–320.

Kononova SV, Nesmeyanova MA. (2002). Phosphonates and their degradation by microorganisms. *Biochemistry (Moscow)* **67:** 184–195.

Koren O, Rosenberg E. (2006). Bacteria associated with mucus and tissues of the coral *Oculina patagonica* in summer and winter. *Appl Environ Microbiol* **72:** 5254–5259.

Kornberg A. (1995). Inorganic polyphosphate: toward making a forgotten polymer unforgettable. *J Bacteriol* **177:** 491–496.

Lafi FF, Garson MJ, Fuerst JA. (2005). Culturable bacterial symbionts isolated from two distinct sponge species (*Pseudoceratina clavata* and *Rhabdastrella globostellata*) from the Great Barrier Reef display similar phylogenetic diversity. *Microb Ecol* **50:** 213–220.

Lamarche MG, Wanner BL, Crépin S, Harel J. (2008). The phosphate regulon and bacterial virulence: a regulatory network connecting phosphate homeostasis and pathogenesis. *FEMS Microbiol Rev* **32:** 461–473.

Luo HW, Bennera R, Long RA, Hu JJ. (2009). Subcellular localization of marine bacterial alkaline phosphatases. *Proc Natl Acad Sci U S A* **106:** 21219–21223.

Martín JF. (2004). Phosphate control of the biosynthesis of antibiotics and other secondary metabolites is mediated by the PhoR-PhoP system: an unfinished story. *J Bacteriol* **186:** 5197–5201.

Mota LJ, Cornelis GR. (2005). The bacterial injection kit: type III secretion systems. *Ann Med* **37:** 234–249.

Mougous JD, Cuff ME, Raunser S, Shen A, Zhou M, Gifford CA *et al.* (2006). A virulence locus of *Pseudomonas aeruginosa* encodes a protein secretion apparatus. *Science* **312:** 1526–1530.

Müller WEG. (2001). Review: how was metazoan threshold crossed? The hypothetical Urmetazoa. *Comp Biochem Phys A* **129:** 433–460.

Müller WEG. (2006). The stem cell concept in sponges (Porifera): metazoan traits. *Semin Cell Dev Biol* **17:** 481–491.

Müller WEG, Blumbach B, Müller IM. (1999). Evolution of the innate and adaptive immune systems: relationships between potential immune molecules in the lowest metazoan phylum (Porifera) and those in vertebrates. *Transplantation* **68:** 1215–1227.

Müller WEG, Brümmer F, Batel R, Müller IM, Schröder HC. (2003). Molecular biodiversity. Case study: Porifera (sponges). *Naturwissenschaften* **90:** 103–120.

Muscholl-Silberhorn A, Thiel V, Imhoff JF. (2007). Abundance and bioactivity of cultured sponge-associated bacteria from the mediterranean sea. *Microb Ecol* **55:** 94–106.

O'Halloran JA, Barbosa TM, Morrissey JP, Kennedy J, O'Gara F, Dobson ADW. (2011). Diversity and antimicrobial activity of *Pseudovibrio* spp. from Irish marine sponges. *J Appl Micobiol* **110:** 1495–1508.

Olson JB, Harmody DK, McCarthy PJ. (2002). *α-Proteobacteria* cultivated from marine sponges display branching rod morphology. *FEMS Microbiol Lett* **211:** 169–173.

Palsson-McDermott EM, O'Neill LAJ. (2004). Signal transduction by the lipopolysaccharide receptor, Toll-like receptor-4. *Immunology* **113:** 153–162.

Paytan A, McLaughlin K. (2007). The oceanic phosphorus cycle. *Chem Rev* **107:** 563–576.

Penesyan A, Tebben J, Lee M, Thomas T, Kjelleberg S, Harder T *et al.* (2011). Identification of the antibacterial compound produced by the marine epiphytic bacterium *Pseudovibrio* sp. D323 and related sponge-associated bacteria. *Mar Drugs* **9:** 1391–1402.

Piel J. (2009). Metabolites from symbiotic bacteria. *Nat Prod Rep* **26:** 338–362.

Poindexter JS. (1981). Oligotrophy - fast and famine existence. *Adv Microb Ecol* **5:** 63–89.

Pratt JT, Ismail AM, Camilli A. (2010). PhoB regulates both environmental and virulence gene expression in *Vibrio cholerae*. *Mol Microbiol* **77:** 1595–1605.

Pukatzki S, McAuley SB, Miyata ST. (2009). The type VI secretion system: translocation of effectors and effector-domains. *Curr Opin Microbiol* **12:** 11–17.

Pukatzki S, Ma AT, Revel AT, Sturtevant D, Mekalanos JJ. (2007). Type VI secretion system translocates a phage tail spike-like protein into target cells where it cross-links actin. *Proc Natl Acad Sci U S A* **104:** 15508–15513.

Pukatzki S, Ma AT, Sturtevant D, Krastins B, Sarracino D, Nelson WC *et al.* (2006). Identification of a conserved bacterial protein secretion system in *Vibrio cholerae* using the *Dictyostelium* host model system. *Proc Natl Acad Sci U S A* **103:** 1528–1533.

Quin LD. (1965). Presence of compounds with a carbon-phosphorus bond in some marine invertebrates. *Biochemistry* **4:** 324–330.

Quinn JP, Kulakova AN, Cooley NA, McGrath JW. (2007). New ways to break an old bond: the bacterial carbon-phosphorus hydrolases and their role in biogeochemical phosphorus cycling. *Environmental Microbiology* **9:** 2392–2400.

Reiswig HM. (1971). Particle feeding in natural populations of three marine Demosponges. *Biol Bull* **141:** 568–591.

Reiswig HM. (1974). Water transport, respiration and energetics of three tropical marine sponges. *J Exp Mar Biol Ecol* **14:** 231–249.

Riesenfeld CS, Murray AE, Baker BJ. (2008). Characterization of the microbial community and polyketide biosynthetic potential in the palmerolide-producing tunicate *Synoicum adareanum*. *J Nat Prod* **71:** 1812–1818.

Rocap G, Larimer FW, Lamerdin J, Malfatti S, Chain P, Ahlgren NA *et al.* (2003). Genome divergence in two *Prochlorococcus* ecotypes reflects oceanic niche differentiation. *Nature* **424:** 1042–1047.

Rupert EE, Barnes RD. (1996). *Invertebrate zoology*, 6th edn. Saunders College Publishing: Fort Worth, TX.

Rypien KL, Ward JR, Azam F. (2010). Antagonistic interactions among coral-associated bacteria. *Environ Microbiol* **12:** 28–39.

Saier MH. (2006). Protein secretion and membrane insertion systems in gram-negative bacteria. *J Membrane Biol* **214:** 75–90.

Santos OCS, Pontes PVML, Santos JFM, Muricy G, Giambiagi-deMarval M, Laport MS. (2010). Isolation, characterization and phylogeny of sponge-associated bacteria with antimicrobial activities from Brazil. *Res Microbiol* **161:** 604–612.

Schut F, Prins RA, Gottschal JC. (1997). Oligotrophy and pelagic marine bacteria: facts and fiction. *Aquat Microb Ecol* **12:** 177–202.

Schwedt A. (2007). Charakterisierung des dominanten Begleitorganismus eines marinen *Beggiatoa*-Konsortiums. Diploma thesis, Universität Hannover, Hannover.

Schwedt A. (2011). Physiology of a marine *Beggiatoa* strain and the accompanying organism *Pseudovibrio* sp. - a facultatively oligotrophic bacterium. Ph.D thesis, Universität Bremen, Bremen.

Sertan-de Guzman AA, Predicala RZ, Bernardo EB, Neilan BA, Elardo SP, Mangalindan GC *et al.* (2007). *Pseudovibrio denitrificans* strain Z143-1, a heptylprodigiosin-producing bacterium isolated from a Philippine tunicate. *FEMS Microbiol Lett* **277:** 188–196.

Shieh WY, Lin YT, Jean WD. (2004). *Pseudovibrio denitrificans* gen. nov., sp. nov., a marine, facultatively anaerobic, fermentative bacterium capable of denitrification. *Int J Syst Evol Microbiol* **54:** 2307–2312.

Sipkema D, Osinga R, Schatton W, Mendola D, Tramper J, Wijffels RH. (2005). Large-scale production of pharmaceuticals by marine sponges: sea, cell, or synthesis? *Biotechnol Bioeng* **90:** 201–222.

Smith DC, Simon M, Alldredge AL, Azam F. (1992). Intense hydrolytic enzyme activity on marine aggregates and implications for rapid particle dissolution. *Nature* **359:** 139–142.

Sultan SZ, Silva AJ, Benitez JA. (2010). The PhoB regulatory system modulates biofilm formation and stress response in El Tor biotype *Vibrio cholerae*. *FEMS Microbiol Lett* **302:** 22–31.

Taylor MW, Radax R, Steger D, Wagner M. (2007). Sponge-associated microorganisms: evolution, ecology, and biotechnological potential. *Microbiol Mol Biol Rev* **71:** 295–374.

Thakur NL, Hentschel U, Krasko A, Pabel CT, Anil AC, Muller WEG. (2003). Antibacterial activity of the sponge *Suberites domuncula* and its primmorphs: potential basis for epibacterial chemical defense. *Aquat Microb Ecol* **31:** 77–83.

Thakur NL, Perovic-Ottstadt S, Batel R, Korzhev M, Diehl-Seifert B, Müller IM *et al.* (2005). Innate immune defense of the sponge *Suberites domuncula* against gram-positive bacteria: induction of lysozyme and AdaPTin. *Mar Biol* **146:** 271–282.

Thiel V, Imhoff JF. (2003). Phylogenetic identification of bacteria with antimicrobial activities isolated from Mediterranean sponges. *Biomol Eng* **20:** 421–423.

Thoms C, Horn M, Wagner M, Hentschel U, Proksch P. (2003). Monitoring microbial diversity and natural product profiles of the sponge *Aplysina cavernicola* following transplantation. *Mar Biol* **142:** 685–692.

Troisfontaines P, Cornelis GR. (2005). Type III secretion: more systems than you think. *Physiology* **20:** 326–339.

Tseng TT, Tyler BM, Setubal JC. (2009). Protein secretion systems in bacterial-host associations, and their description in the Gene Ontology. *BMC Microbiol* **9:** S2.

Vacelet J, Donadey C. (1977). Electron microscope study of the association between some sponges and bacteria. *J Exp Mar Biol Ecol* **30:** 301–314

Van Mooy BAS, Rocap G, Fredricks HF, Evans CT, Devol AH. (2006). Sulfolipids dramatically decrease phosphorus demand by picocyanobacteria in oligotrophic marine environments. *Proc Natl Acad Sci U S A* **103:** 8607–8612.

Van Mooy BAS, Fredricks HF, Pedler BE, Dyhrman ST, Karl DM, Koblížek M *et al.* (2009). Phytoplankton in the ocean use non-phosphorus lipids in response to phosphorus scarcity. *Nature* **458:** 69–72.

Vershinina OA, Znamenskaya LV. (2002). The Pho regulons of bacteria. *Microbiology* **71:** 497–511.

Vizcaino MI. (2011). The chemical defense of *Pseudopterogorgia americana*: a focus on the antimicrobial potential of a *Pseudovibrio* sp. Ph.D thesis, Medical University of South Carolina, Charleston.

Wanner BL. (1993). Gene regulation by phosphate in enteric bacteria. *J Cell Biochem* **51:** 47–54.

Webster NS, Hill RT. (2001). The culturable microbial community of the Great Barrier Reef sponge *Rhopaloeides odorabile* is dominated by an α-proteobacterium. *Mar Biol* **138:** 843–851.

Wehrl M, Steinert M, Hentschel U. (2007). Bacterial uptake by the marine sponge *Aplysina aerophoba*. *Microb Ecol* **53:** 355–365.

White AE. (2009). New insights into bacterial acquisition of phosphorus in the surface ocean. *Proc Natl Acad Sci U S A* **106:** 21013–21014.

White AK, Metcalf WW. (2007). Microbial metabolism of reduced phosphorus compounds. *Annu Rev Microbiol* **61:** 379–400.

Whitman WB, Coleman DC, Wiebe WJ. (1998). Prokaryotes: the unseen majority. *Proc Natl Acad Sci U S A* **95:** 6578–6583.

Wiens M, Korzhev M, Krasko A, Thakur NL, Perovic-Ottstadt S, Breter HJ *et al.* (2005). Innate immune defense of the sponge *Suberites domuncula* against bacteria involves a MyD88-dependent signaling pathway: induction of a perforin-like molecule. *J Biol Chem* **280:** 27949–27959.

Wilkinson CR, Fay P. (1979). Nitrogen fixation in coral reef sponges with symbiotic cyanobacteria. *Nature* **279:** 527–529.

Wu JF, Sunda W, Boyle EA, Karl DM. (2000). Phosphate depletion in the western North Atlantic Ocean. *Science* **289:** 759–762.

Young CL, Ingall ED. (2010). Marine dissolved organic phosphorus composition: insights from samples recovered using combined electrodialysis/reverse osmosis. *Aquatic Geochemistry* **16:** 563–574.

Zavaleta-Pastor M, Sohlenkamp C, Gao JL, Guan ZQ, Zaheer R, Finan TM *et al.* (2010). *Sinorhizobium meliloti* phospholipase C required for lipid remodeling during phosphorus limitation. *Proc Natl Acad Sci U S A* **107:** 302–307.

Zeleznick LD, Myers TC, Titchener EB. (1963). Growth of *Escherichia coli* on methyl- and ethylphosphonic acids. *Biochim Biophys Acta* **78:** 546–547.

Chapter II

The genus *Pseudovibrio* contains metabolically versatile and symbiotically interacting bacteria

Vladimir Bondarev[1] , Michael Richter[2], Jörn Piel[3], Stefano Romano[1], Anne Schwedt[1] and Heide N. Schulz-Vogt[1]

[1]Max Planck Institute for Marine Microbiology, Ecophysiology Group, Celsiusstr. 1, D-28359 Bremen, Germany

[2]Max Planck Institute for Marine Microbiology, Microbial Genomics and Bioinformatics Research Group, Celsiusstr. 1, D-28359 Bremen, Germany

[3]Kekulé-Institut für Organische Chemie und Biochemie, Gerhard-Domagk Str. 1, D-53121 Bonn, Germany

The manuscript has been submitted to the journal *Environmental Microbiology*

Contributions:

The concept of this study was developed together with H. N. Schulz-Vogt. I performed the manual annotation of the genome with the help of M. Richter. I performed the physiological experiments. The manuscript was written in collaboration with H. N. Schulz-Vogt including comments of all co-authors.

Abstract

The majority of strains belonging to the genus *Pseudovibrio* have been isolated from marine invertebrates like tunicates, corals and especially sponges, but the physiology of these bacteria is poorly understood. In this study, we analyze the genomes of two *Pseudovibrio* strains. One is a required symbiont of a cultivated *Beggiatoa* strain, a sulfide oxidizing, autotrophic bacterium. The other one was isolated from a sponge (Enticknap *et al.*, 2006). The data show that both strains are generalistic bacteria capable of importing and oxidizing a wide range of organic and inorganic compounds to meet their carbon, nitrogen, phosphorous and energy requirements under oxic and anoxic conditions. Several physiological traits encoded in the genome were verified in laboratory experiments with a pure culture of the *Pseudovibrio* strain originally associated with *Beggiatoa*. Besides the versatile metabolic abilities of both *Pseudovibrio* strains, our study reveals a number of open reading frames and gene clusters in the genomes that seem to be involved in symbiont-host interactions. *Pseudovibrio* has the genomic potential to attach to host cells, might be capable of interacting with the eukaryotic cell machinery, produce secondary metabolites and may supply the host with cofactors.

Introduction

The first strain of the genus *Pseudovibrio* has been isolated from coastal seawater in 2004 and was described as *Pseudovibrio denitrificans* – a marine, heterotrophic, facultatively anaerobic bacterium capable of denitrification and fermentation (Shieh *et al.*, 2004). Two further type strains, *P. ascidiaceicola* (Fukunaga *et al.*, 2006) and *P. japonicus* (Hosoya and Yokota, 2007), were isolated from a tunicate and coastal seawater, respectively. Physiologically, these isolates were not notably different from *P. denitrificans*. Besides the three type strains, *Pseudovibrio* spp.-related bacteria have been found in various studies throughout the world either by 16S rRNA gene analysis or direct isolation methods (Hentschel *et al.*, 2001; Webster and Hill, 2001; Olson *et al.*, 2002; Thakur *et al.*, 2003; Thiel and Imhoff, 2003; Thoms *et al.*, 2003; Agogué *et al.*, 2005; Lafi *et al.*, 2005; Enticknap *et al.*, 2006; Koren and Rosenberg, 2006; Sertan-de Guzman *et al.*, 2007; Muscholl-Silberhorn *et al.*, 2008; Riesenfeld *et al.*, 2008; Kennedy *et al.*, 2009; Rypien *et al.*, 2010; Santos *et al.*, 2010). Interestingly, besides *P. denitrificans*, *P. japonicus*, and a *Pseudovibrio* spp.-related isolate from coastal, oligotrophic seawater (Agogué *et al.*, 2005), all other strains belonging to this genus discovered until today have been found closely associated with marine invertebrates like tunicates, corals, and sponges. Especially Porifera seem to harbor *Pseudovibrio* populations, e. g., as the dominating species of the culturable bacterial community (Webster and Hill, 2001; Muscholl-Silberhorn *et al.*, 2008). Additionally, *Pseudovibrio* has been found in sponge larvae as the most abundant prokaryote, indicating vertical transmission of these bacteria in their hosts (Enticknap *et al.*, 2006). Such a consistent pattern of *Pseudovibrio* spp. associated with sponges suggests that they are symbionts of those metazoa (Webster and Hill, 2001; Enticknap *et al.*, 2006). Whether the nature of this symbiosis is mutualistic/ commensalistic or whether *Pseudovibrio* spp. rather represent pathogens/parasites is uncertain, but the fact that *Pseudovibrio* spp. have been isolated only from healthy sponges indicates that the bacteria do not harm the host and might be even required for its health (Webster and Hill, 2001). Another shared feature is the production of secondary metabolites by many of the cultured *Pseudovibrio* strains. For instance, heptylprodigiosin, a compound that exhibits antimicrobial activity, was isolated from a pure culture of *P. denitrificans* Z143-1 (Sertan-de Guzman *et al.*, 2007) and the production of additional bioactive compounds could be shown in several other studies (Hentschel *et al.*, 2001; Muscholl-Silberhorn *et al.*, 2008; Kennedy *et al.*, 2009; Santos *et al.*, 2010).

Despite the fact that members of the genus *Pseudovibrio* seem to be ubiquitous and important associates of marine invertebrates and are also found free-living, very little is known about the physiology and interactions with the host. In this study, we analyze the genomes of two *Pseudovibrio* strains. *Pseudovibrio* sp. FO-BEG1 has been isolated from an enrichment culture of a *Beggiatoa* strain, a filamentous, sulfide oxidizing bacterium (Brock and Schulz-Vogt, 2011; Schwedt, 2011). Initially, this *Beggiatoa* strain was sampled from a coral suffering from the black band disease off the coast of Florida, which indicates that the strain *Pseudovibrio* FO-BEG1 could have been associated with the coral at the time of sampling – either in a commensalistic/mutualistic or pathogenic relationship – and is now available as an axenic culture in our lab. Intriguingly, strain FO-BEG1 is also maintained in a co-culture with a *Beggiatoa* sp., which seems to be unable to grow without *Pseudovibrio* and is therefore dependent on strain FO-BEG1. The second strain, *Pseudovibrio sp.* JE062, has been isolated in Florida from the sponge *Mycale laxissima* in the year 2006 and was described as a sponge symbiont by Enticknap *et al.* (2006). The analysis of these genomes gives us an insight into the physiological and symbiotic potential of both *Pseudovibrio* strains and reveals fascinating microorganisms that seem to be adapted to free-living and symbiotic life styles.

Materials and Methods

Growth conditions

For aerobic growth CM medium modified after Shieh *et al.* (2004) was used. After autoclaving, the medium was supplemented with K_2HPO_4 (1.15 mmol l^{-1}), glucose (10 mmol l^{-1} unless stated otherwise), 1 ml l^{-1} tungsten/selenium solution (Brysch *et al.*, 1987), 1 ml l^{-1} trace elements (Widdel and Pfennig, 1984), and 1 ml l^{-1} of four vitamin solutions prepared according to Aeckersberg *et al.* (1991). For measurement of SO_4^{2-} evolution during $S_2O_3^{2-}$ oxidation, 10 mmol l^{-1} $Na_2S_2O_3 \cdot 5\ H_2O$ and 5 mmol l^{-1} glucose were added and 2 g l^{-1} K_2SO_4 from the original recipe was replaced with 0.75 g l^{-1} KCl. To compare growth between a culture with and without $Na_2S_2O_3$, K_2SO_4 was not omitted from the medium and glucose and $Na_2S_2O_3 \cdot 5\ H_2O$ were used in the same concentrations as described above. To investigate the growth with 4-hydroxybenzoic acid and benzoate, both compounds were added in a concentration of 2 mmol l^{-1}, respectively, without any other carbon source. Growth with phosphonoacetate (1 mmol l^{-1}) as phosphorus source was tested by adding this compound as the only phosphorus source and all vitamins were omitted from the medium. For fermentation and denitrification experiments under anoxic conditions, aged

North Sea water was buffered with 50 mmol l^{-1} TRIS, supplemented with NH_4Cl (10 mmol l^{-1}) and the pH adjusted to 8. Preparation of the medium was performed according to Widdel and Bak (1992) in order to prepare the medium anoxically. Cooling was performed under N_2 atmosphere, except for experiments in which N_2 production was measured, in which Ar was used as the atmosphere instead. After autoclavation, the medium was supplemented with 10 mmol l^{-1} glucose, 1 ml l^{-1} tungsten/selenium solution, 1 ml l^{-1} trace elements and 1 ml l^{-1} of four vitamin solutions prepared as described above. $NaNO_3$ (10 mmol l^{-1}) was added for experiments investigating denitrification. To test CO oxidation, CM medium was prepared as described above, containing 400 µmol l^{-1} glucose and supplied with 500 p.p.m. CO to the bottle headspace. For aerobic growth experiments, 250 ml Erlenmeyer flasks were filled with 100 ml medium. For anaerobic growth, 156 ml serum bottles (Wheaton, Millville, USA) were filled anoxically with 50 ml medium and closed with butyl rubber stoppers. For all experiments, 0.1% or 0.5% of a preculture grown aerobically in CM medium was used as inoculum. All growth experiments were performed with *Pseudovibrio* sp. FO-BEG1 in triplicates at 28°C in the dark with shaking at 110 rpm.

Chemical analyses

Bacterial growth was monitored as the optical density ($OD_{600\ nm}$) using an Eppendorf BioPhotometer (Eppendorf AG, Hamburg, Germany). SO_4^{2-} was measured with a Metrohm 761 Compact IC with conductivity detector (Metrohm AG, Herisau, Switzerland) equipped with a Metrosep A Supp 5-100 column with a carbonate eluent (3.2 mmol l^{-1} Na_2CO_3/ 1 mmol l^{-1} $NaHCO_3$ in deionised water) at a flow rate of 0.7 ml min^{-1}. Tetrathionate was measured according to Kamyshny (2009). Glucose and organic acids were determined using a HPLC system (Sykam GmbH) equipped with an anion neutral pre-column (4x20 mm; Sykam GmbH) and an Aminex HPX-87H separation column (300x7.8 mm; Biorad, Munich, Germany) at a temperature of 60 °C. The eluent consisted of 5 mM H_2SO_4 in HPLC-grade water with a flow rate of 0.6 ml min^{-1}. Quantification of glucose, succinate, lactate, formate, acetate, propionate and ethanol was performed with the 7515A RI detector (ERC, Riemerling, Germany); pyruvate was measured with the Sapphire UV-Vis detector at 210 nm (Ecom, Praha, Czech Republic). NO_3^- was quantified with a HPLC system (Sykam GmbH, Eresing, Germany) containing an anion neutral pre-column (4x20 mm; Sykam GmbH) and an IBJ A3 anion separation column (4x60 mm; Sykam GmbH) with a column temperature of 50 °C. The eluent consisted of 25 mmol l^{-1} NaCl and 45% ethanol in deionised water with a flow rate of 1 ml min^{-1}. Detection of NO_3^- was conducted with Linear Uvis 200 (Thermo Fischer

Scientific GmbH, Dreieich, Germany) at 220 nm. N_2 was measured as described by Zedelius *et al.* (2011). CO determination was conducted with a Shimadzu GC-8A (Shimadzu, Duisburg, Germany) gas chromatograph with a Molecular Sieve 5A column (80 to 100; 0.125 in. by 2 m; Restek, Bellefonte, USA) at a flow of 20 ml of synthetic air per minute at 40°C and an RGD2 reduction gas detector (Trace Analytical, Menlo Park, USA).

DNA extraction and sequencing

DNA was extracted from strain FO-BEG1 using the Fast DNA SPIN Kit for Soil (MP Biomedicals LLC, Illkirch, France), according to manufacturers' instructions. 454 sequencing was conducted by LGC Genomics GmbH with a 454 GS FLX System. The Newbler 2.0.00.22 software was used for sequence assembly and quality assessment. Overall, 522919 sequenced reads with an average length of 336.30 bp lead to a 29-fold sequence coverage. In order to close the gaps, a fosmid library with a 1.5-fold physical coverage was created and used for direct sequencing of the fosmid clones. For the residual gaps, 96 specific primers were designed and used for combinatorial PCR on DNA level, the products of which were sequenced via the Sanger method.

Gene prediction, annotation and data mining

Gene prediction was carried out by using the software Glimmer3 (Delcher *et al.*, 2007). Ribosomal RNA genes were detected by using the RNAmmer 1.2 software (Lagesen *et al.*, 2007) and transfer RNAs by tRNAscan-SE (Lowe and Eddy, 1997). Annotation was performed by using the GenDB, version 2.2 system (Meyer *et al.*, 2003), supplemented by the tool JCoast, version 1.6 (Richter *et al.*, 2008). For each predicted open reading frame (ORF) observations have been collected from similarity searches against sequence databases NCBI-nr, Swiss-Prot, KEGG and genomesDB (Richter *et al.*, 2008) and for protein family databases from Pfam (Bateman *et al.*, 2004) and InterPro (Mulder *et al.*, 2005). SignalP has been used for signal peptide predictions (Bendtsen *et al.*, 2004) and TMHMM for transmembrane helix-analysis (Krogh *et al.*, 2001). Predicted protein coding sequences were automatically annotated by the in-house software MicHanThi (Quast, 2006). The MicHanThi software predicts gene functions based on similarity searches using the NCBI-nr (including Swiss-Prot) and InterPro database. The annotation of proteins highlighted within the scope of this study was subject of manual inspection. For all observations regarding putative protein functions, an E value cutoff of 10^{-4} was considered.

Comparison of the shared gene content by reciprocal best matches (RBMs) and functional classification with Kyoto encyclopedia of genes and genomes (KEGG)

Determination of the shared gene content has been performed by a BLAST all versus all search between FO-BEG1 and JE062. Reciprocal best matches were counted by a BLAST result with an E value $<1e^{-5}$ each and a subject coverage of over 65%. For metabolic pathway identification, genes were searched for similarity against the KEGG database. A match was counted if the similarity search resulted in an expectation E value below $1e^{-5}$. All occurring KO (KEGG Orthology) numbers were mapped against KEGG pathway functional hierarchies and statistical analyzed.

Functional classification with cluster of orthologous groups (COG) and calculation of the Average nucleotide identity (ANI)

All predicted ORFs were also searched for similarity against the COG database (Tatusov *et al.*, 2003). A match was counted if the similarity search resulted in an E value below $1e^{-5}$. ANI between the whole-genome sequences of strain FO-BEG1 and the draft genome sequences of strain JE062 was determined by using the *in silico* DNA-DNA hybridization method of the JSpecies (Richter and Rosselló-Móra, 2009) software with default parameters.

Creation of circular genome maps and prediction of ABC and TRAP type transporters

Comparative circular genome maps of the RBMs shared between JE062 and FO-BEG1 have been drawn by using JCoast's plugin for CGView (Stothard and Wishart, 2005). Circular GC-plot and GC-skew representation has been drawn by using DNAPlotter (Carver *et al.*, 2009). As initial step for the identification of the ABC transporters, genes containing the Pfam domain ABC_tran (PF00005) were detected in the genome of strain FO-BEG1. For the identification of the permease and the periplasmic binding protein, the close proximity of genes containing the ABC_tran domain was searched. Only ABC systems with at least one ABC_tran domain, one permease and one periplasmic binding protein were regarded as functioning ABC transporters and substrate specificity was predicted from the annotations of the subunits. In several cases, one subunit (e.g. the permease) was missing in close proximity of genes with the ABC_tran domain. In this case, a single permease gene located on any place in the genome with the same substrate specificity prediction but not belonging to any complete ABC system, was used to complement the transporter system. TRAP transporters were regarded as complete when the subunits DctM, DctQ and DctP were present in close

proximity. When two subunits were identified in close proximity and the third was missing, the single subunit located on any place in the genome not belonging to any complete TRAP system was used to complement the transporter system. In the case of fusion of the DctQ and M subunits in one gene, only the DctP subunit was required to complete the transporter.

Accession numbers

The genome shotgun project of strain FO-BEG1 has been deposited at DDBJ/EMBL/GenBank under the accession number CP003147 for the chromosome and CP003148 for the plasmid. The draft genome sequence of strain JE062 has the DDBJ/EMBL/GenBank accession number ABXL00000000.

Results and Discussion

General genome characteristics

The genome size of strain FO-BEG1 is 5.9 Mbp, including a large plasmid of 0.4 Mbp (**Figure 2.1**). The circular chromosome of 5.5 Mbp contains a large stretch of repeats at position 2,707,040. This area of unknown size could not be bridged with a direct sequencing approach despite the presence of this area on a fosmid, indicating strong secondary structures, and has been masked with the ambiguous nucleotide code 'N'. The G+C content is 52.5 mol% and is consistent with the known values of the described *Pseudovibrio* isolates (Shieh *et al.*, 2004; Fukunaga *et al.*, 2006; Hosoya and Yokota, 2007). Altogether, we found 5,478 ORFs, 398 of which were located on the plasmid, which correspond to about 87% of encoding DNA. Six complete rRNA operons and 69 tRNA encoding regions were annotated, indicating the capability of a quick response to changing conditions and fast growth when nutrients are available. The genome of strain JE062 has not been closed, but there are 19 contigs available with an overall size of 5.7 Mbp, 5,225 ORFs and 52.4 mol% GC content, which is almost identical to the genome of strain FO-BEG1 (**Figure 2.1A and B**). It contains 72 tRNA genes and seven complete rRNA operons. Unfortunately, the repeat-rich area that could not be sequenced in the genome of strain FO-BEG1 shows an ambiguous sequence in strain JE062 as well, and could therefore not be used to close the gap in FO-BEG1.

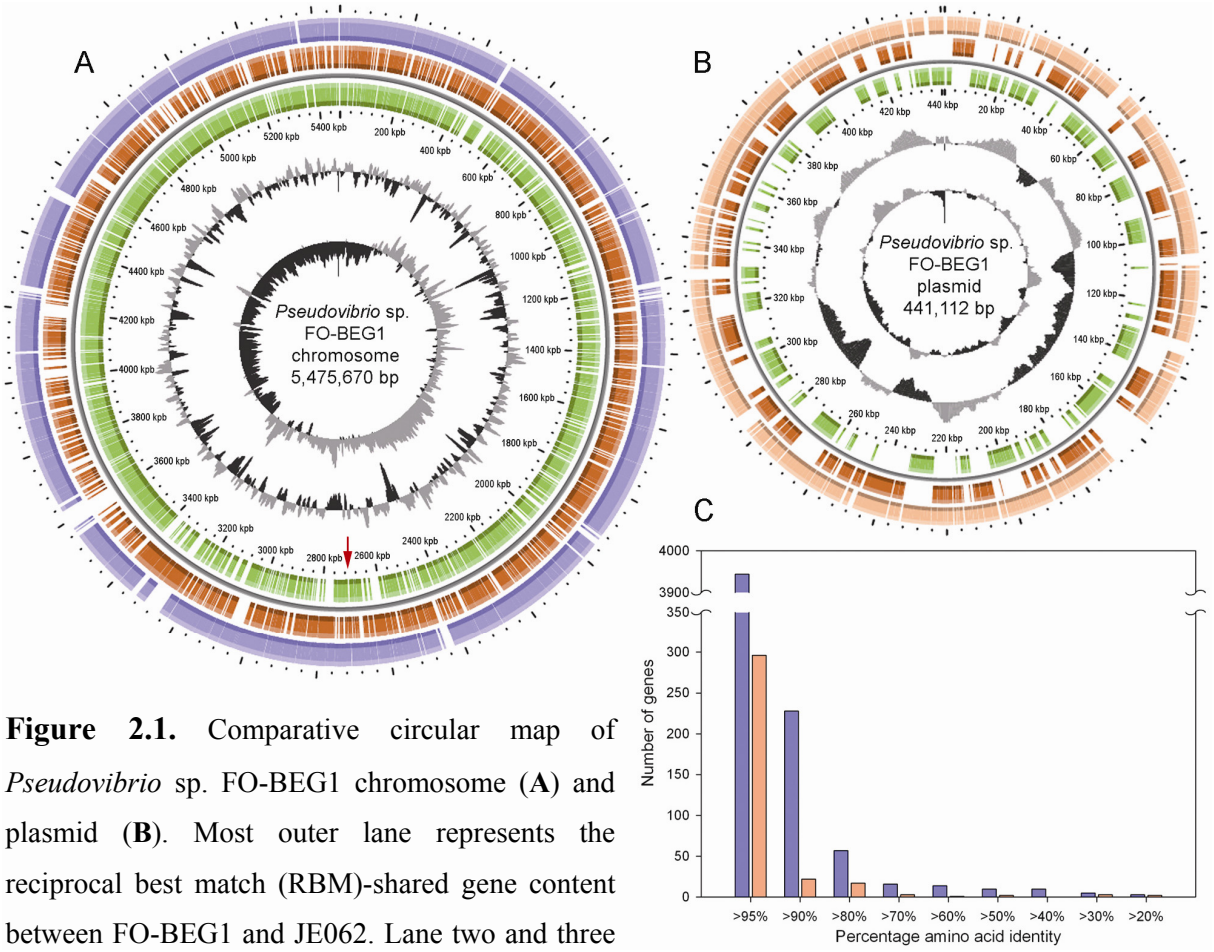

Figure 2.1. Comparative circular map of *Pseudovibrio* sp. FO-BEG1 chromosome (**A**) and plasmid (**B**). Most outer lane represents the reciprocal best match (RBM)-shared gene content between FO-BEG1 and JE062. Lane two and three represent all predicted open reading frames (ORFs) on the lagging (red) and leading (green) strands. The two inner lanes display the GC-plot and the GC-skew. The red arrow indicates the area of unknown size that could not be closed during sequencing. The bar chart (**C**) express the amino acid percentage identity of each RBM shared gene-content between FO-BEG1 and JE062. The blue bar is representing the FO-BEG1 chromosome and orange the corresponding plasmid.

Even though the genome of JE062 is not completely closed we assume that it also contains a plasmid with similar content, since most of the genes identified on the plasmid of FO-BEG1 were allocated in the genome of JE062 (**Figure 2.1B**). **Table 2.1** shows an overview of the genome characteristics of both strains as well as the assignment of the genes to COGs. The shared gene content between FO-BEG1 and the draft genome of JE062 comprises 84.4% (4,287 ORFs, **Figure 2.1C**). An ANI analysis conducted between strains FO-BEG1 and JE062 revealed a 94.5% ANIb (87% genome alignment) and 95.4% ANIm (86% genome alignment) value. The values are in the range of the proposed species definition boundary (Richter and Rosselló-Móra, 2009) indicating a species level degree of similarity.

Table 2.1. General genome features of *Pseudovibrio* sp. FO-BEG1 and JE062, including categorization of the genes into cluster of orthologous group (COG) categories.

Characteristics	FO-BEG1	JE062
Base pairs	5,916,782	5,726,521
G+C content (%)	52.5	52.4
No. of protein-coding genes	5,478	5,225
Percent coding	85.5	85
No. of rRNA operons	6	7
No. of tRNA genes	69	72
COG category		
[J] Translation, ribosomal structure and biogenesis	196	190
[K] Transcription	387	367
[L] Replication, recombination and repair	135	125
[D] Cell cycle control, cell division, chromosome partitioning	21	20
[T] Signal transduction mechanism	138	140
[M] Cell wall/membrane/envelope biogenesis	190	176
[N] Cell motility	153	149
[O] Posttranslational modification, protein turnover, chaperones	135	127
[C] Energy production and conversion	245	245
[G] Carbohydrate transport and metabolism	323	311
[E] Amino acid transport and metabolism	507	492
[F] Nucleotide transport and metabolism	99	92
[H] Coenzyme transport and metabolism	185	181
[I] Lipid transport and metabolism	148	142
[P] Inorganic ion transport and metabolism	291	287
[Q] Secondary metabolites biosynthesis, transport and catabolism	210	204
[R] General function prediction only	598	576
[S] Function unknown	281	272

Physiology

In both genomes we found a number of genes that indicate high metabolic variety of *Pseudovibrio* FO-BEG1 and JE062. Degradation of carbohydrates is most likely performed via the Entner-Doudoroff pathway, which is present in both genomes, due to absence of the phosphofructokinase (PFK), a key enzyme of the glycolysis (Emden-Meyerhoff-Parnas), which is a regularly encountered phenomenon within marine *α-Proteobacteria* (Fürch *et al.*, 2009; Tang *et al.*, 2009; Williams *et al.*, 2009). Besides the PFK, all other enzymes involved in glycolysis can be identified in both genomes, including fructose-1,6-bisphosphatase I, the key enzyme for glyconeogenesis, indicating that the Emden-Meyerhoff-Parnas pathway can

be used for anabolic purposes (**Table S 2.1**). Genes encoding all enzymes of the citric acid cycle and pentose phosphate pathway are present. Additionally, both strains have the genetic potential to degrade aromatic compounds via the β-ketoadipate pathway, which we demonstrated by growing *Pseudovibrio* sp. FO-BEG1 with 4-hydroxybenzoate as the only carbon and energy source under aerobic conditions (**Figure S 2.1A**). Benzoate, however, was not degraded, indicating that either the uptake of benzoate is detained or the hydroxylation of the aromatic ring structure cannot be performed by *Pseudovibrio* FO-BEG1. Under anoxic conditions without nitrate, strain FO-BEG1 metabolized glucose in mixed acid type fermentation, as suggested by the present genes in both strains (**Table S 2.1**), resulting in acidification of the medium and formation of mainly formate, lactate, acetate, and ethanol. Ethanol production during fermentation has not been described for any *Pseudovibrio* strain yet. Additionally, pyruvate, propionate, and succinate have been formed, but to a lesser extent (**Figure S 2.2A**). Production of trace amounts of fumarate was detected, but could not be quantified. As expected, we found the complete set of genes essential for denitrification, including a membrane-bound (*nar*) and a periplasmic nitrate reductase (*nap*). In agreement, we observed a complete denitrification to N_2 in laboratory experiments with strain FO-BEG1 (**Table S 2.1** and **Figure S 2.2C**). For the type strain *P. denitrificans*, simultaneous denitrification and fermentation was described by Shieh *et al*. (2004) and could be confirmed in our experiments for strain FO-BEG1 with acetate, formate, lactate, and ethanol as the main fermentation products (**Figure S 2.2B**). No genes for assimilatory nitrate reduction could be identified in the genome. A set of *sox* genes suggests that both bacteria can use reduced inorganic sulfur compounds as a source of energy to complement heterotrophy. We could show experimentally that the addition of thiosulfate to the medium enhances the aerobic growth of the *Pseudovibrio* sp. FO-BEG1 culture and sulfate is produced over the incubation period (**Figure S 2.1B and C**). No tetrathionate could be measured as an intermediate (results not shown). Therefore, we propose that thiosulfate is oxidized completely to sulfate without any intermediates, as it is known for the typical Sox pathway in α-*Proteobacteria* (for review, see Ghosh and Dam, 2009). We identified genes encoding a small (*cutS*), medium (*cutM*) and large (*cutL*) subunit of the aerobic form II carbon monoxide dehydrogenase (CODH) with the accessory gene *coxG* in the operon (**Table S 2.1**), indicating the capability of CO oxidation. However, uptake of CO could not be demonstrated under tested conditions (results not shown). Interestingly, our results confirm the hypothesis from a recent publication testing CO oxidation in bacteria containing type II CODH genes (Cunliffe, 2011), in which none of the isolates containing only the type II variant was capable of CO oxidation. Only bacteria

containing the form I CODH have been shown to effectively oxidize CO, thereby questioning whether form II CODH is involved in the process of carbon monoxide oxidation, or if it has another primary function not known until now, as suggested by King and Weber (2007).

In both *Pseudovibrio* strains, we found genes for phosphonate import and degradation, which allows the bacteria to cleave the relatively stable C-P bonds of phosphonates (**Table S 2.1**). Thereby, they can metabolize a less accessible phosphorous pool in times of phosphate limitation. We could demonstrate growth of *Pseudovibrio* sp. FO-BEG1 with phosphonoacetate as the only source of phosphorous (**Figure S 2.3A**). Additionally, we could show adaptation of *Pseudovibrio* strain FO-BEG1 to oligotrophic conditions by culturing it with as little as 15 µmol C l^{-1} (0.18 mg C l^{-1}) dissolved organic carbon in the medium (Schwedt, 2011), which shows that *Pseudovibrio* FO-BEG1 is capable of growth under extreme nutrient depletion. The high metabolic variety of *Pseudovibrio* sp. FO-BEG1 and JE062 is also reflected in the analysis of encoded primary transporters. In the genome of strain FO-BEG1 we could identify 31 tripartite ATP-independent periplasmic (TRAP) type transporters (**Table S 2.2**) that are required for import of dicarboxylic acids like malate, succinate and fumarate, one of the highest numbers of TRAP type transporters reported in a genome of a marine prokaryote so far (Wagner-Döbler *et al.*, 2010). In strain JE062 we identified 27 TRAP transporters. Citric acid cycle intermediates seem therefore to be an important source of carbon and energy for the investigated *Pseudovibrio* strains. In addition, we reconstructed over 80 ATP-binding cassette (ABC) transporter systems with predicted substrate specificity from the genomic data of the strain FO-BEG1, including the plasmid, and over 70 ABC transporter systems for JE062 (**Table 2.2 and Table S 2.3**). Sugars, oligopeptides and amino acids are the main substrates that are imported via the ABC systems. A large number of transporters for oligopeptides and amino acids in combination with over 85 genes encoding peptidases and proteases (over 75 genes in strain JE062, see **Table S 2.4**) could help *Pseudovibrio* to hydrolyze complex particulate nutrients into oligopeptides and amino acids, which could serve as nutrition for both, the prokaryote and the host, as has been suggested by Siegl *et al*. (2011). Also iron seems to be an important trace element, for which we identified eight transporters including three siderophores and three transporters for hemin (**Table 2.2**).

Table 2.2. Identified ATP-binding cassette (ABC) and tripartite ATP-independent periplasmic (TRAP) transporters in the genomes of both *Pseudovibrio* strains and their putative functions.

Transporter type and proposed function	Transporters identified	
	FO-BEG1	**JE062**
TRAP transporter for dicarboxylates	**31**	**27**
ABC Transporter for:		
Sugars	**22**	**19**
Oligopeptides	**15**	**13**
Amino acids	**12**	**10**
Putrescine/spermidine	**5**	**5**
Glycerol 3-phosphate	**4**	**4**
Glycine betaine/L-proline	**3**	**3**
Glycine betaine/carnitine/ choline	**1**	**0**
Taurine	**1**	**1**
Thiamine	**1**	**1**
Urea	**1**	**1**
Nopaline	**1**	**1**
Hemin	**3**	**3**
Enterobactin	**1**	**1**
Ferrichrome	**1**	**1**
Anguibactin	**1**	**1**
Iron	**2**	**2**
Manganese/zinc	**2**	**2**
Molybdenum	**1**	**1**
Cobalt	**1**	**1**
Sulfonate	**2**	**2**
Phosphate	**1**	**1**
Phosphonate	**1**	**1**

Vitamin synthesis

Growth of pro- and eukaryotes highly depends on their requirements for cofactors that the organism can or cannot synthesize on its own. Vitamins are important for many different enzymatic processes and the synthesis of some vitamins is mainly accomplished by bacteria, making the prokaryotes a necessary part of the eukaryotic diet or an important partner in symbiotic relationships. The genomes of *Pseudovibrio* sp. FO-BEG1 as well as JE062 contain genes encoding key enzymes of the biosynthesis pathways of biotin (H), thiamin (B_1), pyridoxin (B_6), cobalamin (B_{12}), riboflavin (B_2), folic acid (B_9) and lipoic acid (**Table S 2.5**). Independence of an external vitamin supply was confirmed during aerobic growth in the defined CM medium without the addition of any vitamins, which implies *de novo* synthesis of

all required growth factors by strain FO-BEG1 under tested conditions (**Figure S 2.3B**). *Pseudovibrio* spp. would therefore be a beneficial companions for other prokaryotes or marine invertebrates, since the dependency on an external supply of those vitamins would be relieved.

Bioactive compounds

Symbiotic relationships between bacteria and marine invertebrates, especially sponges, are of special interest, because bacteria associated with sponges often produce novel bioactive compounds (Piel *et al.*, 2004; Taylor *et al.*, 2007; Fisch *et al.*, 2009). In the chromosome of *Pseudovibrio* FO-BEG1 we identified a genomic island of more than 50 kb containing among others a gene cluster of 20 genes predicted to be involved in secondary metabolite production (**Table S 2.6**). The cluster exhibits high sequence similarity to an architecturally almost identical hybrid nonribosomal peptide synthetase-polyketide synthase (NRPS-PKS) system previously reported from many pathogenic and commensal *Escherichia coli* strains (**Figure 2.2**) (Nougayrède *et al.*, 2006). The *E. coli* metabolite, termed colibactin, remains structurally uncharacterized. However, transposon mutagenesis of the gene cluster suggested that colibactin is a pathogenicity determinant that induces DNA double strand breaks in eukaryotic host cells, eventually resulting in cell death. The only significant difference between the gene clusters in *Pseudovibrio* FO-BEG1 and *E. coli* is an additional set of genes in the former, encoding putative transporters and the presence of a different phosphopantetheinyl transferase gene variant likely involved in generating *holo*-proteins from *apo* forms of PKSs and NRPSs (Lambalot *et al.*, 1996). In addition, two *E. coli* genes are fused in the *Pseudovibrio* cluster. Despite these differences, the architecture strongly suggests that the product of the FO-BEG1 cluster is colibactin, providing new opportunities to unveil the identity of this elusive and biomedically relevant compound. Interestingly, we find this more than 50 kb NRPS/PKS fragment only in *Pseudovibrio* sp. FO-BEG1 but not in the genome of strain JE062, with flanking regions downstream and upstream of the inserted fragment highly conserved in synteny in strain JE062 (data not shown), indicating that it has been acquired via horizontal gene transfer. Additionally, the plasmid of strain FO-BEG1 contained an ORF encoding a type III PKS of a size of 7.4 kb, which could also be detected in strain JE062 (**Table S 2.6**).

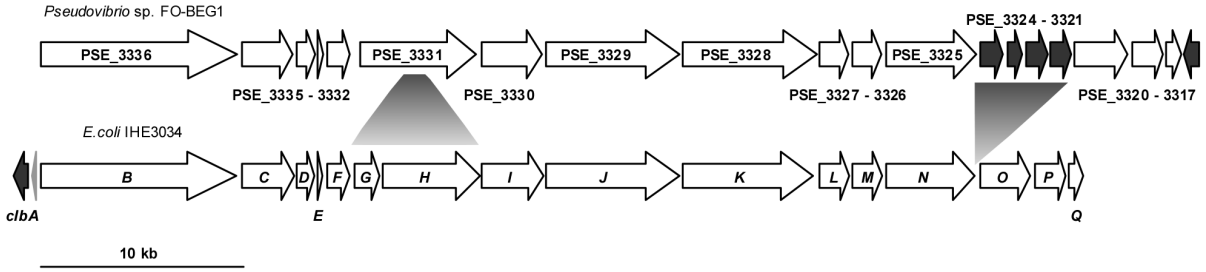

Figure 2.2. Nonribosomal peptide synthetase-polyketide synthase (NRPS-PKS) system in *Pseudovibrio* sp. FO-BEG1 and *Escherichia coli* strain IHE3034. White arrows represent the genes present in *Enterobacteriaceae* and strain FO-BEG1; black arrows represent the open reading frames (ORFs) present only in either *Enterobacteriaceae* or FO-BEG1 but presumably involved in the production of colibactin; the gray arrow shows a gene presumably not involved in the synthesis of colibactin. The symbol at ORF PSE_3331 represents a gene fusion of *E. coli* genes *clbG* and *clbH* in FO-BEG1; the symbol at PSE_3324-3321 represents gene insertion or deletion in strain FO-BEG1 or *E. coli* IHE3034, respectively.

DNA exchange and horizontal gene transfer

The genomes of both *Pseudovibrio* strains show a high metabolic variety. It is reasonable to assume that various genes were acquired via horizontal gene transfer from other microorganisms as is indicated e. g. by the presence of a 50 kb large NPRS-PKS island that can be found only in *Pseudovibrio* sp. FO-BEG1 but not in strain JE062, although both genomes are in general highly similar. In the genome of strain FO-BEG1 we identified a set of genes coding for a complete gene transfer agent (GTA) (in strain JE062 several genes were missing, see **Table S 2.6**), a unit best described as a virus. It harbors small parts of the host DNA and capable of injecting it into appropriate cells, without having negative effects on the host cell (for reviews see Lang and Beatty, 2001; Lang and Beatty, 2007). By this process, *Pseudovibrio* could have taken up and dispersed DNA carried in virus-like particles, thereby gathering genes and establishing a diverse physiology for a symbiotic and a free-living lifestyle. Additionally, we found 14 integrase and 21 transposase elements in the genome of *Pseudovibrio* sp. FO-BEG1 (**Table S 2.6**), 9 of which are located adjacent to the hybrid NRPS-PKS gene cluster, which verifies acquisition of this genomic island via horizontal gene transfer.

Quorum sensing

We could identify 15 genes in strain FO-BEG1 and 14 in strain JE062 containing the LuxR domain, which represents the transcriptional regulator of the acetylated homoserine lactone (AHL) type, allowing the bacterium to detect AHL quorum sensing molecules and to

initiate a response (**Table S 2.7**). Intriguingly, we could not find any *luxI* genes, which code for AHL quorum sensing molecules. This observation leads us to the hypothesis that both *Pseudovibrio* strains do not communicate via AHL within their own species, but seem to use the LuxR as receptors to react to quorum sensing molecules produced by other species and initiate a respective answer. Such a scenario has been described before by Case *et al*. (2008) and was called 'eavesdropping'. The response reaction could include the production of bioactive compounds to repel competing prokaryotes or to protect the host from pathogens or parasites. Alternatively, such LuxR-family 'solos' could participate in interkingdom signaling, as suggested by Subramoni and Venturi (2009), thereby facilitating prokaryote-host interactions of *Pseudovibrio* strains with marine invertebrates.

Growth with *Beggiatoa* sp. 35Flor

Pseudovibrio sp. FO-BEG1 is the single accompanying organism of the *Beggiatoa* strain 35Flor, which is growing in a chemolithoautotrophic sulfide-oxygen-gradient medium (Brock and Schulz-Vogt, 2011; Schwedt, 2011). All attempts to grow *Beggiatoa* without *Pseudovibrio* failed and so far we could not identify the factors required by the *Beggiatoa* strain for autonomous growth. It is known, however, that *Beggiatoa* spp. do not possess catalases (Larkin and Strohl, 1983) and therefore are susceptible to reactive oxygen molecules originating from respiration. Addition of catalase to the medium is known to increase the viability of *Beggiatoa* sp. (Burton and Morita, 1964). We hence hypothesize that *Beggiatoa* sp. 35Flor depends on the radical protection system exhibited by *Pseudovibrio* sp. FO-BEG1 including genes coding for over 20 superoxide dismutases, catalases and peroxidases (**Table S 2.4**). The role of heterotrophic bacteria as scavenger of reactive oxygen species has also been described by Morris *et al*. (2008), which could establish robust growth of cyanobacteria after addition of 'helper' heterotrophs.

Secretion Systems

In the genomes of FO-BEG1 and JE062 we could identify two loci that encode type VI secretion systems (T6SS) as well as one type III secretion system (T3SS) including effector molecules, which indicates the capability of specific interactions with eukaryotes and the possibility of influencing their cell machinery.

The T6SS has been described as a major secretion system in the context of pathogenicity as a virulence factor in morbific bacteria (Mougous *et al.*, 2006; Pukatzki *et al.*,

2006) and a core of 13 highly conserved and essential subunits has been identified for this secretion system (Boyer *et al.*, 2009). In both genomes of the *Pseudovibrio* strains, we found two gene clusters consisting of 12 (cluster I) and 20 (cluster II) genes that encode T6SSs. Cluster II contains the complete set of core subunits and therefore we assume that cluster II could, if expressed, produce a complete and functional type VI secretion system. In cluster I, two core genes are missing in the operon, *hcpI* and *vgrG*, which are main components of the injection apparatus with possible effector functions (Pukatzki *et al.*, 2009; Bönemann *et al.*, 2010). However, homologues of *hcpI* and *vgrG* could be identified in additional copies at other locations in the genomes of FO-BEG1 and JE062 (**Table S 2.8**), which is a phenomenon regularly found in genomes containing T6SS (Pukatzki *et al.*, 2009). The possible role for type VI secretion systems in bacteria has not been completely elucidated so far, but several functions have been attributed to it already. Mainly, T6SS is described as a virulence factor of pathogenic bacteria delivering effector proteins into host cells (Filloux *et al.*, 2008). However, further studies reveal the involvement of T6SS in biofilm formation (Aschtgen *et al.*, 2008), quorum sensing (Weber *et al.*, 2009), interbacterial interactions (Hood *et al.*, 2010) and antipathogenesis (Chow and Mazmanian, 2010; Jani and Cotter, 2010). In conclusion, it can be assumed that the T6SS of both strains are functional since the genomes contain the main structural components of the type VI secretion system.

In addition to the T6SS, we identified a type III secretion system in the genomes of both *Pseudovibrio* strains, which is located in a genomic region encompassing around 35 ORFs with various highly conserved proteins known from T3S systems (Cornelis and Van Gijsegem, 2000) (**Figure 2.3 and Table S 2.8**). Besides the secretion apparatus we also identified genes encoding homologues of three types of effector molecules in the genome of strain FO-BEG1 and two effector molecule types in strain JE062. Those effectors might be directly involved in the establishment of symbiosis between *Pseudovibrio* and its host. YpkA, IpgD (found in both genomes) and YopJ (only in strain FO-BEG1) are effector molecules that affect the cytoskeleton or the innate immune response of the host, respectively. YpkA is a serine/threonine kinase, which has negative effects on cytoskeletal dynamics due to its interaction with actin, thereby contributing to the resistance to phagocytosis (Cornelis, 2002). YpkA is present in three copies in both genomes. In Porifera, specialized amoeboid cells, the archaeocytes, resemble macrophages and eliminate non-self material via phagocytosis (Müller and Müller, 2003). *Pseudovibrio,* expressing and secreting the YpkA effector, could interfere with this process, preventing archaeocytes from digesting *Pseudovibrio* cells. A similar effect

could be induced by a homologue of IpgD found in both genomes, a virulence factor that is responsible for morphological changes of a host cell by increasing membrane detachment from the cytoskeleton (Niebuhr *et al.*, 2000; Niebuhr *et al.*, 2002).

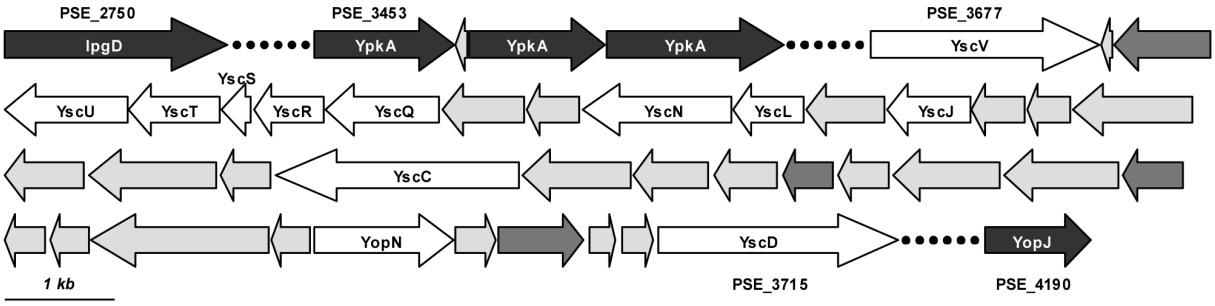

Figure 2.3. Operon coding for type III secretion system (T3SS) subunits and effector proteins. White arrows show annotated homologues of T3SS subunits including the gene name within the arrows; black arrows represent annotated effector homologues; dark gray arrows show annotated genes encoding proteins presumably not involved in T3SS; light gray arrows show hypothetical proteins with unknown function. The locus is indicated above and below some genes for orientation purposes.

In FO-BEG1 we additionally identified a homologue of the YopJ effector exhibiting a serine/threonine acetyltransferase function. By acetylation of serine and threonine residues of mitogen-activated protein (MAP) kinases it prevents phosphorylation of those molecules and therefore inhibits the innate immune response of the organism (Mukherjee *et al.*, 2006). Intriguingly, it has been shown that sponges possess a very efficient innate immune response system, using MAP kinases as the essential component of its response to bacterial endotoxin lipopolysaccharide (LPS) (Böhm *et al.*, 2001; Müller and Müller, 2003). This indicates that homologues of the acetyltransferase YopJ effector in *Pseudovibrio* could prevent phosphorylation of MAP kinases via acetylation, thereby playing a role in the inactivation of the immune answer of the host organism, allowing *Pseudovibrio* to avoid phagocytosis, as described by Bartsev *et al.* (2004) for a *Rhizobium* strain, and to remain in the host for establishment of a symbiosis. This hypothesis is further supported by the fact that a homologue of YopJ (NopJ) was shown to be an effector in symbiotic rhizobia (Deakin and Broughton, 2009) and Lackner *et al*. (2011) demonstrated that T3SS is involved in maintenance of a symbiosis between bacteria and fungi by enhancement of intracellular survival of the prokaryote within the host.

Adhesion

In both genomes we found homologues of genes coding for proteins responsible for adhesion to surfaces or other cells. These proteins, belonging to the group of amyloids, are

extracellular proteinaceous components and are known in Enterobacteriaceae as curli fibers. They are involved in adhesion to surfaces, cell aggregation, biofilm formation and mediate cell-cell adhesion and invasion of host cells (Barnhart and Chapman, 2006). The production of curli fibers in enteric bacteria is dependent on at least six proteins encoded by the operons *csgAB* and *csgDEFG (agf* in *Salmonella*) (Hammar *et al.*, 1995), the latter of which is required for assembly, stability and secretion of the amyloids (Hammar *et al.*, 1995). *csgAB* encodes the structural subunits of the curli fibers, both genes containing characteristic repeat motifs (Hammar *et al.*, 1996). A gene cluster in the genome of *Pseudovibrio* sp. FO-BEG1 resembles the curli formation operon in enteric bacteria (**Figure 2.4**).

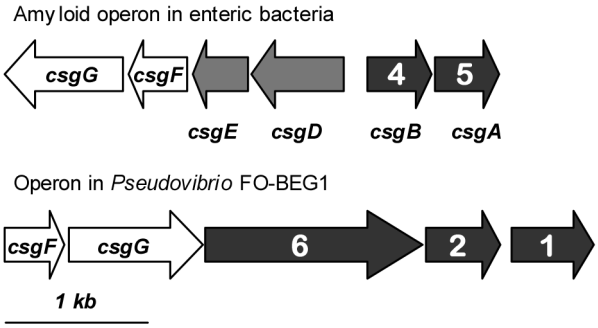

Figure 2.4. Comparison of genes encoding amyloids in Enterobacteriaceae and the operon in *Pseudovibrio* sp. FO-BEG1. White arrows represent homologues of genes in enteric bacteria; gray arrows show genes present in Enterobacteriaceae only; black arrows show genes containing curli repeats, typical motifs of the amyloid structural subunits. The number within the black arrows shows the amount of curli repeats in the according gene.

Homologues of *csgF* and *csgG*, required for stabilization and secretion of the amyloids are found in direct proximity to three genes containing curlin associated repeats as typical structural components of the curli fibers. We hypothesize that the identified operon might code for amyloid structures comparable to curli fibers due to the existence of characteristic curlin repeat motifs and genes involved in the assembly and secretion of such structures, therefore allowing *Pseudovibrio* to attach to other cells or form biofilms or aggregates. Additionally, we identified 35 genes in strain FO-BEG1 and 37 in JE062 containing domains mediating prokaryote-eukaryote interactions, supporting the proposed role of *Pseudovibrio* as a symbiont with possibilities to attach and interact with the host organism (**Table S 2.7**).

Conclusions

In this study, we analyzed highly similar genomes of two *Pseudovibrio* strains that originate from the coast of Florida, the *Pseudovibrio* sp. FO-BEG1 sampled from a coral and maintained over 10 years in co-culture with *Beggiatoa* sp. and *Pseudovibrio* sp. JE062 sampled from a sponge in the same region (Enticknap *et al.*, 2006). The physiology of both strains is extremely versatile and the metabolic traits found in the genome could be partially verified in experiments with strain FO-BEG1. Here, we describe for the first time a *Pseudovibrio* strain that uses aromatic compounds as a carbon and electron source, oxidizes thiosulfate under aerobic conditions and uses phosphonates as a phosphorous source. Notably, strain FO-BEG1 grows under extreme nutrient limitation, which emphasizes its adaptation to life in the open ocean. The metabolic variety is confirmed by the numerous transporter systems that are encoded in the genome. Compared with other marine bacteria, like the prominent *Roseobacter* clade, which is known to be ubiquitous, multitudinous and physiologically versatile (Newton *et al.*, 2010), *Pseudovibrio* seems to be capable of a similarly generalistic life style, exploiting quite a number of sources for energy, nutrients and trace elements.

Aside from metabolic variety, the genomic data of both strains also confirm close associations with marine invertebrates and indicate several potential mechanisms for establishing and maintaining a symbiosis. The most striking discovery is the presence of effector homologues secreted by type III secretion systems, which could affect sponges by interacting with their immune response system (YopJ) or the cytoskeleton (YpkA, IpgD) and thereby have a drastic impact on the cell machinery of the host. Another fascinating discovery is the presence of the hybrid NRPS-PKS system in strain FO-BEG1, which has so far only been described for members of the Enterobacteriaceae family (Putze *et al.*, 2009), producing the bioactive compound colibactin with yet unknown *in-vivo* functions, but arresting eukaryotic cells in the G_2 phase, eventually leading to cell death (Nougayrède *et al.*, 2006). The presence of a gene cluster coding for a cytopathic compound in strain FO-BEG1 emphasizes the impact that *Pseudovibrio* cells might have on marine invertebrates. Intriguingly, strain FO-BEG1 seems to be a required partner in the *Beggiatoa* co-culture, indicating its important symbiotic role not only for marine invertebrates but also for prokaryotes. It is possible that *Pseudovibrio* has positive effects for certain bacteria under *in-*

vivo conditions, e.g. by supplying vitamins or detoxifying metabolic intermediates or reactive oxygen species.

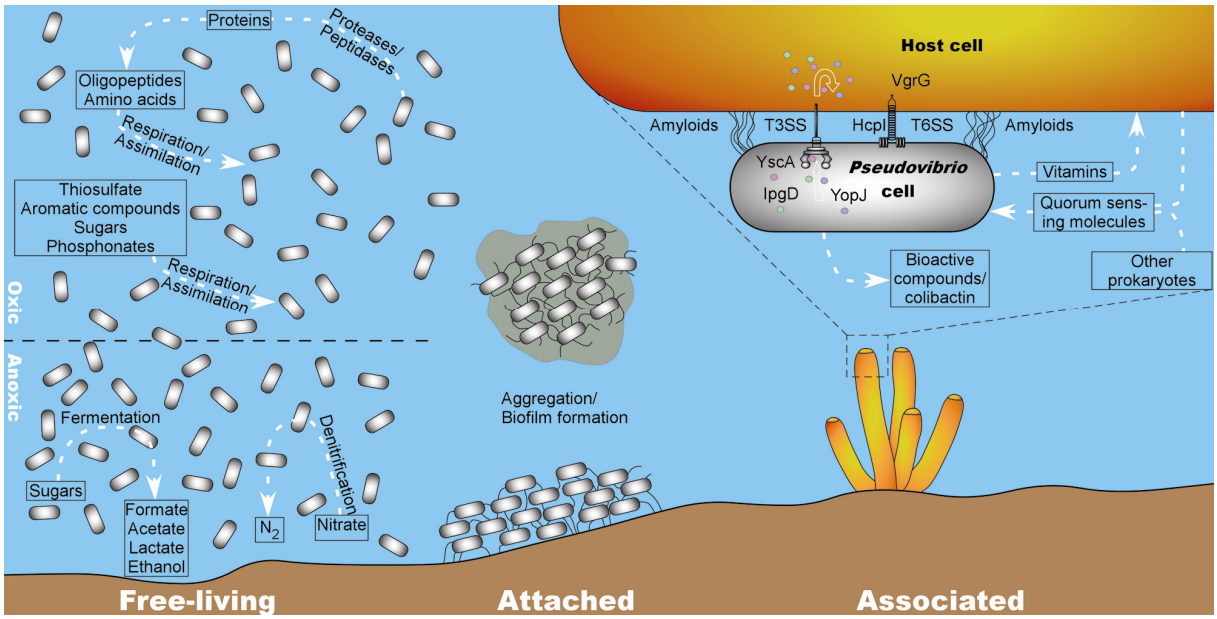

Figure 2.5. Schematic overview of the possible life styles and the physiologic capabilities derived from genetic information of both *Pseudovibrio* genomes. On the left hand side, physiologic abilities are depicted that could be used in free-living, oxic and anoxic conditions. On the right hand side, the attached or associated life style is illustrated. The host organism for the associated life style can be represented by a sponge, coral or tunicate. Biofilm formation, aggregation and attachment to host cells could be performed via e. g. amyloid-like structures. The proposed secretion systems could be involved in prokaryote-eukaryote interactions, influencing the cell machinery of the host. Additionally, *Pseudovibrio* could supply the host with cofactors like vitamins or synthesize secondary metabolites as a defense mechanism against other prokaryotes or the host.

The frequent identification and isolation of *Pseudovibrio* strains in many studies over the last years implies an important but rather unexplored role for this genus in marine habitats. According to the genomic and physiological data on *Pseudovibrio* spp., we propose a free-living and attached or associated life style model for this genus (**Figure 2.5**). As a denitrifying heterotroph, *Pseudovibrio* has an obvious influence on the carbon and nitrogen cycles. Its ecological impact can now be extended to the sulfur and phosphorus cycles due to its ability to metabolize thiosulfate and phosphonates. Additionally, we hypothesize that, due to the predictions based on the genomic data, similar to *E. coli* in humans, *Pseudovibrio* is a commensalistic or even beneficial symbiont of marine invertebrates with a potential to become pathogenic.

Acknowledgments

We thank A. Meyerdierks, M. Mußmann, and R. Amann for comments on the manuscript. For technical support, we thank M. Meyer, S. Menger, C. Probian, and R. Appel. We also thank A. Kamyshny for tetrathionate measurements and K. Imhoff for sulfate determination. This study was funded by the European Research Council and the Max Planck Society.

References

Aeckersberg F, Bak F, Widdel F. (1991). Anaerobic oxidation of saturated hydrocarbons to CO_2 by a new type of sulfate-reducing bacterium. *Arch Microbiol* **156:** 5–14.

Agogué H, Casamayor EO, Bourrain M, Obernosterer I, Joux F, Herndl GJ *et al.* (2005). A survey on bacteria inhabiting the sea surface microlayer of coastal ecosystems. *FEMS Microbiol Ecol* **54:** 269–280.

Aschtgen MS, Bernard CS, De Bentzmann S, Lloubès R, Cascales E. (2008). SciN is an outer membrane lipoprotein required for type VI secretion in enteroaggregative *Escherichia coli*. *J Bacteriol* **190:** 7523–7531.

Barnhart MM, Chapman MR. (2006). Curli biogenesis and function. *Annu Rev Microbiol* **60:** 131–147.

Bartsev AV, Deakin WJ, Boukli NM, McAlvin CB, Stacey G, Malnoe P *et al.* (2004). NopL, an effector protein of *Rhizobium* sp. NGR234, thwarts activation of plant defense reactions. *Plant Physiology* **134:** 871–879.

Bateman A, Coin L, Durbin R, Finn RD, Hollich V, Griffiths-Jones S *et al.* (2004). The Pfam protein families database. *Nucleic Acids Res* **32:** D138–D141.

Bendtsen JD, Nielsen H, von Heijne G, Brunak S. (2004). Improved prediction of signal peptides: SignalP 3.0. *J Mol Biol* **340:** 783–795.

Böhm M, Hentschel U, Friedrich AB, Fieseler L, Steffen R, Gamulin V *et al.* (2001). Molecular response of the sponge *Suberites domuncula* to bacterial infection. *Mar Biol* **139:** 1037–1045.

Bönemann G, Pietrosiuk A, Mogk A. (2010). Tubules and donuts: a type VI secretion story. *Mol Microbiol* **76:** 815–821.

Boyer F, Fichant G, Berthod J, Vandenbrouck Y, Attree I. (2009). Dissecting the bacterial type VI secretion system by a genome wide in silico analysis: what can be learned from available microbial genomic resources? *BMC Genomics* **10:** 104.

Brock J, Schulz-Vogt HN. (2011). Sulfide induces phosphate release from polyphosphate in cultures of a marine *Beggiatoa* strain. *ISME J* **5:** 497–506.

Brysch K, Schneider C, Fuchs G, Widdel F. (1987). Lithoautotrophic growth of sulfate-reducing bacteria, and description of *Desulfobacterium autotrophicum* gen. nov., sp. nov. *Arch Microbiol* **148:** 264–274.

Burton SD, Morita RY. (1964). Effect of catalase and cultural conditions on growth of *Beggiatoa*. *J Bacteriol* **88:** 1755–1761.

Carver T, Thomson N, Bleasby A, Berriman M, Parkhill J. (2009). DNAPlotter: circular and linear interactive genome visualization. *Bioinformatics* **25:** 119–120.

Case RJ, Labbate M, Kjelleberg S. (2008). AHL-driven quorum-sensing circuits: their frequency and function among the Proteobacteria. *ISME J* **2:** 345–349.

Chow J, Mazmanian SK. (2010). A pathobiont of the microbiota balances host colonization and intestinal inflammation. *Cell Host Microbe* **7:** 265–276.

Cornelis GR. (2002). The *Yersinia* Ysc-Yop 'type III' weaponry. *Nat Rev Mol Cell Bio* **3:** 742–752.

Cornelis GR, Van Gijsegem F. (2000). Assembly and function of type III secretory systems. *Annu Rev Microbiol* **54:** 735–774.

Cunliffe M. (2011). Correlating carbon monoxide oxidation with *cox* genes in the abundant Marine Roseobacter Clade. *ISME J* **5:** 685–691.

Deakin WJ, Broughton WJ. (2009). Symbiotic use of pathogenic strategies: rhizobial protein secretion systems. *Nat Rev Microbiol* **7:** 312–320.

Delcher AL, Bratke KA, Powers EC, Salzberg SL. (2007). Identifying bacterial genes and endosymbiont DNA with Glimmer. *Bioinformatics* **23:** 673–679.

Enticknap JJ, Kelly M, Peraud O, Hill RT. (2006). Characterization of a culturable alphaproteobacterial symbiont common to many marine sponges and evidence for vertical transmission via sponge larvae. *Appl Environ Microbiol* **72:** 3724–3732.

Filloux A, Hachani A, Bleves S. (2008). The bacterial type VI secretion machine: yet another player for protein transport across membranes. *Microbiol-SGM* **154:** 1570–1583.

Fisch KM, Gurgui C, Heycke N, van der Sar SA, Anderson SA, Webb VL *et al.* (2009). Polyketide assembly lines of uncultivated sponge symbionts from structure-based gene targeting. *Nat Chem Biol* **5:** 494–501.

Fukunaga Y, Kurahashi M, Tanaka K, Yanagi K, Yokota A, Harayama S. (2006). *Pseudovibrio ascidiaceicola* sp. nov., isolated from ascidians (sea squirts). *Int J Syst Evol Microbiol* **56:** 343–347.

Fürch T, Preusse M, Tomasch J, Zech H, Wagner-Döbler I, Rabus R *et al.* (2009). Metabolic fluxes in the central carbon metabolism of *Dinoroseobacter shibae* and *Phaeobacter gallaeciensis*, two members of the marine *Roseobacter* clade. *BMC Microbiol* **9:** 209.

Ghosh W, Dam B. (2009). Biochemistry and molecular biology of lithotrophic sulfur oxidation by taxonomically and ecologically diverse bacteria and archaea. *FEMS Microbiol Rev* **33:** 999–1043.

Hammar M, Bian Z, Normark S. (1996). Nucleator-dependent intercellular assembly of adhesive curli organelles in *Escherichia coli*. *Proc Natl Acad Sci U S A* **93:** 6562–6566.

Hammar M, Arnqvist A, Bian Z, Olsén A, Normark S. (1995). Expression of two *csg* operons is required for production of fibronectin- and congo red-binding curli polymers in *Escherichia coli* K-12. *Mol Microbiol* **18:** 661–670.

Hentschel U, Schmid M, Wagner M, Fieseler L, Gernert C, Hacker J. (2001). Isolation and phylogenetic analysis of bacteria with antimicrobial activities from the mediterranean sponges *Aplysina aerophoba* and *Aplysina cavernicola*. *FEMS Microbiol Ecol* **35:** 305–312.

Hood RD, Singh P, Hsu FS, Güvener T, Carl MA, Trinidad RRS *et al.* (2010). A type VI secretion system of *Pseudomonas aeruginosa* targets a toxin to bacteria. *Cell Host Microbe* **7:** 25–37.

Hosoya S, Yokota A. (2007). *Pseudovibrio japonicus* sp. nov., isolated from coastal seawater in Japan. *Int J Syst Evol Microbiol* **57:** 1952–1955.

Jani AJ, Cotter PA. (2010). Type VI secretion: not just for pathogenesis anymore. *Cell Host Microbe* **8:** 2–6.

Kamyshny A. (2009). Improved cyanolysis protocol for detection of zero-valent sulfur in natural aquatic systems. *Limnol Oceanogr-Meth* **7:** 442–448.

Kennedy J, Baker P, Piper C, Cotter PD, Walsh M, Mooij MJ *et al.* (2009). Isolation and analysis of bacteria with antimicrobial activities from the marine sponge *Haliclona simulans* collected from irish waters. *Mar Biotechnol* **11:** 384–396.

King GM, Weber CF. (2007). Distribution, diversity and ecology of aerobic CO-oxidizing bacteria. *Nat Rev Microbiol* **5:** 107–118.

Koren O, Rosenberg E. (2006). Bacteria associated with mucus and tissues of the coral *Oculina patagonica* in summer and winter. *Appl Environ Microbiol* **72:** 5254–5259.

Krogh A, Larsson B, von Heijne G, Sonnhammer EL. (2001). Predicting transmembrane protein topology with a hidden Markov model: application to complete genomes. *J Mol Biol* **305:** 567–580.

Lackner G, Moebius N, Hertweck C. (2011). Endofungal bacterium controls its host by an *hrp* type III secretion system. *ISME J* **5:** 252–261.

Lafi FF, Garson MJ, Fuerst JA. (2005). Culturable bacterial symbionts isolated from two distinct sponge species (*Pseudoceratina clavata* and *Rhabdastrella globostellata*) from the Great Barrier Reef display similar phylogenetic diversity. *Microb Ecol* **50:** 213–220.

Lagesen K, Hallin P, Rødland EA, Stærfeldt HH, Rognes T, Ussery DW. (2007). RNAmmer: consistent and rapid annotation of ribosomal RNA genes. *Nucleic Acids Res* **35:** 3100–3108.

Lambalot RH, Gehring AM, Flugel RS, Zuber P, LaCelle M, Marahiel MA *et al.* (1996). A new enzyme superfamily - the phosphopantetheinyl transferases. *Chem Biol* **3:** 923–936.

Lang AS, Beatty JT. (2001). The gene transfer agent of *Rhodobacter capsulatus* and "constitutive transduction" in prokaryotes. *Arch Microbiol* **175:** 241–249.

Lang AS, Beatty JT. (2007). Importance of widespread gene transfer agent genes in *α-Proteobacteria*. *Trends Microbiol* **15:** 54–62.

Larkin JM, Strohl WR. (1983). *Beggiatoa*, *Thiothrix*, and *Thioploca*. *Annu Rev Microbiol* **37:** 341–367.

Lowe TM, Eddy SR. (1997). tRNAscan-SE: a program for improved detection of transfer RNA genes in genomic sequence. *Nucleic Acids Res* **25:** 955–964.

Meyer F, Goesmann A, McHardy AC, Bartels D, Bekel T, Clausen J *et al.* (2003). GenDB - an open source genome annotation system for prokaryote genomes. *Nucleic Acids Res* **31:** 2187–2195.

Morris JJ, Kirkegaard R, Szul MJ, Johnson ZI, Zinser ER. (2008). Facilitation of robust growth of *Prochlorococcus* colonies and dilute liquid cultures by "helper" heterotrophic bacteria. *Appl Environ Microbiol* **74:** 4530–4534.

Mougous JD, Cuff ME, Raunser S, Shen A, Zhou M, Gifford CA *et al.* (2006). A virulence locus of *Pseudomonas aeruginosa* encodes a protein secretion apparatus. *Science* **312:** 1526–1530.

Mukherjee S, Keitany G, Li Y, Wang Y, Ball HL, Goldsmith EJ *et al.* (2006). *Yersinia* YopJ acetylates and inhibits kinase activation by blocking phosphorylation. *Science* **312:** 1211–1214.

Mulder NJ, Apweiler R, Attwood TK, Bairoch A, Bateman A, Binns D *et al.* (2005). InterPro, progress and status in 2005. *Nucleic Acids Res* **33:** D201–D205.

Müller WEG, Müller IM. (2003). Origin of the metazoan immune system: identification of the molecules and their functions in sponges. *Integr Comp Biol* **43:** 281–292.

Muscholl-Silberhorn A, Thiel V, Imhoff JF. (2008). Abundance and bioactivity of cultured sponge-associated bacteria from the mediterranean sea. *Microb Ecol* **55:** 94–106.

Newton RJ, Griffin LE, Bowles KM, Meile C, Gifford S, Givens CE *et al.* (2010). Genome characteristics of a generalist marine bacterial lineage. *ISME J* **4:** 784–798.

Niebuhr K, Jouihri N, Allaoui A, Gounon P, Sansonetti PJ, Parsot C. (2000). IpgD, a protein secreted by the type III secretion machinery of *Shigella flexneri*, is chaperoned by IpgE and implicated in entry focus formation. *Mol Microbiol* **38:** 8–19.

Niebuhr K, Giuriato S, Pedron T, Philpott DJ, Gaits F, Sable J *et al.* (2002). Conversion of PtdIns(4,5)P-2 into PtdIns(5)P by the *S.flexneri* effector IpgD reorganizes host cell morphology. *EMBO J* **21:** 5069–5078.

Nougayrède JP, Homburg S, Taieb F, Boury M, Brzuszkiewicz E, Gottschalk G *et al.* (2006). *Escherichia coli* induces DNA double-strand breaks in eukaryotic cells. *Science* **313:** 848–851.

Olson JB, Harmody DK, McCarthy PJ. (2002). *α-Proteobacteria* cultivated from marine sponges display branching rod morphology. *FEMS Microbiol Lett* **211:** 169–173.

Piel J, Hui DQ, Wen GP, Butzke D, Platzer M, Fusetani N *et al.* (2004). Antitumor polyketide biosynthesis by an uncultivated bacterial symbiont of the marine sponge *Theonella swinhoei*. *Proc Natl Acad Sci U S A* **101:** 16222–16227.

Pukatzki S, McAuley SB, Miyata ST. (2009). The type VI secretion system: translocation of effectors and effector-domains. *Curr Opin Microbiol* **12:** 11–17.

Pukatzki S, Ma AT, Sturtevant D, Krastins B, Sarracino D, Nelson WC *et al.* (2006). Identification of a conserved bacterial protein secretion system in *Vibrio cholerae* using the *Dictyostelium* host model system. *Proc Natl Acad Sci U S A* **103:** 1528–1533.

Putze J, Hennequin C, Nougayrède JP, Zhang WL, Homburg S, Karch H *et al.* (2009). Genetic structure and distribution of the colibactin genomic island among members of the family *Enterobacteriaceae*. *Infect Immun* **77:** 4696–4703.

Quast C. (2006). MicHanThi - design and implementation of a system for the prediction of gene functions in genome annotation projects. Diploma thesis, Universität Bremen, Bremen.

Richter M, Rosselló-Móra R. (2009). Shifting the genomic gold standard for the prokaryotic species definition. *Proc Natl Acad Sci U S A* **106:** 19126–19131.

Richter M, Lombardot T, Kostadinov I, Kottmann R, Duhaime MB, Peplies J *et al.* (2008). JCoast - a biologist-centric software tool for data mining and comparison of prokaryotic (meta)genomes. *BMC Bioinformatics* **9:** 177.

Riesenfeld CS, Murray AE, Baker BJ. (2008). Characterization of the microbial community and polyketide biosynthetic potential in the palmerolide-producing tunicate *Synoicum adareanum*. *J Nat Prod* **71:** 1812–1818.

Rypien KL, Ward JR, Azam F. (2010). Antagonistic interactions among coral-associated bacteria. *Environ Microbiol* **12:** 28–39.

Santos OCS, Pontes PVML, Santos JFM, Muricy G, Giambiagi-deMarval M, Laport MS. (2010). Isolation, characterization and phylogeny of sponge-associated bacteria with antimicrobial activities from Brazil. *Res Microbiol* **161:** 604–612.

Schwedt A. (2011). Physiology of a marine *Beggiatoa* strain and their accompanying organism *Pseudovibrio* sp. - a facultatively oligotrophic bacterium. Ph. D. thesis, Universität Bremen, Bremen.

Sertan-de Guzman AA, Predicala RZ, Bernardo EB, Neilan BA, Elardo SP, Mangalindan GC *et al.* (2007). *Pseudovibrio denitrificans* strain Z143-1, a heptylprodigiosin-producing bacterium isolated from a Philippine tunicate. *FEMS Microbiol Lett* **277:** 188–196.

Shieh WY, Lin YT, Jean WD. (2004). *Pseudovibrio denitrificans* gen. nov., sp. nov., a marine, facultatively anaerobic, fermentative bacterium capable of denitrification. *Int J Syst Evol Microbiol* **54:** 2307–2312.

Siegl A, Kamke J, Hochmuth T, Piel J, Richter M, Liang CG *et al.* (2011). Single-cell genomics reveals the lifestyle of *Poribacteria*, a candidate phylum symbiotically associated with marine sponges. *ISME J* **5:** 61–70.

Stothard P, Wishart DS. (2005). Circular genome visualization and exploration using CGView. *Bioinformatics* **21:** 537–539.

Subramoni S, Venturi V. (2009). LuxR-family 'solos': bachelor sensors/regulators of signalling molecules. *Microbiol-SGM* **155:** 1377–1385.

Tang KH, Feng XY, Tang YJJ, Blankenship RE. (2009). Carbohydrate metabolism and carbon fixation in *Roseobacter denitrificans* OCh114. *PLoS One* **4:** e7233.

Tatusov RL, Fedorova ND, Jackson JD, Jacobs AR, Kiryutin B, Koonin EV *et al.* (2003). The COG database: an updated version includes eukaryotes. *BMC Bioinformatics* **4:** 41.

Taylor MW, Radax R, Steger D, Wagner M. (2007). Sponge-associated microorganisms: evolution, ecology, and biotechnological potential. *Microbiol Mol Biol Rev* **71:** 295–374.

Thakur NL, Hentschel U, Krasko A, Pabel CT, Anil AC, Muller WEG. (2003). Antibacterial activity of the sponge *Suberites domuncula* and its primmorphs: potential basis for epibacterial chemical defense. *Aquat Microb Ecol* **31:** 77–83.

Thiel V, Imhoff JF. (2003). Phylogenetic identification of bacteria with antimicrobial activities isolated from Mediterranean sponges. *Biomolecular Engineering* **20:** 421–423.

Thoms C, Horn M, Wagner M, Hentschel U, Proksch P. (2003). Monitoring microbial diversity and natural product profiles of the sponge *Aplysina cavernicola* following transplantation. *Mar Biol* **142:** 685–692.

Wagner-Döbler I, Ballhausen B, Berger M, Brinkhoff T, Buchholz I, Bunk B *et al.* (2010). The complete genome sequence of the algal symbiont *Dinoroseobacter shibae*: a hitchhiker's guide to life in the sea. *ISME J* **4:** 61–77.

Weber B, Hasic M, Chen C, Wai SN, Milton DL. (2009). Type VI secretion modulates quorum sensing and stress response in *Vibrio anguillarum*. *Environ Microbiol* **11:** 3018–3028.

Webster NS, Hill RT. (2001). The culturable microbial community of the Great Barrier Reef sponge *Rhopaloeides odorabile* is dominated by an α-proteobacterium. *Mar Biol* **138:** 843–851.

Widdel F, Pfennig N. (1984). Dissimilatory sulfate- or sulfur-reducing bacteria. In: Krieg NR, Holt JG (eds). *Bergey's manual of systematic bacteriology*. Williams & Wilkins: Baltimore. pp 663–379.

Widdel F, Bak F. (1992). Gram-negative mesophilic sulfate-reducing bacteria. In: Balows A, Trüper HG, Dworkin M, Harder W, Schleifer KH (eds). *The Prokaryotes*, 2nd edn. Springer: New York. pp 3352–3378.

Williams TJ, Ertan H, Ting L, Cavicchioli R. (2009). Carbon and nitrogen substrate utilization in the marine bacterium *Sphingopyxis alaskensis* strain RB2256. *ISME J* **3:** 1036–1052.

Zedelius J, Rabus R, Grundmann O, Werner I, Brodkorb D, Schreiber F *et al.* (2011). Alkane degradation under anoxic conditions by a nitrate-reducing bacterium with possible involvement of the electron acceptor in substrate activation. *Environ Microbiol Rep* **3:** 125–135.

Supplementary material

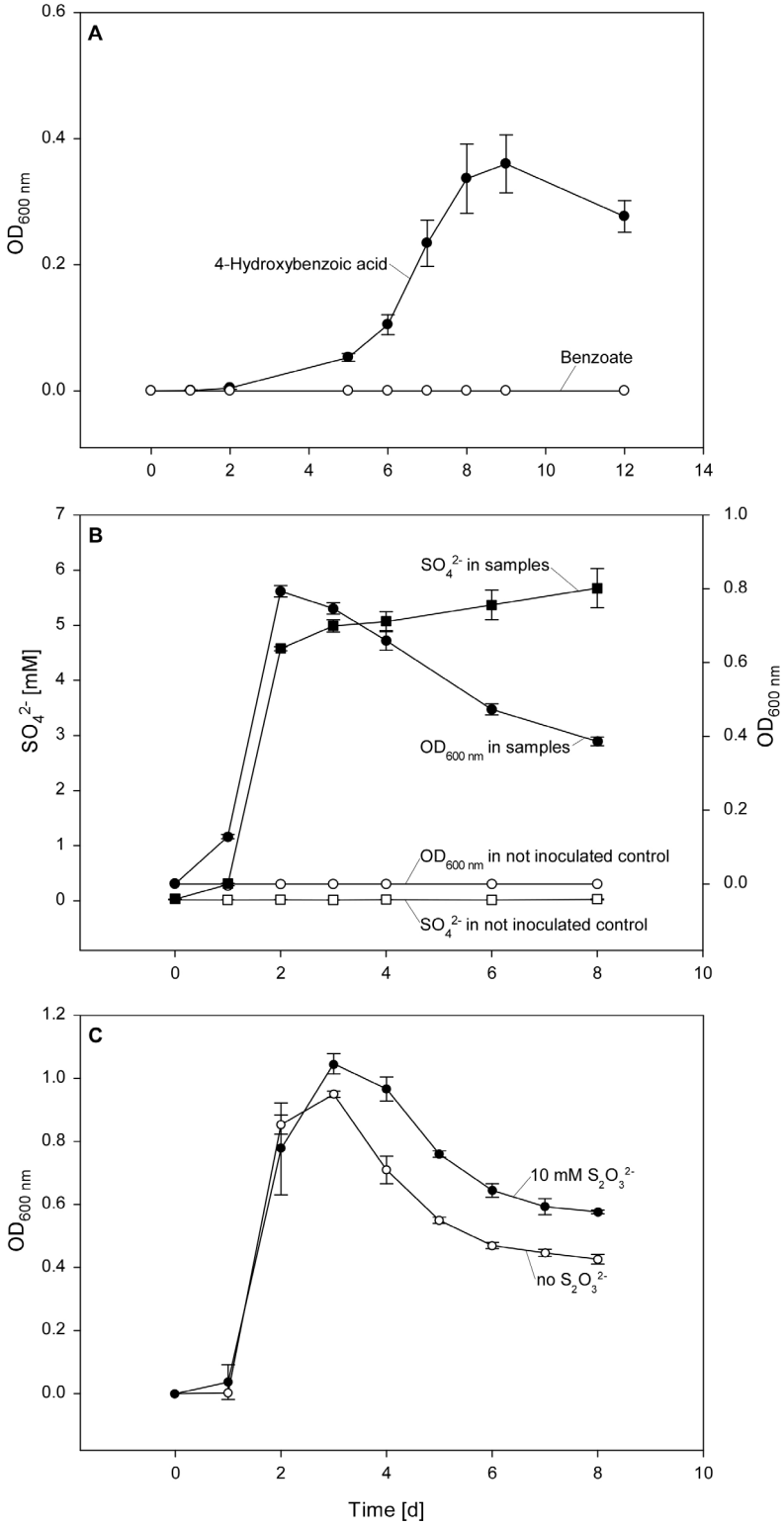

Figure S 2.1. (**A**) Growth of *Pseudovibrio* strain FO-BEG1 with aromatic compounds as the sole carbon and energy source. (**B**) Growth and SO_4^{2-} evolution by *Pseudovibrio* sp. FO-BEG1 under oxic conditions with the addition of 10 mmol l^{-1} $Na_2S_2O_3$ to the medium. Closed squares and circles represent the SO_4^{2-} evolution and optical density in inoculated samples. Open squares and open circles represent SO_4^{2-} evolution and optical density, respectively, in an uninoculated control to exclude chemical oxidation of $Na_2S_2O_3$. Initially, the medium did not contain any SO_4^{2-} in order to decrease the SO_4^{2-} background during the measurements. (**C**) Growth of *Pseudovibrio* sp. FO-BEG1 with and without the addition of 10 mmol l^{-1} $Na_2S_2O_3$ to the medium. The medium for this experiment contains 11.5 mmol l^{-1} K_2SO_4 to ensure that the culture without $Na_2S_2O_3$ contains a sulfur source for growth. Error bars represent the standard deviation in biological triplicates.

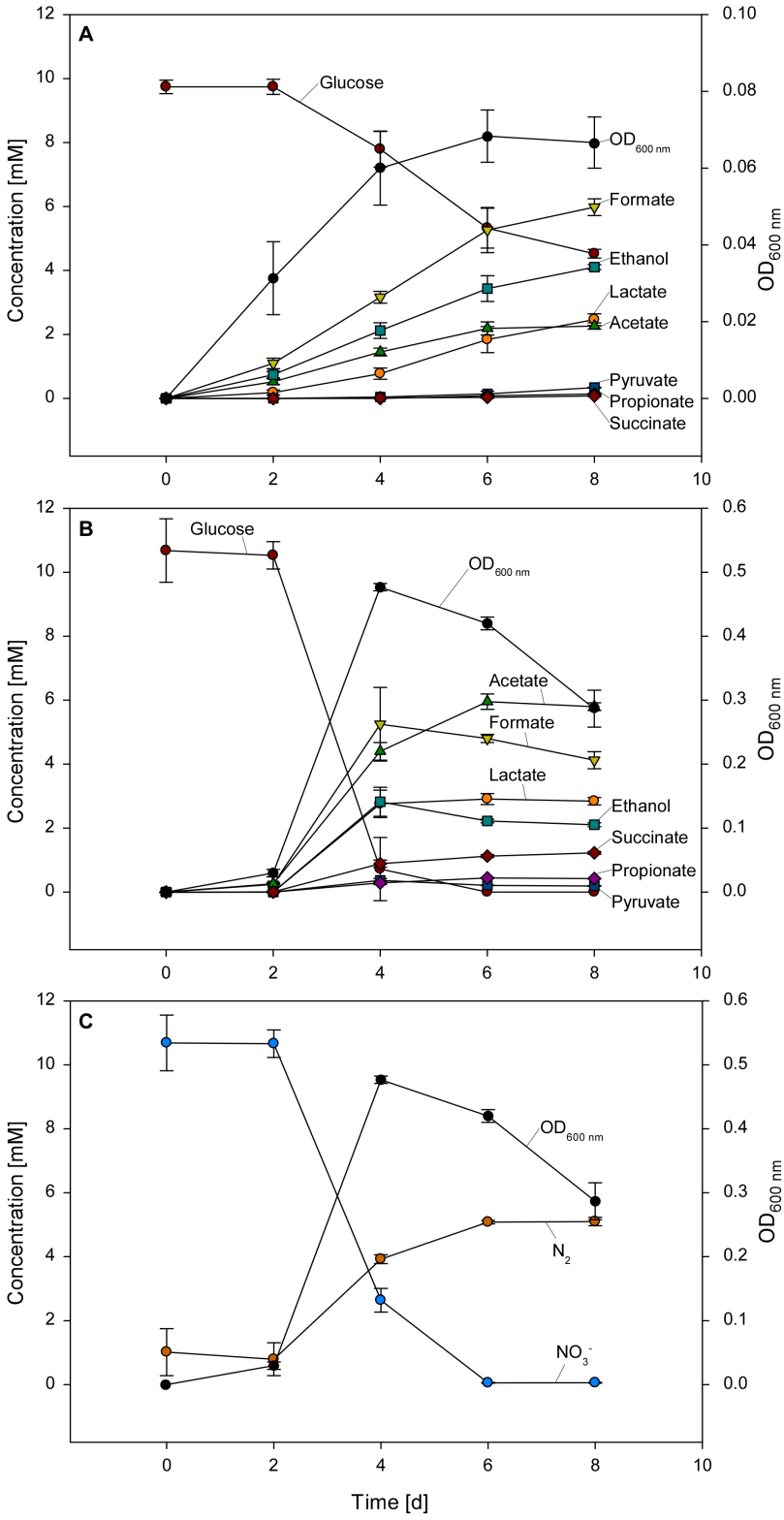

Figure S 2.2. (**A**) Glucose consumption, growth and production of fermentation products by *Pseudovibrio* sp. FO-BEG1 grown under anoxic conditions without NO_3^-. (**B**) Glucose consumption, growth and production of fermentation products during simultaneous denitrification and fermentation by *Pseudovibrio* sp. FO-BEG1 grown under anoxic conditions with addition of 10 mmol l^{-1} NO_3^-. (**C**) Consumption of NO_3^-, evolution of gaseous nitrogen and growth during simultaneous denitrification and fermentation of *Pseudovibrio* sp. FO-BEG1 with 10 mmol l^{-1} NO_3^-. Error bars represent the standard deviation in biological triplicates.

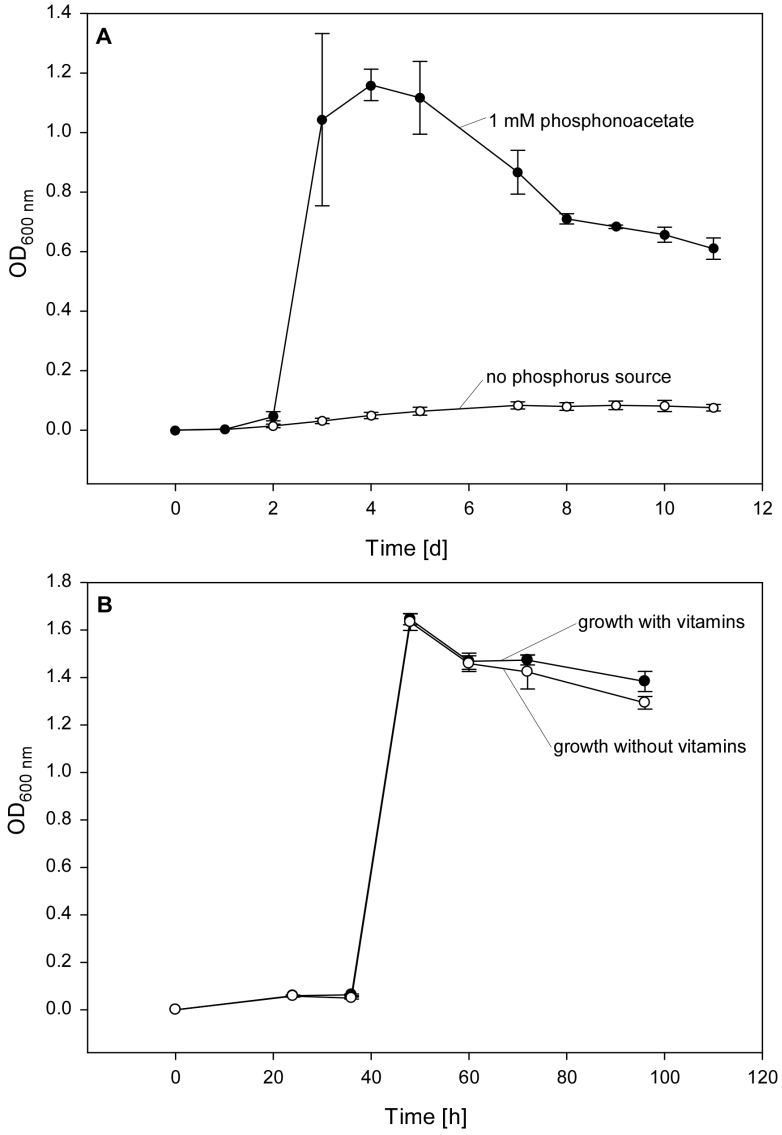

Figure S 2.3. (**A**) Growth of *Pseudovibrio* sp. FO-BEG1 with 1 mmol l^{-1} phosphonoacetate as the only phosphorus source and without the addition of any phosphorus to the medium. (**B**) Growth of *Pseudovibrio* sp. FO-BEG1 with and without the addition of vitamins to the medium. Error bars represent the standard deviation in biological triplicates.

Table S 2.1. Genes detected in the genomes of *Pseudovibrio* sp. FO-BEG1 and JE062 coding for predicted proteins involved in carbon metabolism, denitrification, oxidation of thiosulfate, and phosphonate utilization. Genes that could not be detected in the not closed genome of strain JE062 are indicated with '—'. Absence of a gene name or an EC number indicates that no assignment was made due to missing of these parameters for the respective genes.

Locus FO-BEG1	Locus JE062	Product	Gene name	EC number
		Glycolysis / Gluconeogenesis		
PSE_0520	PJE062_2836	2,3-bisphosphoglycerate-dependent phosphoglycerate mutase	*gpmA*	5.4.2.1
PSE_0524	PJE062_2549	2,3-bisphosphoglycerate-dependent phosphoglycerate mutase	*gpmA*	5.4.2.1
PSE_1032	PJE062_4521	Glucokinase	*glk*	2.7.1.2
PSE_2344	PJE062_1398	Fructose-bisphosphate aldolase	*fbaA*	4.1.2.13
PSE_2526	PJE062_127	Phosphomannomutase/phosphoglucomutase	*algC*	5.4.2.2
PSE_3200	PJE062_1722	Enolase/2-phosphoglycerate dehydratase	*eno*	4.2.1.11
PSE_3383	PJE062_1304	Triose-phosphate isomerase	*tpiA*	5.3.1.1
PSE_4148	PJE062_4782	Glucose-6-phosphate isomerase	*gpi*	5.3.1.9
PSE_4697	PJE062_2190	Glyceraldehyde-3-phosphate dehydrogenase B	*gapB/epd*	1.2.1.12
PSE_4698	PJE062_2252	Phosphoglycerate kinase	*pgk*	2.7.2.3
PSE_4767	PJE062_2266	Pyruvate kinase	*pyk*	2.7.1.40
PSE_3532	PJE062_1635	Fructose-1,6-bisphosphatase class II	*glpX*	3.1.3.37
PSE_0639	PJE062_2867	Phosphoenolpyruvate carboxykinase	*pckA*	4.1.1.49
PSE_4866	PJE062_2056	Pyruvate carboxylase	*pyc*	6.4.1.1
		Entner-Doudoroff pathway		
PSE_0520	PJE062_2836	2,3-bisphosphoglycerate-dependent phosphoglycerate mutase	*gpmA*	5.4.2.1
PSE_0524	PJE062_2549	2,3-bisphosphoglycerate-dependent phosphoglycerate mutase	*gpmA*	5.4.2.1
PSE_1300	PJE062_1936	SMP-30/Gluconolaconase/LRE-like region		3.1.1.17
PSE_1664	PJE062_417	oxidoreductase, short chain dehydrogenase/reductase family protein	*gdh*	1.1.1.47
PSE_1887	PJE062_3941	SMP-30/Gluconolaconase/LRE-like region		3.1.1.17
PSE_1922	PJE062_733	Gluconokinase (Gluconate kinase)	*gntK*	2.7.1.12
PSE_3200	PJE062_1722	Enolase/2-phosphoglycerate dehydratase	*eno*	4.2.1.11
PSE_3907	—	KDPG and KHG aldolase	*eda*	4.1.2.14
PSE_3909	—	2-dehydro-3-deoxygluconokinase	*kdgK*	2.7.1.45
PSE_p0106	PJE062_762	2-dehydro-3-deoxygluconokinase	*kdgK*	2.7.1.45
PSE_p0137	PJE062_797	2-dehydro-3-deoxygluconokinase	*kdgK*	2.7.1.45
PSE_4145	PJE062_4650	Glucose-6-phosphate 1-dehydrogenase	*zwf*	1.1.1.49
PSE_4146	PJE062_4945	Phosphogluconate dehydratase (6-phosphogluconate dehydratase)	*edd*	4.2.1.12
PSE_4147	PJE062_4760	KDPG and KHG aldolase	*eda*	4.1.2.14
PSE_4148	PJE062_4782	Glucose-6-phosphate isomerase	*gpi*	5.3.1.9
PSE_4154	PJE062_4973	SMP-30/Gluconolaconase/LRE-like region		3.1.1.17
PSE_4697	PJE062_2190	Glyceraldehyde-3-phosphate dehydrogenase B	*gapB/epd*	1.2.1.12
PSE_4698	PJE062_2252	Phosphoglycerate kinase	*pgk*	2.7.2.3
PSE_4767	PJE062_2266	Pyruvate kinase	*pyk*	2.7.1.40

Table S 2.1. Continued

Locus FO-BEG1	Locus JE062	Product	Gene	EC
		Pentose phosphate pathway		
PSE_0476	PJE062_2965	6-phosphogluconate dehydrogenase	*gnd*	1.1.1.44
PSE_0628	PJE062_3035	Translaldolase	*tal*	2.2.1.2
PSE_1044	PJE062_4442	Phosphopentomutase	*deoB*	5.4.2.7
PSE_1456	—	Fructose-bisphosphate aldolase	*fbaA*	4.1.2.13
PSE_2114	PJE062_647	Fructose-bisphosphate aldolase	*fbaA*	4.1.2.13
PSE_2344	PJE062_1398	Fructose-bisphosphate aldolase	*fbaA*	4.1.2.13
PSE_2648	PJE062_4217	Ribose-5-phosphate isomerase A	*rpiA*	5.3.1.6
PSE_2884	PJE062_1466	Ribokinase	*rbsK*	2.7.1.15
PSE_3532	PJE062_1635	Fructose-1,6-bisphosphatase class II	*glpX*	3.1.3.11
PSE_4036	PJE062_4566	Ribulose-phosphate 3-epimerase	*rpe*	5.1.3.1
PSE_4437	PJE062_4652	Ribose-phosphate pyrophosphokinase	*prs*	2.7.6.1
PSE_4696	PJE062_2124	Transketolase	*tkt*	2.2.1.1
PSE_1664	PJE062_417	oxidoreductase, short chain dehydrogenase/reductase family protein	*gdh*	1.1.1.47
PSE_1300	PJE062_1936	SMP-30/Gluconolaconase/LRE-like region		3.1.1.17
PSE_1887	PJE062_3941	SMP-30/Gluconolaconase/LRE-like region		3.1.1.17
PSE_4154	PJE062_4973	SMP-30/Gluconolaconase/LRE-like region		3.1.1.17
PSE_1922	PJE062_733	Gluconokinase (Gluconate kinase)	*gntK*	2.7.1.12
PSE_4148	PJE062_4782	Glucose-6-phosphate isomerase	*gpi*	5.3.1.9
PSE_4145	PJE062_4650	Glucose-6-phosphate 1-dehydrogenase	*zwf*	1.1.1.49
		Citric acid cycle		
PSE_0214	PJE062_3108	Aconitate hydratase	*acnA*	4.2.1.3
PSE_0452	PJE062_3422	Aconitate hydratase 2	*acnB*	4.2.1.3
PSE_0603	PJE062_2553	Succinate dehydrogenase cytochrome b556 subunit (Cytochrome b-556)	*sdhC*	1.3.99.1
PSE_0604	PJE062_2930	Succinate dehydrogenase hydrophobic membrane anchor subunit	*sdhD*	1.3.99.1
PSE_0605	PJE062_2640	Succinate dehydrogenase flavoprotein subunit	*sdhA*	1.3.99.1
PSE_0606	PJE062_2569	Succinate dehydrogenase iron-sulfur subunit	*sdhB*	1.3.99.1
PSE_0614	PJE062_3013	Malate dehydrogenase	*mdh*	1.1.1.37
PSE_0615	PJE062_2857	Succinyl-CoA synthetase subunit beta	*sucC*	6.2.1.5
PSE_0616	—	succinyl-CoA synthetase subunit alpha	*sucD*	6.2.1.5
PSE_0617	PJE062_2799	alpha-ketoglutarate decarboxylase	*sucA (odhA)*	1.2.4.2
PSE_0618	PJE062_2606	Dihydrolipoamide acetyltransferase	*sucB*	2.3.1.61
PSE_2580	PJE062_4244	Fumarate hydratase class I	*fumA*	4.2.1.2
PSE_4461	PJE062_4634	Fumarate hydratase class II (Fumarase C)	*fumC*	4.2.1.2
PSE_3294	PJE062_1258	Dihydrolipoyllysine-residue acetyltransferase component of pyruvate dehydrogenase complex (E2)	*pdhC*	2.3.1.12
PSE_3295	PJE062_1014	Pyruvate dehydrogenase E1 component subunit beta	*pdhB*	1.2.4.1
PSE_3296	PJE062_1075	Pyruvate dehydrogenase E1 component subunit alpha	*pdhA*	1.2.4.1
PSE_3391	PJE062_1324	Citrate synthase	*cisY*	2.3.3.1
PSE_4065	PJE062_4617	Isocitrate dehydrogenase	*icd (idhA)*	1.1.1.42
PSE_4461	PJE062_4634	Fumarate hydratase class II (Fumarase C)	*fumC*	4.2.1.2
PSE_4866	PJE062_2056	Pyruvate carboxylase	*pyc*	6.4.1.1
PSE_4928	PJE062_2277	Citrate synthase	*cisY*	2.3.3.1

Table S 2.1. Continued

Locus FO-BEG1	Locus JE062	Product	Gene	EC
		Aromatic compound degradation		
PSE_1913	PJE062_845	Carboxymuconolactone decarboxylase	*pcaC*	4.1.1.44
PSE_2272	PJE062_483	P-hydroxybenzoate hydroxylase (4-hydroxybenzoate 3-monooxygenase)	*pobA*	1.14.13.2
PSE_2278	PJE062_940	3-oxoadipate enol-lactonase	*pcaD*	3.1.1.24
PSE_2279	PJE062_920	Protocatechuate 3,4-dioxygenase beta chain	*pcaH*	1.13.11.3
PSE_2280	PJE062_637	Protocatechuate 3,4-dioxygenase alpha chain	*pcaG*	1.13.11.3
PSE_2281	PJE062_798	3-oxoadipate:succinyl-CoA transferase, subunit A	*pcaI*	2.8.3.12
PSE_2282	PJE062_821	3-oxoadipate:succinyl-CoA transferase, subunit B	*pcaJ*	2.8.3.-
PSE_2283	PJE062_938	Beta-ketoadipyl-CoA thiolase	*pcaF*	2.3.1.16
PSE_2284	PJE062_754	3-carboxy-cis,cis-muconate cycloisomerase	*pcaB*	5.5.1.2
PSE_2827	PJE062_1336	Benzoate 1,2-dioxygenase subunit beta	*benB*	1.14.12.-
PSE_2828	PJE062_1217	Benzoate 1,2-dioxygenase subunit alpha	*benA*	1.14.12.-
PSE_2829	PJE062_1491	Vanillate O-demethylase oxidoreductase	*vanB*	1.14.13.82
		Carbon monoxide oxidation		
PSE_1023	PJE062_4489	Carbon monoxide dehydrogenase subunit G	*coxG*	1.2.99.2
PSE_1024	PJE062_4477	Carbon monoxide dehydrogenase small chain	*coxS*	1.2.99.2
PSE_1025	PJE062_4485	Carbon monoxide dehydrogenase large chain	*coxL*	1.2.99.2
PSE_1027	PJE062_4412	Carbon monoxide dehydrogenase medium chain	*coxM*	1.2.99.2
		Mixed acid fermentation		
PSE_0477	PJE062_2774	L-lactate dehydrogenase	*ldh*	1.1.1.27
PSE_1924	PJE062_844	D-lactate dehydrogenase	*dld*	1.1.1.28
PSE_3254	PJE062_1131	Formate acetyltransferase	*tdcE*	2.3.1.54
PSE_3255	PJE062_1378	Pyruvate formate-lyase activating enzyme	*pflA*	1.97.1.4
PSE_1331	PJE062_1899	Aldehyde-alcohol dehydrogenase	*adhE*	1.1.1.1
PSE_1086	PJE062_4486	Phosphate acetyltransferase (Phosphotransacetylase)	*pta*	2.3.1.8
PSE_1087	PJE062_4379	Acetate kinase	*ackA*	2.7.2.1
PSE_0614	PJE062_3013	Malate dehydrogenase	*mdh*	1.1.1.37
PSE_2580	PJE062_4244	Fumarate hydratase class I	*fumA*	4.2.1.2
PSE_4461	PJE062_4634	Fumarate hydratase class II (Fumarase C)	*fumC*	4.2.1.2
PSE_2225	PJE062_741	Fumarate reductase/succinate dehydrogenase flavoprotein		
PSE_4599	PJE062_2498	Propionyl-CoA carboxylase, beta subunit		
PSE_4597	PJE062_2449	Propionyl-CoA carboxylase alpha chain		
PSE_2418	PJE062_156	Methylmalonyl-CoA mutase large subunit	*mutB*	5.4.99.2
PSE_2419	PJE062_248	Methylmalonyl-CoA mutase small subunit	*mutA*	5.4.99.2
PSE_3421	PJE062_1661	Methylmalonyl-CoA epimerase	*mceE*	5.1.99.1
PSE_1247	PJE062_4342	succinyl-CoA:3-ketoacid-coenzyme A transferase subunit A	*scoA*	2.8.3.5
PSE_1248	PJE062_4358	succinyl-CoA:3-ketoacid-coenzyme A transferase subunit B	*scoB*	2.8.3.5

Table S 2.1. Continued

Locus FO-BEG1	Locus JE062	Product	Gene	EC
		Denitrification		
PSE_0757	PJE062_2921	Respiratory nitrate reductase, alpha subunit	*narG*	1.7.99.4
PSE_0758	PJE062_3029	Respiratory nitrate reductase beta subunit	*narH*	1.7.99.4
PSE_0759	PJE062_2637	Respiratory nitrate reductase, delta subunit	*narJ*	1.7.99.4
PSE_0760	PJE062_2605	Respiratory nitrate reductase, gamma subunit	*narI*	1.7.99.4
PSE_0895	PJE062_2542	Nitrite reductase protein (NO-forming)	*nirN*	1.7.2.1
PSE_0897	PJE062_2612	Denitrification system component NirT	*nirT*	
PSE_0898	PJE062_2813	Nitrite reductase	*nirS*	1.7.2.1
PSE_2203	PJE062_731	Protein NirF	*nriF*	1.7.2.1
PSE_2204	PJE062_627	Nitrite reductase heme biosynthesis D/L protein		
PSE_2205	PJE062_508	Protein NirG	*nirG*	
PSE_2207	PJE062_853	Nitrite reductase	*nirS*	1.7.2.1
PSE_4550	PJE062_2454	Protein NorD	*norD*	1.7.99.7
PSE_4551	PJE062_2491	Protein NorQ	*norQ*	1.7.99.7
PSE_4552	PJE062_2475	Nitric oxide reductase subunit B	*norB*	1.7.99.7
PSE_4553	PJE062_2486	Nitric oxide reductase subunit C	*norC*	1.7.99.7
PSE_3127	PJE062_1200	Regulatory protein NosR	*nosR*	
PSE_3128	PJE062_1080	Nitrous-oxide reductase	*nosZ*	1.7.99.6
PSE_3129	PJE062_1307	nitrous oxide maturation protein NosD	*nosD*	
PSE_3130	PJE062_965	Copper transport ATP-binding protein NosF	*nosF*	
PSE_3131	PJE062_1456	Membrane protein NosY	*nosY*	
PSE_3132	PJE062_1117	NosL protein required for nitrous oxide reduction	*nosL*	
PSE_2100	PJE062_842	Cytochrome c-type protein NapC	*napC*	
PSE_2101	PJE062_629	Nitrate reductase cytochrome c-type subunit (NapB)	*napB*	
PSE_2102	PJE062_585	Nitrate reductase, large subunit, periplasmic		
PSE_2103	PJE062_729	Protein NapD	*napD*	
PSE_2104	PJE062_910	Ferredoxin-type protein NapF	*napF*	
PSE_2105	PJE062_562	Periplasmic nitrate reductase protein	*napE*	
PSE_4539	PJE062_2443	Cytochrome c-type protein NapC	*napC*	
PSE_4540	PJE062_2471	Nitrate reductase cytochrome c-type subunit (NapB)	*napB*	
PSE_4541	PJE062_2490	Ferredoxin-type protein NapH	*napH*	
PSE_4542	PJE062_2479	MauM/NapG ferredoxin-type protein	*napG*	
PSE_4543	PJE062_2442	Nitrate reductase, large subunit, periplasmic		
PSE_4544	PJE062_2506	Protein NapD	*napD*	
		Oxidation of reduced sulfur compounds		
PSE_1359	PJE062_5277	Sulfide dehydrogenase [flavocytochrome c] flavoprotein chain	*soxF*	
PSE_1360	PJE062_5324	Diheme cytochrome c SoxE	*soxE*	
PSE_1361	PJE062_5237	Diheme cytochrome c SoxD	*soxD*	
PSE_1362	PJE062_5256	Sulfur oxidation molybdopterin C protein, SoxC	*soxC*	
PSE_1363	PJE062_5219	Sulfur oxidation B protein	*soxB*	
PSE_1364	PJE062_5333	Diheme cytochrome c SoxA	*soxA*	
PSE_1365	PJE062_5182	Sulfur oxidation Z protein	*soxZ*	
PSE_1366	PJE062_5189	Sulfur oxidation protein SoxY	*soxY*	
PSE_1367	PJE062_5241	Monoheme cytochrome c SoxX	*soxX*	
PSE_1368	PJE062_5328	Thioredoxin SoxW	*soxW*	

Table S 2.1. Continued

Locus FO-BEG1	Locus JE062	Product	Gene	EC
		Phosphonate utilization		
PSE_4849	PJE062_2269	Phosphonate metabolism PhnG	*phnG*	
PSE_4850	PJE062_2196	carbon-phosphorus lyase complex subunit	*phnH*	
PSE_4851	PJE062_2313	Protein PhnI	*phnI*	
PSE_4852	PJE062_2247	Protein PhnJ	*phnJ*	
PSE_4853	PJE062_2188	Phosphonates transport ATP-binding protein PhnK	*phnK*	
PSE_4854	PJE062_2041	Phosphonates transport ATP-binding protein PhnL	*phnL*	
PSE_4857	PJE062_2279	Protein PhnM	*phnM*	
PSE_4858	PJE062_2090	ATP-binding protein PhnN	*phnN*	
PSE_3627	PJE062_1982	Phosphonates transport system permease protein PhnE	*phnE*	
PSE_3628	PJE062_2033	Phosphonates transport system permease protein PhnE	*phnE*	
PSE_3629	PJE062_2039	ABC transporter, phosphonate, periplasmic substrate-binding protein PhnD	*phnD*	
PSE_3630	PJE062_2265	Phosphonates import ATP-binding protein PhnC	*phnC*	

Table S 2.2. Genes detected in the genomes of *Pseudovibrio* sp. FO-BEG1 and JE062 coding for predicted TRAP transporter subunits. Genes that could not be detected in the not closed genome of strain JE062 are indicated with '—'.

Locus FO-BEG1	Locus JE062	Product	Gene
		TRAP Transporter	
PSE_0923	PJE062_2908	TRAP dicarboxylate transporter, DctM subunit	*dctM*
PSE_0924	PJE062_2533	TRAP dicarboxylate transporter, DctQ subunit	*dctQ*
PSE_0925	PJE062_2627	TRAP dicarboxylate transporter, DctP subunit	*dctP*
PSE_1209	PJE062_4388	TRAP dicarboxylate transporter, DctP subunit	*dctP*
PSE_1316	PJE062_1939	TRAP dicarboxylate transporter, DctM subunit	*dctM*
PSE_1317	PJE062_1874	TRAP dicarboxylate transporter, DctQ subunit	*dctQ*
PSE_1426	PJE062_5273	TRAP dicarboxylate transporter, DctP subunit	*dctP*
PSE_1427	PJE062_5331	TRAP dicarboxylate transporter, DctQ subunit	*dctQ*
PSE_1428	PJE062_5225	TRAP dicarboxylate transporter, DctM subunit	*dctM*
PSE_1834	—	TRAP dicarboxylate transporter, DctM subunit	*dctM*
PSE_1835	—	TRAP dicarboxylate transporter, DctQ subunit	*dctQ*
PSE_1836	—	TRAP dicarboxylate transporter, DctP subunit	*dctP*
PSE_1888	PJE062_3892	TRAP dicarboxylate transporter, DctM subunit	*dctM*
PSE_1889	PJE062_3768	TRAP dicarboxylate transporter, DctQ subunit	*dctQ*
PSE_1890	PJE062_3743	TRAP dicarboxylate transporter, DctP subunit	*dctP*
PSE_1919	PJE062_932	TRAP dicarboxylate transporter, DctM subunit	*dctM*
PSE_1920	PJE062_501	TRAP dicarboxylate transporter, DctQ subunit	*dctQ*
PSE_1921	PJE062_925	TRAP dicarboxylate transporter, DctP subunit	*dctP*

Table S 2.2. Continued

Locus FO-BEG1	Locus JE062	Product	Gene
PSE_1925	PJE062_918	TRAP dicarboxylate transporter, fused membrane component DctQM	*dctQM*
PSE_1926	PJE062_600	TRAP dicarboxylate transporter, DctP subunit	*dctP*
PSE_2239	PJE062_646	TRAP transporter solute receptor, TAXI family	
PSE_2240	PJE062_879	TRAP dicarboxylate transporter, fused membrane component DctQM	*dctQM*
PSE_2274	PJE062_919	TRAP dicarboxylate transporter, DctM subunit	*dctM*
PSE_2275	–	TRAP dicarboxylate transporter, DctQ subunit	*dctQ*
PSE_2276	PJE062_523	TRAP dicarboxylate transporter, DctP subunit	*dctP*
PSE_2337	PJE062_584	TRAP transporter solute receptor, TAXI family	
PSE_2338	PJE062_530	TRAP dicarboxylate transporter, fused membrane component DctQM	*dctQM*
PSE_2346	PJE062_1811	TRAP dicarboxylate transporter, DctQ subunit	*dctQ*
PSE_2347	PJE062_1617	TRAP dicarboxylate transporter, DctM subunit	*dctM*
PSE_2348	PJE062_1686	TRAP dicarboxylate transporter, DctP subunit	*dctP*
PSE_2801	PJE062_303	TRAP dicarboxylate transporter, DctP subunit	*dctP*
PSE_2802	PJE062_463	TRAP dicarboxylate transporter, DctQ subunit	*dctQ*
PSE_2803	PJE062_103	TRAP dicarboxylate transporter, DctM subunit	*dctM*
PSE_2830	PJE062_1070	TRAP dicarboxylate transporter, DctP subunit	*dctP*
PSE_2831	PJE062_1159	TRAP dicarboxylate transporter, DctQ subunit	*dctQ*
PSE_2832	PJE062_1444	TRAP dicarboxylate transporter, DctM subunit	*dctM*
PSE_2907	PJE062_1331	TRAP dicarboxylate transporter, fused membrane component DctQM	*dctQM*
PSE_2908	PJE062_1118	TRAP transporter solute receptor, TAXI family protein	
PSE_2946	PJE062_1639	TRAP dicarboxylate transporter, DctP subunit	*dctP*
PSE_2947	PJE062_1073	TRAP dicarboxylate transporter, DctQ subunit	*dctQ*
PSE_2948	PJE062_1496	TRAP dicarboxylate transporter, DctM subunit	*dctM*
PSE_3111	–	TRAP dicarboxylate transporter, DctP subunit	*dctP*
PSE_3112	–	TRAP dicarboxylate transporter, DctQ subunit	*dctQ*
PSE_3113	–	TRAP dicarboxylate transporter, DctM subunit	*dctM*
PSE_3353	PJE062_1507	TRAP dicarboxylate transporter, fused membrane component DctQM	*dctQM*
PSE_3354	PJE062_1151	TRAP transporter solute receptor, TAXI family protein	
PSE_3664	PJE062_1463	TRAP dicarboxylate transporter, DctP subunit	*dctP*
PSE_3665	PJE062_1642	TRAP dicarboxylate transporter, DctQ subunit	*dctQ*
PSE_3666	PJE062_1723	TRAP dicarboxylate transporter, DctM subunit	*dctM*

Table S 2.2. Continued

Locus FO-BEG1	Locus JE062	Product	Gene
PSE_3721	PJE062_1201	TRAP dicarboxylate transporter, DctM subunit	*dctM*
PSE_3722	PJE062_1120	TRAP dicarboxylate transporter, DctQ subunit	*dctQ*
PSE_3723	PJE062_1561	TRAP dicarboxylate transporter, DctP subunit	*dctP*
PSE_3912	–	TRAP dicarboxylate transporter, DctP subunit	*dctP*
PSE_3913	–	TRAP dicarboxylate transporter, DctQ subunit	*dctQ*
PSE_3914	–	TRAP dicarboxylate transporter, DctM subunit	*dctM*
PSE_4136	PJE062_4972	TRAP dicarboxylate transporter- DctP subunit	*dctP*
PSE_4577	PJE062_2484	TRAP dicarboxylate transporter, fused membrane component DctQM	*dctQM*
PSE_4578	PJE062_2464	TRAP transporter solute receptor, TAXI family protein	
PSE_4810	PJE062_2025	TRAP dicarboxylate transporter, DctM subunit	*dctM*
PSE_4811	PJE062_2312	TRAP dicarboxylate transporter, DctQ subunit	*dctQ*
PSE_4812	PJE062_2046	TRAP dicarboxylate transporter, DctP subunit	*dctP*
PSE_4845	PJE062_2117	TRAP dicarboxylate transporter, DctP subunit	*dctP*
PSE_4929	PJE062_2193	TRAP dicarboxylate transporter, DctP subunit	*dctP*
PSE_4930	PJE062_2118	TRAP dicarboxylate transporter, DctM subunit	*dctM*
PSE_4931	PJE062_2335	TRAP dicarboxylate transporter, DctQ subunit	*dctQ*
PSE_4932	PJE062_2112	TRAP dicarboxylate transporter, DctP subunit	*dctP*
PSE_p0100	PJE062_587	TRAP dicarboxylate transporter, DctP subunit	*dctP*
PSE_p0101	PJE062_597	TRAP dicarboxylate transporter, DctQ subunit	*dctQ*
PSE_p0102	PJE062_692	TRAP dicarboxylate transporter, DctM subunit	*dctM*
PSE_p0107	PJE062_891	TRAP dicarboxylate transporter, DctP subunit	*dctP*
PSE_p0108	PJE062_791	TRAP dicarboxylate transporter, DctQ subunit	*dctQ*
PSE_p0109	PJE062_739	TRAP dicarboxylate transporter, DctM subunit	*dctM*
PSE_p0130	PJE062_726	TRAP dicarboxylate transporter, DctP subunit	*dctP*
PSE_p0131	PJE062_678	TRAP dicarboxylate transporter, DctQ subunit	*dctQ*
PSE_p0132	PJE062_526	TRAP dicarboxylate transporter, DctM subunit	*dctM*
PSE_p0325	PJE062_3836	TRAP dicarboxylate transporter, DctQ subunit	*dctQ*
PSE_p0326	PJE062_3646	TRAP dicarboxylate transporter, DctM subunit	*dctM*
PSE_p0327	PJE062_3830	TRAP dicarboxylate transporter, DctP subunit	*dctP*
PSE_p0307	PJE062_3918	TRAP dicarboxylate transporter, DctP subunit	*dctP*
PSE_p0343	PJE062_3801	TRAP dicarboxylate transporter, DctQ subunit	*dctQ*
PSE_p0344	PJE062_3939	TRAP dicarboxylate transporter, DctM subunit	*dctM*
PSE_p0345	PJE062_3906	TRAP dicarboxylate transporter, DctP subunit	*dctP*

Table S 2.2. Continued

Locus FO-BEG1	Locus JE062	Product	Gene
PSE_p0362	PJE062_3865	TRAP dicarboxylate transporter, DctP subunit	*dctP*
PSE_p0363	PJE062_3671	TRAP dicarboxylate transporter, DctQ subunit	*dctQ*
PSE_p0364	PJE062_3954	TRAP dicarboxylate transporter, DctM subunit	*dctM*
PSE_p0369	PJE062_3631	TRAP dicarboxylate transporter, DctM subunit	*dctM*
PSE_p0370	PJE062_3612	TRAP dicarboxylate transporter, DctQ subunit	*dctQ*
PSE_p0371	PJE062_3938	TRAP dicarboxylate transporter, DctP subunit	*dctP*
PSE_p0394	PJE062_3749	TRAP dicarboxylate transporter, DctM subunit	*dctM*
PSE_p0395	PJE062_3639	TRAP dicarboxylate transporter, DctQ subunit	*dctQ*
PSE_p0396	PJE062_3658	TRAP dicarboxylate transporter, DctP subunit	*dctP*

Table S 2.3. Genes detected in the genomes of *Pseudovibrio* sp. FO-BEG1 and JE062 coding for predicted ABC transporter subunits. Genes that could not be detected in the not closed genome of strain JE062 are indicated with '—'. Pfam model specifies the family, to which the identified protein belongs, according with the Pfam database (Bateman *et al.*, 2004). Absence of a gene name indicates that no assignment was made due to missing of this parameter for the respective genes. Predicted substrate specificity was derived from the annotations of the genes belonging to the respective ABC transporter system.

Locus FO-BEG1	Locus JE062	Pfam Model	Product	Gene	Predicted substrate specificity
			ABC Transporter		
PSE_0112	PJE062_3499	ABC_tran	Glycine betaine/L-proline transport ATP-binding protein ProV	*proV*	**Glycine betaine/ L-proline**
PSE_0113	PJE062_3280	BPD_transp_1	Glycine betaine/L-proline transport system permease protein ProW	*proW*	
PSE_0114	PJE062_3213	OpuAC	Glycine betaine-binding protein	*proX*	
PSE_0420	PJE062_3099	Peripla_BP_2	Hemin-binding periplasmic protein HmuT	*hmuT*	**Hemin**
PSE_0421	PJE062_3210	FecCD	Hemin transport system permease protein HmuU	*hmuU*	
PSE_0422	PJE062_3070	ABC_tran	Hemin import ATP-binding protein HmuV	*hmuV*	
PSE_0430	PJE062_3307	OpuAC	Glycine betaine-binding protein	*proX*	**Glycine betaine/ L-proline**
PSE_0431	PJE062_3373	BPD_transp_1	Glycine betaine/L-proline transport system permease protein ProW	*proW*	
PSE_0432	PJE062_3413	ABC_tran	Glycine betaine/L-proline transport ATP-binding protein ProV	*proV*	
PSE_0437	PJE062_3357	SBP_bac_5	Periplasmic dipeptide transport protein	*dppA*	**Oligopeptide**
PSE_0438	PJE062_3451	BPD_transp_1	Dipeptide transport system permease protein DppB	*dppB*	
PSE_0439	PJE062_3076	BPD_transp_1	Dipeptide transport system permease protein DppC	*dppC*	
PSE_0440	PJE062_3241	ABC_tran	Dipeptide transport ATP-binding protein DppD	*dppD*	
PSE_0441	PJE062_3337	ABC_tran	Dipeptide transport ATP-binding protein DppF	*dppF*	
PSE_0443	PJE062_3229	Peripla_BP_1	D-ribose-binding protein	*rbsB*	**Sugar**
PSE_0444	PJE062_3285	ABC_tran	Ribose import ATP-binding protein RbsA	*rbsA*	
PSE_0445	PJE062_3140	BPD_transp_2	Ribose transport system permease protein RbsC	*rbsC*	

Table S 2.3. Continued

Locus FO-BEG1	Locus JE062	Pfam Model	Product	Gene	Predicted substrate specificity
PSE_0470	PJE062_2829	BPD_transp_1	sn-glycerol-3-phosphate transport system permease protein UgpE	*ugpE*	**Glycerol-3-phosphate**
PSE_0471	PJE062_2766	BPD_transp_1	sn-glycerol-3-phosphate transport system permease protein UgpA	*ugpA*	
PSE_0472	PJE062_3014	SBP_bac_1	sn-glycerol-3-phosphate-binding periplasmic protein UgpB	*ugpB*	
PSE_0473	PJE062_2743	ABC_tran	sn-glycerol-3-phosphate import ATP-binding protein UgpC	*ugpC*	
PSE_0528	PJE062_2554	SBP_bac_5	peptide ABC transporter, periplasmic peptide-binding protein		**Oligopeptide**
PSE_0529	PJE062_2658	SBP_bac_5	peptide ABC transporter, periplasmic peptide-binding protein		
PSE_0530	PJE062_2902	BPD_transp_1	peptide ABC transporter, permease protein		
PSE_0531	PJE062_2946	BPD_transp_1	peptide ABC transporter permease protein		
PSE_0532	PJE062_2818	ABC_tran	peptide ABC transporter, ATP-binding protein		
PSE_0587	PJE062_2984	FecCD	Hemin transport system permease protein HmuU	*hmuU*	**Hemin**
PSE_0588	PJE062_2677	Peripla_BP_2	Hemin-binding periplasmic protein HmuT	*hmuT*	
PSE_0589	PJE062_2700	ABC_tran	Hemin import ATP-binding protein HmuV	*hmuV*	
PSE_0680	PJE062_2538	SBP_bac_1	sn-glycerol-3-phosphate-binding periplasmic protein UgpB	*ugpB*	**Glycerol-3-phosphate**
PSE_0681	PJE062_2885	BPD_transp_1	sn-glycerol-3-phosphate transport system permease protein UgpA	*ugpA*	
PSE_0682	PJE062_2602	BPD_transp_1	sn-glycerol-3-phosphate transport system permease protein UgpE	*ugpE*	
PSE_0683	PJE062_2790	ABC_tran	sn-glycerol-3-phosphate import ATP-binding protein UgpC	*ugpC*	
PSE_0763	PJE062_2800	Bmp	ABC transporter, periplasmic binding protein		**Sugar**
PSE_0765	PJE062_2960	ABC_tran	Ribose import ATP-binding protein RbsA	*rbsA*	
PSE_0766	PJE062_2751	BPD_transp_2	sugar ABC transporter, permease protein		
PSE_0767	PJE062_2698	BPD_transp_2	sugar ABC transporter, permease protein		

Table S 2.3. Continued

Locus FO-BEG1	Locus JE062	Pfam Model	Product	Gene	Predicted substrate specificity
PSE_0856	PJE062_2634	ABC_tran	High-affinity branched-chain amino acid transport ATP-binding protein LivF (LIV-I protein F)	*livF*	**Amino acid**
PSE_0857	PJE062_2943	ABC_tran	High-affinity branched-chain amino acid transport ATP-binding protein LivG (LIV-I protein G)	*livG*	
PSE_0858	PJE062_2995	BPD_transp_2	High-affinity branched-chain amino acid transport system permease protein LivM (LIV-I protein M)	*livM*	
PSE_0859	PJE062_2944	BPD_transp_2	High-affinity branched-chain amino acid transport system permease protein LivH (LIV-I protein H)	*livH*	
PSE_0860	PJE062_2831	ANF_receptor	branched-chain amino acid ABC transporter, periplasmic substrate-binding protein		
PSE_0900	PJE062_2932	ABC_tran	Maltose/maltodextrin import ATP-binding protein MalK	*malK*	**Sugar**
PSE_0901	PJE062_2619	SBP_bac_1	sugar uptake ABC transporter periplasmic solute-binding protein		
PSE_0902	PJE062_2590	BPD_transp_1	sugar uptake ABC transporter permease protein		
PSE_0903	PJE062_2733	BPD_transp_1	sugar uptake ABC transporter permease protein		
PSE_0914	PJE062_2898	SBP_bac_1	sugar ABC transporter, periplasmic sugar-binding protein		**Sugar**
PSE_0915	PJE062_2980	BPD_transp_1	sugar ABC transporter, permease protein		
PSE_0916	PJE062_2684	BPD_transp_1	sugar ABC transporter, permease protein		
PSE_0918	PJE062_2573	ABC_tran	Lactose transport ATP-binding protein LacK	*lacK*	
PSE_0933	PJE062_2872	BPD_transp_1	Taurine transport system permease protein TauC	*tauC*	**Taurine**
PSE_0934	PJE062_2914	ABC_tran	Taurine import ATP-binding protein TauB	*tauB*	
PSE_0935	PJE062_2710	SBP_bac_3	Taurine-binding periplasmic protein	*tauA*	
PSE_1036	PJE062_4410	SBP_bac_1	uncharacterized ABC-type transport system, periplasmic component/surface lipoprotein		**Sugar**
PSE_1037	PJE062_4371	ABC_tran	Ribose import ATP-binding protein RbsA	*rbsA*	
PSE_1038	PJE062_4507	BPD_transp_2	permease protein, ABC-type sugar transporter		
PSE_1039	PJE062_4366	BPD_transp_2	sugar ABC transporter, permease protein		

Table S 2.3. Continued

Locus FO-BEG1	Locus JE062	Pfam Model	Product	Gene	Predicted substrate specificity
PSE_1120	PJE062_4425	ABC_tran	High-affinity branched-chain amino acid transport ATP-binding protein LivG (LIV-I protein G)	*livG*	**Amino acid**
PSE_1121	PJE062_4370	ABC_tran	High-affinity branched-chain amino acid transport ATP-binding protein LivF (LIV-I protein F)	*livF*	
PSE_1122	PJE062_4385	BPD_transp_2	High-affinity branched-chain amino acid transport system permease protein LivH (LIV-I protein H)	*livH*	
PSE_1123	PJE062_4430	BPD_transp_2	High-affinity branched-chain amino acid transport system permease protein LivM (LIV-I protein M)	*livM*	
PSE_1124	PJE062_4454	ANF_receptor	ABC branched amino acid transporter family, periplasmic substrate-binding protein		
PSE_1141	PJE062_2757	TonB_dep_Rec	Ferrichrome-iron receptor	*fhuA*	**Enterobactin**
PSE_1142	PJE062_2912	Peripla_BP_2	Ferrienterobactin-binding periplasmic protein	*fepB*	
PSE_1143	PJE062_2884	FecCD	Ferric enterobactin transport system permease protein FepD	*fepD*	
PSE_1144	PJE062_3038	FecCD	Ferric enterobactin transport system permease protein FepG	*fepG*	
PSE_1145	PJE062_2878	ABC_tran	Ferric enterobactin transport ATP-binding protein FepC	*fepC*	
PSE_1213	PJE062_4405	BPD_transp_2	High-affinity branched-chain amino acid transport system permease protein LivM (LIV-I protein M)	*livM*	**Amino acid**
PSE_1214	PJE062_4382	BPD_transp_2	High-affinity branched-chain amino acid transport system permease protein LivH (LIV-I protein H)	*livH*	
PSE_1215	PJE062_4456	ABC_tran	High-affinity branched-chain amino acid transport ATP-binding protein LivF (LIV-I protein F)	*livF*	
PSE_1216	PJE062_4457	ABC_tran	High-affinity branched-chain amino acid transport ATP-binding protein LivG (LIV-I protein G)	*livG*	
PSE_1217	PJE062_4428	SBF	P3 protein (Solute carrier family 10 member 3)		
PSE_1243	PJE062_4352	SBP_bac_1	Putrescine-binding periplasmic protein	*potF*	**Putrescine/ Spermidine**
PSE_1244	PJE062_4362	ABC_tran	Putrescine transport ATP-binding protein PotG	*potG*	
PSE_1245	PJE062_4348	BPD_transp_1	Putrescine transport system permease protein PotH	*potH*	
PSE_1246	PJE062_4343	BPD_transp_1	Putrescine transport system permease protein PotI	*potI*	

Table S 2.3. Continued

Locus FO-BEG1	Locus JE062	Pfam Model	Product	Gene	Predicted substrate specificity
PSE_1292	PJE062_1965	ABC_tran	Lactose transport ATP-binding protein LacK	*lacK*	
PSE_1294	PJE062_1894	SBP_bac_1	ABC transporter, substrate-binding protein		**Sugar**
PSE_1296	PJE062_1958	BPD_transp_1	sugar ABC transporter, permease protein,		
PSE_1297	PJE062_1975	BPD_transp_1	sugar ABC transporter, permease protein		
PSE_1322	PJE062_1888	ABC_tran	Zinc import ATP-binding protein ZnuC	*znuC*	
PSE_1323	PJE062_1960	ABC-3	High-affinity zinc uptake system membrane protein ZnuB	*znuB*	**Zinc**
PSE_1324	—	FUR	Zinc uptake regulation protein (Zinc uptake regulator)	*zur*	
PSE_2536	PJE062_14	SBP_bac_9	High-affinity zinc uptake system protein ZnuA	*znuA*	
PSE_1389	PJE062_5224	BPD_transp_1	sugar uptake ABC transporter permease protein		
PSE_1390	PJE062_5312	BPD_transp_1	sugar uptake ABC transporter permease protein		**Sugar**
PSE_1391	PJE062_5176	SBP_bac_1	extracellular solute-binding protein family 1		
PSE_1392	PJE062_5319	ABC_tran	Maltose/maltodextrin import ATP-binding protein MalK	*malK*	
PSE_1675	PJE062_116	SBP_bac_9	Manganese-binding lipoprotein MntA / periplasmic zinc-binding protein TroA	*mntA/troA*	
PSE_1676	PJE062_387	ABC_tran	Manganese transport system ATP-binding protein MntB / zinc transport system ATP-binding protein TroB	*mntB/troB*	**Manganese**
PSE_1677	PJE062_164	ABC-3	Manganese transport system membrane protein MntC / zinc transport system membrane protein TroC	*mntC/troC*	
PSE_1678	PJE062_301	ABC-3	Manganese transport system membrane protein MntD / zinc transport system membrane protein TroD	*mntD/troD*	
PSE_1679	PJE062_321	SBP_bac_1	Spermidine/putrescine-binding periplasmic protein 2	*potD*	
PSE_1681	PJE062_41	ABC_tran	Spermidine/putrescine import ATP-binding protein PotA	*potA*	**Putrescine/ Spermidine**
PSE_1682	PJE062_317	BPD_transp_1	Putrescine transport system permease protein PotH	*potH*	
PSE_1683	PJE062_261	BPD_transp_1	Spermidine/putrescine transport system permease protein PotC	*potC*	

Table S 2.3. Continued

Locus FO-BEG1	Locus JE062	Pfam Model	Product	Gene	Predicted substrate specificity
PSE_1688	PJE062_408	SBP_bac_1	phosphate ABC transporter, periplasmic binding protein	*pstS*	
PSE_1689	PJE062_354	BPD_transp_1	Phosphate transport system permease protein PstC	*pstC*	
PSE_1690	PJE062_413	BPD_transp_1	Phosphate transport system permease protein PstA	*pstA*	**Phosphate**
PSE_1691	PJE062_39	ABC_tran	Phosphate import ATP-binding protein PstB 1	*pstB*	
PSE_1692	PJE062_279	PhoU	Phosphate transport system protein PhoU	*phoU*	
PSE_1815	PJE062_176	Peripla_BP_1	periplasmic substrate-binding protein, ABC-type sugar transporter		
PSE_1816	PJE062_31	BPD_transp_2	sugar ABC transporter, permease protein		**Sugar**
PSE_1817	PJE062_162	ABC_tran	sugar ABC transporter, ATP-binding protein		
PSE_1875	PJE062_2861	SBP_bac_1	ABC sugar transporter extracellular solute-binding protein, family 1		
PSE_1876	PJE062_2615	BPD_transp_1	ABC-type sugar transport system, permease component		**Sugar**
PSE_1877	PJE062_3016	BPD_transp_1	ABC-type sugar transport system, permease component		
PSE_1878	PJE062_2608	ABC_tran	ABC-type sugar transport system, ATPase component		
PSE_1900	PJE062_4447	SBP_bac_1	Thiamine-binding periplasmic protein	*thiB*	
PSE_1901	PJE062_4491	BPD_transp_1	Thiamine transport system permease protein ThiP	*thiP*	**Thiamine**
PSE_1902	PJE062_4514	ABC_tran	Thiamine import ATP-binding protein ThiQ	*thiQ*	
PSE_1931	PJE062_859	NMT1	ABC-type sulfonate transport system periplasmic component		
PSE_1932	PJE062_632	BPD_transp_1	Aliphatic sulfonates transport permease protein SsuC	*ssuC*	**Sulfonates**
PSE_1933	PJE062_685	ABC_tran	Aliphatic sulfonates import ATP-binding protein SsuB	*ssuB*	
PSE_1938	PJE062_519	SBP_bac_1	iron(III) ABC transporter, substrate-binding protein		
PSE_1939	PJE062_888	BPD_transp_1	iron(III) transport system permease protein FbpB	*fbpB*	**Iron**
PSE_1940	PJE062_677	ABC_tran	Fe(3+) ions import ATP-binding protein FbpC	*fbpC*	

Table S 2.3. Continued

Locus FO-BEG1	Locus JE062	Pfam Model	Product	Gene	Predicted substrate specificity
PSE_1957	PJE062_572	SBP_bac_1	Sugar-binding periplasmic protein		
PSE_1958	PJE062_541	BPD_transp_1	ABC-type sugar transport systems, permease components		**Sugar**
PSE_1959	PJE062_553	BPD_transp_1	ABC sugar transporter inner membrane binding protein		
PSE_1960	PJE062_599	ABC_tran	Sugar ABC transporter, ATP-binding protein		
PSE_1987	PJE062_601	ABC_tran	Oligopeptide transport ATP-binding protein OppF	*oppF*	
PSE_1988	PJE062_645	ABC_tran	Oligopeptide transport ATP-binding protein OppD	*oppD*	
PSE_1989	PJE062_931	BPD_transp_1	Oligopeptide transport system permease protein OppC	*oppC*	**Oligopeptide**
PSE_1990	PJE062_886	BPD_transp_1	oligopeptide transport system permease protein OppB	*oppB*	
PSE_1991	PJE062_540	SBP_bac_5	Periplasmic oligopeptide-binding protein	*oppA*	
PSE_2045	PJE062_684	SBP_bac_5	oligopeptide ABC transporter, periplasmic oligopeptide-binding protein		
PSE_2048	PJE062_902	ABC_tran	Oligopeptide transport ATP-binding protein OppF	*oppF*	
PSE_2049	PJE062_662	ABC_tran	Oligopeptide transport ATP-binding protein OppD	*oppD*	**Oligopeptide**
PSE_2050	PJE062_554	BPD_transp_1	Glutathione transport system permease protein GsiD	*gsiD*	
PSE_2051	PJE062_901	BPD_transp_1	Glutathione transport system permease protein GsiC	*gsiC*	
PSE_2052	PJE062_642	SBP_bac_5	Glutathione-binding protein GsiB	*gsiB*	
PSE_2195	PJE062_510	SBP_bac_3	extracellular solute-binding protein family 3		
PSE_2196	PJE062_602	BPD_transp_1	Inner membrane amino-acid ABC transporter permease protein YecS		**Amino acid**
PSE_2532	PJE062_402	ABC_tran	Cysteine/glutathione ABC transporter membrane/ATP-binding component		
PSE_2229	PJE062_837	ABC_tran	ABC sugar transporter, ATPase subunit		
PSE_2230	PJE062_711	BPD_transp_2	ABC sugar transporter, inner membrane subunit		**Sugar**
PSE_2231	PJE062_898	Peripla_BP_1	ABC sugar transporter, periplasmic ligand binding protein		
PSE_2242	PJE062_557	ABC_tran	Fe(3+) ions import ATP-binding protein FbpC	*fbpC*	
PSE_2243	PJE062_594	BPD_transp_1	iron(III) transport system permease protein FbpB	*fbpB*	**Iron**
PSE_2244	PJE062_592	SBP_bac_1	Iron(III) binding periplasmic protein	*fpbA*	

Table S 2.3. Continued

Locus FO-BEG1	Locus JE062	Pfam Model	Product	Gene	Predicted substrate specificity
PSE_2252	PJE062_905	SBP_bac_5	Oligopeptide-binding protein AppA	*appA*	**Oligopeptide**
PSE_2253	PJE062_503	BPD_transp_1	Oligopeptide transport system permease protein OppB	*oppB*	
PSE_2254	PJE062_809	BPD_transp_1	Oligopeptide transport system permease protein OppC	*oppC*	
PSE_2255	PJE062_799	ABC_tran	Glutathione import ATP-binding protein GsiA	*gsiA*	
PSE_2267	PJE062_899	SBP_bac_3	Cystine-binding periplasmic protein		**Amino acid**
PSE_2268	PJE062_509	BPD_transp_1	polar amino acid ABC transporter, inner membrane subunit		
PSE_2531	—	ABC_tran	Cysteine/glutathione ABC transporter membrane/ATP-binding component		
PSE_2358	PJE062_12	ABC_tran	Ferrichrome transport ATP-binding protein FhuC	*fhuC*	**Ferrichrome**
PSE_2359	PJE062_245	FecCD	Ferrichrome transport system permease protein FhuG	*fhuG*	
PSE_2360	PJE062_4	FecCD	Ferrichrome transport system permease protein FhuB	*fhuB*	
PSE_2361	PJE062_378	Peripla_BP_2	Iron(III) dicitrate-binding periplasmic protein	*fecB*	
PSE_2389	PJE062_334	ABC_tran	ABC transporter, ATP-binding protein		**Oligopeptide**
PSE_2390	PJE062_243	SBP_bac_5	Periplasmic oligopeptide-binding protein	*oppA*	
PSE_2391	PJE062_43	BPD_transp_1	Oligopeptide transport system permease protein OppB	*oppB*	
PSE_2392	—	BPD_transp_1	Oligopeptide transport system permease protein OppC	*oppC*	
PSE_2393	PJE062_72	ABC_tran	Glutathione import ATP-binding protein GsiA	*gsiA*	
PSE_2493	PJE062_418	ABC_tran	Glutathione import ATP-binding protein GsiA	*gsiA*	**Oligopeptide**
PSE_2494	PJE062_435	SBP_bac_5	Periplasmic oligopeptide-binding protein	*oppA*	
PSE_2495	PJE062_318	BPD_transp_1	Oligopeptide transport system permease protein AppB	*appB*	
PSE_2496	PJE062_225	BPD_transp_1	Oligopeptide transport system permease protein AppC	*appC*	
PSE_2513	PJE062_36	BPD_transp_1	aliphatic sulfonates transport permease protein SsuC	*ssuC*	**Sulfonates**
PSE_2514	PJE062_24	ABC_tran	Aliphatic sulfonates import ATP-binding protein SsuB	*ssuB*	
PSE_2515	PJE062_383	SBP_bac_1	Putative aliphatic sulfonates-binding protein	*ssuA*	

Table S 2.3. Continued

Locus FO-BEG1	Locus JE062	Pfam Model	Product	Gene	Predicted substrate specificity
PSE_2520	PJE062_357	ABC_tran	Glutathione import ATP-binding protein GsiA	*gsiA*	**Oligopeptide**
PSE_2521	PJE062_204	BPD_transp_1	Glutathione transport system permease protein GsiD	*gsiD*	
PSE_2522	PJE062_434	BPD_transp_1	Glutathione transport system permease protein GsiC	*gsiC*	
PSE_2523	PJE062_42	SBP_bac_5	Glutathione-binding protein GsiB	*gsiB*	
PSE_2141	PJE062_513	ABC_tran	ATP-binding component of ABC transporter		
PSE_2564	PJE062_4100	BPD_transp_1	Nopaline transport system permease protein NocM	*nocM*	**Nopaline**
PSE_2565	PJE062_4285	BPD_transp_1	Nopaline transport system permease protein NocQ	*nocQ*	
PSE_2566	PJE062_4170	SBP_bac_3	Nopaline-binding periplasmic protein		
PSE_2567	PJE062_4189	SBP_bac_3	Nopaline-binding periplasmic protein		
PSE_2568	PJE062_4253	SBP_bac_3	Nopaline-binding periplasmic protein		
PSE_2638	PJE062_4138	SBP_bac_5	periplasmic dipeptide binding protein	*dppA*	**Oligopeptide**
PSE_2639	PJE062_4284	BPD_transp_1	Dipeptide transport system permease protein DppB	*dppB*	
PSE_2640	PJE062_4303	BPD_transp_1	Dipeptide transport system permease protein DppC	*dppC*	
PSE_2641	PJE062_4336	ABC_tran	Dipeptide transport ATP-binding protein DppD	*dppD*	
PSE_2642	PJE062_4101	ABC_tran	Dipeptide transport ATP-binding protein DppF	*dppF*	
PSE_2643	PJE062_4114	SBP_bac_5	periplasmic dipeptide transport protein	*dppA*	
PSE_2783	PJE062_1514	Peripla_BP_2	periplasmic binding protein		
PSE_2784	PJE062_1111	FecCD	Hemin transport system permease protein HmuU	*hmuU*	**Hemin**
PSE_2785	PJE062_1709	ABC_tran	Hemin import ATP-binding protein HmuV	*hmuV*	
PSE_2808	PJE062_1377	SBP_bac_5	Periplasmic alpha-galactoside-binding protein		
PSE_2809	PJE062_1731	BPD_transp_1	Oligopeptide transport system permease protein AppB	*appB*	**Oligopeptide**
PSE_2810	PJE062_1776	BPD_transp_1	Oligopeptide transport system permease protein AppC	*appC*	
PSE_2811	PJE062_1552	ABC_tran	Oligopeptide transport ATP-binding protein AppD	*appD*	

Table S 2.3. Continued

Locus FO-BEG1	Locus JE062	Pfam Model	Product	Gene	Predicted substrate specificity
PSE_2816	PJE062_1140	SBP_bac_1	sugar ABC transporter, periplasmic sugar-binding protein		
PSE_2817	PJE062_1562	BPD_transp_1	sugar ABC transporter, permease protein		**Sugar**
PSE_2818	PJE062_1154	BPD_transp_1	sugar ABC transporter, permease protein		
PSE_2819	PJE062_1225	ABC_tran	sugar ABC transporter, ATP-binding protein		
PSE_2868	PJE062_1053	SBP_bac_5	Oligopeptide-binding protein appA	*appA*	
PSE_2869	PJE062_1539	BPD_transp_1	Oligopeptide transport system permease protein AppB	*appB*	
PSE_2870	PJE062_1757	BPD_transp_1	Oligopeptide transport system permease protein AppC	*appC*	**Oligopeptide**
PSE_2871	PJE062_1524	ABC_tran	Oligopeptide transport ATP-binding protein AppD	*appD*	
PSE_2872	PJE062_1035	ABC_tran	Oligopeptide transport ATP-binding protein AppF	*appF*	
PSE_2879	PJE062_1337	RbsD_FucU	High affinity ribose transport protein RbsD	*rbsD*	
PSE_2880	PJE062_1777	ABC_tran	Ribose import ATP-binding protein RbsA	*rbsA*	**Sugar**
PSE_2881	PJE062_1423	BPD_transp_2	Ribose transport system permease protein RbsC	*rbsC*	
PSE_2882	PJE062_1180	Peripla_BP_1	D-ribose-binding periplasmic protein	*rbsB*	
PSE_2918	PJE062_1472	SBP_bac_1	extracellular solute-binding protein, family 1		
PSE_2919	PJE062_1003	BPD_transp_1	Maltose transport system permease protein MalF	*malF*	**Sugar**
PSE_2920	PJE062_1476	BPD_transp_1	Maltodextrin transport system permease protein MalD	*malD*	
PSE_2921	PJE062_1533	ABC_tran	Maltose/maltodextrin import ATP-binding protein MalK	*malK*	
PSE_2963	PJE062_1648	ANF_receptor	ABC transporter, urea, substrate-binding, UrtA	*urtA*	
PSE_2964	PJE062_1405	BPD_transp_2	urea ABC transporter, permease protein UrtB	*urtB*	
PSE_2965	PJE062_1553	BPD_transp_2	urea ABC transporter, permease protein UrtC	*urtC*	**Urea**
PSE_2966	PJE062_1288	ABC_tran	urea ABC transporter, ATP-binding protein UrtD	*urtD*	
PSE_2967	PJE062_1589	ABC_tran	urea ABC transporter, ATP-binding protein UrtE	*urtE*	
PSE_2977	PJE062_1645	BPD_transp_1	Glycine betaine/L-proline transport system permease protein ProW	*proW*	
PSE_2978	PJE062_1063	ABC_tran	Glycine betaine/L-proline transport ATP-binding protein ProV	*proV*	**Glycine betaine/ L-proline**
PSE_2979	PJE062_1143	OpuAC	Substrate-binding region of ABC-type glycine betaine transport system		

Table S 2.3. Continued

Locus FO-BEG1	Locus JE062	Pfam Model	Product	Gene	Predicted substrate specificity
PSE_2987	PJE062_1332	OpuAC	Choline-binding protein	*opuBC*	**Glycine betaine/ carnitine/choline**
PSE_2988	–	BPD_transp_1	Glycine betaine/carnitine/choline transport system permease protein OpuCD	*opuCD*	
PSE_2989	PJE062_1578	ABC_tran	Glycine betaine/carnitine/choline transport ATP-binding protein OpuCA	*opuCA*	
PSE_2990	PJE062_1498	BPD_transp_1	Glycine betaine/carnitine/choline transport system permease protein OpuCB	*opuCB*	
PSE_3097	PJE062_1174	Peripla_BP_2	Ferric anguibactin-binding protein	*fatB*	**Ferric anguibactin**
PSE_3098	PJE062_1095	FecCD	Ferric anguibactin transport system permease protein FatD	*fatD*	
PSE_3099	PJE062_1044	FecCD	Ferric anguibactin transport system permease protein FatC	*fatC*	
PSE_3100	PJE062_1329	ABC_tran	Ferrichrome transport ATP-binding protein FhuC	*fhuC*	
PSE_3153	PJE062_1631	ANF_receptor	Leu/Ile/Val-binding protein homolog	*livB*	**Amino acid**
PSE_3154	PJE062_1741	BPD_transp_2	High-affinity branched-chain amino acid transport system permease protein LivH (LIV-I protein H)	*livH*	
PSE_3155	PJE062_1386	BPD_transp_2	High-affinity branched-chain amino acid transport system permease protein LivM (LIV-I protein M)	*livM*	
PSE_3156	PJE062_1557	ABC_tran	High-affinity branched-chain amino acid transport ATP-binding protein LivG (LIV-I protein G)	*livG*	
PSE_3157	PJE062_1394	ABC_tran	High-affinity branched-chain amino acid transport ATP-binding protein LivF (LIV-I protein F)	*livF*	
PSE_3176	PJE062_1668	SBP_bac_1	ABC transporter periplasmic binding protein		**Sugar**
PSE_3177	PJE062_1420	BPD_transp_2	sugar ABC transporter, permease protein		
PSE_3178	PJE062_1239	BPD_transp_2	sugar ABC transporter, permease protein		
PSE_3179	PJE062_1523	ABC_tran	Ribose import ATP-binding protein RbsA	*rbsA*	

Table S 2.3. Continued

Locus FO-BEG1	Locus JE062	Pfam Model	Product	Gene	Predicted substrate specificity
PSE_3515	PJE062_1371	ABC_tran	Glutamate/glutamine/aspartate/asparagine transport ATP-binding protein BztD	*bztD*	**Amino acid**
PSE_3516	PJE062_1361	BPD_transp_1	Glutamate/glutamine/aspartate/asparagine transport system permease protein BztC	*bztC*	
PSE_3517	–	BPD_transp_1	Glutamate/glutamine/aspartate/asparagine transport system permease protein BztB	*bztB*	
PSE_3518	–	SBP_bac_3	Glutamate/glutamine/aspartate/asparagine-binding protein BztA	*bztA*	
PSE_3627	PJE062_1374	BPD_transp_1	Phosphonates transport system permease protein PhnE	*phnE*	**Phosphonate**
PSE_3628	PJE062_1147	BPD_transp_1	Phosphonates transport ATP-binding protein PhnL	*phnL*	
PSE_3629	PJE062_1356	SBP_bac_3	ABC transporter, phosphonate, periplasmic substrate-binding protein PhnD	*phnD*	
PSE_3630	PJE062_1025	ABC_tran	Phosphonates import ATP-binding protein PhnC	*phnC*	
PSE_3640	PJE062_1291	SBP_bac_1	ABC transporter, substrate binding protein (sugar)		**Sugar**
PSE_3641	PJE062_983	BPD_transp_1	ABC transporter, membrane spanning protein (sugar)		
PSE_3642	PJE062_1417	BPD_transp_1	ABC transporter, membrane spanning protein (sugar)		
PSE_3644	PJE062_1309	ABC_tran	ABC transporter, nucleotide binding/ATPase protein (sugar)		
PSE_3646	PJE062_1305	Peripla_BP_1	periplasmic binding protein/LacI transcriptional regulator		**Amino acid**
PSE_3647	PJE062_1083	SBP_bac_3	putative amino acid uptake ABC transporter periplasmic solute-binding protein		
PSE_3648	PJE062_1302	BPD_transp_1	Amino acid uptake ABC transporter permease protein		
PSE_3653	PJE062_1142	SBP_bac_1	Putrescine-binding periplasmic protein	*potF*	**Putrescine/ Spermidine**
PSE_3654	PJE062_1571	ABC_tran	Putrescine transport ATP-binding protein PotG	*potG*	
PSE_3655	PJE062_1526	BPD_transp_1	Putrescine transport system permease protein PotH	*potH*	
PSE_3656	PJE062_1564	BPD_transp_1	Putrescine transport system permease protein PotI	*potI*	

Table S 2.3. Continued

Locus FO-BEG1	Locus JE062	Pfam Model	Product	Gene	Predicted substrate specificity
PSE_3671	PJE062_1069	ABC_tran	High-affinity branched-chain amino acid transport ATP-binding protein LivF (LIV-I protein F)	*livF*	**Amino acid**
PSE_3672	PJE062_1719	ABC_tran	High-affinity branched-chain amino acid transport ATP-binding protein LivG (LIV-I protein G)	*livG*	
PSE_3673	PJE062_1499	BPD_transp_2	High-affinity branched-chain amino acid transport system permease protein LivM (LIV-I protein M)	*livM*	
PSE_3674	PJE062_1484	BPD_transp_2	High-affinity branched-chain amino acid transport system permease protein LivH (LIV-I protein H)	*livH*	
PSE_3675	PJE062_1325	ANF_receptor	Leu/Ile/Val-binding protein homolog 4	*livB*	
PSE_3919	–	BPD_transp_1	Maltose transport system permease protein MalG	*malG*	**Sugar**
PSE_3920	–	BPD_transp_1	Maltose transport system permease protein MalF	*malF*	
PSE_3921	–	SBP_bac_1	Maltose-binding periplasmic protein	*malE*	
PSE_3924	–	ABC_tran	Maltose/maltodextrin import ATP-binding protein MalK	*malK*	
PSE_3948	PJE062_4678	SBP_bac_1	extracellular solute-binding protein, family 1		**Sugar**
PSE_3950	–	BPD_transp_1	Multiple sugar-binding transport system permease protein MsmF	*msmF*	
PSE_3951	PJE062_5134	BPD_transp_1	L-arabinose transport system permease protein AraQ	*araQ*	
PSE_3953	PJE062_4603	ABC_tran	Alpha-glucoside transport ATP-binding protein AglK	*aglK*	
PSE_4021	PJE062_4745	ANF_receptor	Leu/Ile/Val-binding protein homolog	*livB*	**Amino acid**
PSE_4023	PJE062_44581	ABC_tran	High-affinity branched-chain amino acid transport ATP-binding protein LivF (LIV-I protein F)	*livF*	
PSE_4024	PJE062_4641	ABC_tran	High-affinity branched-chain amino acid transport ATP-binding protein LivG (LIV-I protein G)	*livG*	
PSE_4025	PJE062_4545	BPD_transp_2	High-affinity branched-chain amino acid transport system permease protein LivM (LIV-I protein M)	*livM*	
PSE_4026	PJE062_5154	BPD_transp_2	High-affinity branched-chain amino acid transport system permease protein LivH (LIV-I protein H)	*livH*	

Table S 2.3. Continued

Locus FO-BEG1	Locus JE062	Pfam Model	Product	Gene	Predicted substrate specificity
PSE_4503	PJE062_4774	BPD_transp_1	ABC transporter permease protein		
PSE_4504	PJE062_4712	BPD_transp_1	spermidine/putrescine ABC transporter membrane component		**Putrescine/ Spermidine**
PSE_4505	PJE062_5011	SBP_bac_1	extracellular solute-binding protein family 1		
PSE_4506	PJE062_4906	ABC_tran	putrescine/spermidine ABC transporter ATPase		
PSE_4557	PJE062_4521	ABC_tran	Dipeptide transport ATP-binding protein DppF	*dppF*	
PSE_4558	PJE062_2508	ABC_tran	Dipeptide transport ATP-binding protein DppD	*dppD*	
PSE_4559	PJE062_2469	BPD_transp_1	Dipeptide transport system permease protein DppC	*dppC*	**Oligopeptide**
PSE_4560	PJE062_2453	BPD_transp_1	Dipeptide transport system permease protein DppB	*dppB*	
PSE_4561	PJE062_2480	SBP_bac_5	Periplasmic dipeptide transport protein	*dppA*	
PSE_4562	PJE062_2473	ABC_tran	Maltose/maltodextrin import ATP-binding protein MalK	*malK*	
PSE_4564	PJE062_2457	BPD_transp_1	Maltose transport system permease protein MalG	*malG*	**Sugar**
PSE_4565	PJE062_2513	BPD_transp_1	Maltose transport system permease protein MalF	*malF*	
PSE_4566	PJE062_2461	SBP_bac_1	sugar ABC transporter, periplasmic sugar-binding protein		
PSE_4804	PJE062_2295	ABC_tran	High-affinity branched-chain amino acid transport ATP-binding protein BraG	*braG*	
PSE_4805	PJE062_2276	ANF_receptor	branched-chain amino acid ABC transporter, periplasmic branched-chain amino acid binding protein		
PSE_4806	PJE062_2012	BPD_transp_2	High-affinity branched-chain amino acid transport system permease protein BraE	*braE*	**Amino acid**
PSE_4807	PJE062_2240	BPD_transp_2	High-affinity branched-chain amino acid transport system permease protein BraD	*braD*	
PSE_4808	PJE062_2180	ABC_tran	High-affinity branched-chain amino acid transport ATP-binding protein BraF	*braF*	
PSE_4831	PJE062_2307	SBP_bac_5	Glutathione-binding protein GsiB	*gsiB*	
PSE_4832	PJE062_2293	BPD_transp_1	Dipeptide transport system permease protein DppB	*dppB*	**Oligopeptide**
PSE_4833	PJE062_2270	BPD_transp_1	Dipeptide transport system permease protein DppC	*dppC*	
PSE_4834	PJE062_2181	ABC_tran	Glutathione import ATP-binding protein GsiA	*gsiA*	

Table S 2.3. Continued

Locus FO-BEG1	Locus JE062	Pfam Model	Product	Gene	Predicted substrate specificity
PSE_4895	PJE062_2134	ABC_tran	amino-acid ABC transporter ATP-binding protein YecC	*yecC*	
PSE_4896	PJE062_2061	BPD_transp_1	amino-acid ABC transporter permease protein PatM	*patM*	**Amino acid**
PSE_4897	PJE062_2075	SBP_bac_3	amino-acid ABC transporter-binding protein PatH	*patH*	
PSE_4935	PJE062_2212	ABC_tran	Molybdenum import ATP-binding protein ModC	*modC*	
PSE_4936	PJE062_2256	BPD_transp_1	Molybdenum transport system permease protein ModB	*modB*	**Molybdenum**
PSE_4937	PJE062_2348	SBP_bac_1	Molybdate-binding periplasmic protein	*modA*	
PSE_4960	PJE062_2103	BioY	BioY protein	*bioY*	
PSE_4961	PJE062_2002	CbiQ	Cobalt transport protein	*cbiQ*	**Cobalt**
PSE_4962	PJE062_2254	ABC_tran	Cobalt import ATP-binding protein CbiO 1	*cbiO*	
PSE_5060	PJE062_4022	SBP_bac_1	ABC-type sugar transport system, periplasmic component		
PSE_5062	PJE062_4017	BPD_transp_1	sn-glycerol-3-phosphate transport system permease protein UgpE	*ugpE*	
PSE_5063	PJE062_3999	BPD_transp_1	sn-glycerol-3-phosphate transport system permease protein UgpA	*ugpA*	**Glycerol-3-phosphate**
PSE_5064	PJE062_3997	ABC_tran	sn-glycerol-3-phosphate import ATP-binding protein UgpC	*ugpC*	
PSE_5065	PJE062_4020	ABC_tran	sn-glycerol-3-phosphate import ATP-binding protein UgpC	*ugpC*	
PSE_p0066	PJE062_3787	Peripla_BP_1	D-ribose-binding protein	*rbsB*	
PSE_p0067	PJE062_3695	ABC_tran	Putative ribose/galactose/methyl galactoside import ATP-binding protein	*rgmG*	**Sugar**
PSE_p0068	PJE062_3689	BPD_transp_2	Galactoside transport system permease protein MglC	*mglC*	
PSE_p0070	PJE062_3838	ABC_tran	sn-glycerol-3-phosphate import ATP-binding protein UgpC	*ugpC*	
PSE_p0071	PJE062_3875	BPD_transp_1	sn-glycerol-3-phosphate transport system permease protein UgpE	*upgE*	**Glycerol-3-phosphate**
PSE_p0072	PJE062_3669	BPD_transp_1	sn-glycerol-3-phosphate transport system permease protein UgpA	*upgA*	
PSE_p0073	PJE062_3794	SBP_bac_1	sn-glycerol-3-phosphate-binding periplasmic protein UgpB	*upgB*	

Table S 2.3. Continued

Locus FO-BEG1	Locus JE062	Pfam Model	Product	Gene	Predicted substrate specificity
PSE_p0079	PJE062_3869	SBP_bac_1	ABC transporter, periplasmic binding-protein		
PSE_p0080	—	BPD_transp_1	Lactose transport system permease protein LacF	*lacF*	**Sugar**
PSE_p0081	—	BPD_transp_1	Multiple sugar-binding transport system permease protein MsmG	*msmG*	
PSE_p0082	PJE062_3781	ABC_tran	Maltose/maltodextrin import ATP-binding protein MalK	*malK*	
PSE_p0179	PJE062_3795	BPD_transp_1	Spermidine/putrescine transport system permease protein PotB	*potB*	
PSE_p0180	PJE062_3917	BPD_transp_1	Putrescine transport system permease protein PotH	*potH*	**Putrescine/ Spermidine**
PSE_p0181	PJE062_3909	SBP_bac_1	ABC transporter, periplasmic substrate-binding protein		
PSE_p0182	PJE062_3834	ABC_tran	Spermidine/putrescine import ATP-binding protein PotA	*potA*	
PSE_p0206	PJE062_3717	ABC_tran	sugar ABC transporter, ATP-binding protein		
PSE_p0210	PJE062_3844	BPD_transp_1	L-arabinose transport system permease protein AraQ	*araQ*	
PSE_p0211	PJE062_3654	BPD_transp_1	starch degradation products transport system permease protein AmyD	*amyD*	**Sugar**
PSE_p0212	PJE062_3625	SBP_bac_1	ABC-type sugar transport system, periplasmic component		
PSE_p0237	PJE062_3796	ABC_tran	Oligopeptide transport ATP-binding protein AppF	*appF*	
PSE_p0238	PJE062_3619	BPD_transp_1	Oligopeptide transport system permease protein AppC	*appC*	**Oligopeptide**
PSE_p0239	PJE062_3887	BPD_transp_1	Oligopeptide transport system permease protein AppB	*appB*	
PSE_p0240	PJE062_3972	SBP_bac_5	Periplasmic dipeptide transport protein	*dppA*	
PSE_p0350	PJE062_3636	ABC_tran	Oligopeptide transport ATP-binding protein AppF	*appF*	
PSE_p0351	—	ABC_tran	Oligopeptide transport ATP-binding protein OppD	*oppD*	
PSE_p0352	PJE062_3745	BPD_transp_1	Probable D,D-dipeptide transport system permease protein DdpC	*dppC*	**Oligopeptide**
PSE_p0353	PJE062_3770	BPD_transp_1	Glutathione transport system permease protein GsiC	*gsiC*	
PSE_p0354	PJE062_3690	SBP_bac_5	Periplasmic dipeptide transport protein	*dppA*	

Table S 2.4. Genes detected in the genomes of *Pseudovibrio* sp. FO-BEG1 and JE062 coding for predicted peptidases/proteases and proteins involved in protection against reactive oxygen species (ROS). Genes that could not be detected in the not closed genome of strain JE062 are indicated with '—'. Absence of a gene name or an EC number indicates that no assignment was made due to missing of these parameters for the respective genes.

Locus FO-BEG1	Locus JE062	Product	Gene	EC
		Peptidases /Proteases		
PSE_0001	PJE062_3184	Peptidase M23/M37 family protein		
PSE_0229	PJE062_3278	Peptidase family M48		
PSE_0251	PJE062_3407	Peptidase family S41		
PSE_0273	PJE062_3414	D-alanyl-D-alanine carboxypeptidase	*dacC*	
PSE_0434	—	Peptidase family M48		
PSE_0464	—	Peptidase M75, Imelysin		
PSE_0466	PJE062_2551	Peptidase M75, Imelysin		
PSE_0494	PJE062_2791	Peptidase M22, glycoprotease		
PSE_0563	PJE062_2577	Pyrrolidone-carboxylate peptidase	*pcp*	3.4.19.3
PSE_0669	PJE062_2688	Peptidase family S49		
PSE_0709	PJE062_2578	Peptidase family S41		
PSE_0710	PJE062_2576	Peptidase M23		
PSE_0811	PJE062_2788	Peptidase family U32		
PSE_0812	PJE062_2571	Peptidase family U32		
PSE_0992	PJE062_2365	Penicillin-insensitive murein endopeptidase precursor/D-alanyl-D-alanine-endopeptidase	*mepA*	3.4.24.-
PSE_1070	PJE062_4381	Type IV leader peptidase family		
PSE_1080	PJE062_4511	Cytosol aminopeptidase/leucine aminopeptidase	*pepA*	3.4.11.1
PSE_1106	PJE062_4512	Peptidase M19, renal dipeptidase		
PSE_1182	—	Dipeptidase 1/Microsomal dipeptidase		
PSE_1188	—	Metallopeptidase family M24		
PSE_1495	PJE062_5268	Peptidase M16 family protein		
PSE_1496	PJE062_5323	Peptidase M16 family protein		
PSE_1498	PJE062_5212	Lipoprotein signal peptidase	*lspA*	3.4.23.36
PSE_1533	PJE062_182	Peptidase U62, modulator of DNA gyrase		
PSE_1565	PJE062_241	Peptidase M16 family protein		
PSE_1568	PJE062_410	D-alanyl-D-alanine carboxypeptidase		
PSE_1618	PJE062_92	Peptidase family S49		
PSE_1833	—	Peptidase M24		
PSE_1842	—	Peptidase M24		
PSE_2257	PJE062_671	Peptidase M23B		
PSE_2285	PJE062_817	Peptidase family M20/M25/M40		
PSE_2356	PJE062_223	Peptidase family M20/M25/M40		
PSE_2396	PJE062_57	Peptidase M19, renal dipeptidase		
PSE_2422	PJE062_398	Peptidase family M20/M25/M40		
PSE_2435	PJE062_293	Protease 2/Oligopeptidase B	*ptrB*	3.4.21.83
PSE_2461	PJE062_207	Peptidase U35, phage prohead HK97		
PSE_2472	PJE062_117	Phage cell wall peptidase, NlpC/P60		
PSE_2490	PJE062_382	Aminopeptidase N (Alpha-aminoacylpeptide hydrolase)	*ampN*	3.4.11.2
PSE_2733	PJE062_4294	Cytosol aminopeptidase/Leucine aminopeptidase	*ampA*	3.4.11.1

Table S 2.4. Continued

Locus FO-BEG1	Locus JE062	Product	Gene	EC
PSE_2795	PJE062_1383	Peptidase family M20/M25/M40		
PSE_2941	PJE062_1153	Peptidase family M20/M25/M40		
PSE_2997	PJE062_1623	Prolyl oligopeptidase family		
PSE_3040	–	Clp protease		
PSE_3062	–	Peptidase M15		
PSE_3141	PJE062_1066	D-alanyl-D-alanine carboxypeptidase	*dacA*	3.4.16.4
PSE_3234	PJE062_1678	Peptidase M23B		
PSE_3404	PJE062_1716	Peptidase family M50		3.4.24.-
PSE_3468	PJE062_1772	Peptidase M23B		
PSE_3475	–	Peptidase family M48		
PSE_3524	–	Peptidyl-dipeptidase dcp (Dipeptidyl carboxypeptidase)	*dcp*	3.4.15.5
PSE_3609	PJE062_1430	Signal peptidase I	*lepB*	3.4.21.89
PSE_3808	PJE062_3548	D-alanyl-D-alanine carboxypeptidase	*dacF*	3.4.16.4
PSE_3821	–	Clp protease		3.4.21.92
PSE_3979	PJE062_5150	Transglutaminase-like cysteine peptidase		
PSE_3998	PJE062_4868	Methionine aminopeptidase (MAP) (Peptidase M)	*map*	3.4.11.18
PSE_4028	PJE062_4576	Peptidase S58, DmpA		
PSE_4247	PJE062_5063	Xaa-Pro aminopeptidase 1	*xpp1*	3.4.11.9
PSE_4285	PJE062_5046	Peptidase T	*pepT*	3.4.11.4
PSE_4388	PJE062_5031	Prolyl oligopeptidase family		
PSE_4435	PJE062_4791	Xaa-Pro dipeptidase	*pepQ*	3.4.13.9
PSE_4669	PJE062_2225	M42 glutamyl aminopeptidase		
PSE_4674	PJE062_2053	Cell division protease FtsH homolog	*ftsH*	3.6.4.3
PSE_4759	PJE062_2089	Oligoendopeptidase F homolog		
PSE_4873	PJE062_2076	Peptidase family M48		
PSE_4884	PJE062_2338	O-sialoglycoprotein endopeptidase (Glycoprotease)	*gcp*	3.4.24.57
PSE_4893	PJE062_1994	Peptidase family M20/M25/M40		
PSE_4926	PJE062_2084	Peptidase U32		
PSE_5035	PJE062_4092	Peptidase S58, DmpA		
PSE_0055	PJE062_3479	CAAX protease family protein		
PSE_0097	PJE062_3209	ATP-dependent protease La, LON		
PSE_0489	PJE062_2770	ATP-dependent protease peptidase subunit	*hslV*	3.4.25.-
PSE_0491	PJE062_2610	ATP-dependent hsl protease ATP-binding subunit HslU	*hslU*	
PSE_0494	PJE062_2791	Peptidase M22, glycoprotease		
PSE_0709	PJE062_2578	Peptidase family S41		
PSE_0869	PJE062_2969	Serralysin		3.4.24.40
PSE_0880	PJE062_3017	zinc protease pqqL	*pqqL*	3.4.99.-
PSE_2435	PJE062_293	Protease 2/Oligopeptidase B	*ptrB*	3.4.21.83
PSE_2484	PJE062_401	Serine protease	*degP1*	3.4.21.-
PSE_2726	PJE062_4115	Serine protease		
PSE_3446	PJE062_1826	ATP-dependent protease La	*lon*	3.4.21.53
PSE_3447	PJE062_1775	ATP-dependent Clp protease ATP-binding subunit clpX	*clpX*	
PSE_3448	PJE062_1602	ATP-dependent Clp protease proteolytic subunit (Endopeptidase Clp)	*clpP*	3.4.21.92
PSE_3805	PJE062_3583	ATP-dependent Clp protease ATP-binding subunit clpA	*clpA*	

Table S 2.4. Continued

Locus FO-BEG1	Locus JE062	Product	Gene	EC
PSE_3806	PJE062_3584	ATP-dependent Clp protease adapter protein clpS 1	*ClpS*	
PSE_3852	PJE062_4839	Serine protease		
PSE_4208	PJE062_5075	Intracellular protease 1 (Intracellular protease I)	*pfpI*	
PSE_4228	PJE062_4726	Trypsin-like serine protease		
PSE_4718	PJE062_1984	Zinc protease		
PSE_4884	PJE062_2338	O-sialoglycoprotein endopeptidase (Glycoprotease)	*gcp*	3.4.24.57
		Protection against reactive oxygen species		
PSE_0143	PJE062_3455	Copper/zinc superoxide dismutase	*sodC*	1.15.1.1
PSE_2428	PJE062_90	Manganese/iron superoxide dismutase	*sodF*	1.15.1.1
		Catalase		
PSE_1899	PJE062_693	Peroxidase/catalase (Catalase-peroxidase)	*catA*	1.11.1.6
PSE_4005	PJE062_4983	Catalase	*catA*	1.11.1.6
PSE_0100	PJE062_3343	Cytochrome c551 peroxidase (Cytochrome c peroxidase) (CCP)	*ccpR*	
PSE_0180	PJE062_3475	Thioredoxin peroxidase	*tdx*	
PSE_0181	PJE062_3303	Alkylhydroperoxidase AhpD	*ahpD*	
PSE_0722	—	Peroxiredoxin, OsmC-like protein	*osmC*	
PSE_1918	PJE062_770	Alkyl hydroperoxide reductase/ Thiol specific antioxidant/ Mal allergen		
PSE_1949	PJE062_923	Di-heme cytochrome c peroxidase		
PSE_2025	PJE062_566	Alkylhydroperoxidase AhpD		
PSE_2156	PJE062_603	Alkyl hydroperoxide reductase/ Thiol specific antioxidant/ Mal allergen		
PSE_2209	PJE062_579	Alkyl hydroperoxide reductase/ Thiol specific antioxidant/ Mal allergen		
PSE_2511	PJE062_470	Alkyl hydroperoxide reductase/ Thiol specific antioxidant/ Mal allergen		
PSE_2926	PJE062_1164	Di-heme cytochrome c peroxidase		
PSE_3314	—	Alkyl hydroperoxide reductase/ Thiol specific antioxidant/ Mal allergen		
PSE_3466	PJE062_1662	Alkyl hydroperoxide reductase/ Thiol specific antioxidant/ Mal allergen		
PSE_3521	PJE062_1626	Phosphatidic acid phosphatase type 2/haloperoxidase		
PSE_3918	—	Alkyl hydroperoxide reductase/ Thiol specific antioxidant/ Mal allergen		
PSE_4045	PJE062_4776	Alkyl hydroperoxide reductase/ Thiol specific antioxidant/ Mal allergen		
PSE_4466	PJE062_4550	Organic hydroperoxide resistance protein		
PSE_5045	PJE062_4053	Di-heme cytochrome c peroxidase		
PSE_5046	PJE062_4061	Di-heme cytochrome c peroxidase		
PSE_p0159	PJE062_3672	Di-heme cytochrome c peroxidase		
PSE_p0165	PJE062_3748	Alkylhydroperoxidase AhpD		
PSE_p0321	PJE062_3655	Alkylhydroperoxidase AhpD		

Table S 2.5. Genes detected in the genomes of *Pseudovibrio* sp. FO-BEG1 and JE062 coding for predicted proteins involved vitamin synthesis. Genes that could not be detected in the not closed genome of strain JE062 are indicated with '—'. Absence of a gene name or an EC number indicates that no assignment was made due to missing of these parameters for the respective genes.

Locus FO-BEG1	Locus JE062	Product	Gene	EC
		Vitamin B1 Thiamine[a)]		
PSE_0621	PJE062_2616	Thiamine-phosphate pyrophosphorylase	*thiE*	2.5.1.3
PSE_0622	PJE062_2638	Hydroxyethylthiazole kinase	*thiM*	2.7.1.50
PSE_0906	PJE062_2968	Thiamine biosynthesis protein ThiF	*thiF*	2.7.7.-
PSE_0907	PJE062_2761	Thiamine-phosphate pyrophosphorylase	*thiE*	2.5.1.3
PSE_0908	PJE062_2880	Thiazole biosynthesis protein ThiG	*thiG*	
PSE_0909	PJE062_2900	ThiS, thiamine-biosynthesis	*thiS*	
PSE_0910	PJE062_2986	Thiamine biosynthesis oxidoreductase ThiO	*thiO*	1.4.3.19
PSE_0911	PJE062_2936	Thiamine biosynthesis protein ThiC	*thiC*	
PSE_3819	PJE062_5088	Thiamine-phosphate pyrophosphorylase	*thiE*	2.5.1.3
PSE_4137	PJE062_5017	Phosphomethylpyrimidine kinase	*thiD*	2.7.4.7
PSE_4138	PJE062_4585	Hydroxyethylthiazole kinase	*thiM*	2.7.1.50
PSE_4699	PJE062_2332	Thiamine-phosphate pyrophosphorylase	*thiE*	2.5.1.3
PSE_1900	PJE062_4447	Thiamine-binding periplasmic protein	*thiB*	
PSE_1901	PJE062_4491	Thiamine transport system permease protein ThiP	*thiP*	
PSE_1902	PJE062_4514	Thiamine import ATP-binding protein ThiQ	*thiQ*	
PSE_3582	PJE062_1837	Thiamine-monophosphate kinase	*thiL*	
PSE_2998	PJE062_1279	Cysteine desulfurase, NifS	*nifS/iscS*	2.8.1.7
PSE_1658	PJE062_60	1-deoxy-D-xylulose-5-phosphate synthase	*dxpS*	2.2.1.7
PSE_3005	PJE062_1473	TENA/THI-4/PQQC family	*tenA*	3.5.99.2
PSE_4898	PJE062_2346	TENA/THI-4/PQQC family	*tenA*	3.5.99.2
		Vitamin B2 Riboflavin[b)]		
PSE_1646	PJE062_256	Riboflavin biosynthesis protein RibBA (3,4-dihydroxy-2-butanone 4-phosphate synthase/GTP cyclohydrolase-2)	*ribBA*	3.5.4.25/ 4.1.99.12
PSE_0835	PJE062_3009	Riboflavin biosynthesis protein RibD (Diaminohydroxyphosphoribosylaminopyrimidine deaminase/5-amino-6-(5-phosphoribosylamino)uracil reductase)	*ribD*	3.5.4.26/ 1.1.1.93
PSE_3584	PJE062_1363	Riboflavin synthase beta chain	*risB*	
PSE_3585	—	Riboflavin synthase alpha chain	*risA*	2.5.1.9
PSE_3586	PJE062_977	Riboflavin biosynthesis protein RibD (Diaminohydroxyphosphoribosylaminopyrimidine deaminase/5-amino-6-(5-phosphoribosylamino)uracil reductase)	*ribD*	3.5.4.26/ 1.1.1.193
PSE_1503	PJE062_5201	Riboflavin biosynthesis protein ribF (Riboflavin kinase/ FMN adenylyltransferase)	*ribF*	2.7.1.26/ 2.7.7.2
		Vitamin B9 Folic acid[c)]		
PSE_0236	PJE062_3408	GTP cyclohydrolase 1	*folE*	3.5.4.16
PSE_3972	PJE062_4864	GTP cyclohydrolase 1	*folE*	3.5.4.16
PSE_2813	PJE062_994	Alkaline phosphatase		3.1.3.1
PSE_5052	PJE062_3977	Alkaline phosphatase		3.1.3.1
PSE_3836	PJE062_4956	Dihydroneopterin aldolase (DHNA)	*folB*	4.1.2.25

Table S 2.5. Continued

Locus FO-BEG1	Locus JE062	Product	Gene	EC
PSE_0133	PJE062_3459	2-amino-4-hydroxy-6-hydroxymethyldihydropteridine pyrophosphokinase	*folK*	2.7.6.3
PSE_0134	PJE062_3328	Dihydropteroate synthase (DHPS)	*folP*	2.5.1.15
PSE_0339	PJE062_3466	Bifunctional protein folC (Folylpolyglutamate synthase/Dihydrofolate synthase)	*folC*	6.3.2.12/ 6.3.2.17
PSE_4234	–	Dihydrofolate reductase type III DHFR	*folA*	1.5.1.3
		Vitamin B12 Cobalamin[d)]		
PSE_0073	PJE062_3117	Aerobic cobaltochelatase subunit CobS	*cobS*	6.6.1.2
PSE_0074	PJE062_3423	Aerobic cobaltochelatase subunit CobT	*cobT*	6.6.1.2
PSE_0272	PJE062_3130	Cobalamin (vitamin B12) biosynthesis CobW-like	*cobW*	
PSE_0298	PJE062_3171	Cobyrinic acid a,c-diamide synthase		
PSE_0823	PJE062_2890	Sirohydrochlorin cobaltochelatase (CbiX)	*cbiX*	4.99.1.3
PSE_0824	PJE062_2592	Precorrin-8X methylmutase/Precorrin isomerase CobH/CbiC	*cobH/cbiC*	1.7.7.1/ 5.4.1.2
PSE_0825	PJE062_2904	Precorrin-6Y C(5,15)-methyltransferase CobL/CbiE/CbiT	*cobL/cbiE/cbiT*	2.1.1.132
PSE_0826	PJE062_3055	Precorrin-2 C(20)-methyltransferase CobI/CbiL	*cobI/cbiL*	2.1.1.130
PSE_0827	PJE062_3024	Precorrin-3B C(17)-methyltransferase CobJ/CibH/GbiG	*cobJ/cibH/cbiG*	2.1.1.131
PSE_0828	PJE062_2713	Precorrin-4 C(11)-methyltransferase CobM/CbiF	*cobM/cbiF*	2.1.1.133
PSE_0829	PJE062_2999	Cobyrinic acid A,C-diamide synthase CobB/CbiA	*cobB/cbiA*	6.3.5.9
PSE_0830	PJE062_2731	Uroporphyrinogen-III C-methyltransferase	*cobA*	2.1.1.107
PSE_0832	PJE062_2996	Cobalt-precorrin-6A synthase	*cbiD*	
PSE_0833	PJE062_2650	Precorrin-6A reductase CobK/CbiJ	*cobK/cbiJ*	1.3.1.54
PSE_2555	PJE062_4304	Cobalamin (5'-phosphate) synthase CobS/CobV	*cobS/cobV*	2.7.8.26
PSE_2556	PJE062_4127	Nicotinate-nucleotide-dimethylbenzimidazole phosphoribosyltransferase (CobT/CobU)	*cobT/cobU*	2.4.2.21
PSE_3492	PJE062_1509	Cobalamin biosynthesis protein CobD/CbiB	*cobD/cbiB*	6.3.1.10
PSE_3493	PJE062_1793	Cobyric acid synthase CobQ/CobB	*cobQ/cobB*	6.3.5.10
PSE_3494	PJE062_1191	Cob(I)yrinic acid a,c-diamide adenosyltransferase (CobA/CobO)	*cobA/cobO*	2.5.1.17
PSE_3495	PJE062_1559	Aerobic cobaltochelatase subunit cobN	*cobN*	6.6.1.2
PSE_3496	PJE062_1259	Cobalamin (vitamin B12) biosynthesis CobW	*cobW*	
PSE_3497	PJE062_1011	Bifunctional adenosylcobalamin biosynthesis protein CobP/CobU (Adenosylcobinamide kinase/Adenosylcobinamide-phosphate guanylyltransferase)	*cobP/cobU*	2.7.1.156/ 2.7.7.62
PSE_4445	PJE062_4542	Cob(II)yrinic acid a,c-diamide reductase	*bluB*	1.16.8.1
PSE_4713	–	Cobyrinic acid a,c-diamide synthase CobQ/CobB	*cobQ/cobB*	
PSE_4818	PJE062_2023	Cobalamin (vitamin B12) biosynthesis CobW	*cobW*	
PSE_3491	PJE062_1667	Threonine-phosphate decarboxylase CobC/CobD	*cobC/cobD*	4.1.1.81
		Vitamin B6 Pyridoxine[e)]		
PSE_4671	PJE062_1992	Phosphoserine aminotransferase (PdxF)	*serC/pdxF*	2.6.1.52

Table S 2.5. Continued

Locus FO-BEG1	Locus JE062	Product	Gene	EC
PSE_1564	PJE062_153	Threonine synthase	*thrC*	4.2.3.1
PSE_2728	PJE062_4225	4-hydroxythreonine-4-phosphate dehydrogenase	*pdxA*	1.1.1.262
PSE_4205	PJE062_4768	Pyridoxine 5'-phosphate synthase	*pdxJ*	2.6.99.2
PSE_p0050	PJE062_3885	Pyridoxamine kinase	*pdxY*	2.7.1.35
PSE_0084	–	Pyridoxine kinase/Pyridoxal kinase/Pyridoxamine kinase	*pdxK*	2.7.1.35
PSE_1669	PJE062_333	Pyridoxine/pyridoxamine 5'-phosphate oxidase	*pdxH*	1.4.3.5
PSE_1658	PJE062_60	1-deoxy-D-xylulose-5-phosphate synthase	*dxpS*	2.2.1.7
		Vitamin H Biotin[f)]		
PSE_3083	PJE062_1792	Biotin synthase	*bioB*	2.8.1.6
PSE_3084	PJE062_1708	8-amino-7-oxononanoate synthase	*bioF*	2.3.1.47
PSE_3085	PJE062_1407	Dethiobiotin synthetase	*bioD*	6.3.3.3
PSE_3086	PJE062_1813	Adenosylmethionine-8-amino-7-oxononanoate aminotransferase	*bioA*	2.6.1.62
PSE_3087	PJE062_1055	3-oxoacyl-[acyl-carrier-protein] synthase 3	*bioZ*	2.3.1.180
		Lipoic acid[g)]		
PSE_3289	PJE062_975	Lipoyl synthase	*lipA*	2.8.1.8
PSE_3828	PJE062_4856	Octanoyltransferase	*lipB*	2.3.1.181

[a)] Thiamin (Vitamin B1)

For the biosynthesis of vitamin B_1, thiazole and pyrimidine must be synthesized via different pathways and then combined to thiamin phosphate (Begley *et al.*, 1999; Jurgenson *et al.*, 2009). We identified genes encoding the enzymes of the pyrimidine branch as well as the proteins responsible for the formation of thiazole, including TihO for aerobic formation of dehydroglycine as the final step of the thiazole formation and the key enzyme ThiE performing the linkage of thiazole and pyrimidine to thiamin phosphate and the subsequent phosphorylation to the vitamin thiamin pyrophosphate via ThiL (Jurgenson *et al.*, 2009).

[b)] Riboflavin (Vitamin B2)

Vitamin B_2 is required for numerous reactions and processes and is produced by plants and microorganisms, but must be taken up by animals (Fischer and Bacher, 2005). The presence of the key enzymes GTP cyclohydrolase II, which is required for the conversion of GTP as the first step of the pathway, riboflavin synthase and lumazine synthase, catalyzing the formation of riboflavin and the re-utilization of the by-product 5-amino-6-ribitylamino-2,4(1*H*,3*H*)-pyrimidinedion, respectively, as well as other enzymes described to be required for this *de novo* synthesis (Fischer and Bacher, 2005) in both genomes indicates the capability to produce vitamin B_2 by both strains.

c) Folic acid (Vitamin B9)

Tetrahydrofolate, a biochemical derivate of the folic acid, serves as a donor and acceptor of one-carbon units in a number of anabolic and catabolic processes (Bermingham and Derrick, 2002). All enzymes reported to be required for the formation of folate have been detected in strain FO-BEG1 (in JE062, the dehydrofolate reductase is missing), except for DHNE and DHPP. The roles of 7,8-dihydoneopterin triphosphate epimerase (DHNE) and 7,8-dihydroneopterin triphosphate pyrophosphohydrolase (DHPP) are not clarified yet (Bermingham and Derrick, 2002) and it is questionable, whether they are at all involved in the *de novo* synthesis of folic acid. The capability of strain FO-BEG1 to grow without the external supply of vitamins implies that folate is synthesized in this strain.

d) Cobalamin (Vitamin B12)

The *de novo* synthesis of cobalamin is restricted to prokaryotes and the vitamin must be taken up by other living organisms for the function of several enzymes like methionine synthase and methylmalony-CoA mutase (Martens *et al.*, 2002). The biosynthesis of vitamin B_{12} is a complex process that requires an array of enzymes. Two pathways exist for the *de novo* synthesis of cobalamin – the aerobic synthesis, in which cobalt is inserted into the molecule via the proteins CobN, CobS and CobT, and the anaerobic pathway with CbiX as the enzyme responsible for cobalt insertion. Genes for both pathways are present in analyzed genomes of *Pseudovibrio*, CobG, however, a key enzyme in the oxygen-dependent pathway, seems to be missing. A cobalamin biosynthesis pathway of similar structure has been reported for the *Roseobacter* clade already and vitamin B_{12} production has indeed been shown in *Dinoroseobacter shibae* DFL12, a symbiont of marine algae (Wagner-Döbler *et al.*, 2010).

e) Pyridoxine (Vitamin B6)

Only prokaryotes and plants can *de novo* synthesize vitamin B_6, other eukaryotes must take it up. It is a cofactor of over 100 enzymatic reactions, predominantly in the amino acid metabolism (Fitzpatrick *et al.*, 2007). In both genomes we could identify genes *pdxA, pdxJ* and *dxpS* coding for the key enzymes of the so-called DXP-dependent pathway, which leads to the condensation of the vitamer pyridoxine 5´-phosphate (PNP) (Fitzpatrick *et al.*, 2007). Furthermore, the synthesized PNP can be interconverted via the salvage pathway, which is completely present in the genome, into other vitamer forms of vitamin B_6 (Mooney *et al.*, 2009).

f) Biotin (Vitamin H)

A complete operon for the synthesis of biotin consisting of *bioB, bioF, bioD, bioA and bioZ* was found in the genome of *Pseudovibrio* FO-BEG1 and JE062. The arrangement of the genes is identical with the described operon of *Mesorhizobium* sp. (Sullivan *et al.*, 2001), a symbiotic α-proteobacterium found in the soil, containing the unique gene *bioZ* that is proposed to be involved in pimeloyl-CoA synthesis in the first steps of biotin formation (Guillén-Navarro *et al.*, 2005; Streit and Entcheva, 2003). Importantly, the operon is functional and has been proven to produce biotin if expressed.

g) Lipoic acid

For the endogenous synthesis of lipoic acid as a branch from the fatty acid biosynthesis, LipB and LipA are required, a lipoyl (octanoyl)-transferase and an enzyme catalyzing the sulfur insertion into the molecule, respectively (Booker, 2004). Genes encoding both proteins were identified in both genomes.

References

Begley TP, Downs DM, Ealick SE, McLafferty FW, Van Loon APGM, Taylor S *et al.* (1999). Thiamin biosynthesis in prokaryotes. *Arch Microbiol* **171:** 293–300.

Bermingham A, Derrick JP. (2002). The folic acid biosynthesis pathway in bacteria: evaluation of potential for antibacterial drug discovery. *BioEssays* **24:** 637–648.

Booker SJ. (2004). Unraveling the pathway of lipoic acid biosynthesis. *Chem Biol* **11:** 10–12.

Fischer M, Bacher A. (2005). Biosynthesis of flavocoenzymes. *Nat Prod Rep* **22:** 324–350.

Fitzpatrick TB, Amrhein N, Kappes B, Macheroux P, Tews I, Raschle T. (2007). Two independent routes of *de novo* vitamin B_6 biosynthesis: not that different after all. *Biochem J* **407:** 1–13.

Guillén-Navarro K, Encarnación S, Dunn MF. (2005). Biotin biosynthesis, transport and utilization in rhizobia. *FEMS Microbiol Lett* **246:** 1591–1565.

Jurgenson CT, Begley TP, Ealick SE. (2009). The structural and biochemical foundations of thiamin biosynthesis. *Annu Rev Biochem* **78:** 569–603.

Martens JH, Barg H, Warren MJ, Jahn D. (2002). Microbial production of vitamin B_{12}. *Appl Microbiol Biotechnol* **58:** 275–285.

Mooney S, Leuendorf JE, Hendrickson C, Hellmann H. (2009). Vitamin B6: a long known compound of surprising complexity. *Molecules* **14:** 329–351.

Streit WR, Entcheva P. (2003). Biotin in microbes, the genes involved in its biosynthesis, its biochemical role and perspectives for biotechnological production. *Appl Microbiol Biotechnol* **61:** 21–31.

Sullivan JT, Brown SD, Yocum RR, Ronson CW. (2001). The *bio* operon on the acquired symbiosis island of *Mesorhizobium* sp. strain R7A includes a novel gene involved in pimeloyl-CoA synthesis. *Microbiol-SGM* **147:** 1315–1322.

Wagner-Döbler I, Ballhausen B, Berger M, Brinkhoff T, Buchholz I, Bunk B *et al.* (2010). The complete genome sequence of the algal symbiont *Dinoroseobacter shibae*: a hitchhiker's guide to life in the sea. *ISME J* **4:** 61–77.

Table S 2.6. Genes detected in the genomes of *Pseudovibrio* sp. FO-BEG1 and JE062 coding for predicted integrases, transposases, subunits of the gene transfer agent (GTA) and genes of the NRPS/PKS cluster. Genes that could not be detected in the not closed genome of strain JE062 are indicated with '—'. Absence of a gene name indicates that no assignment was made due to missing of this parameter for the respective genes. For the NRPS/PKS cluster, sequence similarity to the genes of the colibactin producing *E. coli* CFT073 strain is given.

Locus FO-BEG1	Locus JE062	Product	Gene
		GTA	
PSE_2457	PJE062_203	Phage DNA Packaging Protein	
PSE_2458	PJE062_274	Phage portal protein, HK97	
PSE_2459	PJE062_167	hypothetical protein	
PSE_2460	PJE062_351	hypothetical protein	
PSE_2461	PJE062_207	Peptidase U35, phage prohead HK97	
PSE_2462	PJE062_422	Phage major capsid protein, HK97 family	
PSE_2463	—	Phage conserved hypothetical protein, phiE125 gp8	
PSE_2464	—	Phage head-tail adaptor	
PSE_2465	PJE062_282	conserved hypothetical protein	
PSE_2466	PJE062_363	Phage major tail protein, TP901-1 family	
PSE_2467	—	Gene transfer agent (GTA) like protein	
PSE_2468	—	Conserved hypothetical phage protein	
PSE_2469	PJE062_443	Phage minor tail protein	
PSE_2470	PJE062_201	Gene transfer agent protein	
PSE_2471	PJE062_275	Phage conserved hypothetical protein BR0599	
PSE_2472	PJE062_117	Phage cell wall peptidase, NlpC/P60	
PSE_2473	PJE062_155	Gene transfer agent (GTA) orfg15, like protein	
		Integrases	
PSE_0066	PJE062_3298	Phage integrase family	
PSE_0453	PJE062_3485	Phage integrase family	
PSE_0457	—	Phage integrase family	
PSE_0623	PJE062_2786	Phage integrase family	
PSE_0748	PJE062_2951	Phage integrase family	
PSE_1819	—	Phage integrase family	
PSE_3013	PJE062_3594	Phage integrase family	
PSE_3106	—	Phage integrase family	
PSE_3107	—	Phage integrase family	
PSE_3108	—	Phage integrase family	
PSE_3364	—	Phage integrase family	
PSE_3365	—	Phage integrase family	
PSE_3929	PJE062_5158	Phage integrase family	
PSE_4169	PJE062_1148	Phage integrase family	
		Transposases	
PSE_1176	—	ISCc3, transposase OrfA	
PSE_1177	—	ISCc3, transposase OrfB	
PSE_1204	—	ISCc3, transposase OrfB	
PSE_1205	—	ISCc3, transposase OrfA	

Table S 2.6. Continued

Locus FO-BEG1	Locus JE062	Product	Gene
PSE_2059	–	Transposase	
PSE_2315	–	ISCc3, transposase OrfA	
PSE_2316	–	ISCc3, transposase OrfB	
PSE_3120	–	ISCc3, transposase OrfA	
PSE_3121	–	ISCc3, transposase OrfB	
PSE_3337	–	ISCc3, transposase OrfA	
PSE_3338	–	ISCc3, transposase OrfB	
PSE_3339	–	ISCc3, transposase OrfB	
PSE_3340	–	Transposon Tn7 transposition protein TnsE	*tnsE*
PSE_3341	–	Transposon Tn7 transposition protein TnsD	*tnsD*
PSE_3342	–	Transposon Tn7 transposition protein TnsC	*tnsC*
PSE_3344	–	Transposon Tn7 transposition protein TnsB	*tnsB*
PSE_3345	–	Transposon Tn7 transposition protein TnsA	*tnsA*
PSE_3361	–	ISCc3, transposase OrfA	
PSE_3362	–	ISCc3, transposase OrfB	
PSE_4189	–	Transposase	
PSE_p0146	–	Transposase IS4 family protein	

Locus FO-BEG1	Locus JE062	Product	Gene	Evalue / identity [%] to *E. coli* CFT073
		NRPS-PKS		
PSE_3317	–	4'-phosphopantetheinyl transferase	*hetI*	–
PSE_3318	–	Cadicidin biosynthesis thioesterase		8.0E-56 / 44%
PSE_3319	–	Beta-lactamase class C		1.0E-53 / 34%
PSE_3320	–	Polyketide synthase		4.0E-103 / 43%
PSE_3321	PJE062_617*	Protein containing DUF214, permase predicted		–
PSE_3322	PJE062_571*	Protein containing DUF214, permase predicted		–
PSE_3323	PJE062_611*	Lipoprotein-releasing system ATP-binding protein LolD	*lolD*	–
PSE_3324	–	Secretion protein HlyD	*hlyD*	–
PSE_3325	–	Non-ribosomal peptide synthetase		2.0E-145 / 34%
PSE_3326	–	Multi antimicrobial extrusion protein MatE		4.0E-78 / 49%
PSE_3327	–	Asp-tRNAAsn/Glu-tRNAGln amidotransferase A subunit		2.0E-89 / 43%
PSE_3328	–	Peptide synthetase		0.0 / 43%
PSE_3329	–	Non-ribosomal peptide synthetase		0.0 / 38%
PSE_3330	–	Polyketide synthase		0.0 / 51%
PSE_3331	–	Non-ribosomal peptide synthase		0.0 / 39%
PSE_3332	–	Acyl-CoA dehydrogenase domain protein		3.0E-79 / 50%
PSE_3333	–	Hypothetical protein		2.0E-12 / 56%

Table S 2.6. Continued

Locus FO-BEG1	Locus JE062	Product	Gene	Evalue / identity [%] to *E. coli* CFT073
PSE_3334	─	3-hydroxybutyryl-CoA dehydrogenase	*hbd*	1.0E-85 / 64%
PSE_3335	─	Polyketide synthase		1.0E-178 / 44%
PSE_3336	─	Polyketide synthase		0.0 / 40%
PSE_p0217	PJE062_3951	Type III polyketide synthase		─
		Genes marked with * encode an ABC transporter		

Table S 2.7. Genes detected in the genomes of *Pseudovibrio* sp. FO-BEG1 and JE062 coding for predicted proteins involved in attachment, protein-protein interactions and predicted LuxR transcriptional regulators. Genes that could not be detected in the not closed genome of strain JE062 are indicated with '─'. Absence of a gene name or an EC number indicates that no assignment was made due to missing of these parameters for the respective genes.

Locus FO-BEG1	Locus JE062	Product	Gene	EC
		ORFs containing ankyrin repeat domains[a)]		
PSE_0544	PJE062_2814	ankyrin repeat protein		
PSE_2079	─	ankyrin repeat protein		
PSE_3116	─	ankyrin repeat protein		
		ORFs containing tetratricopeptide repeat domains[a)]		
PSE_0098	PJE062_3465	Thioredoxin		
PSE_0865	PJE062_3032	Methyltransferase type 12		2.1.1.-
PSE_1079	PJE062_4509	Tetratricopeptide repeat protein		
PSE_1686	PJE062_118	Tetratricopeptide repeat protein		
PSE_2479	PJE062_323	Cytochrome c-type biogenesis protein CycH	*cycH*	
PSE_2694	PJE062_4181	Tetratricopeptide repeat protein		
PSE_3163	PJE062_1441	Tetratricopeptide repeat protein		
PSE_3476	─	peptidase M48, Ste24p		
PSE_3705	PJE062_1339	type III secretion system chaperone protein B		
PSE_4003	PJE062_4620	Tetratricopeptide repeat protein		
PSE_4676	PJE062_2205	Tol-Pal system YbgF		
PSE_4741	PJE062_2047	Tetratricopeptide repeat protein		
PSE_4770	PJE062_2250	Tetratricopeptide repeat protein		
PSE_4880	PJE062_2166	HemY domain protein	*hemY*	
PSE_p0011	PJE062_3638	Methyltransferase type 12		2.1.1.-
		ORFs containing Sel1 domains[a)]		
PSE_0262	PJE062_3497	Sel1 domain protein repeat-containing protein		
PSE_1737	PJE062_108	Sel1 domain protein repeat-containing protein		

Table S 2.7. Continued

Locus FO-BEG1	Locus JE062	Product	Gene	EC
PSE_1793	PJE062_380	Sel1 domain protein repeat-containing protein		
PSE_2549	PJE062_4185	Sel1 domain protein repeat-containing protein		
PSE_3010	PJE062_1367	Sel1 domain protein repeat-containing protein		
PSE_4219	PJE062_4679	Sel1 domain protein repeat-containing protein		
PSE_4221	PJE062_5026	Sel1 domain protein repeat-containing protein		
PSE_4700	PJE062_2257	Sel1 domain protein repeat-containing protein		
		Invasion associated locus B[a)]		
PSE_1550	PJE062_305	Invasion associated locus B	*ialB*	
PSE_1999	PJE062_658	Invasion associated locus B	*ialB*	
PSE_2098	PJE062_650	Invasion associated locus B	*ialB*	
PSE_2110	PJE062_550	Invasion associated locus B	*ialB*	
PSE_3194	PJE062_1243	Invasion associated locus B	*ialB*	
		Genes associated with amyloid production		
PSE_4342	PJE062_4994	Curlin associated repeat		
PSE_4343	PJE062_4861	Curlin associated repeat		
PSE_4344	PJE062_5083	Curlin associated repeat		
PSE_4345	PJE062_4741	Curli production assembly/transport component CsgG	*csgG*	
PSE_4346	PJE062_4746	Curli production assembly/transport component CsgF	*csgF*	
		Genes containing YadA domains[a)]		
PSE_2099	PJE062_871	protein containing YadA-like, C-terminal domain		
PSE_2111	PJE062_850	protein containing YadA-like, C-terminal domain		
		Genes containing TadE-like domains[a)]		
PSE_1084	PJE062_4462	TadE-like protein		
PSE_1085	PJE062_4380	TadE-like protein		
		LuxR transcriptional regulator		
PSE_1326	PJE062_1887	transcriptional regulator, LuxR family protein	*luxR*	
PSE_1528	PJE062_237	transcriptional regulator, LuxR family protein	*luxR*	
PSE_1752	PJE062_454	transcriptional regulator, LuxR family protein	*luxR*	
PSE_1756	PJE062_469	transcriptional regulator, LuxR family protein	*luxR*	
PSE_2176	PJE062_945	transcriptional regulator, LuxR family protein	*luxR*	
PSE_2420	PJE062_63	transcriptional regulator, LuxR family protein	*luxR*	

Table S 2.7. Continued

Locus FO-BEG1	Locus JE062	Product	Gene	EC
PSE_4321	PJE062_5001	transcriptional regulator, LuxR family protein	*luxR*	
PSE_4710	PJE062_2349	transcriptional regulator, LuxR family protein	*luxR*	
PSE_4867	PJE062_2072	transcriptional regulator, LuxR family protein	*luxR*	
PSE_4891	–	transcriptional regulator, LuxR family protein	*luxR*	
PSE_4980	PJE062_4013	transcriptional regulator, LuxR family protein	*luxR*	
PSE_4981	PJE062_3991	transcriptional regulator, LuxR family protein	*luxR*	
PSE_4982	PJE062_4089	transcriptional regulator, LuxR family protein	*luxR*	
PSE_p0055	PJE062_3730	transcriptional regulator, LuxR family protein	*luxR*	
PSE_p0305	PJE062_3930	transcriptional regulator, LuxR family protein	*luxR*	

[a)] Homologues of genes presumably involved in attachment and prokaryote-eukaryote interactions

Genomes of sponge-associated microorganisms often show an overrepresentation of eukaryotic domains mediating protein-protein interactions, especially ankyrin repeat (AR) and tetratricopeptide repeat (TPR) domains containing genes, which are thought to play a role in bacteria-host interactions (Liu *et al.*, 2011; Siegl *et al.*, 2011; Thomas *et al.*, 2010). Genes containing AR or TRP repeat domains could also be identified in the genome of both *Pseudovibrio* strains. Additionally, we found genes containing YadA and TadE domains, known to be required for binding to host tissue (Hoiczyk *et al.*, 2000) and adherence to surfaces (Kachlany *et al.*, 2001), respectively. Open reading frames containing Sel1 repeats were detected in both *Pseudovibrio* genomes. Those repeats were found in great abundance in an amoeba symbiont (Schmitz-Esser *et al.*, 2010) and are thought to mediate prokaryote-eukaryote interactions (Mittl and Schneider-Brachert, 2007). We also identified five homologues of "invasion-associated locus B" genes in genomes of strain FO-BEG1 and JE062. In *Bartonella bacilliformis* the invasion-associated locus B gene (*ialB*) was shown to have a direct role in human erythrocyte parasitism and was needed for adherence and invasion of the erythrocytes by the bacterium (Coleman and Minnick, 2001). In summary, we identified a number of different protein homologues and genes with repeat motifs assumed to be involved in prokaryote-eukaryote interactions, supporting the proposed role of *Pseudovibrio* as a symbiont with possibilities to attach, invade and interact with the host organism.

References

Coleman SA, Minnick MF. (2001). Establishing a direct role for the *Bartonella bacilliformis* invasion-associated locus B (IalB) protein in human erythrocyte parasitism. *Infect Immun* **69:** 4373–4381.

Hoiczyk E, Roggenkamp A, Reichenbecher M, Lupas A, Heesemann J. (2000). Structure and sequence analysis of *Yersinia* YadA and *Moraxella* UspAs reveal a novel class of adhesins. *EMBO J* **19:** 5989–5999.

Kachlany SC, Planet PJ, DeSalle R, Fine DH, Figurski DH. (2001). Genes for tight adherence of *Actinobacillus actinomycetemcomitans*: from plaque to plague to pond scum. *Trends Microbiol* **9:** 429–437.

Liu MY, Kjelleberg S, Thomas T. (2011). Functional genomic analysis of an uncultured δ-proteobacterium in the sponge *Cymbastela concentrica*. *ISME J* **5:** 427–435.

Mittl PRE, Schneider-Brachert W. (2007). Sel1-like repeat proteins in signal transduction. *Cell Signal* **19:** 20–31.

Schmitz-Esser S, Tischler P, Arnold R, Montanaro J, Wagner M, Rattei T *et al.* (2010). The genome of the amoeba symbiont "*Candidatus* Amoebophilus asiaticus" reveals common mechanisms for host cell interaction among amoeba-associated bacteria. *J Bacteriol* **192:** 1045–1057.

Siegl A, Kamke J, Hochmuth T, Piel J, Richter M, Liang CG *et al.* (2011). Single-cell genomics reveals the lifestyle of *Poribacteria*, a candidate phylum symbiotically associated with marine sponges. *ISME J* **5:** 61–70.

Thomas T, Rusch D, DeMaere MZ, Yung PY, Lewis M, Halpern A *et al.* (2010). Functional genomic signatures of sponge bacteria reveal unique and shared features of symbiosis. *ISME J* **4:** 1557–1567.

Table S 2.8. Genes detected in the genomes of *Pseudovibrio* sp. FO-BEG1 and JE062 coding for predicted subunits of the type III and type VI secretion systems. Genes that could not be detected in the not closed genome of strain JE062 are indicated with '—'. Absence of a gene name indicates that no assignment was made due to missing of this parameter for the respective genes. For the type III secretion system, sequence similarity to the best SwissProt hit is given.

Locus FO-BEG1	Locus JE062	Product	Gene	Evalue / identity [%] to SwissProt Hit
		Type III secretion system		
PSE_2750	PJE062_4298	Inositol phosphate phosphatase IpgD	*ipgD*	5.0E-18 / 27%
PSE_3453	PJE062_1387	Protein kinase YpkA	*ypkA*	5.0E-11 / 26%
PSE_3455	PJE062_1601	Protein kinase YpkA	*ypkA*	4.0E-10 / 26%
PSE_3456	PJE062_1751	Protein kinase YpkA	*ypkA*	2.0E-12 / 28%
PSE_3677	PJE062_1314	Low calcium response locus protein D (LcrD)	*yscV*	0.0 / 54%
PSE_3678	—	hypothetical protein		
PSE_3679	PJE062_1029	dienelactone hydrolase and related enzymes		
PSE_3680	PJE062_1817	Yop proteins translocation protein U	*yscU*	4.0E-62 / 41%
PSE_3681	PJE062_1687	Yop proteins translocation protein T	*yscT*	8.0E-22 / 38%
PSE_3682	PJE062_1490	Yop proteins translocation protein S	*yscS*	2.0E-5 / 52%
PSE_3683	PJE062_1016	Yop proteins translocation protein R	*yscR*	8.0E-49 / 57%
PSE_3684	PJE062_1246	Yop proteins translocation protein Q	*yscQ*	0.0060 / 30%
PSE_3685	PJE062_1406	hypothetical protein		
PSE_3686	PJE062_1474	hypothetical protein		
PSE_3687	PJE062_1036	Yop proteins secretion ATPase	*yscN*	2.0E-147 / 66%
PSE_3688	PJE062_1156	Yop proteins translocation protein L	*yscL*	8.0E-9 / 26%
PSE_3689	PJE062_996	hypothetical protein		
PSE_3690	PJE062_1724	Yop proteins translocation J	*yscJ*	1.0E-42 / 47%
PSE_3691	PJE062_1825	hypothetical protein		
PSE_3692	PJE062_1134	hypothetical protein		
PSE_3693	PJE062_1461	hypothetical protein		
PSE_3694	PJE062_969	hypothetical protein		
PSE_3695	PJE062_1844	hypothetical protein		
PSE_3696	PJE062_1796	hypothetical protein		
PSE_3697	PJE062_1006	Yop proteins translocation protein C	*yscC*	1.0E-8 / 24%
PSE_3698	PJE062_1665	hypothetical protein		
PSE_3699	PJE062_991	hypothetical protein		
PSE_3700	PJE062_1656	hypothetical protein		
PSE_3701	PJE062_1486	Tetratricopeptide region		
PSE_3702	PJE062_1647	hypothetical protein		
PSE_3703	PJE062_962	hypothetical protein		
PSE_3704	PJE062_1171	hypothetical protein		
PSE_3705	PJE062_1339	type III secretion system chaperone protein B		
PSE_3706	PJE062_1315	hypothetical protein		
PSE_3707		hypothetical protein		
PSE_3708	PJE062_1165	hypothetical protein		
PSE_3709	PJE062_1353	hypothetical protein		
PSE_3710	—	membrane-bound Yop targeting protein YopN	*yopN*	*6.0E-14 / 25%

Table S 2.8. Continued

Locus FO-BEG1	Locus JE062	Product	Gene	Evalue / identity [%] to SwissProt Hit
PSE_3711	–	hypothetical protein		
PSE_3712	PJE062_1659	Cyclic nucleotide-binding domain		
PSE_3713	PJE062_1450	hypothetical protein		
PSE_3714	PJE062_1254	hypothetical protein		
PSE_3715	PJE062_1816	Yop proteins translocation protein D	*yscD*	0.045 / 21%
PSE_4190	–	Effector protein YopJ (Virulence factor YopJ)	*yopJ*	6.0E-22 / 29%
		* No SwissProt Hit, BlastP Hit instead		
		Type VI secretion system cluster I		
PSE_1854	PJE062_773	ImpA domain protein	*impA*	
PSE_1855	PJE062_714	Type VI secretion protein IcmF	*icmF*	
PSE_1856	PJE062_893	type VI secretion protein, VC_A0107 family		
PSE_1857	PJE062_506	type VI secretion protein EvpB	*evpB*	
PSE_1858	PJE062_730	type VI secretion system, lysozyme-related protein		
PSE_1859	PJE062_884	type VI secretion protein, VC_A0110 family		
PSE_1860	PJE062_596	type VI secretion protein, VC_A0111 family		
PSE_1861	PJE062_492	FHA domain protein	*fha*	
PSE_1862	PJE062_933	type VI secretion lipoprotein, VC_A0113 family		
PSE_1863	PJE062_502	type VI secretion protein, VC_A0114 family		
PSE_1864	PJE062_588	type IV / VI secretion system DotU	*dotU*	
PSE_1865	PJE062_641	ATPase, type VI secretion system ClpV1	*clpV1*	
		Type VI secretion system cluster II		
PSE_2844	PJE062_1121	Type VI secretion protein IcmF	*icmF*	
PSE_2845	PJE062_1271	Type IV / VI secretion system, DotU/OmpA/MotB	*dotU/ompA/motB*	
PSE_2846	PJE062_1112	type VI secretion protein, VC_A0114 family		
PSE_2847	PJE062_1027	type VI secretion lipoprotein, VC_A0113 family		
PSE_2848	PJE062_1673	FHA domain protein	*fha*	
PSE_2849	PJE062_1460	hypothetical protein		
PSE_2850	PJE062_1178	hypothetical protein		
PSE_2851	PJE062_1054	Rhs element Vgr protein		
PSE_2852	PJE062_1408	hypothetical protein		
PSE_2853	PJE062_1012	type VI secretion protein, EvpB/VC_A0108 family		
PSE_2854	PJE062_1728	voltage-gated sodium channel		
PSE_2855	PJE062_1703	ATPase, type VI secretion system ClpV1	*clpV1*	
PSE_2856	PJE062_1167	type VI secretion protein, VC_A0111 family		
PSE_2857	PJE062_1049	type VI secretion protein, VC_A0110 family		

Table S 2.8. Continued

Locus FO-BEG1	Locus JE062	Product	Gene	Evalue / identity [%] to SwissProt Hit
PSE_2858	PJE062_1774	type VI secretion system lysozyme-related protein		
PSE_2859	PJE062_1348	virulence protein, SciE type	*sciE*	
PSE_2860	PJE062_988	SciM protein	*sciM*	
PSE_2861	PJE062_1094	Cytoplasmic protein SciI	*sciI*	
PSE_2862	PJE062_1199	Cytoplasmic protein SciH	*sciH*	
PSE_2863	PJE062_1550	ImpA domain protein	*impA*	
PSE_p0119	–	Rhs-family protein	*rhs*	
PSE_p0120	–	hypothetical protein		
PSE_p0121	–	FHA domain protein	*fha*	
PSE_p0122	–	type VI secretion system Vgr family protein	*vgr*	
PSE_p0123	–	hypothetical protein		
PSE_p0124	–	Type VI secretion system effector, Hcp1	*hcp1*	
PSE_1192	PJE062_748	Type VI secretion system effector, Hcp1 family	*hcp1*	
PSE_1193	–	ypothetical protein		
PSE_1194	–	hypothetical protein		
PSE_1195	PJE062_528	hypothetical protein		
PSE_1196	PJE062_779	Type VI secretion system Vgr family protein	*vgr*	

Chapter III

Isolation of facultatively oligotrophic bacteria

Anne Schwedt[1], Vladimir Bondarev[1], Michael Seidel[1,2], Thorsten Dittmar[1,2], Heide N. Schulz-Vogt[1]

[1]Max Planck Institute for Marine Microbiology, Ecophysiology Group, Celsiusstr. 1, D-28359 Bremen, Germany

[2]Max Planck Institute for Marine Microbiology, Marine Geochemistry Group, Institute for Chemistry and Biology of the Marine Environment, Carl von Ossietzky University of Oldenburg, Carl-von-Ossietzky-Str. 9-11, D-26129 Oldenburg, Germany

Manuscript in preparation

Contributions:

The concept of this study was developed by A. Schwedt and H. N. Schulz-Vogt. I developed the cell enumeration technique for low cell numbers and performed counting of the tested isolates. The manuscript was written by A. Schwedt including comments of all co-authors.

This work has already been published in the dissertation of Anne Schwedt as chapter 4.2 with the title: “Facultatively oligotrophic bacteria isolated from the habitat of large sulfide-oxidizers”. The authors and contributions remained unchanged, but the manuscript was partially adapted and corrected to fit better in the context of this thesis.

Abstract

Marine bacteria in the open ocean are exposed to an extremely low amount of nutrients. However, there exist nutrient hotspots, such as marine snow particles, attached to which, bacteria can exhibit high growth rates. Bacteria able to grow under both, nutrient affluence and deficiency are called facultative oligotrophs. In the present study, we introduce a cultivation strategy for the isolation of facultatively oligotrophic bacteria, the CANgrow-method (changing availability of nutrients growth-method). In this method, three initial transfer steps in pure artificial seawater without the addition of organic substrates pre-select for bacteria multiplying under oligotrophic conditions. Pure cultures are obtained by three subsequent transfers of single colonies on organic-rich solid medium. Finally, at least seven transfers in pure artificial seawater ensure oligotrophic growth. Phylogenetically, the isolated strains belong to three different groups, which are not closely related, the *Actinobacteria*, *α*- and *γ-Proteobacteria*. This leads us to suspect that the ability of common heterotrophic bacteria to multiply under extreme nutrient limitation is largely underestimated, and that facultative oligotrophy is more widespread among known heterotrophs than so far recognized.

Introduction

The biggest habitat on earth is the ocean, large parts of which are characterized by extremely low concentrations of available nutrients and energy sources. The dissolved organic carbon (DOC) concentration in the open ocean is in the range of 0.4 to 1 mg C l^{-1} (Schut *et al.*, 1997; Hansell *et al.*, 2009) and is thus lower than in most other environments. Hence, the open ocean is referred to as an oligotrophic environment, a term that was introduced by Weber (1907) more than a century ago to describe nutrient deficiency in contrast to the term eutrophic, denoting nutrient affluence. There are several definitions of oligotrophy, but it is generally accepted that bacteria are referred to as oligotrophic when they are able to grow in medium containing less than 0.5 mg C l^{-1} (Ishida *et al.*, 1989). A bacterial strain is called obligately oligotrophic, when growth is inhibited by high substrate concentrations, which is in contrast to a facultatively oligotrophic strain that can also grow in organic-rich medium (Ishida *et al.*, 1989). Facultative oligotrophs are therefore successful in environments with changing nutrient conditions. As the open ocean is low in energy sources and nutrients, a high proportion of marine, planktonic bacteria is likely capable of oligotrophic growth. Different strategies have been developed during the past decades for the isolation of marine bacteria, but only few pure cultures of oligotrophic bacteria exist so far. Whenever a complex organic-rich medium is used for the isolation and cultivation, the concentrations of substrates are considerably higher than in the natural habitat (ZoBell, 1941) and might inhibit the growth of obligately oligotrophic bacteria. On the other hand, if an extremely substrate deficient medium is used for the isolation and cultivation, the substrate concentrations and also the cell numbers are close to detection limit (Button *et al.*, 1993). So far, all approaches to cultivate oligotrophic bacteria reported in the literature either used natural seawater (e.g. Carlucci and Shimp, 1974; Ammerman *et al.*, 1984; Button *et al.*, 1993; Connon and Giovannoni, 2002) that has generally a DOC concentration of 0.4 to 1 mg C l^{-1} (Schut *et al.*, 1997; Hansell *et al.*, 2009) or artificial seawater supplemented with at least 0.1 to 3 mg fixed C l^{-1} (e.g. Van der Kooij *et al.*, 1980; Ishida *et al.*, 1982). A common routine for the isolation of bacteria growing in natural seawater is the dilution-to-extinction method (Button *et al.*, 1993), which has been refined by Connon and Giovannoni (2002) to enable the parallel identification of many cultures after dilution-to-extinction with so-called high-throughput culturing (HTC). Zengler *et al.* (2002) developed a second high-throughput cultivation method by combining single cell encapsulation with flow cytometry. This allows the detection and isolation of those bacteria able to grow in natural seawater.

In the present study we introduce a new strategy for the isolation of facultatively oligotrophic bacteria, which relies on the change from oligotrophic to eutrophic conditions, called the CANgrow-method (changing availability of nutrients growth-method). In contrast to earlier methods, the artificial oligotrophic medium is defined and much lower in nutrients and three initial transfers strongly pre-select for bacteria, which can grow under extreme nutrient deficiency. Subsequently, three transfers on nutrient rich agar plates select for facultatively oligotrophic bacteria and are used to obtain pure cultures. Finally, the ability of the isolates to grow oligotrophically is ensured by at least seven transfers in pure artificial seawater.

Material and Methods

Samples

The first isolate, *Pseudovibrio* sp. FO-BEG1, was originally grown in co-culture with a marine *Beggiatoa* strain (Kamp *et al.*, 2008; Brock and Schulz-Vogt, 2011). The *Pseudovibrio* strain seems to be required for the growth of the sulfide oxidizing *Beggiatoa* strain and was therefore further studied in pure culture. As the *Pseudovibrio* isolate was observed to grow in controls without the addition of any electron donor, it inspired the development of the CANgrow-method, as described below, and stimulated our search for further strains of facultatively oligotrophic bacteria. The new strains were isolated from oceanic bottom water overlaying Namibian sediments that harbor different large sulfur bacteria (sample aquisition described in Salman *et al.*, 2011). All samples were stored at 4 °C. In addition to the new isolates the *Pseudovibrio denitrificans* type stain (DSM number 17465) was purchased from the German culture collection DSMZ (Deutsche Sammlung von Mikroorganismen und Zellkulturen GmbH, Braunschweig, Germany) and cultivated under oligotrophic conditions.

Growth media and cultivation conditions

For cultivation and isolation two different media were used, an oligotrophic and an eutrophic medium. The liquid, oligotrophic medium contained 30.3 g NaCl, 3.3 g $MgCl_2 \cdot 6\ H_2O$, 2.8 g $MgSO_4 \cdot 2\ H_2O$, 0.44 g $CaCl_2 \cdot 2\ H_2O$, 0.7 g KCl, 50 µl 2 mol l^{-1} NaOH, 2 ml 1 mol l^{-1} $NaHCO_3$, 1 ml 1 mmol l^{-1} K_2HPO_4 and 1 ml trace elements solution in 1 liter deionized water (Optilab-Standard Water System, MembraPure, Bodenheim, Germany). The trace elements solution was composed of 2.1 mg l^{-1} $FeSO_4 \cdot 7\ H_2O$, 13 ml l^{-1} HCl (25%),

60 mg l^{-1} H_3BO_3, 100 mg l^{-1} $MnCl_2 \cdot 4\ H_2O$, 190 mg l^{-1} $CoCl_2 \cdot 6\ H_2O$, 24 mg l^{-1} $NiCl_2 \cdot 6\ H_2O$, 2 mg l^{-1} $CuCl_2 \cdot 2\ H_2O$, 144 mg l^{-1} $ZnSO_4 \cdot 7\ H_2O$ and 36 mg l^{-1} $Na_2MoO_4 \cdot 2\ H_2O$. The oligotrophic medium was prepared under synthetic air atmosphere (20% O_2 in N_2; H_2O <3 ppm-mol, C_nH_m <0.1 ppm-mol, CO <1 ppm-mol, CO_2 <1 ppm-mol). For at least the last three transfer steps all glassware, aluminum foil and NaCl was combusted (480 °C, 3 h) and teflon stoppers were used to close the cultivation bottles (Wheaton 125 ml serum bottles clear, Wheaton, Millville, NJ, USA). This medium was used for all oligotrophic cultivation experiments. The solid, eutrophic medium contained 2 g polypeptone, 0.5 g Bacto yeast extract (Becton, Dickinson and Company Sparks (BD), MD, USA), 30 g NaCl, 5 g $MgCl_2 \cdot 6\ H_2O$, 0.005 g $CaCl_2 \cdot 2\ H_2O$, 0.005 g $Na_2MoO_4 \cdot 7\ H_2O$, 0.004 g $CuCl_2 \cdot 2\ H_2O$, 0.006 g $FeCl_3 \cdot 6\ H_2O$, 15 g agar in 1 liter deionized water. The pH was adjusted to pH 8 using 1 mol l^{-1} NaOH. All incubations in oligotrophic and eutrophic media were performed without shaking, in the dark, at 28 °C.

CANgrow-method (changing availability of nutrients growth-method)

For isolation, 50 ml of oligotrophic medium were inoculated with 100 µl seawater sample (from off shore Namibia) or *Beggiatoa* sp. culture. The cultures were transferred (100 µl enrichment in 50 ml fresh medium) at least three times in oligotrophic medium with incubation periods between the transfers of at least one week. Aliquots of the oligotrophic enrichments were then plated on eutrophic, solid medium and single colonies were transferred three times on eutrophic medium. Finally, at least another seven transfers (100 µl culture in 50 ml fresh medium) were performed in liquid, oligotrophic medium (**Figure 3.1**).

Sequencing of 16S rRNA genes and phylogenetic analysis

Eutrophically grown colonies were picked and directly transferred to a polymerase chain reaction (PCR) mix containing 1×PCR MasterMix (Promega, Mannheim, Germany) and 1 µmol l^{-1} of each primer (GM3F and GM4R in Muyzer *et al.*, 1995). The PCR program applied was as follows: initial denaturation at 95 °C for 5 minutes, 32 cycles of 95 °C for 1 minute, 50 °C for 30 seconds and 72 °C for 90 seconds followed by a final elongation at 72 °C for seven minutes. PCR products were cloned using the TOPO TA Cloning® Kit for Sequencing (Invitrogen, Karlsruhe, Germany) according to manufacture's instructions. Sequencing of the cloned inserts was performed using the Big Dye Cycle Sequencing Kit (Applied Biosystems, Carlsbad, CA, USA) and sequences were analyzed on an ABI Genetic Analyzer 3130x (Applied Biosystems, Carlsbad, CA, USA). Nearly full-length sequences

were assembled with SeqMan (Lasergene software package, DNAStar, Madison, WI, USA) and deposited in the DDBJ/EMBL/GenBank databases under accession numbers FR716535 to FR716549. Phylogenetic analysis of the 16S rRNA gene sequences was performed using the ARB software package (Ludwig *et al.*, 2004) and release 102 of the SILVA SSURef database (Pruesse *et al.*, 2007). Tree reconstruction with maximum likelihood and neighbour joining methods was performed using 0, 30 and 50% positional conservatory filters that exclude highly variable regions. Finally a consensus tree based on the different reconstruction methods was built. A total number of 102 nearly full-length sequences were used for initial calculation to stabilize tree topology. Displayed in the final tree (**Figure 3.2**) are the sequences of the 15 isolates grouped with their closest relatives.

Cell counts

Samples from oligotrophic cultures were taken and 1 ml culture was stained for 20 minutes with SYBR Green (SYBR Green I 10,000×, Sigma, Taufkirchen, Germany) diluted 1:5000 and filtered onto black 0.22 µm GTTP Isopore Membrane Filters (Millipore, Schwalbach, Germany) using a Bio-Dot apparatus (Bio-Rad, München, Germany) with a filtration diameter of 3 mm. Cells were counted under a fluorescence microscope (Axiophot, Zeiss, Jena, Germany) with an excitation of 450 to 490 nm and an emission of 515 to 565 nm (filter set 10, Zeiss, Jena, Germany).

Measurement of dissolved organic carbon (DOC)

Dissolved organic carbon (DOC) was measured in the oligotrophic medium using a Shimadzu TOC-VCPH total organic carbon analyzer (Shimadzu, Kyoto, Japan). Acidification of samples was performed with 1% v/v 2 mol l^{-1} HCl followed by sparging with synthetic air in order to remove inorganic carbon. The detection limit of the method was 5 µmol C l^{-1} (0.06 mg C l^{-1}) and the analytical accuracy was confirmed with reference material (deep Atlantic seawater) and low carbon water from the consensus reference materials program (D.A. Hansell, University of Miami, Coral Gables, FL, USA).

Results

Isolation of facultatively oligotrophic bacteria

Applying the newly developed CANgrow-method, which favors slowly growing facultatively oligotrophic bacteria (**Figure 3.1**), we obtained 15 isolates of marine bacteria that were able to adapt from oligotrophic to eutrophic growth conditions and vice versa within

3 to 5 days. We were able to obtain pure cultures of these strains by transferring single colonies from organic-rich agar plates and could show that these colonies were able to grow oligotrophically by at least seven transfers in pure artificial seawater.

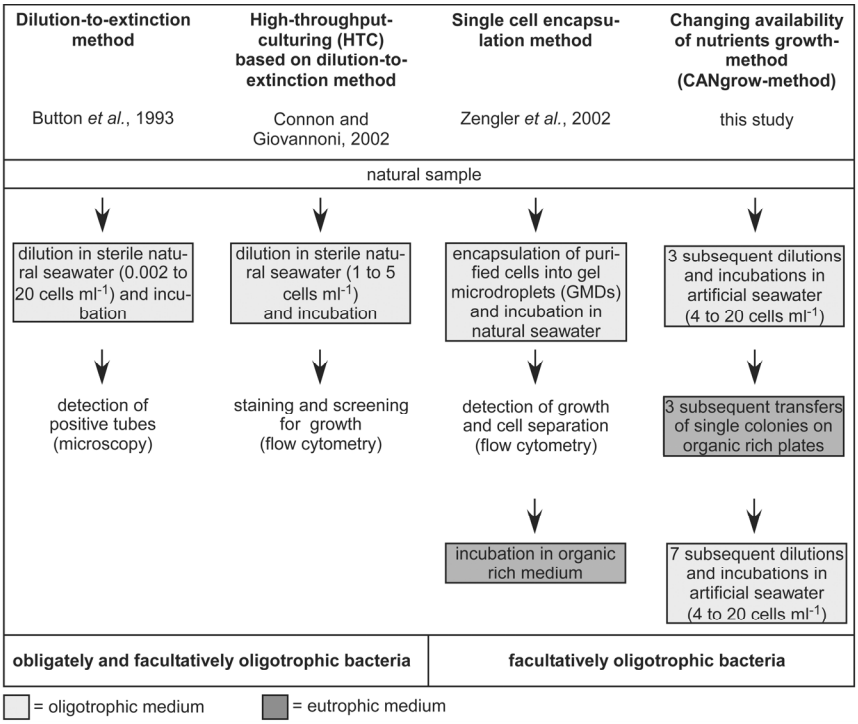

Figure 3.1. Comparison of strategies for the isolation of oligotrophic bacteria. Three different methods for the isolation of obligately or facultatively oligotrophic bacteria are compared with the newly developed CANgrow-method (Changing availability of nutrients growth-method).

Phylogeny of the isolates

Bacteria from three different phyla were isolated with the CANgrow-method (**Figure 3.2**). Except for two isolates, which were closely related to *Arthrobacter* spp. (*Actinobacteria*) on 16S rRNA gene level (99.8 to 99.9% identity to closest related strain), all isolates were members of the *Proteobacteria*. One of these isolates showed >99.5% sequence identity to the α-proteobacterium *Pseudovibrio denitrificans*. The remaining 12 isolates were members of the *γ-Proteobacteria*, two of them grouping with *Kangiella* spp. (96.4% identity to closest related strain) and ten with *Marinobacter* spp. (98.7 to 100% identity to closest related strain).

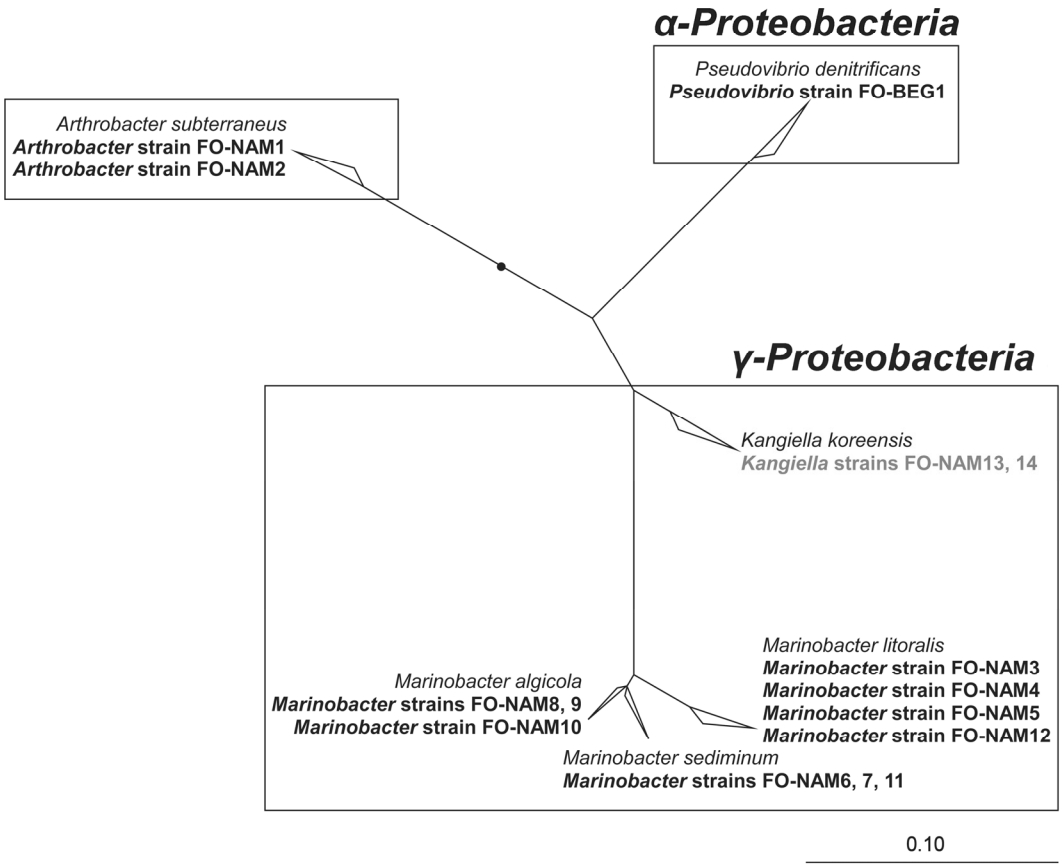

Figure 3.2. Phylogenetic trees based on a total number of 102 nearly full-length sequences were calculated with maximum likelihood and neighbor joining methods using different positional conservatory filters. The displayed tree is an excerpt from the consensus tree that was inferred based on the different reconstruction approaches. The 14 new isolates and strain FO-BEG1 are grouped with the most closely related type strains. Isolated strains listed in one line feature an identical 16S rRNA gene sequence, whereas isolated strains listed directly one below the other are 99.6 to 99.9% identical in their 16S rRNA gene sequence. The isolates FO-NAM13, 14 were only able to grow for six transfers under oligotrophic conditions and are therefore marked grey in the tree.

Oligotrophic growth

The artificial seawater contained a DOC concentration of 0.18 ± 0.06 mg C l^{-1} (15 ± 5 µmol C l^{-1}). Growth curves in oligotrophic artificial seawater medium (**Figure 3.3**) were obtained for one isolate from each phylogenetic group (*Actinobacteria*, *α*- and *γ-Proteobacteria*). We observed a clear increase in cell numbers starting from 4 to 20 cells ml^{-1} to a final density of 10^4 to 10^5 cells ml^{-1}. The proteobacterial isolates showed growth after 2 days and reached the stationary phase after 5 to 7 days of incubation. Both actinobacterial isolates were characterized by delayed growth that was detectable after 12 days. Here, the stationary phase was reached after about 20 days of incubation. Moreover, all

isolates except for the two isolated *Kangiella* strains were able to grow after at least seven transfers in the oligotrophic seawater medium. The two isolates closely related to *Kangiella* spp. were not able to grow after more than six transfers under oligotrophic conditions. The isolates closely related to *Marinobacter* spp. reached the highest final cell numbers (**Figure 3.3D**) whereas the actinobacterial isolates showed lowest final cell densities (**Figure 3.3C**). Furthermore, we observed oligotrophic growth for the type strain *Pseudovibrio denitrificans* (DSM number 17465) and the growth curve (**Figure 3.3B**) showed the same pattern as the *Pseudovibrio* isolate FO-BEG1 (**Figure 3.3A**). The isolate FO-BEG1 is currently growing in the 26th oligotrophic transfer in highly purified artificial seawater.

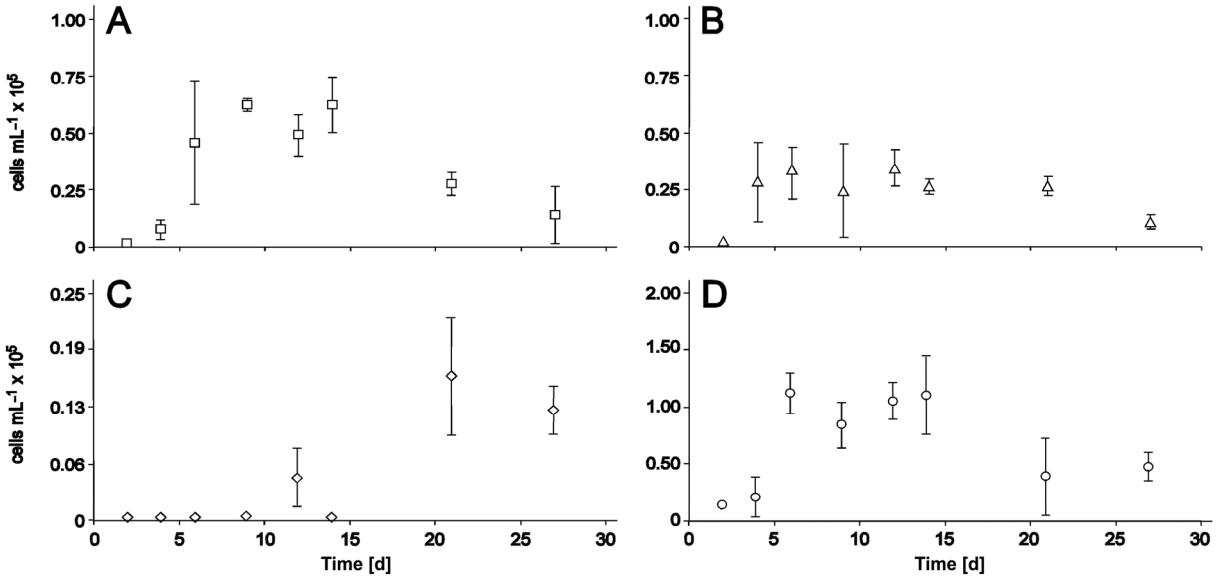

Figure 3.3. Oligotrophic growth curves in dependence of incubation time of (**A**) strain FO-BEG1 (*α-Proteobacteria*, related to *Pseudovibrio* spp.), (**B**) *Pseudovibrio denitrificans* type strain (*α-Proteobacteria*), (**C**) isolate FO-NAM2 (*Actinobacteria*, related to *Arthrobacter* spp.) and (**D**) isolate FO-NAM6 (*γ-Proteobacteria*, related to *Marinobacter* spp.). Error bars represent the standard deviation of biological replicates.

Discussion

Isolation of facultatively oligotrophic bacteria with the CANgrow-method

Each strategy that is applied for the isolation of bacteria selects for a specific physiological type of bacteria. Most approaches used recently for the isolation of oligotrophic bacteria are based on the dilution to extinction method (Button *et al.*, 1993; Connon and Giovannoni, 2002) and thereby select for abundant microorganisms. In contrast to this, the CANgrow-method favors bacteria, which might not have been particularly abundant in the original inoculum but can adapt fast to changes in nutrient availability. Previous studies have

shown that many bacteria isolated under oligotrophic conditions can adapt to nutrient-rich media (Yanagita *et al.*, 1977; MacDonell and Hood, 1982; Carlucci *et al.*, 1986). Also, the single-cell encapsulation method (Zengler *et al.*, 2002) is based on oligotrophic growth followed by eutrophic growth conditions. This cultivation approach is similar to ours (**Figure 3.1**), but we used artificial seawater with a very low DOC concentration rather than natural seawater. The measured DOC concentration of 0.18 mg C l^{-1} is two to five times lower than in natural seawater (Schut *et al.*, 1997; Hansell *et al.*, 2009). Nevertheless, we are certain to observe true growth under these extremely oligotrophic conditions, because we performed at least seven transfers in purified artificial seawater with each of the isolated strains and 25 transfers for strain FO-BEG1. The initial cell number after each transfer was 4 to 20 cells ml^{-1}. Thus, 9 to 15 divisions must have occurred between two consecutive transfers to account for a final cell number of 10^4 to 10^5 cells ml^{-1} as observed at the end of the growth phase (**Figure 3.3**). This accounts for 60 to 100 divisions during a total of 7 incubations. Therefore, we conclude that all isolates are viable under oligotrophic conditions by the definition of Button *et al.* (1993), who characterized organisms as viable after having performed 13 divisions, which we observe already after 1 to 2 transfers.

The trophic states of marine bacteria – oligotrophy versus eutrophy

Already 30 years ago (Ishida and Kadota, 1981), it was suspected that there exist two types of oligotrophic bacteria: *i*) organisms, which disappear with increasing man-made eutrophication and *ii*) organisms, which can adapt fast to man-made eutrophication. We did not isolate bacteria from the oligotrophic open ocean but from water directly overlaying marine sediments. All of the isolated strains were able to adapt fast to the nutrient deficiency of the initial isolation medium. Our observation that facultatively oligotrophic bacteria can also be isolated from non-oligotrophic water indicates that these bacteria might be more widespread and not limited to nutrient-poor environments. For example, they might attach to marine snow particles (e.g. Alldredge *et al.*, 1986; Smith *et al.*, 1992; Azam and Malfatti, 2007 and references therein), which represent nutrient hot spots for heterotrophic bacteria, and possibly sink down with these particles. We assume that many facultatively oligotrophic bacteria have been overlooked so far, because they were not searched for in non-oligotrophic environments. Likewise, many already known heterotrophic bacteria may be capable of growing under much lower nutrient conditions than currently assumed.

Diverse phylogeny of facultatively oligotrophic bacteria

The isolated bacterial strains belong to different phylogenetic groups, namely *α-Proteobacteria*, *γ-Proteobacteria* and *Actinobacteria*. Based on the 16S rRNA gene data, the isolated α-proteobacterium (FO-BEG1) is highly identical to the *Pseudovibrio denitrificans* type strain, which is described as a heterotrophic, facultatively anaerobic microorganism capable of performing complete denitrification (Shieh *et al.*, 2004). With our experiments, we have shown for the first time that the *Pseudovibrio denitrificans* type strain as well as the isolated *Pseudovibrio* strain FO-BEG1 are able to multiply and build up biomass under extreme nutrient limitation. Likewise, growth under oligotrophic conditions as observed for the isolates FO-NAM13 and FO-NAM14 (related to *Kangiella* spp.), has so far never been described for any member of the genus *Kangiella*. Long-term starvation and survival but no growth in the absence of external nutrients has previously been reported for *Arthrobacter* spp. and was proposed to be fueled by internally stored reserve material (Zevenhuizen, 1966). In our study, isolates FO-NAM1, FO-NAM2 (related to *Arthrobacter* spp.) were transferred in oligotrophic medium more than seven times and active growth was always observed. Hence, we assume that the cells gained energy and built up biomass from an external source, since we determined growth and not only survival. Bacteria belonging to the genus *Marinobacter* are known to be diverse in physiology (e.g. Gauthier *et al.*, 1992; Huu *et al.*, 1999) and substrate uptake under low nutrient conditions was shown for *Marinobacter arcticus* (Button *et al.*, 2004), but oligotrophic growth was not studied in detail whereas the isolates FO-NAM3 to FO-NAM12 (related to *Marinobacter* spp.) actively grow under nutrient deficiency.

Cell numbers of the isolated strains growing under oligotrophic conditions differed between the phylogenetic groups. The cell numbers of isolates related to *Marinobacter* spp. were higher than cell numbers of the other isolates, whereas the isolates related to *Kangiella* spp. did not grow for more than six transfers. This suggests that different phylotypes vary in their capabilities of adapting to oligotrophic growth conditions. Taken together, our data indicate that the ability to switch between extreme nutrient deficiency and affluence of substrate is not unusual or restricted to a certain phylogenetic group, even if the level of adaptation might differ. Therefore, we propose that the ability to grow under extreme substrate limitation is much more widespread among known heterotrophic bacteria than currently recognized.

Acknowledgments

This study was funded by the European Research Council and the Max Planck Society. We thank A.-C. Kreutzmann for helpful remarks on the manuscript, V. Salman, M. Friebe, and M. Meyer for technical support and the members of the Meteor cruise M76 (April – June 2008) for providing samples.

References

Alldredge AL, Cole JJ, Caron DA. (1986). Production of heterotrophic bacteria inhabiting macroscopic organic aggregates (marine snow) from surface waters. *Limnol Oceanogr* **31:** 68–78.

Ammerman JW, Fuhrman JA, Hagström A, Azam F. (1984). Bacterioplankton growth in seawater: I. Growth kinetics and cellular characteristics in seawater cultures. *Mar Ecol Prog Ser* **18:** 31–39.

Azam F, Malfatti F. (2007). Microbial structuring of marine ecosystems. *Nat Rev Microbiol* **5:** 782–791.

Brock J, Schulz-Vogt HN. (2011). Sulfide induces phosphate release from polyphosphate in cultures of a marine *Beggiatoa* strain. *ISME J* **5:** 497–506.

Button DK, Robertson B, Gustafson E, Zhao XM. (2004). Experimental and theoretical bases of specific affinity, a cytoarchitecture-based formulation of nutrient collection proposed to supercede the Michaels-Menten paradigm of microbial kinetics. *Appl Environ Microbiol* **70:** 5511–5521.

Button DK, Schut F, Quang P, Martin R, Robertson BR. (1993). Viability and isolation of marine bacteria by dilution culture: theory, procedures, and initial results. *Appl Environ Microbiol* **59:** 881–891.

Carlucci AF, Shimp SL. (1974). Isolation and growth of a marine bacterium in low concentrations of substrate. In: Colwell RR, Morita RY (eds). *Ocean environment microbial activities*. University Park Press: Baltimore. pp 363–367.

Carlucci AF, Shimp SL, Craven DB. (1986). Growth- characteristics of low-nutrient bacteria from the Northeast and Central Pacific-Ocean. *FEMS Microbiol Ecol* **38:** 1–10.

Connon SA, Giovannoni SJ. (2002). High-throughput methods for culturing microorganisms in very-low-nutrient media yield diverse new marine isolates. *Appl Environ Microbiol* **68:** 3878–3885.

Gauthier MJ, Lafay B, Christen R, Fernandez L, Acquaviva M, Bonin P *et al.* (1992). Marinobacter hydrocarbonoclasticus gen. nov., sp. nov., a new, extremely halotolerant, hydrocarbon-degrading marine bacterium. *Int J Syst Bacteriol* **42:** 568–576.

Hansell DA, Carlson CA, Repeta DJ, Schlitzer R. (2009). Dissolved organic matter in the ocean a controversy stimulates new insights. *Oceanography* **22:** 202–211.

Huu NB, Denner EBM, Ha DTC, Wanner G, Stan-Lotter H. (1999). *Marinobacter aquaeolei* sp. nov., a halophilic bacterium isolated from a Vietnamese oil-producing well. *Int J Syst Bacteriol* **49:** 367–375.

Ishida Y, Kadota H. (1981). Growth patterns and substrate requirements of naturally occurring obligate oligotrophs. *Microb Ecol* **7:** 123–130.

Ishida Y, Imai I, Miyagaki T, Kadota H. (1982). Growth and uptake kinetics of a facultatively oligotrophic bacterium at low nutrient concentrations. *Microb Ecol* **8:** 23–32.

Ishida Y, Fukami K, Eguchi M, Yoshinaga I. (1989). Strategies for growth of oligotrophic bacteria in the pelagic environment. In: Hattori T, Ishida Y, Maruyama Y, Morita RY, Uchida A (eds). *Recent advances in microbial ecology*. Janpan Scientific Society Press: Japan. pp 89–93.

Kamp A, Roy H, Schulz-Vogt HN. (2008). Video-supported analysis of *Beggiatoa* filament growth, breakage, and movement. *Microb Ecol* **56:** 484–491.

Ludwig W, Strunk O, Westram R, Richter L, Meier H, Yadhukumar *et al.* (2004). ARB: a software environment for sequence data. *Nucleic Acids Res* **32:** 1363–1371.

MacDonell MT, Hood MA. (1982). Isolation and characterization of ultramicrobacteria from a Gulf Coast Estuary. *Appl Environ Microbiol* **43:** 566–571.

Muyzer G, Teske A, Wirsen CO, Jannasch HW. (1995). Phylogenetic relationships of *Thiomicrospira* species and their identification in deep-sea hydrothermal vent samples by denaturing gradient gel-electrophoresis of 16S rDNA fragments. *Arch Microbiol* **164:** 165–172.

Pruesse E, Quast C, Knittel K, Fuchs BM, Ludwig WG, Peplies J *et al.* (2007). SILVA: a comprehensive online resource for quality checked and aligned ribosomal RNA sequence data compatible with ARB. *Nucleic Acids Res* **35:** 7188–7196.

Salman V, Amann R, Girnth AC, Polerecky L, Bailey JV, Høgslund S *et al.* (2011). A single-cell sequencing approach to the classification of large, vacuolated sulfur bacteria. *Syst Appl Microbiol* **34:** 243–259.

Schut F, Prins RA, Gottschal JC. (1997). Oligotrophy and pelagic marine bacteria: facts and fiction. *Aquat Microb Ecol* **12:** 177–202.

Shieh WY, Lin YT, Jean WD. (2004). *Pseudovibrio denitrificans* gen. nov., sp. nov., a marine, facultatively anaerobic, fermentative bacterium capable of denitrification. *Int J Syst Evol Microbiol* **54:** 2307–2312.

Smith DC, Simon M, Alldredge AL, Azam F. (1992). Intense hydrolytic enzyme activity on marine aggregates and implications for rapid particle dissolution. *Nature* **359:** 139–142.

Van der Kooij D, Visser A, Hijnen WAM. (1980). Growth of *Aeromonas hydrophila* at low concentrations of substrates added to tap water. *Appl Environ Microbiol* **39:** 1198–1204.

Weber CA. (1907). Aufbau und Vegetation der Moore Norddeutschlands. *Botanische Jahrbuecher fuer Systematik, Pflanzengeschichte und Pflanzengeographie / Beiblatt*. pp 19–34.

Yanagita T, Ichikawa T, Tsuji T, Kamata Y, Ito K, Sasaki M. (1977). Two trophic groups of bacteria, oligotrophs and eutrophs: their distribution in fresh and sea water areas in the central northern Japan. *J Gen Appl Microbiol* **24:** 59–88.

Zengler K, Toledo G, Rappe M, Elkins J, Mathur EJ, Short JM *et al.* (2002). Cultivating the uncultured. *Proc Natl Acad Sci U S A* **99:** 15681–15686.

Zevenhuizen LPTM. (1966). Formation and function of glycogen-like polysaccharide of Arthrobacter. *Anton Van Lee J M S* **32:** 356–372.

ZoBell CE. (1941). Studies on marine bacteria. I. The cultural requirements of heterotroophic aerobes. *J Mar Rev* **4:** 41–75.

Chapter IV

Pseudovibrio denitrificans^{T} versus *Pseudovibrio* sp. FO-BEG1 – a comparison

Vladimir Bondarev[1], Nora Buddruhs[2], Heide N. Schulz-Vogt[1]

[1]Max Planck Institute for Marine Microbiology, Ecophysiology Group, Celsiusstr. 1, D-28359 Bremen, Germany

[2]Leinbniz Institut DSMZ – Deutsche Sammlung von Mikroorganismen und Zellkulturen GmbH, Inhoffenstraße 7B, D-38124 Braunschweig, Germany

Manuscript in preparation

Contributions:

The concept of this study was developed together with H. N. Schulz-Vogt. I performed the physiological tests and evaluation of the data. Biolog® experiments were performed together with N. Buddruhs. The manuscript was written in collaboration with H. N. Schulz-Vogt including comments of N. Buddruhs.

Abstract

The genus *Pseudovibrio* contains three species: *Pseudovibrio denitrificans, Pseudovibrio ascidiaceicola* and *Pseudovibrio japonicus*. The latter two are closer related to each other than to *P. denitrificans*. The main physiological characteristic of the genus is the facultative anaerobic growth with fermentative or denitrifying metabolisms. The three currently known species differ mainly in substrate specificity and enzyme activity profiles. The new strain described here, *Pseudovibrio* sp. FO-BEG1, has been isolated from a co-culture containing as a second partner a lithotrophic *Beggiatoa* species. This *Pseudovibrio* strain shows 99.6% sequence identity to the 16S rRNA gene of the *P. denitrificans* type strain and less than 98.7% to *P. ascidiaceicola* and *P. japonicus*. In this study, we present a genotypic and phenotypic comparison of *Pseudovibrio* sp. FO-BEG1 and the type strain of *P. denitrificans,* revealing a DNA-DNA hybridization identity of 66.3% (±2%) and several physiological differences in substrate usage, like the inability of *P. denitrificans*^{T} to grow on succinic acid, malic acid, α-ketoglutaric acid and fumaric acid, which are intermediates of the citric acid cycle. The differences between the two strains shown in the present study are not sufficient to justify a phylogenetic diversion into two different species and we therefore propose that *Pseudovibrio* sp. FO-BEG1 is a strain within the *Pseudovibrio denitrificans* species.

Introduction

The *Pseudovibrio* genus belongs to the *Rhodobacteraceae* family of the *α-Proteobacteria* and contains three type species, the first of which, *Pseudovibrio denitrificans*, has been described in 2004 as a flagellated, facultatively anaerobic bacterium capable of fermentation and denitrification and was isolated from coastal waters in Taiwan (Shieh *et al.*, 2004). Sequentially, two further species were described: *Pseudovibrio ascidiaceicola* (Fukunaga *et al.*, 2006), which had been isolated from a tunicate, and *Pseudovibrio japonicus*, isolated from coastal waters in Japan (Hosoya and Yokota, 2007). They shared a 16S rRNA gene sequence identity to *P. denitrificans* of 98.9% and 98.3%, respectively. The physiology of all three species was similar, including the capability of fermentation and denitrification, with substrate spectra and enzyme activity profiles differing in the utilization of several carbon compounds as well as the activities of chemotrypsin, α-glucosidase, arginine dihydrolase, valine arylamidase, napthol-AS-BI-phosphohydrolase and N-acetyl-glucosaminidase (Fukunaga *et al.*, 2006; Hosoya and Yokota, 2007). The assignment into different species was determined due to the phenotypic differences and the low DNA-DNA hybridization (DDH) values of less than 30% and 35% for *P. ascidiaceicola* and *P. japonicus*, respectively, compared to *P. denitrificans* and below 35% between *P. ascidiaceicola* and *P. japonicus* (Fukunaga *et al.*, 2006; Hosoya and Yokota, 2007).

The novel strain *Pseudovibrio* sp. FO-BEG1 has been isolated from a black-band diseased coral in Florida and was maintained in co-culture with *Beggiatoa* sp. before establishment of an axenic culture by Schwedt (Schwedt, 2007; Schwedt, 2011). Genome sequencing and annotation as well as physiological investigations of strain FO-BEG1 expanded the knowledge about this genus and illustrated its metabolic versatility and simultaneous adaptation to a host-associated life style (**Chapter II**). The main aim of this study was the characterization of the differences of strain FO-BEG1 compared to the *Pseudovibrio denitrificans* type strain by using a polyphasic approach in order to derive the phylogenetic affiliation and to assign FO-BEG1 either as a new strain to the species *Pseudovibrio denitrificans* or as a new species to the genus *Pseudovibrio*.

Materials and Methods

Used strains and cultivation conditions

Pseudovibrio denitrificans^{T} (DSM 17465) was purchased from the German culture collection DSMZ (Leibniz-Institut DSMZ-Deutsche Sammlung von Mikroorganismen und Zellkulturen GmbH, Braunschweig, Germany) and cultivated on PY agar plates according to Shieh *et al.* (2004). PY agar plates contained the following constituents per liter deionized water: 2 g polypeptone (Becton, Dickinson and Company Sparks (BD), MD, USA); 0.5 g yeast extract (BD); 30 g NaCl; 5 g $MgCl_2 \cdot 6\ H_20$; 0.005 g $CaCl_2$; 0.005 g $Na_2MoO_4 \cdot 7\ H_2O$; 0.004 g $CuCl_2 \cdot 2\ H_2O$; 0.006 g $FeCl_3 \cdot 6\ H_2O$; 15 g Bacto Agar (BD) and the pH was adjusted to 8. For the growth experiments, liquid PY medium without agar was prepared and the amount of polypeptone and yeast extract was reduced to 0.2 g and 0.05 g, respectively. The tested substrates glucose, succinic acid and fumaric acid were added in a final concentration of 10 mmol l^{-1}. Growth was monitored as the optical density ($OD_{600\ nm}$) using an Eppendorf BioPhotometer (Eppendorf AG, Hamburg, Germany). *Pseudovibrio* sp. FO-BEG1 was grown in CM medium modified after (Shieh *et al.*, 2004) as described in the Materials and Methods part in **Chapter II**.

DNA-DNA hybridization (DDH)

DNA-DNA hybridization was performed by the DSMZ. Cells were disrupted by using a French pressure cell (Thermo Spectronic) and the DNA in the crude lysate was purified by chromatography on hydroxyapatite as described by Cashion *et al.* (1977). DNA-DNA hybridization was carried out as described by De Ley *et al.* (1970) under consideration of the modifications described by Huss *et al.* (1983) using a model Cary 100 Bio UV/VIS-spectrophotometer equipped with a Peltier-thermostatted 6×6 multicell changer and a temperature controller with *in-situ* temperature probe (Varian).

Extraction and analysis of fatty acids

Fatty acid analysis was performed by the DSMZ. Fatty acid methyl esters from 40 mg cells scraped from Petri dishes were obtained by saponification, methylation, and extraction using minor modifications of the method of Miller (1982) and Kuykendall *et al.* (1988). The fatty acid methyl esters mixtures were separated using Sherlock Microbial Identification System (MIS) (MIDI, Microbial ID, Newark, DE, USA) which consisted of an Agilent model 6890N gas chromatograph fitted with a 5% phenyl-methyl silicone capillary column

(0.2 mm × 25 m), a flame ionization detector, Agilent model 7683A automatic sampler, and a HP-computer with MIDI data base (Hewlett-Packard Co., Palo Alto, CA, USA). Peaks were automatically integrated and fatty acid names and percentages calculated by the MIS Standard Software (Microbial ID). The gas chromatographic parameters were as follows: carrier gas, ultra-high-purity hydrogen; column head pressure 60 kPa; injection volume 2 µl; column split ratio, 100:1; septum purge 5 ml min^{-1}; column temperature, 170 to 270 °C at 5 °C min^{-1}; injection port temperature, 240 °C and detector temperature, 300 °C.

API tests

API API 20 E, API 20 NE, API ZYM and API 50 CH tests were performed by the DSMZ according to manufacturer's instructions. Cells were resuspended in the inoculation fluid containing 3% NaCl in order to increase the salinity. The stripes were incubated for 48 hours and visually evaluated.

Biolog® experiments

For the Biolog® experiment, Phenotype MicroArray (PM) plates 1 and 2 were used. 12 ml of the inoculation fluid was prepared as follows: 10 ml of the IF-0 solution (Biolog®, Hayward CA, USA) were mixed with 1.2 ml artificial sea salts (containing 200 g l^{-1} NaCl; 40 g l^{-1} $NaSO_4$; 30 g l^{-1} $MgCl_2 \cdot 6\ H_2O$; 5 g l^{-1} KCl; 2.5 g l^{-1} NH_4Cl; 2 g l^{-1} KH_2PO_4; 1.5 g l^{-1} $CaCl_2 \cdot 2\ H_2O$), 0.428 ml deionised water, 0.12 ml vitamin solution (containing 2 mg l^{-1} biotin; 20 mg l^{-1} niacin; 8 mg l^{-1} 4-aminobenzoic acid; 1 mg l^{-1} thiamine), 0.012 ml trace elements (containing 13 ml l^{-1} HCl 25%; 2.1 g l^{-1} $FeSO_4 \cdot 7\ H_2O$; 5.2 g l^{-1} $Na_2EDTA \cdot 2\ H_2O$; 30 mg l^{-1} H_3BO_3; 2.1 g l^{-1} $FeSO_4 \cdot 7\ H_2O$; 100 mg l^{-1} $MnCl_2 \cdot 4\ H_2O$; 190 mg l^{-1} $CoCl_2 \cdot 6\ H_2O$; 24 mg l^{-1} $NiCl_2 \cdot 6\ H_2O$; 2 mg l^{-1} $CuCl_2 \cdot 2\ H_2O$; 144 mg l^{-1} $ZnSO_4 \cdot 7\ H_2O$; 36 mg l^{-1} $Na_2MoO_4 \cdot 2\ H_2O$), 0.12 ml carbonate buffer (1.8 mmol l^{-1} final concentration) and 0.12 ml DyeD (Biolog®). Colonies from marine broth agar plates (37.4 g l^{-1} Difco™ Marine Broth (BD) and 15 g l^{-1} Bacto Agar (BD) grown for two days at 28 °C were dissolved in this inoculation fluid until an absorption of 85% was achieved, measured with a turbidimeter (Biolog®). 100 µl of this solution were used for inoculation of each well of the PM1 and PM2 plates. For incubation at 28 °C, the plates were placed in the GEN III OmniLog II system (Biolog®) and the color development was measured every 15 minutes for 96 hours.

Calculation of the phylogenetic tree

Phylogenetic analysis of the 16S rRNA gene sequences was performed using ARB (Ludwig *et al.*, 2004) and the release 102 of the SILVA SSURef database (Pruesse *et al.*, 2007), which contained the 16S rRNA gene sequence of *Pseudovibrio denitrificans*^{T}. The 16S rRNA gene sequence of *Pseudovibrio* sp. FO-BEG1 was extracted from the sequenced genome of strain FO-BEG1. Tree reconstruction was performed with the maximum likelihood method and a total of nineteen full-length 16S rRNA gene sequences. Calculation included gene sequence information between positions 100 and 1479 (according to *E. coli* numbering) and stability of the tree was verified by bootstraps calculation with 1000 runs. Members of other *α-Proteobacteria* groups were included in the analysis to verify the phylogenetic affiliation within the *α-Proteobacteria*. The tree was rooted with nine *Arthrobacter* sp. as the outgroup.

Results

Genotypic characteristics

The analysis of the *Pseudovibrio* sp. FO-BEG1 16S rRNA gene sequence revealed an identity of 99.6% to *P. denitrificans*^{T} and 98.4% and 98% to *P. ascidiaceicola* and *P. japonicus*, respectively. The topology of a phylogenetic tree calculated from the multiple sequence alignment based on 16S rRNA gene sequence information confirmed the phylogenetic affiliation of those two strains to *P. denitrificans*^{T}. *P. ascidiaceicola* and *P. japonicus* were separated from *P. denitrificans*^{T} and clustered on a separate branch (**Figure 4.1**). On the other hand, DNA-DNA hybridization resulted in a hybridization level of 66.3% (±2%) between *P. denitrificans* type strain and *Pseudovibrio* sp. FO-BEG1, indicating a separation of the two strains into separate species.

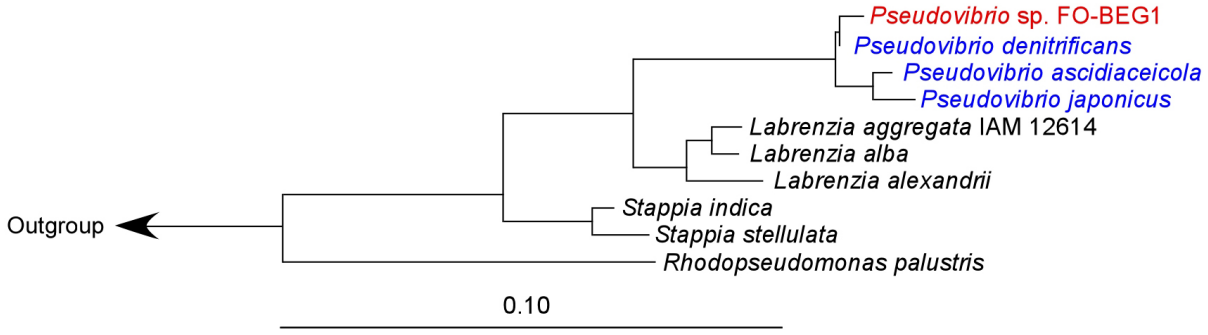

Figure 4.1. Maximum likelihood phylogenetic tree based on 16S rRNA gene sequence analysis showing the three described species within the genus *Pseudovibrio* (blue) and the new strain FO-BEG1 (red). The closely related members of the *α-Proteobacteria* are shown in black. Bootstrap values for all nodes shown were >78%.

Phenotypic characteristics

Both strains, *P. denitrificans*^{T} and *Pseudovibrio* sp. FO-BEG1, form beige colonies with an entire margin on PY agar approximately 24 to 36 hours after inoculation. After 3 days of growth, colonies of *P. denitrificans*^{T} became darker, in contrast to colonies of strain FO-BEG1, which are consistent in color. Colony consistency was rather viscous in the case of strain FO-BEG1 and more buoyant for *P. denitrificans*^{T}. Cells of both strains were mainly straight or curved rods and were motile by the means of one or several flagella (Shieh *et al.*, 2004) . In defined, aerobic, liquid medium (CM) supplemented with glucose, ammonia, trace elements and vitamins (see Materials and Methods of **Chapter II**) growth could only be observed for strain FO-BEG1, but not for the type strain *P. denitrificans*. None of the strains grew in defined medium under anaerobic, fermenting or denitrifying conditions, but when the medium was prepared with aged North Sea water (see Materials and Methods of **Chapter II**), strain FO-BEG1, but not *P. denitrificans*^{T}, was capable to grow (results not shown).

Table 4.1: Cellular fatty acid content of *P. denitrificans*^{T} and *Pseudovibrio* sp. FO-BEG1. Values are percentages of all recorded fatty acids.

Fatty acid	*Pseudovibrio* sp. FO-BEG1	*Pseudovibrio denitrificans*^{T}
16:0	5.19	6.15
17:0	0.62	0.32
16:0 3OH	0.42	0.58
18:1 ω7*c*	82.23	76.37
18:0	3.18	2.65
11 methyl 18:1 ω7*c*	–	0.24
19:0 cyclo ω8*c*	1.67	7.13
19:0 10 methyl	–	0.24
18:0 3OH	2.11	2.15
Summed feature 2 14:0 3-OH and/or 16:1 iso I	2.00	1.85
Summed feature 3 15:0 iso 2-OH and/or 16:1ω7*c*	2.08	1.95

Both strains exhibited a similar cellular fatty acid profile (**Table 4.1**). *Pseudovibrio* sp. FO-BEG1 differed in having a higher amount of the unsaturated fatty acid 18:1 ω7*c* and lower amounts of 19:0 cyclo ω8*c*.

API tests

The commercially available API systems (bioMérieux) consist of a strip with several microwells containing different enzymatic substrates, including a buffer, for the research of enzymatic activities, or different carbon substrates for the investigation of their assimilation and fermentation. The tests are evaluated by investigation of the color, produced during the enzymatic reaction with an added reagent or by the color change of the pH indicator during fermentative acidification. The analysis of API 20 E, API 20 NE, API ZYM and API 50 CH showed high consistency between the tested strains, except for mannose, N-acetylglucosamin, malate, maltose assimilation as well as weak esterase, acid phosphatase and naphtol-AS-BI-phosphorylhydrolase activity, which were positive for *Pseudovibrio* sp. FO-BEG1 and negative for *P. denitrificans*^{T} (**Table 4.2**).

Biolog® experiments

Biolog® experiments were performed with PM1 and PM2 plates containing 190 different carbon sources (Bochner, 2009), in which the strains were tested for metabolic activity by the measurement of color development when the tetrazolium dye was reduced to the colored formazan crystals (Smith and McFeters, 1997). In both plates, the negative control well, which did not contain any carbon substrate, showed metabolic activity for both strains (**Figure S 4.2A and B**). Therefore, the highest measured negative control value of the respective PM plate was taken as a threshold for all other measurements. Values below that threshold represented absence of metabolic activity; values above represented metabolic activity for the respective substrate. Since the analysis was performed in triplicates, at least two curves exceeding the threshold were considered positive. Differences between *P. denitrificans*^{T} and strain FO-BEG1, where FO-BEG1 showed metabolic activity and the type strain did not, were the following: succinic acid, L-aspartic acid, D,L-α-glycerolphosphate, D-galactonic acid-γ-lactone, D,L-malic acid, Tween 40, α-ketoglutaric acid, α-ketobutyric acid, lactulose, fumaric acid, bromosuccinic acid, D-malic acid, L-malic acid, glucuronamide, D-fucose, 3-0-β-D-galacto-pyranosyl-D-arabinose, γ-aminobutyric acid, α-methyl-D-galactoside, butyric acid, caproic acid, citraconic acid, D-lactic acid methyl ester, succinamic acid, L-isoleucine, L-leucine, L-phenylalanine and L-pyroglutamic acid. On the other hand, the type

strain showed metabolic activity on L-arabinose, D-threonine and acetoacetic acid, but strain FO-BEG1 did not.

Table 4.2: Characteristics of *P. denitrificans*^{T} and *Pseudovibrio* sp. FO-BEG1 as obtained by API 20 E, API 20 NE, API ZYM and API 50 CHE tests. Symbol + represents a positive, - represents a negative and (+) represents a weak positive response.

Combined results from API 20 E, API 20 NE, API ZYM, and API 50 CHE	***Pseudovibrio* sp. FO-BEG1**	***Pseudovibrio denitrificans*^{T}**
Assimilation of:		
Mannose, N-acetylglucosamine, maltose, malate	+	-
Glucose, arabinose, mannitol, gluconate, caprate, adipate, citrate, phenylacetate	-	-
Activity of:		
Alkaline phosphatase, leucin-arylamidase, trypsin, chemotrypsin, N-acetyl-glucosaminidase, β-galacto-sidase, gelatinase	+	+
Lipase, valin-arylamidase, cystin-arylamidase, α-galactosidase, β-glucuronidase, β-glucosidase, α-mannosidase, α-fructosidase, tryptophan desaminase, urease, ornithin decarboxylase, lysin decarboxylase, arginin dihydrolase	-	-
α-Glucosidase, esterase lipase	(+)	(+)
Esterase, acid phosphatase, naphtol-AS-BI-phosphoryl-hydrolase	(+)	-
Nitrate reduction	+	+
Indole production	+	+
Gelatine hydrolysis	+	+
Esculin hydrolysis	+	+
VP reaction	-	-
H_2S production	-	-
Fermentation of:		
Glucose, sucrose, D-arabinose, ribose, mannose, maltose, sucrose, trehalose, D-turanose	+	+
Mannitol, inositol, rhamnose, amygdalin, L-arabinose, glycerol, erythritol, D-xylose, L-xylose, adonitol, β-D-xyloside, galactose, fructose, sorbose, dulicitol, sorbitol, α-D-mannoside, α-D-glucoside, N-acetylglucosamine, arbutin, esculin, salicin, cellobiose, lactose, inulin, melezitose, raffinose, starch, glycogen, xylitol, gentio-biose, D-lyxose, D-tagatose, D-fucose, L-fucose, D-arabitol, L-arabitol, gluconate, 2-ketogluconate, 5-ketogluconate	-	-
Melibiose	(+)	(+)

To confirm the results obtained by Biolog®, growth experiments of the type strain with selected substrates (glucose, malic acid and fumaric acid) were performed. Indeed, growth with glucose was significantly higher than with malic or fumaric acid in *Pseudovibrio denitrificans*^{T}. Cultures grown on the latter two substrates only achieved optical density comparable to the control (**Figure S 4.1**).

Discussion

Genotypic characterization

According to Stackebrandt and Ebers (2006), two species can be delineated if the identity of the 16S rRNA gene is below 98.7%. If the value lies above 98.7%, the affiliation must be determined by other factors like physiological and genomic differences and chemotaxonomic data. The identity of the 16S rRNA gene of strain FO-BEG1 compared to both *P. ascidiaceicola* and *P. japonicus* is below the threshold of 98.7%. Furthermore, both species cluster on a branch separated from *P. denitrificans*^{T} and strain FO-BEG1 (**Figure 4.1**), which justifies the allocation of the first three into different species. The 16S rRNA gene sequence identity of more than 99.5% indicates a close phylogenetic relationship of strain FO-BEG1 to *P. denitrificans*^{T}. The G+C content of the genome of *P. denitrificans*^{T} accounted for 51.7% (Shieh *et al.*, 2004) and 52.5% for *Pseudovibrio* strain FO-BEG1, being rather similar. DNA-DNA hybridization levels of the type strain with strain FO-BEG1 were 64.9% and 67.7% and thus lie below the threshold of 70% determined for organisms assigned to the same species (Schleifer, 2009; Tindall *et al.*, 2010). Accordingly, the two strains are considered to be classified into two different species. However, due to a common reproducibility bias of around 10% (De Ley *et al.*, 1970), the establishment of a new species based mainly on DDH levels is not reliable and needs to be confirmed by physiological and chemotaxonomic data.

Phenotypic characterization

Analysis of the cellular fatty acid composition of strain FO-BEG1 and *P. denitrificans*^{T} (**Table 4.1**) supports the close relation between the two strains, with the unsaturated 18:1 ω7*c* being the major fatty acid. The measured values are comparable to those published for the other *Pseudovibrio* strains (Fukunaga *et al.*, 2006; Hosoya and Yokota, 2007). It is, however, difficult to compare absolute values as the method is strongly dependent on the growth status of the bacteria and different growth conditions might result in a different

fatty acids profile (Tindall *et al.*, 2010). This observation is well reflected in the fact that the FAME data published for the description of *P. japonicus* and *P. ascidiaceicola*, report the lack of the fatty acid 19:0 cyclo ω8*c* for *P. denitrificans*^{T}, whereas in our study it made up more than 7%.

In the API tests, both strains differed in the assimilation of four carbon compounds and the activity of three enzymes out of 92 tests performed. With the Biolog® system, we tested 190 carbon compounds, for 72 of which both strains showed metabolic activity, 88 were tested negative for both strains and for 30 the metabolic reaction differed. Interestingly, 16 of the substrates tested negative for *Pseudovibrio denitrificans*^{T} represent acids, including intermediates of the citric acid cycle, like α-ketoglutaric acid, succinic acid, fumaric acid and malic acid. Since we do not have any indications for the deficiency or malfunction of the citric acid cycle in the type strain, we conclude that the import of the acids is impaired due to missing transporters. Even though the results show that the physiology of both strains is similar, differences in substrate usage indicate adaptations of their metabolic capabilities to different conditions, which strongly suggests the separation into two different species. It should be taken into consideration, however, that the metabolic differences could result from long-term cultivation on different media, since adaptation to culture conditions have been observed numerous times (Zengler, 2009 and references therein), resulting in physiological changes of the bacteria. The DSMZ type strain has been cultivated on the undefined medium PY1071, containing yeast extract and polypeptone, for ca. two years, whereas strain FO-BEG1 has been isolated under oligotrophic conditions (**Chapter III**) and cultivated under defined conditions with glucose as carbon source (**Chapter II**) for more than 2 years.

The intention to use Biolog® for this study was the testing of metabolic activity of both strains on almost 200 substrates in a short amount of time. The drawback of this method, however, was the high background due to metabolic activity of both strains in the negative control well not containing any substrate. This background activity could be either due to contamination of the inoculum with organic material while using colonies from agar plates, or a possible respiration of internally stored carbon compounds e.g. polyhydroxyalkanoates (Jendrossek, 2009). Also growth on vitamins supplied to the inoculum fluid may be an explanation. For future experiments, the Biolog® setup could be improved by using a less sensitive dye for the detection of metabolic activity. Additionally, we identified some discrepancies between Biolog® tests and performed growth experiments. As has been

described in **Chapter II** of this thesis, growth of strain FO-BEG1 could be observed with 4-hydroxybenzoate as the sole carbon and energy source. In the Biolog® experiment (**Figure S 4.2**), this substrate was not metabolized. A reason for this discrepancy could be either the high background of the Biolog® measurements or due to the fact, that 4-hydroxybenzoate is used rather slowly by this strain (highest OD600 is achieved after 9 days, see **Chapter II**) and was overlooked by the Biolog® measurements lasting only 4 days. It is therefore conceivable that metabolic activities with substrates, which are used slowly by the bacteria, are determined false negative within Biolog® experiments. Therefore, we suggest that Biolog® is a useful tool to get a broad overview of metabolic capabilities of bacterial strains, but that substrates of interest should be tested in actual growth experiments.

In conclusion, the genotypic and phenotypic characterization of *Pseudovibrio denitrificans*^{T} DSM 17465 and *Pseudovibrio* sp. FO-BEG1 reveals some differences but also many similarities between the two analyzed strains. The distinctions are mainly based on the physiological data of different substrate utilization. Even though different metabolic abilities and substrate utilization profiles were the basis for the assignment into different species of *P. denitrificans*, *P. ascidiaceicola*, and *P. japonicus* (Shieh *et al.*, 2004; Fukunaga *et al.*, 2006; Hosoya and Yokota, 2007), the experimental data were supported by low DNA-DNA hybridization values, which is not the case in our analysis. Therefore, we propose, according with the current state of knowledge, to assign *Pseudovibrio* sp. FO-BEG1 as a new strain to the *Pseudovibrio denitrificans* species. However, we suggest further physiologic and phylogenetic analysis, which might result in the identification of major differences in the metabolism of both strains and consequent formation of a new species for *Pseudovibrio* sp. FO-BEG1.

Acknowledgments

We thank J. Harder for many fruitful discussions and V. Salman for comments on the manuscript. For technical support we thank M. Meyer and S. Menger. This study was funded by the European Research Council and the Max Planck Society.

References

Bochner BR. (2009). Global phenotypic characterization of bacteria. *FEMS Microbiol Rev* **33:** 191–205.

Cashion P, Holder-Franklin MA, McCully J, Franklin M. (1977). A rapid method for the base ratio determination of bacterial DNA. *Anal Biochem* **81:** 461–466.

De Ley J, Cattoir H, Reynaerts A. (1970). The quantitative measurement of DNA hybridization from renaturation rates. *Europ J Biochem* **12:** 133–142.

Fukunaga Y, Kurahashi M, Tanaka K, Yanagi K, Yokota A, Harayama S. (2006). *Pseudovibrio ascidiaceicola* sp. nov., isolated from ascidians (sea squirts). *Int J Syst Evol Microbiol* **56:** 343–347.

Hosoya S, Yokota A. (2007). *Pseudovibrio japonicus* sp. nov., isolated from coastal seawater in Japan. *Int J Syst Evol Microbiol* **57:** 1952–1955.

Huss VAR, Festl H, Schleifer KH. (1983). Studies on the spectrophotometric determination of DNA hybridization from renaturation rates. *Syst Appl Microbiol* **4:** 184–192.

Jendrossek D. (2009). Polyhydroxyalkanoate granules are complex subcellular organelles (carbonosomes). *J Bacteriol* **191:** 3195–3202.

Kuykendall LD, Roy MA, O'neill JJ, Devine TE. (1988). Fatty acids, antibiotic resistance, and deoxyribonucleic acid homology groups of *Bradyrhizobium japonicum*. *Int J Syst Bacteriol* **38:** 358–361.

Ludwig W, Strunk O, Westram R, Richter L, Meier H, Yadhukumar *et al.* (2004). ARB: a software environment for sequence data. *Nucleic Acids Res* **32:** 1363–1371.

Miller LT. (1982). Single derivatization method for routine analysis of bacterial whole-cell fatty acid methyl esters, including hydroxy acids. *J Clin Microbiol* **16:** 584–586.

Pruesse E, Quast C, Knittel K, Fuchs BM, Ludwig WG, Peplies J *et al.* (2007). SILVA: a comprehensive online resource for quality checked and aligned ribosomal RNA sequence data compatible with ARB. *Nucleic Acids Res* **35:** 7188–7196.

Schleifer KH. (2009). Classification of *Bacteria* and *Archaea*: past, present and future. *Syst Appl Microbiol* **32:** 533–542.

Schwedt A. (2007). Charakterisierung des dominanten Begleitorganismus eines marinen *Beggiatoa*-Konsortiums. Diploma thesis, Universität Hannover, Hannover.

Schwedt A. (2011). Physiology of a marine *Beggiatoa* strain and the accompanying organism *Pseudovibrio* sp. - a facultatively oligotrophic bacterium. Ph.D thesis, Universität Bremen, Bremen.

Shieh WY, Lin YT, Jean WD. (2004). *Pseudovibrio denitrificans* gen. nov., sp. nov., a marine, facultatively anaerobic, fermentative bacterium capable of denitrification. *Int J Syst Evol Microbiol* **54:** 2307–2312.

Smith JJ, McFeters GA. (1997). Mechanisms of INT (2-(4-iodophenyl)-3-(4-nitrophenyl)-5-phenyl tetrazolium chloride), and CTC (5-cyano-2,3-ditolyl tetrazolium chloride) reduction in *Escherichia coli* K-12. *J Microbiol Methods* **29:** 161–175.

Stackebrandt E, Ebers J. (2006). Taxonomic parameters revisited: tarnished gold standards. *Microbiology Today* **33:** 152–155.

Tindall BJ, Rosselló-Móra R, Busse HJ, Ludwig W, Kämpfer P. (2010). Notes on the characterization of prokaryote strains for taxonomic purposes. *Int J Syst Evol Microbiol* **60:** 249–266.

Zengler K. (2009). Central Role of the Cell in Microbial Ecology. *Microbiol Mol Biol Rev* **73:** 712–729.

Supplementary material

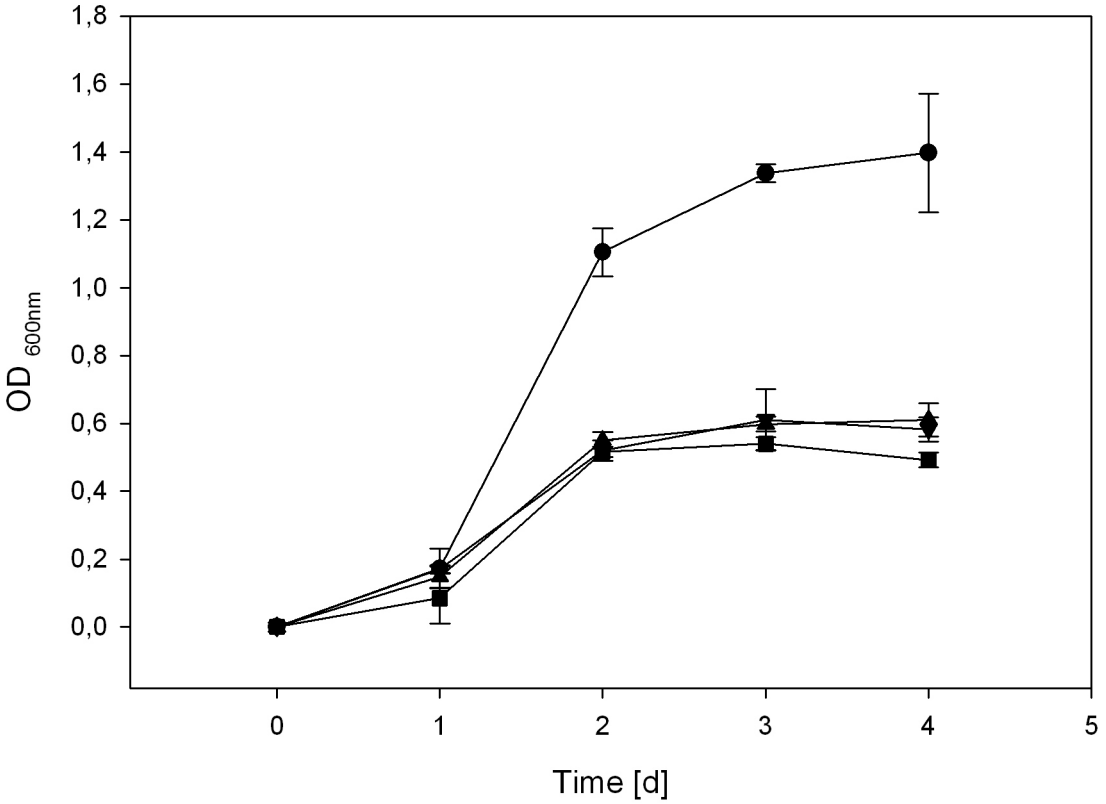

Figure S 4.1. Growth of *P. denitrificans* type strain cultivated in PY medium with reduced polypeptone and yeast extract concentrations with the addition of 10 mmol l^{-1} glucose (●), 10 mmol l^{-1} succinic acid (▼), 10 mmol l^{-1} fumaric acid (▲) and the control containing only PY with reduced polypeptone and yeast extract concentrations (■). Error bars represent the standard deviation of biological triplicates.

Figure S 4.2. Metabolic activity of *P. denitrificans*^{T} (blue chart) and *Pseudovibrio* sp. FO-BEG1 (red chart) tested with Biolog PM1 (A) and PM2 (B), each well containing different substrates designated in the heading. The color of the heading indicates metabolic activity of both strain on the respective substrate (orange), the absence of metabolic activity for both strains (white) or a different response of both strains (green). The black chart represents measured color development in a sterile control. The horizontal red and blue lines mark the threshold, which has been determined according to the maximal measured values in the negative control.

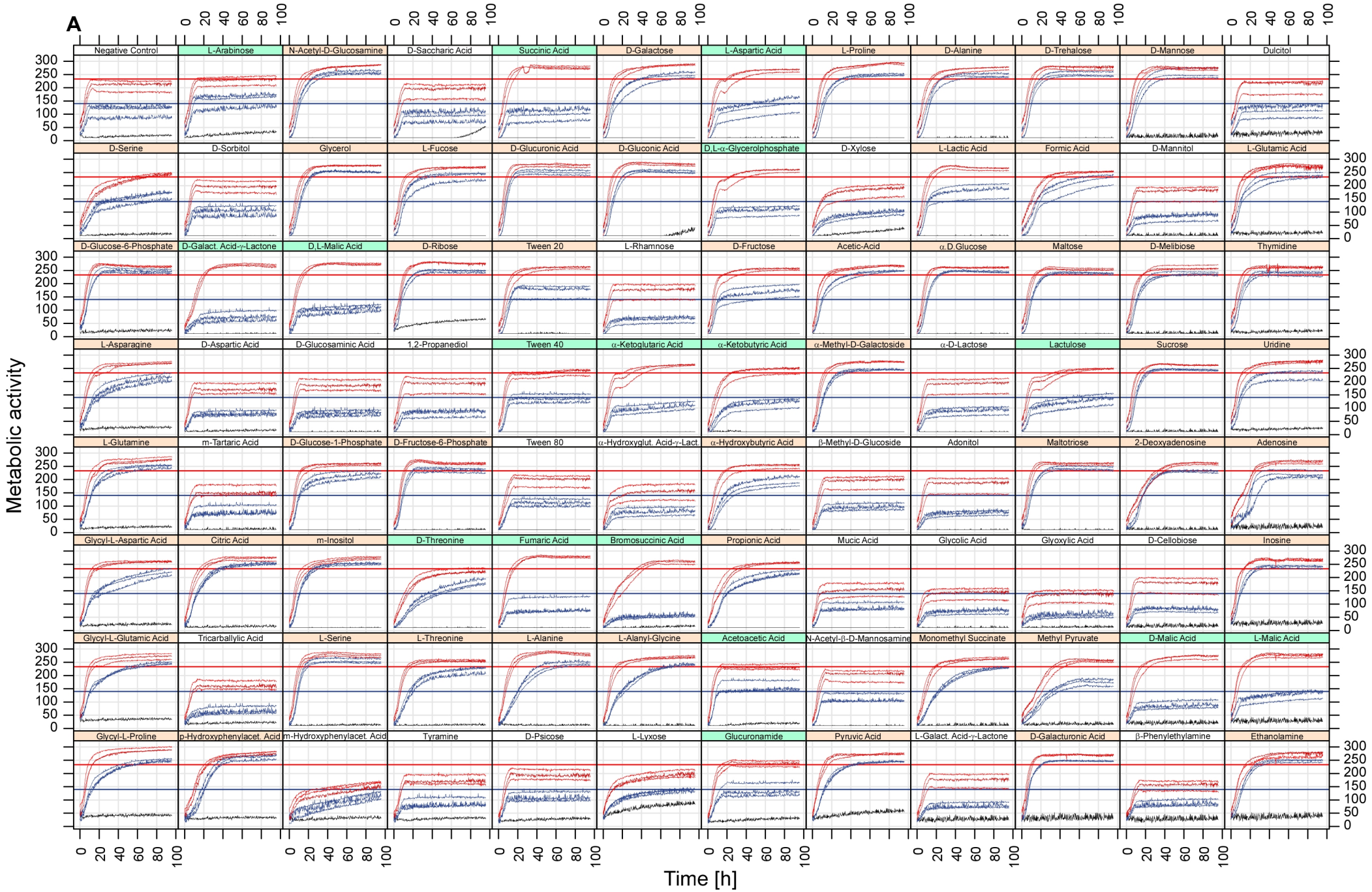
A
Negative Control
L-Arabinose
N-Acetyl-D-Glucosamine
D-Saccharic Acid
Succinic Acid
D-Galactose
L-Aspartic Acid
L-Proline
D-Alanine
D-Trehalose
D-Mannose
Dulcitol
D-Serine
D-Sorbitol
Glycerol
L-Fucose
D-Glucuronic Acid
D-Gluconic Acid
D,L-α-Glycerolphosphate
D-Xylose
L-Lactic Acid
Formic Acid
D-Mannitol
L-Glutamic Acid
D-Glucose-6-Phosphate
D-Galact. Acid-γ-Lactone
D,L-Malic Acid
D-Ribose
Tween 20
L-Rhamnose
D-Fructose
Acetic-Acid
α.D.Glucose
Maltose
D-Melibiose
Thymidine
L-Asparagine
D-Aspartic Acid
D-Glucosaminic Acid
1,2-Propanediol
Tween 40
α-Ketoglutaric Acid
α-Ketobutyric Acid
α-Methyl-D-Galactoside
α-D-Lactose
Lactulose
Sucrose
Uridine
L-Glutamine
m-Tartaric Acid
D-Glucose-1-Phosphate
D-Fructose-6-Phosphate
Tween 80
α-Hydroxyglut. Acid-γ-Lact.
α-Hydroxybutyric Acid
β-Methyl-D-Glucoside
Adonitol
Maltotriose
2-Deoxyadenosine
Adenosine
Glycyl-L-Aspartic Acid
Citric Acid
m-Inositol
D-Threonine
Fumaric Acid
Bromosuccinic Acid
Propionic Acid
Mucic Acid
Glycolic Acid
Glyoxylic Acid
D-Cellobiose
Inosine
Glycyl-L-Glutamic Acid
Tricarballylic Acid
L-Serine
L-Threonine
L-Alanine
L-Alanyl-Glycine
Acetoacetic Acid
N-Acetyl-β-D-Mannosamine
Monomethyl Succinate
Methyl Pyruvate
D-Malic Acid
L-Malic Acid
Glycyl-L-Proline
p-Hydroxyphenylacet. Acid
m-Hydroxyphenylacet. Acid
Tyramine
D-Psicose
L-Lyxose
Glucuronamide
Pyruvic Acid
L-Galact. Acid-γ-Lactone
D-Galacturonic Acid
β-Phenylethylamine
Ethanolamine
Metabolic activity
Time [h]

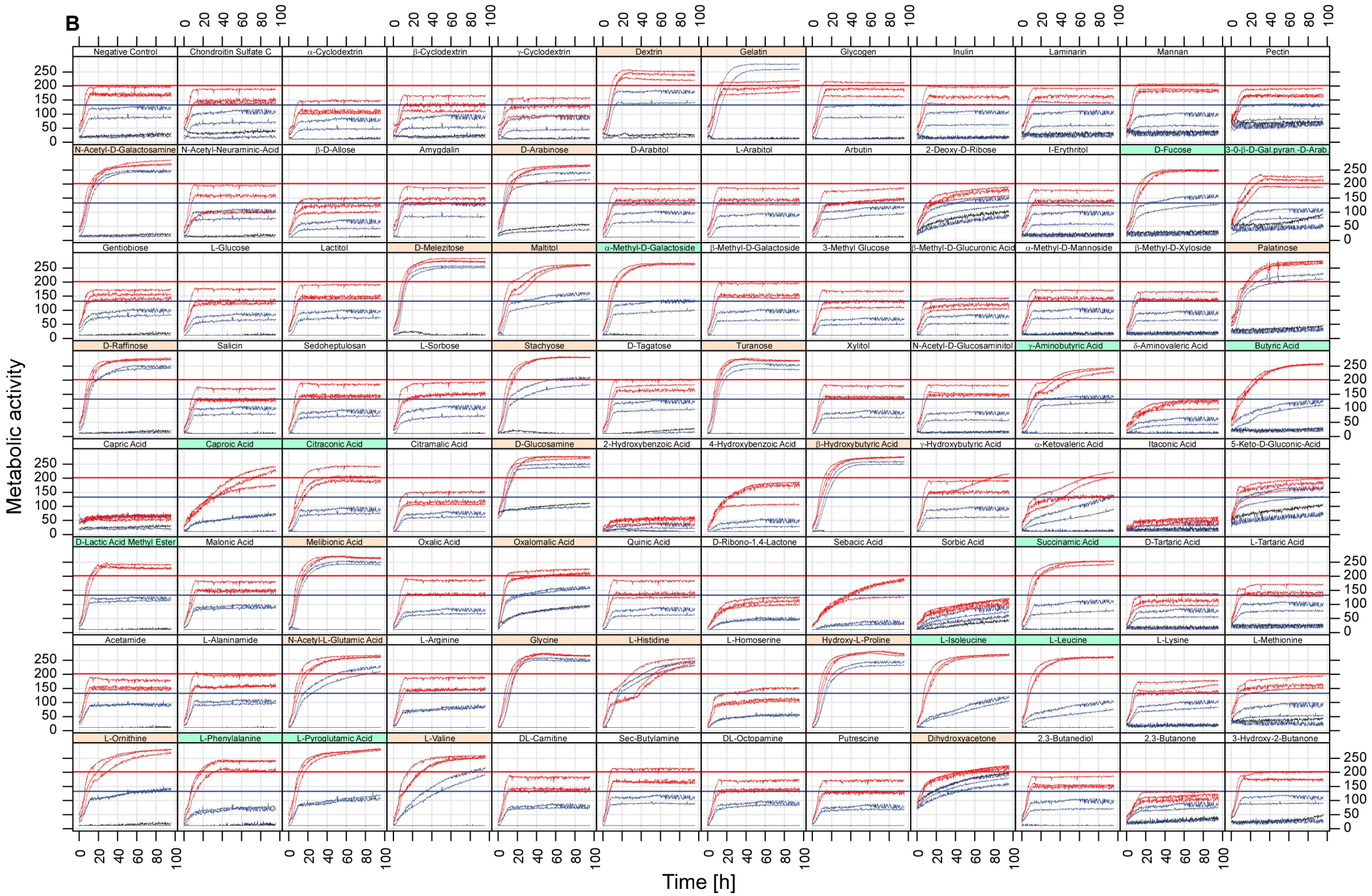
B
Negative Control
Chondroitin Sulfate C
α-Cyclodextrin
β-Cyclodextrin
γ-Cyclodextrin
Dextrin
Gelatin
Glycogen
Inulin
Laminarin
Mannan
Pectin
N-Acetyl-D-Galactosamine
N-Acetyl-Neuraminic-Acid
β-D-Allose
Amygdalin
D-Arabinose
D-Arabitol
L-Arabitol
Arbutin
2-Deoxy-D-Ribose
I-Erythritol
D-Fucose
3-0-β-D-Gal.pyran.-D-Arab.
Gentiobiose
L-Glucose
Lactitol
D-Melezitose
Maltitol
α-Methyl-D-Galactoside
β-Methyl-D-Galactoside
3-Methyl Glucose
β-Methyl-D-Glucuronic Acid
α-Methyl-D-Mannoside
β-Methyl-D-Xyloside
Palatinose
D-Raffinose
Salicin
Sedoheptulosan
L-Sorbose
Stachyose
D-Tagatose
Turanose
Xylitol
N-Acetyl-D-Glucosaminitol
γ-Aminobutyric Acid
δ-Aminovaleric Acid
Butyric Acid
Capric Acid
Caproic Acid
Citraconic Acid
Citramalic Acid
D-Glucosamine
2-Hydroxybenzoic Acid
4-Hydroxybenzoic Acid
β-Hydroxybutyric Acid
γ-Hydroxybutyric Acid
α-Ketovaleric Acid
Itaconic Acid
5-Keto-D-Gluconic-Acid
D-Lactic Acid Methyl Ester
Malonic Acid
Melibionic Acid
Oxalic Acid
Oxalomalic Acid
Quinic Acid
D-Ribono-1,4-Lactone
Sebacic Acid
Sorbic Acid
Succinamic Acid
D-Tartaric Acid
L-Tartaric Acid
Acetamide
L-Alaninamide
N-Acetyl-L-Glutamic Acid
L-Arginine
Glycine
L-Histidine
L-Homoserine
Hydroxy-L-Proline
L-Isoleucine
L-Leucine
L-Lysine
L-Methionine
L-Ornithine
L-Phenylalanine
L-Pyroglutamic Acid
L-Valine
DL-Carnitine
Sec-Butylamine
DL-Octopamine
Putrescine
Dihydroxyacetone
2,3-Butanediol
2,3-Butanone
3-Hydroxy-2-Butanone
Metabolic activity
Time [h]

Chapter V

Response to phosphate limitation in *Pseudovibrio* sp. strain FO-BEG1

Vladimir Bondarev[1], Stefano Romano[1], Thorsten Dittmar[2], Martin Kölling[3], Heide N. Schulz-Vogt[1]

[1]Max Planck Institute for Marine Microbiology, Ecophysiology Group, Celsiusstr. 1, D-28359 Bremen, Germany

[2]Max Planck Institute for Marine Microbiology, Marine Geochemistry Group, Institute for Chemistry and Biology of the Marine Environment, Carl von Ossietzky University of Oldenburg, Carl-von-Ossietzky-Str. 9-11, D-26129 Oldenburg, Germany

[3]MARUM Center for Marine Environmental Sciences, University of Bremen, Leobener Strasse, D-28359 Bremen, Germany

Manuscript in preparation

Contributions:

The concept of this study was developed together with S. Romano and H. N. Schulz-Vogt. The physiological experiments were performed together with S. Romano. The manuscript was written in collaboration with S. Romano and H. N. Schulz-Vogt.

Abstract

Phosphate (P_i) starvation in bacteria induces a response, which regulates the expression of proteins involved in acquisition of phosphorus from different sources including high-affinity transporter and degradation enzymes. Furthermore, P_i-starvation often positively regulates the production of secondary metabolites. *Pseudovibrio* sp. FO-BEG1 reacts to phosphate limitation by the secretion of a colored substance. In order to characterize this response in detail, we performed chemical, physiological and proteomic analyses of strain FO-BEG1 grown under P_i-limited and P_i-surplus conditions and conducted an initial molecular analysis of the substances secreted under both conditions via Fourier transform ion cyclotron resonance mass spectrometry (FT-ICR-MS). The physiological experiments, supported by the proteomic analysis, demonstrate that under P_i-limited conditions, strain FO-BEG1 exhibits a similar response to phosphate starvation like other bacteria, e.g. *Escherichia coli* or *Bacillus subtilis*, including induction of high-affinity transporters for phosphates and phosphonates and enzymes responsible for the cleavage of phosphate residues from organic molecules like the alkaline phosphatase. Further adaptations to P_i-starvation are modifications of the cellular envelope and up-regulation of proteins involved in protein export and the oxidative stress response. Additionally, along with the secretion of the colored substance, a simultaneous increase of soluble iron in the medium can be observed, indicating that one of the secreted molecules binds iron. Dissolved organic matter (DOM) extraction and subsequent dissolved organic carbon (DOC) determination demonstrate that the amount of DOC secreted into the medium is three-fold higher under P_i-starvation. FT-ICR-MS analysis of the DOM extracts reveals statistically significant differences between P_i-limited and P_i-surplus cultures. In summary, the response to phosphate starvation exhibited by *Pseudovibrio* sp. FO-BEG1 induces acquisition mechanisms for phosphorus-containing compounds and the secretion of yet unidentified, possibly iron containing extracellular metabolites. The function and structure of these compounds is to be determined.

Introduction

Phosphorus is a fundamental element for all living organisms. It is required for the phosphate backbone in DNA and RNA, represents the hydrophilic head group in membrane forming phospholipids and is essential for the cellular energy metabolism as phosphoanhydride-bound phosphate in ATP molecules (Paytan and McLaughlin, 2007). In marine environments, phosphorus availability is known to control primary production and to be the ultimate limiting nutrient over geological time scales (Paytan and McLaughlin, 2007 and references therein). Therefore, bacteria in marine ecosystems are well adapted to varying concentrations of phosphorus, available mainly in the form of phosphate (P_i) and organophosphates, and are especially adapted to phosphorus scarcity. On the one hand, as a response to long-term starvation, phosphorus requirements per cell can be decreased, either by the substitution of phospholipids with sulfur- and/or nitrogen-containing lipids (Van Mooy *et al.*, 2009) or by genome streamlining, leading to a reduction of the genetic information of a microorganism and a lower demand of phosphorus for DNA replication (Giovannoni *et al.*, 2005). On the other hand, a direct and immediate response to phosphorus limitation is crucial for bacterial cell survival. This task is accomplished by the PhoR-PhoB two-component system consisting of a sensor kinase, PhoR, and the corresponding response regulator PhoB, which acts as a transcriptional regulator (Wanner, 1993). Under P_i-limited conditions, PhoR phosphorylates PhoB, which, in turn, activates gene transcription of the phosphate (Pho) regulon (Wanner, 1993). The induced genes of the Pho regulon primarily encode proteins involved in phosphate assimilation and metabolism. A typical response to phosphate limitation is the expression of the high-affinity phosphate-specific transporter (Pst) and uptake systems for organophosphates like *sn*-glycerol-3-phosphate (G3P) or phosphonates (Wanner, 1993). Additionally, enzymes involved in the acquisition of phosphates like phosphomonoesterases (e.g. alkaline phosphatase (AP) and 5'-nucleotidase) and phosphodiesterases are induced (Vershinina and Znamenskaya, 2002).

Intriguingly, besides the activation of a metabolism that is directed towards phosphorus acquisition, which is an obvious reaction during the limitation, phosphate homeostasis has been frequently reported to be the trigger for secondary metabolite production in a wide range of microorganisms, including proteobacteria, gram-positive bacteria and filamentous fungi (Martín, 2004). The secreted compounds are produced by microorganisms e.g. in order to prevail against competitors or as signaling molecules for

interaction with eukaryotes like plants (Maplestone *et al.*, 1992; Vining, 1992). Additionally, in several studies, evidence is provided for the connection of the Pho regulon to the expression of virulence factors (Lamarche *et al.*, 2008 and references therein). Mutations in the *phoR* and *phoB* genes result e.g. in a decreased production of virulence factors (von Krüger *et al.*, 2006) and lead to impaired colonization of host tissue, compared with wild type strains (von Krüger *et al.*, 1999). Additionally, mutations in the Pst system, which seems to be connected with the regulation process of PhoR-PhoB (Lamarche *et al.*, 2008), result in decrease of virulence, reduced resistance to antimicrobial substances (e.g. Lamarche *et al.*, 2005) and diminished type III secretion systems activity (Rao *et al.*, 2004).

Bacterial strains belonging to the *Pseudovibrio* genus have often been isolated from marine invertebrates, mainly from sponges, and are therefore assumed to be their symbionts (Taylor *et al.*, 2007). *Pseudovibrio* isolates are frequently reported to produce secondary metabolites with antimicrobial characteristics, as reported by e.g. Hentschel *et al.* (2001), Santos *et al.* (2010), and O'Halloran *et al.* (2011). However, only few of these bioactive compounds have been characterized, including heptylprodigiosin (Sertan-de Guzman *et al.,* 2007), tropodithietic acid (TDA) (Penesyan *et al.*, 2011), the bile acid glycocholic acid (GCA) as well as the newly described polypeptide Pseudovibrocin (Vizcaino, 2011). In our previous work, we analyzed the genome and the physiology of the *Pseudovibrio* sp. strain FO-BEG1 (**Chapter II**). Apart from a versatile metabolism, we identified possible mechanisms mediating prokaryote-eukaryote interactions, e.g. type III and type VI secretion systems including potential effectors.

In this study, we investigated the physiological response of *Pseudovibrio* sp. FO-BEG1 to phosphate limitation. One of the major aspects of the reaction to P_i-starvation was the secretion of a yellowish-orange substance into the medium by the investigated strain **(Figure 5.1)**. A proteomic approach was performed in order to analyze up- and down-regulated proteins under phosphate starvation as well as regulated proteins during the transition from the early to the late growth phase under P_i-limitation. Additionally, initial investigations of the extracellular components, including mass-spectrometrical analyses, were performed.

Materials and Methods

Medium preparation and growth conditions

Pseudovibrio sp. FO-BEG1 was grown in an artificial sea water medium containing 30 g l^{-1} NaCl, 3 g l^{-1} $MgCl_2 \cdot 6\ H_2O$, 2 g l^{-1} K_2SO_4, 0.54 g l^{-1} NH_4Cl, 0.005 g l^{-1} $CaCl_2$, 6 g l^{-1} TRIS-HCl and the pH was adjusted to 8. After autoclaving, the medium was supplied with 10 mmol l^{-1} glucose, 1 ml l^{-1} tungsten/selenium solution (Brysch *et al.*, 1987), 1 ml l^{-1} trace elements (Widdel and Pfennig, 1984) and 1 ml l^{-1} of four vitamin solutions prepared according to Aeckersberg *et al.* (1991). Phosphate limited cultures contained 0.1 mmol l^{-1} and phosphate surplus cultures contained 1.2 mmol l^{-1} of phosphate. Cultivation was performed in 250 ml Erlenmeyer flasks filled with 100 ml medium at 28 °C in the dark with shaking at 130 rpm. Bacterial growth was monitored by means of optical density ($OD_{600\ nm}$), which was measured using an Eppendorf BioPhotometer (Eppendorf AG, Hamburg, Germany).

Determination of ammonia, glucose, trace elements and ultraviolet-visible light (UV-Vis) absorption spectra

Ammonia was measured using a flow injection analysis (FIA) system as described by Hall and Aller (1992). 30 mmol l^{-1} NaOH with 0.2 mol l^{-1} sodium citrate tribasic dihydrate and 50 µmol l^{-1} HCl were used as carrier and receiver phase, respectively. Glucose was determined using a HPLC system (Sykam GmbH, Eresing, Germany) equipped with an anion neutral pre-column (4x20 mm; Sykam GmbH) and an Aminex HPX-87H separation column (300x7.8 mm; Biorad, Munich, Germany) at a temperature of 60 °C. The eluent consisted of 5 mM H_2SO_4 in HPLC-grade water with a flow rate of 0.6 ml min^{-1}. Quantification of glucose was performed with a 7515A RI detector (ERC, Riemerling, Germany). Residual trace elements in the supernatant were measured with an Inductively Coupled Plasma-Optical Emission Spectrometer (ICP-OES). Samples for the ICP-OES measurement were collected during growth, centrifuged at 11,000 × *g* for 10 minutes, filtered with 0.22 µm pore size Millipore filters (Millipore, Bedford, MA, USA) diluted 1:10 in 1% supra-pure HNO_3 (Merck, Darmstadt, Germany) and stored at 4 °C until further analysis. The following elements were detected: iron, cobalt, and bor. Zinc, manganese, molybdenum, nickel, copper, and selenium were also analyzed by the ICP-OES method, but the amount of these trace elements was below the detection limit. The UV-Vis spectra of the supernatant were recorded using a Beckman DU 640 spectrophotometer (Beckman Coulter, Fullerton, CA, USA). Two ml of the

respective culture were centrifuged at 11,000 × *g* for 10 minutes and the recovered supernatant was used for recording the UV-Vis spectra with the sterile medium as a blank.

Alkaline phosphatase activity, phosphate determination, polyphosphate (poly P_i) and polyhydroxyalkanoate (PHA) staining

Alkaline phosphatase activity was assessed using *para*-nitrophenyl phosphate (pNPP; Sigma-Aldrich, Steinheim, Germany). The turbidity of the cultures was measured and 1 ml of the cultures was used for the assay. pNPP was added to a final concentration of 540 µmol l^{-1}. Absorbance at 420 and 550 nm were monitored every 30 minutes for two hours using a Beckman DU 640 spectrophotometer. All procedures during the assay were performed at room temperature. The units of alkaline phosphatase, expressed in Miller (Slauch and Silhavy, 1991), were calculated using the formula $10^3 \times [A_{420} - (1.75 \times A_{550})] / T \times OD_{600\ nm} \times V$, where A_{420} and A_{550} represent the absorbance at the respective wavelength after the incubation time T given in min. $OD_{600\ nm}$ is the turbidity of cultures at 600 nm and V is the volume in ml used in the assay. Presence of poly P_i during growth of the cells was monitored by staining with 4',6-diamidino-2-phenylindole (DAPI). Residual phosphate concentrations were determined colorimetrically by the ascorbic acid method modified after Hansen and Koroleff (1999) using a Beckman DU 640 Spectrophotometer or a SpectroDirect Spectrophotometer (Aqualytic, Dortmund, Germany). For poly P_i staining cultures were sampled and fixed for one hour at room temperature with 1% formaldehyde. 10 µl of a DAPI solution (1 g l^{-1} in deionized water) was added to 100 µl of the sample and incubated over night. Inclusions were observed by fluorescence microscopy using an Axioplan universal microscope (Zeiss, Oberkochen, Germany) with a HBO 50 mercury lamp (Osram, München, Germany) for UV light and a UV-G 365 filter set (G 365 exciter filter, FT 395 chromatic beam splitter and an LP 420 barrier filter, Zeiss, Oberkochen, Germany). For polyhydroxyalkanoate (PHA) staining, 90 µl of the culture were incubated for five minutes with 10 µl Nile Red (25 mg l^{-1} in dimethyl sulfoxide; Sigma-Aldrich). The inclusions were observed using the same microscope as described above with filter set 15 (Zeiss), with excitation at 546 nm and recording the emitted light at 590 nm.

Proteomic analysis – sampling, cell lysis and Bradford assay

Proteomic analysis of the soluble protein fraction was performed by TopLab GmbH. Samples were collected at one third of the maximum turbidity ($OD_{600\ nm}$) in both P_i-surplus and P_i-limited cultures. Moreover, for the P_i-limited culture, a third sample was taken in the

late exponential phase. Samples were centrifuged at 11,000 × *g* for 10 minutes, the supernatant was discarded, cells were frozen immediately and stored at –80 °C until further analysis. Cell lyses was performed on ice by means of sonication (tip from Benedelin Sonoplus; Bandelin Electronics, Germany) for six times ten seconds with a power amplitude of 25%. Subsequently, the samples were shaken for 20 minutes to improve the solubilization of the proteins. Then the samples were centrifuged at 20,000 × *g* for 30 minutes to remove cellular debris. The supernatant was transferred into a low-bind tube for subsequent labeling. An aliquot was used to determine the protein concentration by Bradford assay (Bradford, 1976).

Isotope-coded protein label (ICPL) labeling, sodium dodecyl sulfate-polyacrylamide gel electrophoresis (SDS-PAGE) and protein cleavage

For each ICPL labeling reaction with the SERVA ICPL™ Quadruplex-Kit (SERVA, GmbH, Germany), 100 µg total protein were used. Labeling was performed according to manufacturer's instructions. The acetone precipitated ICPL labeled proteins were dissolved in SDS sample buffer. SDS-PAGE was performed according to Laemmli (1970) using 4 to 20% gradient gels for separation (SERVA*Gel*™, SERVA Electrophoresis GmbH, Germany). Afterwards the gel was stained with colloidal Coomassie Blue. After the run each SDS-PAGE lane was sliced in five pieces. For each slice the protein content was estimated to be 20 µg based on the total load of 100 µg and stained intensity. Prior to the digestion, the proteins were destained using 50 mmol l^{-1} NH_4HCO_3 in 30% acetonitrile. The reduction and alkylation was performed during the ICPL labeling. In-gel digestion was performed overnight with sequencing grade trypsin (SERVA Electrophoresis GmbH, Germany) using a protein to enzyme ratio of 200:1 in 10 mmol l^{-1} NH_4HCO_3. Then, Glu-C MS grade (Protea® Chemicals, South Africa) was added using a protein to enzyme ratio of 50:1. The cleavage was performed for approximately 8 hours at room temperature. The peptides were extracted and acidified with 1% formic acid for subsequent mass spectrometry analysis.

Liquid chromatography electrospray ionization mass spectrometry (LC-ESI-MS/MS) after tryptic and Glu-C cleavage

For nano LC-ESI-MS/MS, approximately a quarter of the digest was used. One-dimensional nano-LC separation was performed on a multi-dimensional liquid chromatography system (Ettan MDLC, GE Healthcare, Germany). Peptides were separated with an analytical column (C18 PepMap 100, 3 µm bead size, 75 µm i.d.; 15 cm length;

Dionex LC Packings, USA) with a three step 120 minutes linear gradient (A: 0.1% formic acid, B: 84% acetonitrile and 0.1% formic acid) at a flow rate of 260 nl min^{-1}. The gradient used was: 0 to 30% B in 80 minutes, 30 to 60% B in 30 minutes and 60 to 100% B in 10 minutes. Mass spectrometry (MS) was performed on a linear ion trap mass spectrometer (Thermo LTQ, Thermo Scientific, USA) operating in positive polarity mode online coupled to the nano-LC system. For electrospray ionization, a distal coated SilicaTip (FS-360-50-15-D-20) and a needle voltage of 1.4 kV was used. The MS method consisted of a cycle combining one full MS scan (mass range: 300 to 2000 *m/z*) with then data dependent MS/MS events (CID; 35% collision energy). The dynamic exclusion was set to 30 seconds.

ICPL quantification, database queries and data analysis

The raw data were converted to mzXML format using the software Trans-Proteomic Pipeline. Then, the peak detection, deconvolution, deisotoping and quantification of the peaks was done using ICPL-ESIQuant. The data were normalized by the median of all ratios. The quadruplet detection was first performed for each run separately. Subsequently, the detected quadruplets of the reference runs were used to search for incomplete quadruplets in the biological sample runs for each corresponding slice. This way, complete and incomplete quadruplets, which result from highly regulated proteins, were quantified. The MASCOT identification data were imported with a threshold ion score of 20. The Glu-C cleavage specificity was set for Glu. The fasta sequences of the annotated *Pseudovibrio* sp. FO-BEG1 genome (available at DDBJ/EMBL/GenBank under the accession number CP003147 for the chromosome and CP003148 for the plasmid) were used to build a specific database. For each LC-ESI-MS/MS run four separate database queries were done, using one of the ICPL labels as second fixed modification. For database searches a mass tolerance of 50 ppm in the MS mode and 0.5 Da in the MS/MS mode with two missed cleavages was set.

Protein identification was based on the following criteria: *i*) at least two peptides must be present to identify a protein, single peptides were excluded from further analysis; *ii*) the standard deviation of the peptide intensity ratio was set to a threshold of 50%, however, if the standard deviation value did not change the regulation of the protein (e.g. from up-regulated to not-regulated), the protein was kept in the analysis; *iii*) regulated proteins with standard deviation values above 50% were investigated manually, and if all ratios of the identified peptides belonging to the protein were below the threshold set for regulation, the protein was kept in the analysis. The regulatory ratios based on the peak intensity ratios lead to the

following regulation: proteins, which are up-regulated have a ratio between 1 and infinity and down-regulated proteins have a ration between 1 and 0, whereas the threshold for significant regulation was set to 2 and 0.5, respectively. However, this representation of the data shows an asymmetrical and not weighted regulation. Therefore, the following calculations were done for the regulation ratios: *i*) for all ratios, the decadic logarithm was found, *ii*) the values of the peptides belonging to one protein were averaged to have the weighted mean value, *iii*) the decadic logarithm was then converted back, and *iv*) for down-regulated proteins, the inverse of the ratio was multiplied by –1, resulting in negative values. In the following, the significant regulation is therefore given as ≥2 for up-regulated and ≤–2 for down-regulated proteins. The regulated proteins were further divided into 15 arbitrarily defined categories: carbon metabolism, phosphorus metabolism, amino acid and nucleotide metabolism, protein and peptide metabolism, transport and secretion (including electron and proton translocating proteins), fatty acid and lipid metabolism, cell wall and membrane biogenesis, translation, transcription and DNA metabolism, regulation of transcription, stress response, detoxification and iron metabolism, cofactor and vitamin synthesis, chemotaxis and motility, secondary metabolite production, proteins with only a general function prediction and proteins with an unknown function. SignalP has been used for the signal peptide predictions (Bendtsen *et al.*, 2004) and TMHMM for the transmembrane helix-analysis (Krogh *et al.*, 2001). Prediction of protein localization was performed with subCELlular LOcalization (CELLO) predictor (Yu *et al.*, 2006).

Solid phase extraction of dissolved organic matter (SPE-DOM), dissolved organic carbon (DOC) measurements and Fourier transform ion cyclotron resonance mass spectrometry (FT-ICR-MS) of the DOC

Samples were taken in both P_i-surplus ($+P_i$) and P_i-limited ($-P_i$) cultures immediately after the inoculation (T_0), at the beginning of the growth phase (T_1) and in the stationary phase (T_3). One more sample was taken for the P_i-limited cultures in the late growth phase (T_2). Samples were centrifuged at 11,000 × *g* for 10 minutes and filtered into 150 ml glass serum-bottles using Acrodisc 25 mm syringe filters with a 0.2 µm GHP membrane (Pall Life Sciences, Ann Arbor, MI, USA) and acidified to pH 2 with 25% HCl. Except for T_0, all samples were prepared in triplicates. Samples were stored at 4 °C until further analysis. DOM was extracted for all time points using the solid phase extraction of dissolved organic matter (SPE-DOM) method (Dittmar *et al.*, 2008). DOC was analyzed using a Shimadzu TOC-VCPH total organic carbon analyzer (Shimadzu, Kyoto, Japan). The DOM extracts were 1:2

diluted with deionized water, adjusted to a DOC concentration of 20 ppm with methanol and deionized water (50:50 v/v), filtered using 0.2 µm PTFE filter (Rotilabo, Carl Roth GmbH, Karlsruhe, Germany) and further analyzed with a solariX FT-ICR-MS (Bruker Daltonik GmbH, Bremen, Germany) with a 15.0 Tesla magnet system. An Apollo II ion source was used for the electrospray ionization in the negative and positive mode. All data were acquired with a time domain size of 4 megaword and a detection range of *m/z* 150 to 2000. The acquired mass spectra were analyzed with the Data Analysis software Version 4.0 SP4 (Bruker Daltonik GmbH). Calibration of the mass spectra was performed as follows. One $-P_i$ T_3 sample was spiked with 330 ppm sodium trifluoroacetic acid (Sigma-Aldrich) and measured in the positive ionization mode. In the negative ionization mode, the $-P_i$ T_3 sample was spiked with 0.05 ppm L-arginine (Sigma-Aldrich). The resulting mass spectra were calibrated internally with a reference mass list for the trifluoroacetic acid or L-arginine, respectively, and, according with this internal calibration, a molecular formula was assigned for the residual peaks of the sample in the respective ionization mode. The molecular formulas were assigned in the elemental composition in the following ranges: $C_{1-\infty}$ $H_{1-\infty}$ $O_{1-\infty}$ N_{0-2} S_{0-1} P_0. Then, molecular formula were chosen that appear in all other measured spectra with a maximal error of 0.1 ppm and a two new calibration lists were created based on these data with an standard deviation error of less than 0.05 ppm. The new calibration lists were subsequently used for calibration of all other acquired mass spectra in the negative and positive ionization mode, respectively. Additionally, the FT-ICR mass spectrometer was calibrated externally every day by measuring a deep sea water extract (Nelha pool) at a concentration of 20 ppm as a standard.

Statistical analysis

All FT-ICR-MS data were analyzed by means of non-metric multidimensional scaling (NMDS). This statistical method gives an overview of the relatedness of the profiles of secreted compounds under different culturing conditions and at different time point. The analysis was performed by calculating similarity among samples by means of the Bray-Curtis similarity index. NMDS and the relative stress value, which is a measure that reflects the degree of deviation of NMDS distances from original matrix distances, were carried out by means of the PAST program (http://folk.uio.no/ohammer/past/). For each the sum of the first four hundreds peaks was used for the normalization of the intensity of all peaks. The normalized peak intensities were then used for all statistical analyses performed.

Bioactivity test of the P_i-limited supernatant of a *Pseudovibrio* sp. FO-BEG1 culture

The bioactivity of the supernatant was tested to verify the effect on the growth on other common marine heterotrophic strains. One ml of the freshly collected supernatant from a stationary phase P_i-limited culture was spread on a Difco™ Marine Broth (Becton, Dickinson and Company Sparks (BD), MD, USA) agar plate, consisting of 37.4 g l^{-1} Marine Broth and 15 g l^{-1} Bacto Agar (BD). Afterwards the following strains were streaked on the plate: *Altreromonas macleodii* (DSM 6062), *Oceanobacillus iheyensis* (DSM 14371), *Marinobacter algicola* (DSM 16394), *Kytococcus sedentarius* (DSM 20547), and *Exiguobacterium sibiricum* (DSM 17290). As a control, the supernatant of a *Pseudovibrio* sp. FO-BEG1 culture was used that was grown under P_i-surplus.

Results

Growth under phosphate limited conditions

Growth as well as glucose and ammonia concentrations under P_i-limited and P_i-surplus conditions have been monitored and are shown in **Figure 5.2A**. As expected, growth of the P_i-limited culture was slower and the maximum $OD_{600\ nm}$ was depressed, compared to the P_i-surplus conditions. The calculated growth rate was μ=0.167 in P_i-surplus and μ=0.051 in P_i-limited conditions. According to the differing growth rates, glucose and ammonia utilization differed among both conditions, with increased consumption of the two substrates under P_i-surplus conditions. The increase in ammonia after 36 hours in the P_i-surplus culture is most likely due to cell lysis and the subsequent degradation of released proteins, peptides, and amino acids.

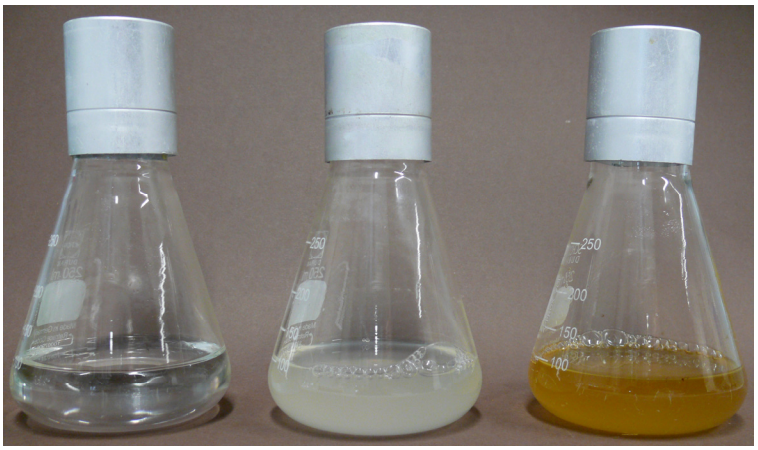

Figure 5.1. Photograph of Erlenmeyer flasks containing sterile medium (left), *Pseudovibrio* sp. FO-BEG1 culture in the stationary phase grown in a medium with surplus of phosphate (1.2 mmol l^{-1}; center) and in a medium limited in phosphate (0.1 mmol l^{-1}; right).

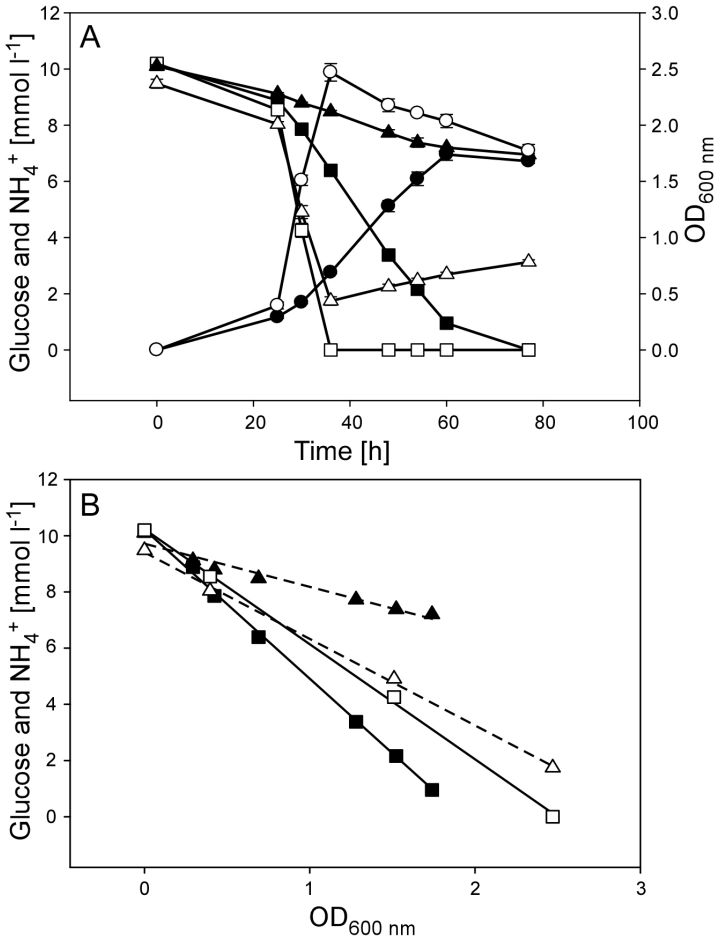

Figure 5.2. (**A**) Growth (circles) of a P_i-surplus and a P_i-limited culture as well as the ammonia (triangles) and glucose (squares) utilization over time. Open symbols represent the P_i-surplus, filled ones the P_i-limited culture. Error bars represent the standard deviation of biological triplicates. (**B**) Utilization of glucose (squares) and ammonia (triangles) per unit turbidity in P_i-surplus (open symbols) and P_i-limited cultures (filled symbols) in dependence of time (taken from **Figure 5.2A**). According to the slope, the utilization of glucose is 4.1 and 5.3 mmol l^{-1} per unit optical density (continuous line) and ammonia 1.5 and 3.1 mmol l^{-1} per unit optical density (dashed line) in the P_i-surplus and P_i-limited cultures, respectively.

When the optical density is plotted against the measured concentrations of glucose or ammonia at the respective time points, it becomes evident that the uptake of ammonia per increased optical density unit is two-fold lower in the P_i-limited culture (**Figure 5.2B**). However, uptake of glucose is higher under P_i-starvation, even though the resulting maximum turbidity of the P_i-limited culture is significantly lower than in the P_i-surplus (**Figure 5.2B**). Therefore, the presence of polyhydroxyalkanoates (PHA), as a possible storage compound under excess of glucose, was investigated via Nile Red staining in both cultures. Bright fluorescent intracellular inclusions have been detected in the P_i-starved culture, indicating that those contain more PHA than cultures grown in P_i-surplus medium (**Figure 5.3**).

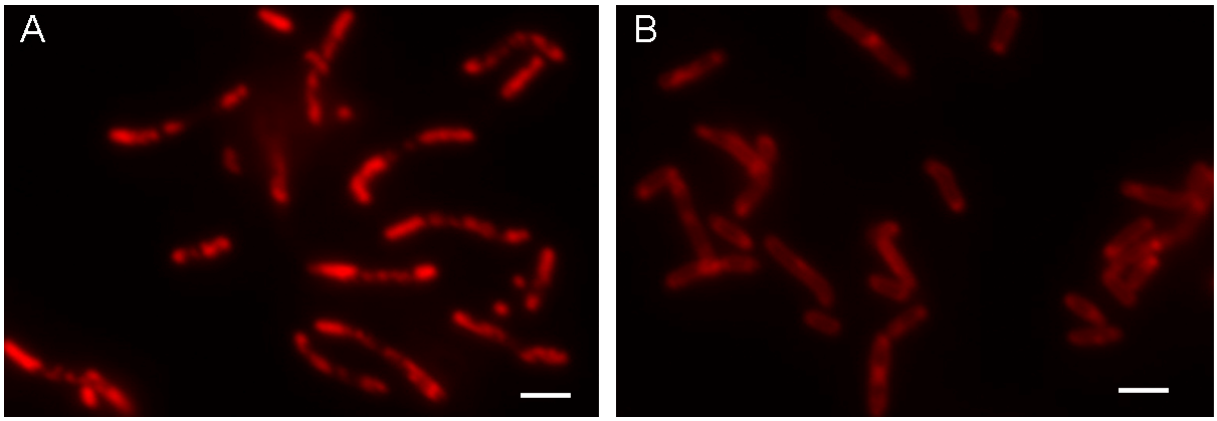

Figure 5.3. *Pseudovibrio* sp. FO-BEG1 cells stained with Nile Red after 35 hours of growth. The Nile Red stain visualizes bacterial cells by binding to the membranes. Additionally, polyhydroxyalkanoates (PHA) are visible as intense bright inclusions within the bacterial cells. (**A**) Cells grown under P_i-limitation, (**B**) cells grown under P_i-surplus. Scale bars 2 µm.

The initial concentration of phosphate of 1.2 mmol l^{-1} in the P_i-surplus culture decreased to around 0.5 mmol l^{-1} after 60 hours of growth, whereas the primary concentration of 0.1 mmol l^{-1} under P_i-limited conditions declined below the detection limit after 24 hours (**Figure 5.4**). Nevertheless, growth under phosphate limiting conditions continued for 36 hours until the beginning of the stationary phase at 60 hours.

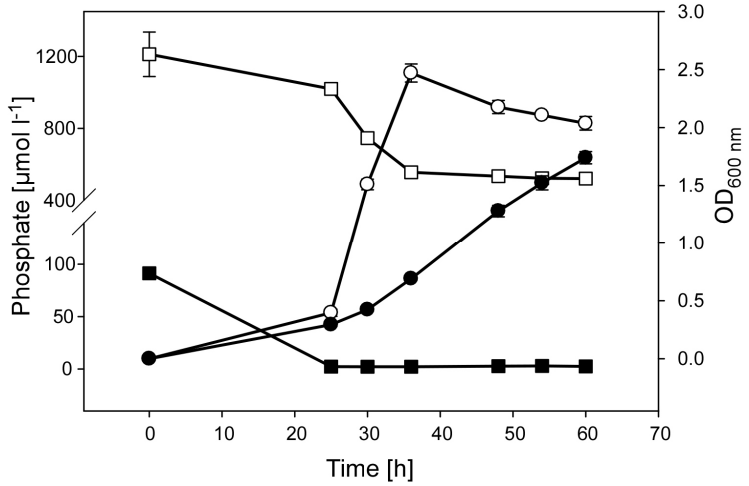

Figure 5.4. Phosphate concentration (squares) and growth as the optical density at 600 nm (circles) in P_i-surplus (open symbols) and P_i-limited (filled symbols) cultures. Error bars represent the standard deviation of biological triplicates.

To verify whether the growth was supplied by an internal phosphorus storage, we investigated the polyphosphate (poly P_i) content of *Pseudovibrio* cells under P_i-limited and P_i-surplus conditions by staining the cells with 4',6-diamidino-2-phenylindole (DAPI). DAPI binds to DNA and is usually used for cell enumeration, however, it was also shown to bind to polyphosphate, thereby shifting the emission maximum from 460 nm (blue signal) to 525 nm (yellow signal) (Tijssen *et al.*, 1982). Over the sampling time of 60 hours we could not observe an obvious decrease of poly P_i within the cells (**Figure 5.5**). Moreover, we noticed

morphological changes of the cells grown with different supply of phosphorus. After 60 hours, cells grown under P_i-surplus conditions were straight or slightly curved rods with a volume of 1.3 (±0.43) μm^3, whereas cells grown under P_i-limited conditions became longer, resulting in a final cell volume of 3.0 (±0.93) μm^3.

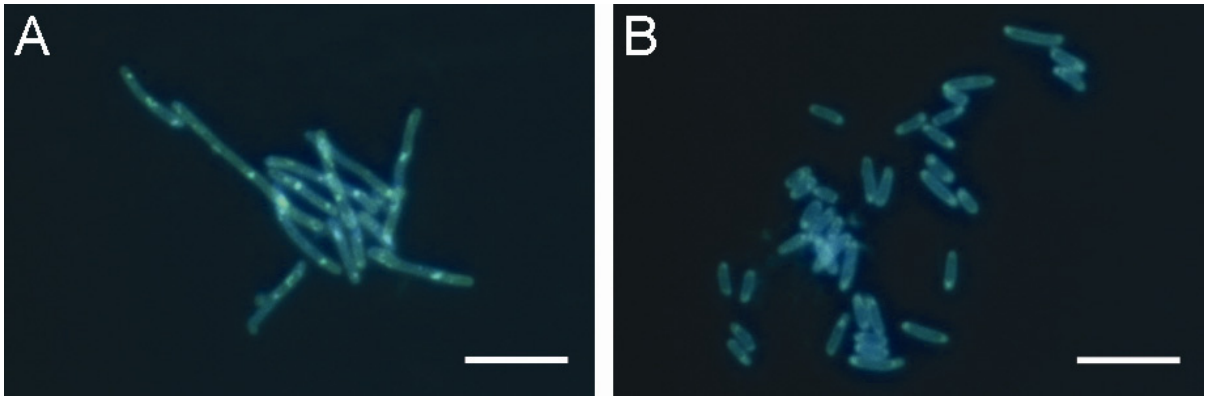

Figure 5.5. *Pseudovibrio* sp. FO-BEG1 stained with 4',6-diamidino-2-phenylindole (DAPI) after 60 hours of growth. The blue signal represents DAPI bound to DNA, whereas the yellow signal represents DAPI bound to polyphosphate. (**A**) Cells grown under P_i-limitation, (**B**) cells grown under P_i-surplus. Scale bars 5 µm.

In order to monitor the changes in the utilization behavior of supplied trace elements by the P_i-limited and P_i-surplus culture of *Pseudovibrio* sp. FO-BEG1, we performed inductively coupled plasma optical emission spectrometry (ICP-OES) measurements during the investigated time period. Iron (Fe) and cobalt (Co) differed markedly between the two tested conditions (**Figure 5.6**), whereas the amount of other elements was either similar between both conditions or below the detection limit. The uptake of cobalt was increased by approximately 0.01 mg l^{-1} after 44 hours in the phosphate-limited culture, although the growth rate and the maximum optical density were lower than under P_i-surplus conditions. The measurement of iron in the cell-free control showed that the amount of iron decreased in the first 24 hours and was stable afterwards, indicating that less iron is in solution, possibly due to precipitation and interactions with phosphate, since the decrease of Fe in the P_i-surplus culture was higher. Interestingly, comparable to the cobalt measurements, we noticed a higher uptake of iron between 24 and 40 hours of incubation in the P_i-limited culture (0.104 mg l^{-1}) compared to the P_i-surplus conditions (0.036 mg l^{-1}), representing approximately one-third of what has been used under phosphate limitation. After 40 hours, the amount of dissolved iron starts to increase again in the P_i-limited culture, whereas it remains constant under P_i-surplus conditions.

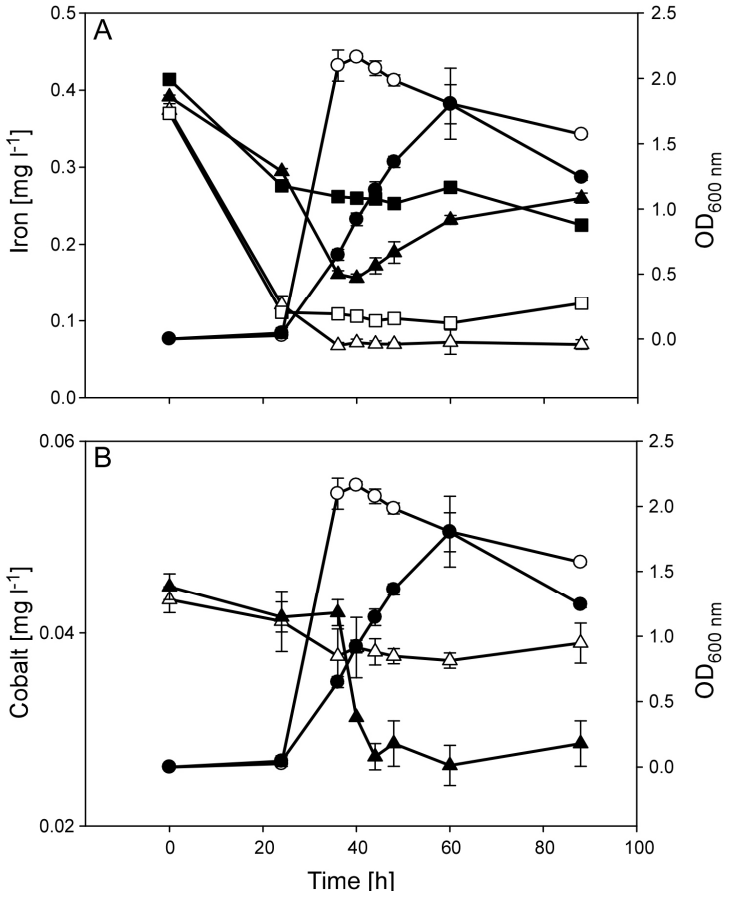

Figure 5.6. Amount of iron (**A**) and cobalt (**B**) in the supernatant of cultures grown under P_i-surplus (open symbols) and P_i-limited (filled symbols) conditions. Triangles represent the amount of the respective element in inoculated samples, whereas the error bars show the standard deviation. In the case of iron, the squares show the amount of the respective element in non-inoculated controls. Circles show the optical density at 600 nm.

It is known that phosphate limitation induces activity of the alkaline phosphatase (AP), an enzyme that cleaves the phosphoester bond between an organic compound and its phosphate residue (Coleman, 1992). To analyze if strain FO-BEG1 has the same response to P_i-starvation, we performed an alkaline phosphatase assay with cultures grown under P_i-limited and P_i-surplus conditions (**Figure 5.7**). Under P_i-surplus conditions, low AP activity could be shown over the analyzed time period, induced in the stationary phase of the growth. Under P_i-starvation, however, AP activity was detected after 37 hours and increased up to its maximum at 48 hours after inoculation, which is approximately 10-fold higher than the activity measured in P_i-surplus cultures. AP activity was also measured before 24 hours, but due to the extremely low absorbance at 420, 550 and 600 nm in the beginning of the growth and the resulting errors in the calculated values, they are not presented here.

Phosphate limitation induces production of a colored substance

During growth under P_i-limitation, *Pseudovibrio* sp. FO-BEG1 secreted, possibly among other metabolites, a yet unidentified yellowish-orange substance which was detected visually as well as in recorded ultraviolet and visible light (UV/Vis) absorption spectra. The secretion of the compounds was initiated between 36 and 48 hours of growth and the amount gradually increased until the end of the measurements at 77 hours (**Figure 5.8**). In the UV/Vis

spectra the main peak was detected at 323 nm, including a small shoulder around 303 nm as well as a broad shoulder between 350 and 380 nm with the maximum around 375 nm. Under P_i-surplus conditions, no production of colored substances could be observed, which was confirmed by the UV/Vis absorption spectra (**Figure 5.8**).

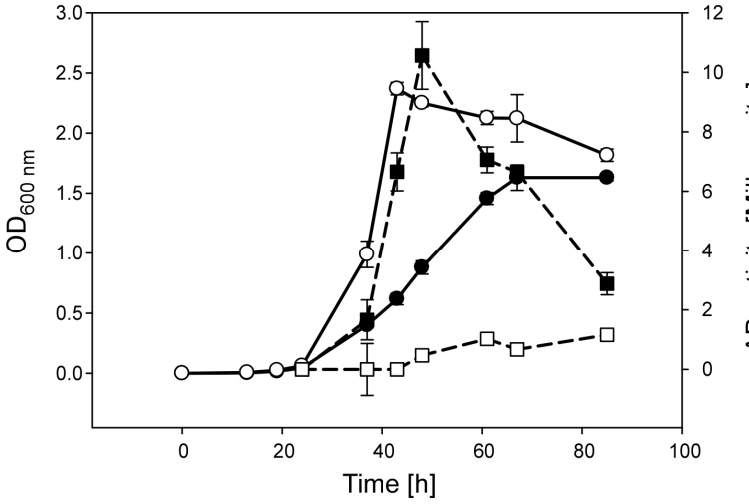

Figure 5.7. Optical density at 600 nm (circles, continuous line) and alkaline phosphatase (AP) activity expressed in miller units (squares, dashed line) in P_i-surplus (open symbols) and P_i-limited (filled symbols) cultures. Error bars represent the standard deviation of biological triplicates.

The supernatant of P_i-starved cultures was analyzed for antimicrobial activities. For this, one ml of the sterile supernatant of P_i-limited cultures grown until the stationary phase was spread on agar plates and the plates were inoculated either with *Alteromonas macleodii*, *Oceanobacillus iheyensis*, *Marinobacter algicola, Kytococcus sedentarius* or *Exiguobacterium sibiricum*. However, under the experimental conditions no inhibition effect of the used supernatant was visible for the tested strains when compared with supernatant of P_i-surplus cultures (results not shown).

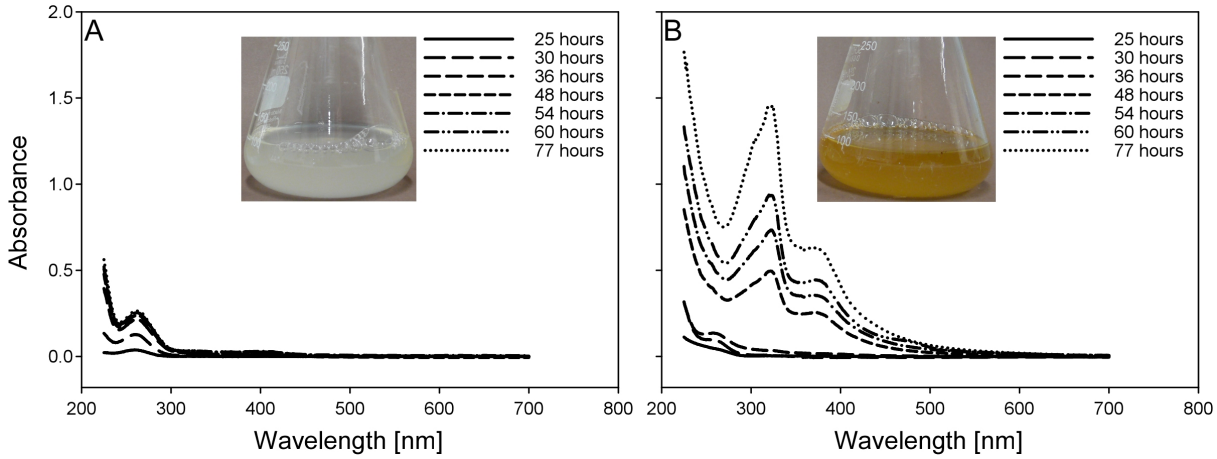

Figure 5.8. Absorbance spectra of ultraviolet and visible light in the supernatant of P_i-surplus (**A**) and P_i-limited (**B**) cultures over a time period of 77 hours. Photographs demonstrate the visual appearance of the respective cultures after 77 hours

To verify that the substances secreted during P_i-starvation are organic molecules, we performed solid phase extraction of the dissolved organic matter (DOM) from the supernatant at different time points in P_i-surplus and P_i-limited cultures (**Figure 5.9A**). The dissolved organic carbon (DOC) content of both extracts was measured, resulting in approximately 3-fold higher DOC in the extracts of the P_i-limited culture compared with the extracts of the P_i-surplus culture after 60 hours of growth (**Figure 5.9A**).

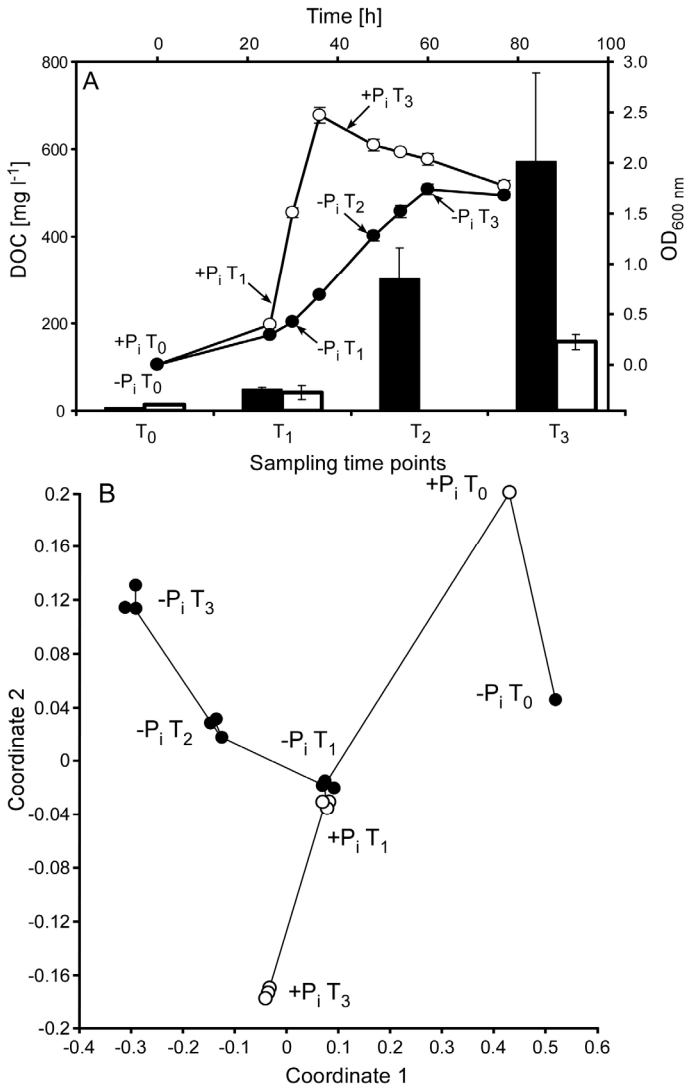

Figure 5.9. (**A**) Dissolved organic carbon (DOC) measurements (bars) of the solid phase extraction of the P_i-limited (filled) and P_i-surplus (open) supernatant. The growth is represented in circles, the open symbols show P_i-surplus and filled symbols P_i-limitation. Sampling points are shown on the growth curve. Error bars represent the standard deviation of biological triplicates. (**B**) Non-metric multidimensional scaling (NMDS) plot, representing the statistical difference between P_i-limited (filled circles) and P_i-surplus (open circles) cultures sampled at the respective time points measured via FT-ICR-MS in the negative ionization mode. Except for T_0 taken for both conditions, all time points were analyzed in triplicates, represented by three circles per each time point in the plot.

In order to analyze the differences in the secreted DOM, we performed mass-spectrometrical measurements with the FT-ICR-MS of the extracted supernatant-DOM from cultures grown under P_i-limited and P_i-surplus conditions. All peaks with their respective intensities were extracted from the MS data and cross-matched between all tested conditions and time points, which are indicated in **Figure 5.9A**. Overall, we detected over 100,000 peaks in the negative ionization mode, of which over 6,500 and 500 were identified only in DOM extracts of P_i-limited and the P_i-surplus cultures, respectively. In the positive ionization mode, over 65,000 peaks were detected, with over 5,000 present only in DOM extracts of P_i-limited

cultures and over 2,000 only in DOM extracts of P_i-surplus cultures. This data were used for statistical analysis via non-metric multidimensional scaling (NMDS) (**Figure 5.9B**). The low NMDS stress level (0.061) suggests that the groupings on a 2-D plot are a reliable depiction of biological divergence. At the beginning of the growth phase the secretome of both cultures is highly similar, but the samples taken from the P_i-limited culture after the appearance of the yellow compound are significantly different from those collected from the P_i-surplus culture, as visualized in the NMDS plot (**Figure 5.9B**).

Proteomic analysis of *Pseudovibrio* sp. FO-BEG1 grown under different conditions

In order to investigate differences in the protein expression during P_i-starvation compared to P_i-surplus, we performed a proteomic analysis employing the ICPL method, which is based on stable isotope labeling of free amino acid groups in intact proteins and their subsequent separation, fractionation and mass-spectrometrical analysis. Due to the different labels applied for the different conditions, the ratios of peak intensities of the MS data can be used for relative quantification of the proteins (Schmidt *et al.*, 2005). However, a major drawback of the quantitative proteomics is that the mass spectrometer is exposed to an enormous amount of peptides in a sample and therefore – depending on the pre-separation of proteins in a gel and liquid chromatography – can detect only a fraction of the proteins (Bantscheff *et al.*, 2007; Malmström *et al.*, 2011). Therefore, a mass-spectrometry based proteome can be regarded as a shotgun approach in which not necessarily all proteins of interest will be identified and quantified.

Three conditions were investigated in the proteomic analysis: early growth phase of P_i-surplus ($+P_i$) and early ($-P_i$ T_1) as well as late ($-P_i$ T_2) growth phase of P_i-limitation, whereupon the $-P_i$ T_1 was selected as the reference (**Figure 5.10**). Proteins were regarded as regulated when the change in the expression was ≥2-fold for up-regulated and ≤–2-fold for down-regulated proteins. The regulated proteins were then divided into 15 arbitrarily defined categories (see Materials and Methods). In the following, the results of the proteomic approach will be separated into four categories of protein expression: *i*) up-regulation and *ii*) down-regulation under P_i-limitation will refer to different expression of proteins under phosphate-limited ($-P_i$ T_1) compared to phosphate-surplus conditions ($+P_i$). Additionally, *iii*) up- and *iv*) down-regulation of proteins in the late growth phase of P_i-limitation ($-P_i$ T_2) is compared to the early growth phase of P_i-limitation ($-P_i$ T_1) (**Figure 5.10**). The analysis was performed in biological duplicates, the proteome of which has been analyzed separately in

ICPL run 1 and ICPL run 2. ICPL run 3 represents a reference run and contains all pooled samples in order to identify proteins that are absent at one condition but present at the other. Proteins represented by incomplete quadruplets in the MS data cannot be quantified and therefore are only valued as turned on or off at the respective conditions.

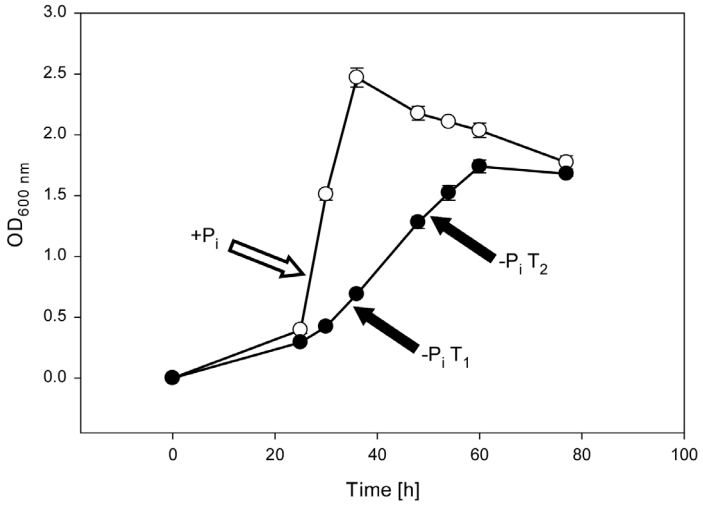

Figure 5.10. Sampling points for the proteomic analysis. The P_i-surplus-culture (open circles) was sampled in the early growth phase, whereas the P_i-limited culture (filled circles) was sampled during the early ($–P_i$ T_1) and the late ($–P_i$ T_2) growth phase. $–P_i$ T_1 was used as a reference for the proteomic analysis.

In the proteomic study, we were able to identify and to quantify 698 proteins, which represent 12.7% of all predicted ORFs in the genome of strain FO-BEG1. The proteomic analysis was performed with biological duplicates and 544 out of 698 proteins (about 78%) were detected in both replicates. In this case, the expression ratios for identical proteins from the two replicates were used for further analysis. A number of 154 (22%) of all detected proteins could only be quantified in one replicate. Nevertheless, these proteins were used for further analysis, but they were marked with an asterisk in the tables to refer to absence of reproducibility in biological replicates (**Table S 5.1** and **Table S 5.2**). Out of 698 quantified proteins, 17.8% (124 proteins) were significantly regulated during P_i-starvation. Out of these, the expression of 102 proteins was up-regulated and of 22 down-regulated under P_i-limited conditions (**Figure 5.11**). 90 proteins (12.9%) were significantly regulated during the transition from the early to the late growth phase under P_i-limited conditions, 14 of which were up- and 76 down-regulated (**Figure 5.12**). All regulated proteins can be found in **Table S 5.1** (up- and down-regulated under P_i-starvation) and **Table S 5.2** (up- and down-regulated in the late growth phase of P_i-starvation). In the following results and discussion, however, we will focus on those proteins that are known to be regulated during phosphate starvation as found in other studies (e.g. von Krüger *et al.*, 2006; Rodríguez-García *et al.*, 2007; Crépin *et al.*, 2008) as well as those that we consider important for the comprehension of the answer initiated by *Pseudovibrio* sp. FO-BEG1 to phosphate starvation and the secretion of extracellular compounds.

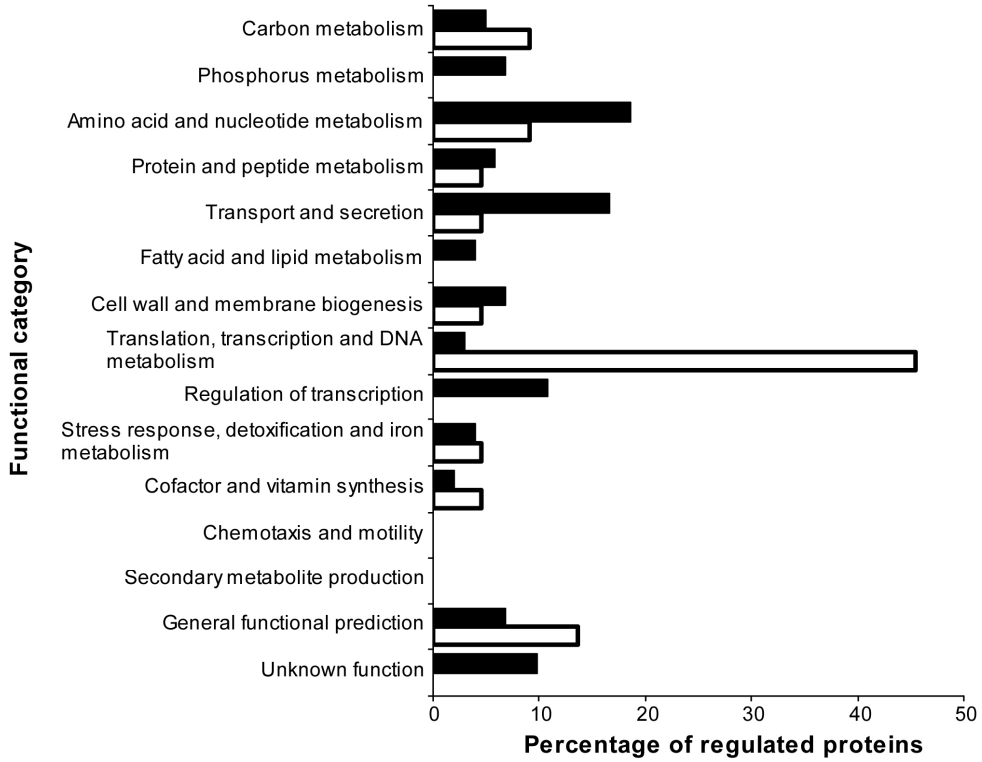

Figure 5.11. Categorization of the differentially expressed proteins under P_i-starvation shown as the percentage of the total amount of either up- (102) or down- (22) regulated proteins. Black and white bars represent up- and down-regulated proteins, respectively.

Phosphate starvation induces up-regulation of proteins involved in a variety of metabolic processes

Phosphate limitation triggered the upregulation of enzymes involved in the phosphorus acquisition, storage, and metabolism. Four out of five subunits of the high-affinity phosphate import system PstS, PstA, and PstB (PstC was not detected in the proteome) were up-regulated 20.9-fold, 4.5-fold and 8.5-fold respectively, and the expression of PhoU was turned on under P_i-starvation. Furthermore, three subunits of ABC transporters for *sn*-glycerol-3-phosphate (*sn*-G3P), an organophosphate compound that can serve as a phosphorus source, were up-regulated between 4.6-fold and 12.5-fold. Those three subunits belong to two different loci encoding *sn*-G3P ABC transporters, indicating that at least two transporters for that kind of substrate were up-regulated under P_i-limited conditions. Additionally, PhnD and PhnC, subunits from the phosphonate ABC transporter, were highly up-regulated along with proteins involved in phosphonate degradation, PhnI, PhnJ, and PhnM. PhoH, a predicted ATPase and a part of the phosphate starvation response in *E. coli* (Kim *et al.*, 1993) was 7-fold up-regulated. Expression of the phosphate acetyltransferase was up-regulated 13.3-fold and of the acetate kinase 7.4-fold. Both enzymes are involved in the

synthesis of acetyl phosphate from acetyl-CoA (Ingram-Smith *et al.*, 2006), which can directly phosphorylate PhoB (McCleary and Stock, 1994) and might therefore be directly involved in the phosphate starvation response. Polyphosphate kinase I, an enzyme that is involved in polyphosphate (poly P_i) metabolism in the cells (Ahn and Kornberg, 1990), was overexpressed.

Besides proteins directly assigned to the phosphorus metabolism, other proteins that were considered to be involved in phosphate acquisition were up-regulated as well. Generally, these proteins are involved in DNA and nucleotide degradation. AMP nucleosidase cleaves AMP irreversibly into a phosphate-containing sugar and adenine (Hurwitz *et al.*, 1957). The 5'-nucleotidase and 2',3'-cyclic nucleotide 2'-phosphodiesterase/3'-nucleotidase were up-regulated, and the expression of a ribonuclease was detected only under P_i-starvation. Activities of these proteins eventually lead to the cleavage of the phosphodiester bonds and liberation of phosphates from the nucleosides. The expression of deoxyguanosinetriphosphate triphosphohydrolase, which releases the unusual product triphosphate from GTP, could likewise be detected only under P_i-limited conditions.

Enzymes involved in carbon conversion are also affected by P_i-limitation. Phasins are proteins that are required for the surface formation of polyhydroxyalkanoates (PHA), which are carbon storage compounds in bacteria. Under P_i-limited conditions, one out of two phasins encoded in the *Pseudovibrio* sp. FO-BEG1 genome was up-regulated. The second phasin was also identified as up-regulated in the proteomic analysis, but was excluded from further analysis due to low statistical significance. Ferritin is a protein required for storage of iron, which is made out of 24 identical subunits and exhibits a hollow, sphere-like structure that can accommodate up to 4500 iron atoms (Andrews, 2010). Furthermore, protection against reactive oxygen species (ROS) has been proposed for ferritins (Chiancone *et al.*, 2004 and references therein). Two bacterioferritins, specific prokaryotic forms containing haem, have been found up-regulated under phosphate limiting conditions. Additional up-regulated proteins involved in defense against oxidative stress were the alkylhydroperoxidase as well as the glutathione synthase, the latter producing the antioxidant glutathione (Kullisaar *et al.*, 2010; Zhang *et al.*, 2010 and references therein).

One UDP-sulfoquinovose biosynthetic protein was up-regulated 22.2-fold. This enzyme is essential for the sulfoquinovosyldiacylglycerol (SQDG) synthesis, a phosphorus-

free, sulfur-containing membrane lipid (Benning, 2007). In accordance with this observation, two enoyl-CoA hydratase/isomerase-related proteins, a 3-oxoacyl reductase, and a phosphatidic acid phosphatase – enzymes which are involved in fatty acid and lipid metabolism – were found up-regulated and could be involved in degradation of phospholipids. The 3-oxoacyl reductase could, on the contrary, be involved in the synthesis of new, phosphorus-free membrane lipids. Phosphomannomutase/phosphoglucomutase catalyzes the second step in the synthesis of alginate, an exopolysaccharide, involved in the establishment of biofilms in *Pseudomonas aeruginosa* (Ramsey and Wozniak, 2005). We could identify a second enzyme required for the first and third step of alginate synthesis (Gacesa, 1998), which is located in direct proximity of the phosphomannomutase/phosphoglucomutase (but it was not detected in the proteomic approach). However, no further proteins involved in this process could be identified in the genome. Two proteins containing the SPFH domain, which are members of the band 7 protein family, have been identified in the genome of *Pseudovibrio* sp. FO-BEG1, both of which are present in the proteomic analysis and are up-regulated under P_i-limitation. One protein (PSE_4595) shows a 2.5-fold upregulation, the other one, however, is just below the threshold with an increased expression of 1.9-fold (results not shown). Proteins with the SPFH domain are found in prokaryotes and eukaryotes and are involved in membrane associated-processes with a variety of functions like vesicle trafficking, assembly of complexes and operation of membrane channels (Boehm *et al.*, 2009). Additionally, two OmpA/MotB-like proteins were found up-regulated just below the threshold (1.9-fold) (results not shown). OmpA is a major membrane component in *E. coli* and, besides being a porine (Nikaido, 2003), has various functions, including connection of the outer membrane to peptidoglycan, adhesion and invasion of host cells, avoidance of the immune response of the host and biofilm formation (Wang, 2002; Smith *et al.*, 2007). Along with OmpA, the periplasmic protein TolB, which has been shown to form a complex with the outer membrane and to interact with OmpA, is up-regulated 2.3 fold. TolB belongs to the Tol-Pal proteins and is involved in the outer membrane stability (Lazzaroni *et al.*, 1999; Lloubès *et al.*, 2001).

Under P_i-limited conditions, 16.7% (17 proteins) belonging to the transport and secretion category were found to be up-regulated. 14 of the 17 proteins are ABC type transporter, 9 of which encode subunits for phosphate, phosphonate and *sn*-G3P import and have been mentioned already. The other subunits belong to predicted ABC systems dedicated to the transport of di- and oligopeptides, spermidine/putrescine, and maltose/maltodextrin and show an increase in expression from 2.6-fold up to 12.5-fold. One subunit of a TRAP

transporter system for dicarboxylates was slightly up-regulated, along with TrkA, a subunit of a potassium uptake channel. In the genome of strain FO-BEG1 three homologues of TolC proteins are present, two of which have been identified in the proteomic study. One TolC homologue is up-regulated 3.7-fold, but the other one is below the threshold (1.6-fold, data not shown). TolC, as an outer membrane factor (OMF), represents a subunit of the type I secretion system and is required for the export of proteins across both membranes into the environment.

Among proteins that are involved in the protein and peptide metabolism, six proteins are up-regulated under P_i-limited conditions. These proteins possess chaperone functions in order to assist in the protein folding process, to repair misfolded or denatured proteins or to degrade them – a process which is catalyzed by proteases and peptidases. For instance, a homologue of PmbA, a protein required for the maturation and secretion of a microcin antibiotic, is up-regulated 2.4-fold (Rodríguez-Sáinz *et al.*, 1990).

Under phosphate starvation, transcriptional regulators are also induced. Among others, we have found two homologues of the phage shock protein PspA to be up-regulated 2.1- and 3.3-fold, respectively. PspA is part of the bacterial response to membrane stress that is generally induced by impairment of the inner membrane integrity, resulting in a decline in the proton motive force, and by outer membrane secretins that are used for adherence to host cells and the export of virulence factors of pathogenic bacteria (Darwin, 2005; Joly *et al.*, 2010). As a part of the two-component system PhoP-PhoQ, where PhoQ represents the membrane-associated sensor kinase and is present in the genome of strain FO-BEG1 (PSE_2476), the response regulator PhoP (PSE_2475) has been found 11.1-fold upregulated. *Salmonella* is one of the best studied model organisms concerning PhoP-PhoQ functions and it has been shown that the system regulates virulence and many changes in the bacterial cell envelope (Groisman, 2001). Furthermore, the expression of a member of the multiple antibiotic resistance regulator (MarR) protein family has been induced under phosphate limited conditions. The MarR regulator family is known to regulate diverse cellular functions including virulence, stress response, and resistance to antibiotics and organic solvents (Ellison and Miller, 2006; Perera and Grove, 2010).

The vast majority (>45%) of down-regulated proteins under P_i-starvation (and therefore up-regulated in P_i-surplus) belong to the transcription, translation and DNA

metabolism category (**Figure 5.11**). Growth under P_i-starvation is retarded, which is reflected in the down-regulation of tRNA genes and subunits of ribosomes. Additionally, enzymes like glucose-6-phosphate isomerase involved in the glycolysis pathway and citrate synthase, which catalyzes a key reaction in the tricarboxylic acid cycle, are down-regulated under P_i-limited conditions.

Changes in the protein expression during the late growth phase of P_i-limitation and the prediction of secreted proteins

Changes in the proteome during the transition from early to late growth phase under P_i-limited conditions are characterized mainly by decrease of anabolic processes, which is represented by down-regulation of proteins involved in translation, transcription and DNA metabolism, amino acid and nucleotide metabolism, and energy generation represented by the transport and secretion category (**Figure 5.12**). Among the up-regulated proteins in the late growth phase we find, among others, a phospholipase, which is most likely involved in phosphate acquisition, two subunits of TRAP transporters, and a phasin that, as described before, is involved in PHA granule formation. Three out of 14 up-regulated proteins belong to the stress response, detoxification and iron metabolism category, whereas two of the three proteins are involved in the glutathione synthesis. The last one, a major ferric-iron binding protein, is 6-fold up-regulated in the late growth phase of P_i-limitation, however, it is also found 4.6-fold down-regulated in the early growth phase of P_i-limitation (meaning that it is up-regulated under P_i-surplus conditions), indicating that it is not involved in the specific response to phosphate starvation. For three out of 14 up-regulated proteins in the late growth phase of P_i-limitation only general functional predictions are available (**Figure 5.12**).

One of the questions of the present study was the characterization of the secreted compounds. To identify proteins with the potential to be secreted, we analyzed the regulated fraction of proteins for the presence of a transmembrane domain, a signal peptide, and the predicted localization (**Table S 5.1** and **Table S 5.2**). Proteins containing a transmembrane domain are localized either in the inner or in the outer membrane and therefore are unlikely to be completely secreted. Therefore, our major interest was in proteins with a signal peptide, but without a transmembrane domain, of which fifteen were up-regulated under P_i-limitation. Furthermore, five proteins were up-regulated and three down-regulated in the late growth phase of phosphate starvation. However, only one of these proteins (PSE_1012), a hypothetical protein with unknown functions, has a predicted extracellular localization.

Additionally, the hypothetical protein PSE_3716 has a predicted extracellular localization, but does not contain a signal peptide.

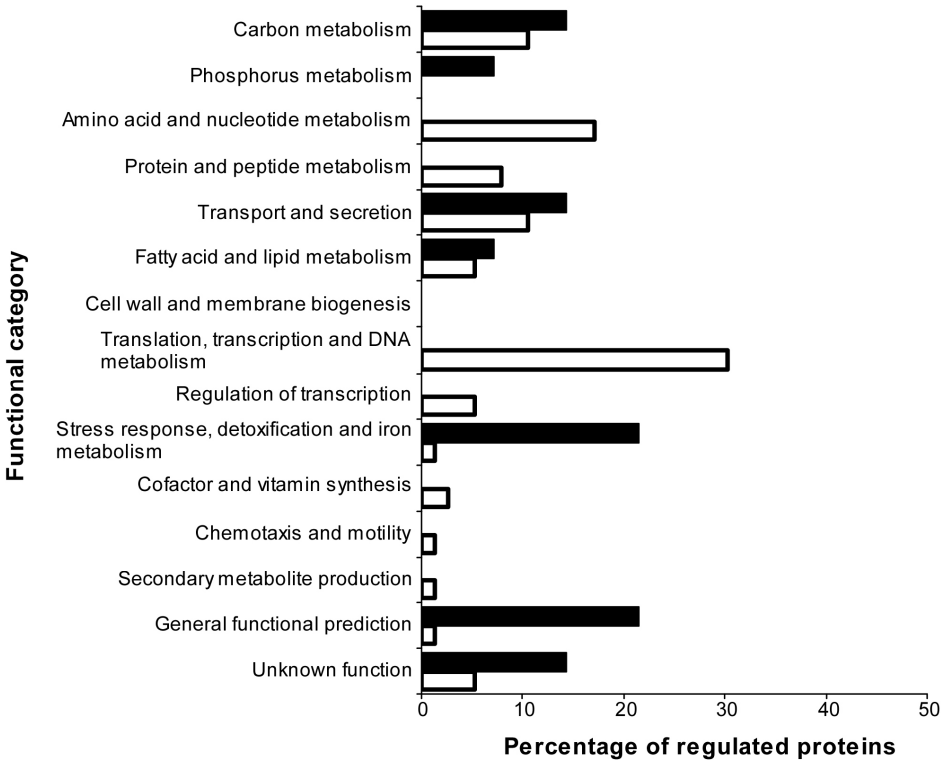

Figure 5.12. Categorization of the differentially expressed proteins in the late growth phase compared to early growth phase under P_i-starvation shown as the percentage of the total amount of either up- (14) or down- (76) regulated proteins. Black and white bars represent up- and down-regulated proteins, respectively.

Discussion

In the present study, the physiological response to phosphate limitation of *Pseudovibrio* sp. FO-BEG1 was investigated. Strain FO-BEG1 was cultivated in a defined medium containing glucose as the carbon and ammonia as the nitrogen source. The phosphate content was 1.2 and 0.1 mmol l^{-1} in the P_i-surplus and P_i-limited cultures, respectively. The P_i-limited culture contained more than a five-fold lower amount of phosphorus than is required for the utilization of 10 mmol l^{-1} glucose according to the Redfield ratio, which is verified by an observed decrease of about 650 mmol l^{-1} phosphate in the P_i-surplus culture (**Figure 5.4**). Phosphate limitation induces morphological changes in cells of strain FO-BEG1, represented by significant cell elongation. This phenomenon has been described e.g. in *Vibrio* strains and can be attributed to the increase of the cellular surface by using a surplus of carbon present in the medium in order to enhance uptake efficiency of the limited nutrients (Løvdal *et al.*, 2008). Alternatively, activation of the SOS response, which is commonly induced by

exposure to stress, can inhibit cell division (e.g. van der Veen *et al.*, 2010), leading to elongated cells as observed in the case of strain FO-BEG1 (**Figure 5.5**).

Phosphate limitation affects the physiology of *Pseudovibrio* sp. FO-BEG1

The P_i-limited cultures are characterized by a low final cell density, a lower growth rate and decreased uptake of ammonia and glucose (**Figure 5.2**). Especially the assimilation of ammonia per unit optical density is reduced by almost half, when compared to P_i-surplus conditions (**Figure 5.2B)**, which is a phenomenon that cannot be explained so far. The differences in the growth rate are also reflected in the proteomic data. Nutrient repression results in down-regulation of tRNA genes and ribosomal subunits for protein synthesis, of DNA replication and repair enzymes and of proteins involved in major carbon utilization cycles like glycolysis and the tricarboxylic acid cycle. Intriguingly, when glucose utilization is considered per optical density unit, it becomes evident that under P_i-starvation the cells take up more glucose per $OD_{600\ nm}$ (**Figure 5.2**). The increased consumption of glucose indicates that this substrate may be used for other purposes than growth, being most likely the accumulation of carbon storage compounds in the form of polyhydroxyalkanoates (PHA). The proteomic analysis shows up-regulation of a phasin, a protein that covers the outer surface of the PHA granules (Steinbüchel *et al.*, 1995). Furthermore, staining with Nile Red illustrates that after 35 hours cells in the P_i-limited condition accumulate more PHA than cells grown in the P_i-surplus medium (**Figure 5.3**), confirming that the synthesis of PHA under P_i-starvation is increased. Production of the carbon storage compound polyhydroxybutyrate (PHB) under P_i-limited conditions is a known response, which was shown for instance in a *Synechocystis* strain, storing 6.7% more PHB under P_i-starvation (Panda and Mallick, 2006).

The Pho regulon presumably controls the P_i-starvation of strain FO-BEG1

The phosphate starvation response has been extensively studied in different *E. coli*, *Bacillus*, *Vibrio*, and *Streptomyces* strains and is controlled by the PhoR-PhoB two-component regulatory system, which is strongly up-regulated under the P_i-limited conditions (Hoi *et al.*, 2006; Rodríguez-García *et al.*, 2007; Crépin *et al.*, 2008). Even though we identified homologues of PhoR and PhoB in the genome of *Pseudovibrio* sp. FO-BEG1 (PSE_1687 and PSE_1693, respectively, data not shown) we could not detect these components in the proteomic analysis. PhoR is a membrane bound histidine kinase (Lamarche *et al.*, 2008) and therefore was likely to be removed during protein preparation, since the procedure was optimized for cellular and not membrane proteins. PhoB, however, could have

been missed due to the fact that in a quantitative mass spectrometry proteomic approach not all proteins are detected (Bantscheff *et al.*, 2007). One of the major proteins induced during phosphate starvation is the alkaline phosphatase PhoA (VanBogelen *et al.*, 1996; Hoi *et al.*, 2006). Alkaline phosphatase (AP) related genes have been identified in the genome of strain FO-BEG1 in two different loci (PSE_2813 and PSE_5052) and both have predicted periplasmic localization (results not shown). An increase in alkaline phosphatase activity is associated with the induction of the P_i-starvation response, since PhoA is controlled by the Pho regulon (Wanner, 1993). We could not detect any of the predicted homologues of the alkaline phosphatases in the proteomic analysis. However, we have shown an increase in AP activity 37 hours after inoculation in a whole cells assay (**Figure 5.7**). This indicates that the alkaline phosphatase is indeed produced as a response to P_i-starvation and it was simply not detected during the proteomic analysis.

Furthermore, considerable up-regulation of proteins described in other proteomic approaches to be directly controlled by the Pho regulon or involved in the response to P_i-starvation have been detected in the proteomic study, including the high-affinity ABC transport system for phosphate, phosphonate import and degradation proteins, highly affine ABC transporter systems for organophosphates (*sn*-G3P) as well as DNA- and nucleotide-degrading enzymes, especially 5'-nucleotidase, AMP nucleosidase, and 2',3'-cyclic nucleotide 2'-phosphodiesterase/3'-nucleotidase (Voigt *et al.*, 2006; von Krüger *et al.*, 2006; Rodríguez-García *et al.*, 2007; Tetu *et al.*, 2009). We therefore propose that, despite the absence of the PhoR-PhoB proteins in the proteomic analysis, *Pseudovibrio* sp. FO-BEG1 utilizes the PhoR-PhoB two-component regulatory system after exposure to P_i-starvation, thereby up-regulating proteins involved in acquisition of phosphorus for the cell metabolism.

Polyphosphate is not completely degraded under P_i-limited conditions

In the P_i-limited culture, phosphate in the medium was used up completely after 24 hours. However, pronounced growth was observed in the following 36 hours, leading to the conclusion that intracellular poly P_i could be the source for the required phosphorus, which then was analyzed via DAPI staining. Unfortunately, the DAPI staining technique used in this study does not allow quantification of the stored polyphosphate, but its decreasing amount in the cells can be visualized, as shown by Brock and Schulz-Vogt (2011), and therefore the complete exhaustion of polyphosphate should clearly be recognizable. Remarkably, we could not detect polyphosphate decrease in the cells over the incubation time under P_i-limited

conditions, despite the fact that poly P_i is regarded, among other functions, as a phosphorus reservoir (Kornberg, 1995) and could have been accessed under tested conditions to increase cellular biomass. The proteomic data confirm this observation. Only the polyphosphate kinase I was found up-regulated, an enzyme that is actually proposed to reversibly catalyze polyphosphate synthesis (Brown and Kornberg, 2008). In contrast, the polyphosphate kinase II and the exopolyphosphatase are considered as polyphosphate-degrading enzymes, generating GTP or ATP, respectively (Brown and Kornberg, 2008). Homologues of both enzymes are present in the genome of strain FO-BEG1 (PSE_0394 and PSE_2770, respectively), however, none has been detected in the proteomic analysis indicating that poly P_i might indeed be rather accumulated than degraded during P_i-starvation. These observations are in agreement with the findings of Grillo and Gibson (1979), who have shown increased poly P_i synthesis under phosphate starvation by a *Synechococcus* strain.

The cell envelope is modified and protection against reactive oxygen species is increased in *Pseudovibrio* sp. FO-BEG1 during P_i-starvation

During P_i-limitation, cells must utilize the present phosphorus economically. In order to decrease their demand for phosphorus and to recover already incorporated phosphorus, bacterial cells are known to exchange phospholipids with phosphorus-free lipids (Geiger *et al.*, 1999; Van Mooy *et al.*, 2006). Results of the proteomic analysis imply that a similar response is activated in *Pseudovibrio* sp. FO-BEG1 and the cell envelope is modified during P_i-starvation. Phospholipids are presumably substituted with SQDG since an UDP-sulfoquinovose biosynthetic protein and enzymes involved in degradation and synthesis of lipids are up-regulated. However, degradation of membrane lipids could have another physiological background. It has been shown that P_i-starved *E. coli* cells experience severe damage from peroxides, which are predominantly affecting lipids (Moreau *et al.*, 2001). Peroxidation of lipids is regarded as particularly harmful due to a successive chain reaction that continuously oxidizes membranes within the cell and eventually affects proteins and DNA (Dedon *et al.*, 1998; Refsgaard *et al.*, 2000). Moreau *et al.* (2001) have shown that P_i-starved cells antagonize this process with the alkylhydroperoxidase that can detoxify the formed lipid hydro-peroxides, and which is an enzyme that was also up-regulated in the P_i-limited culture of FO-BEG1. It is therefore conceivable that enzymes involved in the degradation of lipids are also up-regulated in order to "remove" the disordered lipids, which have been detoxified but are not functioning any longer.

Furthermore, iron plays an important role when it comes to oxidative stress. Damaging of iron-sulfur clusters by reactive oxygen species (ROS) can result in the release of Fe^{2+}, which, in turn, reacts with H_2O_2 and produces reactive hydroxyl radicals that oxidize proteins, lipids and DNA (Storz and Imlay, 1999). The increase of bacterioferritin-like proteins in the cell could provide a possibility to store and protect the cell from the dangerous Fe^{2+}, since iron is stored as Fe^{3+} in ferritins and Fe^{2+} is oxidized at the ferroxidase center of the ferritin complex (Chiancone *et al.*, 2004). Remarkably, the oxidation of two Fe^{2+} is performed with one H_2O_2 in the bacterioferritin (Bou-Abdallah *et al.*, 2002), thereby reducing the reactive peroxide to water and avoiding the production of hydroxyl radicals from the regular oxidation of H_2O_2 with Fe^{2+}. Therefore, bacterioferritin can be regarded, besides an iron storage compound, as an extremely important component of the ROS protection machinery. Also the upregulation of the glutathione synthase indicates that protection against ROS plays an important role under P_i-starvation. Even though this tripeptide has been investigated thoroughly in eukaryotes and is regarded as an important antioxidant and detoxification molecule (Pompella *et al.*, 2003), details about the function of glutathione in prokaryotes are still unknown. Nevertheless, protective roles and antioxidative activities have been proposed for glutathione in prokaryotes (e.g. Kullisaar *et al.*, 2010; Zhang *et al.*, 2010), indicating that it could play an important role in protecting *Pseudovibrio* cells from oxygen radicals. Additionally, two subunits of a high-affinity ABC transporter for the polyamines spermidine/putrescine were highly up-regulated under P_i-limitation. One of the suggested roles for spermidine is DNA protection against ROS (Khan *et al.*, 1992; Ha *et al.*, 1998). Therefore, spermidine could provide another mechanism to counter oxidative stress in *Pseudovibrio* sp. FO-BEG1, which would explain the increased requirement of this polyamine by the cells.

Supporting the theory that the cell surface and membranes are heavily modified under tested conditions, we observe an increased expression of the PspA protein as part of the bacterial response to conditions impairing membrane integrity. This might be a result of altered membrane properties due to the phospholipid-exchange process or mislocalization of secretins, outer membrane subunits of the type II secretion system, considering that they might be involved in export of molecules under P_i-limitation (Darwin, 2005). Furthermore, we see a slight increase in expression of two membrane protein homologues of OmpA (just below the threshold of 2-fold) and of the periplasmic TolB. Both are required for the structural integrity of the outer membrane and are known to form a complex together

(Lloubès *et al.*, 2001; Godlewska *et al.*, 2009). Mutations or deletion of the PhoR-PhoB system hamper adhesion and virulence in e.g. *E. coli* (Lamarche *et al.*, 2008 and references therein). Intriguingly, TolB and OmpA were shown to be involved in pathogenesis, adhesion, invasion and evasion of the immune system in the host (Lloubès *et al.*, 2001; Smith *et al.*, 2007; Godlewska *et al.*, 2009). Since *Pseudovibrio* spp. are associated with marine invertebrates, it is tempting to speculate that the up-regulation of these proteins can be of importance for the establishment and maintenance of a symbiosis with marine invertebrates. Additionally, it is possible that up-regulation of a protein required for alginate synthesis leads to an increased alginate-related exopolysaccharide layer in *Pseudovibrio*, thereby protecting it from endocytosis, as has been proposed for sponge symbionts in general (Wilkinson *et al.*, 1984; Friedrich *et al.*, 1999)

TolC could be involved in secretion of metabolites in strain FO-BEG1

One of the important aspects of P_i-limitation of *Pseudovibrio* sp. FO-BEG1 is the release of one or more compounds into the medium, which becomes visually detectable by the appearance of a yellow color in the medium under P_i-starvation (**Figure 5.8**). The applied proteomic approach was not specifically adjusted for isolation of membrane bound proteins, therefore conclusions about involved secretion mechanisms are difficult to draw. Nevertheless, expression of TolC, an outer membrane factor of the type I secretion system, was found up-regulated, indicating that this could be one of the export mechanisms for the secreted compounds. In the genome, in direct proximity to *tolC*, we found two other subunits that are required for a working export system: the ATP utilizing pump (PSE_3719) and the membrane fusion protein, which connects the outer membrane with the inner membrane (PSE_3718). In fact, the outer membrane factor TolC can be also recruited by proteins of other transport families like the major facilitator superfamily (MFS) and restance-nodulation-division (RND), thereby functioning as a versatile channel for secretion of a variety of substances, ranging from small antimicrobial peptides like bacteriocins, to hydrolytic enzymes and large endotoxins (Young and Holland, 1999; Holland *et al.*, 2005).

Differences in extracellular metabolome are confirmed by the FT-ICR-MS analysis

The identity and function of the secreted compounds remains elusive at this moment. The analysis for the presence of signal peptides and their predicted localization in up-regulated proteins during P_i-limitation resulted in two candidate proteins (PSE_1012 and PSE_3716), both of which are uncharacterized so far. The closest annotated hit for PSE_1012

is a phosphatase-related protein, but we could not observe phosphatase activity in the supernatant of P_i-limited cells (results not shown). For PSE_3716, no activity predictions exist so far. Besides being proteins, the secreted material could alternatively be small molecules, like metabolites, oligo- or polypeptides. This part of the extracellular metabolome was accessed via the extraction of the dissolved organic matter from the culture supernatant and the measurement of the samples via FT-ICR-MS. The DOC analysis showed a strongly increased amount of dissolved organic carbon in the P_i-limited compared to the P_i-surplus cultures (**Figure 5.9A)**, confirming the secretion of organic compounds. Furthermore, the analysis of the secretome via FT-ICR-MS provided mass spectra, which show statistically different molecular fingerprints between the medium of the P_i-limited and the P_i-surplus culture (**Figure 5.9B**), verifying that not only more DOM is secreted under P_i-starvation, but that it is also significantly dissimilar to the DOM found in the supernatant of the P_i-surplus cultures. Further analysis of the acquired MS data is required in order to conclude chemical composition of differently secreted substances under the tested conditions

Particularly interesting are the ICP-OES measurements of iron and cobalt, showing an increased uptake of Co and Fe under P_i-starvation. For the higher usage of Co we lack an explanation. Iron, however, seems to be of major importance under P_i-limitation. On the one hand, increased uptake of iron corresponds with increased bacterioferritin synthesis for storage and simultaneous detoxification of radical oxygen species. On the other hand, after 40 hours of incubation, iron in the medium increases again together with an intensification of the yellowish-orange color in the medium. This can be interpreted in two ways: either one of the secreted compounds, presumably the one that is responsible for the color, contains iron, or the secreted compound acts as a siderophores-like molecule, solubilzing the iron bound to the precipitates in order to take it up into the cells. So far, we do not have any evidence that bioactive compounds with antimicrobial activities are among the secreted compounds since the performed tests did not show any inhibition effects with the tested strains. From the proteomic point of view, the up-regulation of a PmbA homologue, a protein that is required for microcin processing and secretion, is the so far only indication that secondary metabolites could be produced and secreted by *Pseudovibrio* sp. FO-BEG1 under phosphate limitation, but this needs to be further investigated.

In summary, we conclude that *i*) P_i-starvation in *Pseudovibrio* sp. FO-BEG1 induces a response, which is comparable to the in-depth analyzed responses of e.g. *E. coli* and

Bacillus species (Hoi *et al.*, 2006; Crépin *et al.*, 2008), and that this response is presumably regulated by the PhoR-PhoB regulon in strain FO-BEG1; *ii*) P_i-starvation stimulates an increased accumulation of storage compounds for carbon, phosphorus and iron; *iii*) oxidative stress is a major issue during P_i-starvation of the FO-BEG1 culture and conclusively, protection systems are up-regulated; *iv*) P_i-limitation induces the secretion of one or several molecules into the medium, introducing the yellow color. The ultimate identity and function of this compound will, however, be subject of future investigations.

Acknowledgments

We thank J. Harder for many fruitful discussions and, V. Salman for comments on the manuscript. For technical support, we thank M. Meyer, S. Menger, C. Probian, and R. Appel. We also thank I. Ulber for help with the DOM extraction and DOC measurements, K. Klaproth for FT-ICR-MS measurements, and S. Pape for ICP-OES measurements. This study was funded by the European Research Council and the Max Planck Society.

References

Aeckersberg F, Bak F, Widdel F. (1991). Anaerobic oxidation of saturated hydrocarbons to CO_2 by a new type of sulfate-reducing bacterium. *Arch Microbiol* **156:** 5–14.

Ahn KH, Kornberg A. (1990). Polyphosphate kinase from *Escherichia coli* – purification and demonstration of a phosphoenzyme intermediate. *J Biol Chem* **265:** 11734–11739.

Andrews SC. (2010). The Ferritin-like superfamily: evolution of the biological iron storeman from a rubrerythrin-like ancestor. *Biochim Biophys Acta* **1800:** 691–705.

Bantscheff M, Schirle M, Sweetman G, Rick J, Kuster B. (2007). Quantitative mass spectrometry in proteomics: a critical review. *Anal Bioanal Chem* **389:** 1017–1031.

Bendtsen JD, Nielsen H, von Heijne G, Brunak S. (2004). Improved prediction of signal peptides: SignalP 3.0. *J Mol Biol* **340:** 783–795.

Benning C. (2007). Questions remaining in sulfolipid biosynthesis: a historical perspective. *Photosynth Res* **92:** 199–203.

Boehm M, Nield J, Zhang PP, Aro EM, Komenda J, Nixon PJ. (2009). Structural and mutational analysis of band 7 proteins in the cyanobacterium *Synechocystis* sp. strain PCC 6803. *J Bacteriol* **191:** 6425–6435.

Bou-Abdallah F, Lewin AC, Le Brun NE, Moore GR, Chasteen ND. (2002). Iron detoxification properties of *Escherichia coli* bacterioferritin - attenuation of oxyradical chemistry. *J Biol Chem* **277:** 37064–37069.

Brock J, Schulz-Vogt HN. (2011). Sulfide induces phosphate release from polyphosphate in cultures of a marine *Beggiatoa* strain. *ISME J* **5:** 497–506.

Brown MRW, Kornberg A. (2008). The long and short of it - polyphosphate, PPK and bacterial survival. *Trends Biochem Sci* **33:** 284–290.

Brysch K, Schneider C, Fuchs G, Widdel F. (1987). Lithoautotrophic growth of sulfate-reducing bacteria, and description of *Desulfobacterium autotrophicum* gen. nov., sp. nov. *Arch Microbiol* **148:** 264–274.

Chiancone E, Ceci P, Ilari A, Ribacchi F, Stefanini S. (2004). Iron and proteins for iron storage and detoxification. *Biometals* **17:** 197–202.

Coleman JE. (1992). Structure and mechanism of alkaline phosphatase. *Annu Rev Bioph Biom* **21:** 441–483.

Crépin S, Lamarche MG, Garneau P, Séguin J, Proulx J, Dozois CM *et al.* (2008). Genome-wide transcriptional response of an avian pathogenic *Escherichia coli* (APEC) *pst* mutant. *Bmc Genomics* **9:** 568.

Darwin AJ. (2005). The phage-shock-protein response. *Mol Microbiol* **57:** 621–628.

Dedon PC, Plastaras JP, Rouzer CA, Marnett LJ. (1998). Indirect mutagenesis by oxidative DNA damage: formation of the pyrimidopurinone adduct of deoxyguanosine by base propenal. *Proc Natl Acad Sci U S A* **95:** 11113–11116.

Dittmar T, Koch B, Hertkorn N, Kattner G. (2008). A simple and efficient method for the solid-phase extraction of dissolved organic matter (SPE-DOM) from seawater. *Limnol Oceanogr Methods* **6:** 230–235.

Ellison DW, Miller VL. (2006). Regulation of virulence by members of the MarR/SlyA family. *Curr Opin Microbiol* **9:** 153–159.

Friedrich AB, Merkert H, Fendert T, Hacker J, Proksch P, Hentschel U. (1999). Microbial diversity in the marine sponge *Aplysina cavernicola* (formerly *Verongia cavernicola*) analyzed by fluorescence in situ hybridization (FISH). *Mar Biol* **134:** 461–470.

Gacesa P. (1998). Bacterial alginate biosynthesis - recent progress and future prospects. *Microbiol-UK* **144:** 1133–1143.

Geiger O, Röhrs V, Weissenmayer B, Finan TM, Thomas-Oates JE. (1999). The regulator gene *phoB* mediates phosphate stress-controlled synthesis of the membrane lipid diacylglyceryl-*N,N,N*-trimethylhomoserine in *Rhizobium* (*Sinorhizobium*) *meliloti*. *Mol Microbiol* **32:** 63–73.

Giovannoni SJ, Tripp HJ, Givan S, Podar M, Vergin KL, Baptista D *et al.* (2005). Genome streamlining in a cosmopolitan oceanic bacterium. *Science* **309:** 1242–1245.

Godlewska R, Wiśniewska K, Pietras Z, Jagusztyn-Krynicka EK. (2009). Peptidoglycan-associated lipoprotein (Pal) of Gram-negative bacteria: function, structure, role in

pathogenesis and potential application in immunoprophylaxis. *FEMS Microbiol Lett* **298:** 1–11.

Grillo JF, Gibson J. (1979). Regulation of phosphate accumulation in the unicellular cyanobacterium *Synechococcus*. *J Bacteriol* **140:** 508–517.

Groisman EA. (2001). The pleiotropic two-component regulatory system PhoP-PhoQ. *J Bacteriol* **183:** 1835–1842.

Ha HC, Sirisoma NS, Kuppusamy P, Zweier JL, Woster PM, Casero RA. (1998). The natural polyamine spermine functions directly as a free radical scavenger. *Proc Natl Acad Sci U S A* **95:** 11140–11145.

Hall PO, Aller RC. (1992). Rapid, small-volume, flow injection analysis for ΣCO_2 and NH_4^+ in marine and freshwaters. *Limnol Oceanogr* **37:** 1113–1119.

Hansen HP, Koroleff F. (1999). Determination of nutrients. In: Grasshoff K, Kremling K, Ehrhardt M (eds). *Methods of seawater analysis*. Wiley-VCH: Weinheim. pp 159–226.

Hentschel U, Schmid M, Wagner M, Fieseler L, Gernert C, Hacker J. (2001). Isolation and phylogenetic analysis of bacteria with antimicrobial activities from the mediterranean sponges *Aplysina aerophoba* and *Aplysina cavernicola*. *FEMS Microbiol Ecol* **35:** 305–312.

Hoi LT, Voigt B, Jürgen B, Ehrenreich A, Gottschalk G, Evers S *et al.* (2006). The phosphate-starvation response of *Bacillus licheniformis*. *Proteomics* **6:** 3582–3601.

Holland IB, Schmitt L, Young J. (2005). Type 1 protein secretion in bacteria, the ABC-transporter dependent pathway. *Mol Membr Biol* **22:** 29–39.

Hurwitz J, Heppel LA, Horecker BL. (1957). The enzymatic cleavage of adenylic acid to adenine and ribose 5-phosphate. *J Biol Chem* **226:** 525–540.

Ingram-Smith C, Martin SR, Smith KS. (2006). Acetate kinase: not just a bacterial enzyme. *Trends Microbiol* **14:** 249–253.

Joly N, Engl C, Jovanovic G, Huvet M, Toni T, Sheng X *et al.* (2010). Managing membrane stress: the phage shock protein (Psp) response, from molecular mechanisms to physiology. *FEMS Microbiol Rev* **34:** 797–827.

Khan AU, Di Mascio P, Medeiros MHG, Wilson T. (1992). Spermine and spermidine protection of plasmid DNA against single-strand breaks induced by singlet oxygen. *Proc Natl Acad Sci U S A* **89:** 11428–11430.

Kim SK, Makino K, Amemura M, Shinagawa H, Nakata A. (1993). Molecular analysis of the *phoH* gene, belonging to the phosphate regulon in *Escherichia coli*. *J Bacteriol* **175:** 1316–1324.

Kornberg A. (1995). Inorganic polyphosphate: toward making a forgotten polymer unforgettable. *J Bacteriol* **177:** 491–496.

Krogh A, Larsson B, von Heijne G, Sonnhammer EL. (2001). Predicting transmembrane protein topology with a hidden Markov model: application to complete genomes. *J Mol Biol* **305:** 567–580.

Kullisaar T, Songisepp E, Aunapuu M, Kilk K, Arend A, Mikelsaar M *et al.* (2010). Complete glutathione system in probiotic *Lactobacillus fermentum* ME-3. *Appl Biochem Micro+* **46:** 481–486.

Laemmli UK. (1970). Cleavage of structural proteins during assembly of the head of bacteriophage T4. *Nature* **227:** 680–685.

Lamarche MG, Wanner BL, Crépin S, Harel J. (2008). The phosphate regulon and bacterial virulence: a regulatory network connecting phosphate homeostasis and pathogenesis. *FEMS Microbiol Rev* **32:** 461–473.

Lamarche MG, Dozois CM, Daigle F, Caza M, Curtiss R, Dubreuil JD *et al.* (2005). Inactivation of the *pst* system reduces the virulence of an avian pathogenic *Escherichia coli* O78 strain. *Infect Immun* **73:** 4138–4145.

Lazzaroni JC, Germon P, Ray MC, Vianney A. (1999). The Tol proteins of *Escherichia coli* and their involvement in the uptake of biomolecules and outer membrane stability. *FEMS Microbiol Lett* **177:** 191–197.

Lloubès R, Cascales E, Walburger A, Bouveret E, Lazdunski C, Bernadac A *et al.* (2001). The Tol-Pal proteins of the *Escherichia coli* cell envelope: an energized system required for outer membrane integrity? *Res Microbiol* **152:** 523–529.

Løvdal T, Skjoldal EF, Heldal M, Norland S, Thingstad TF. (2008). Changes in morphology and elemental composition of *Vibrio splendidus* along a gradient from carbon-limited to phosphate-limited growth. *Microb Ecol* **55:** 152–161.

Malmström L, Malmström J, Aebersold R. (2011). Quantitative proteomics of microbes: principles and applications to virulence. *Proteomics* **11:** 2947–2956.

Maplestone RA, Stone MJ, Williams DH. (1992). The evolutionary role of secondary metabolites - a review. *Gene* **115:** 151–157.

Martín JF. (2004). Phosphate control of the biosynthesis of antibiotics and other secondary metabolites is mediated by the PhoR-PhoP system: an unfinished story. *J Bacteriol* **186:** 5197–5201.

McCleary WR, Stock JB. (1994). Acetyl phosphate and the activation of two-component response regulators. *J Biol Chem* **269:** 31567–31572.

Moreau PL, Gérard F, Lutz NW, Cozzone P. (2001). Non-growing *Escherichia coli* cells starved for glucose or phosphate use different mechanisms to survive oxidative stress. *Mol Microbiol* **39:** 1048–1060.

Nikaido H. (2003). Molecular basis of bacterial outer membrane permeability revisited. *Microbiol Mol Biol Rev* **67:** 593–656.

O'Halloran JA, Barbosa TM, Morrissey JP, Kennedy J, O'Gara F, Dobson ADW. (2011). Diversity and antimicrobial activity of *Pseudovibrio* spp. from Irish marine sponges. *J Appl Micobiol* **110:** 1495–1508.

Panda B, Mallick N. (2006). Enhanced poly-β-hydroxybutyrate accumulation in a unicellular cyanobacterium, *Synechocystis* sp. PCC 6803. *Lett Appl Microbiol* **44:** 194–198.

Paytan A, McLaughlin K. (2007). The oceanic phosphorus cycle. *Chem Rev* **107:** 563–576.

Penesyan A, Tebben J, Lee M, Thomas T, Kjelleberg S, Harder T *et al.* (2011). Identification of the antibacterial compound produced by the marine epiphytic bacterium *Pseudovibrio* sp. D323 and related sponge-associated bacteria. *Marine Drugs* **9:** 1391–1402.

Perera IC, Grove A. (2010). Molecular mechanisms of ligand-mediated attenuation of DNA binding by MarR family transcriptional regulators. *J Mol Cell Biol* **2:** 243–254.

Pompella A, Visvikis A, Paolicchi A, De Tata V, Casini AF. (2003). The changing faces of glutathione, a cellular protagonist. *Biochem Pharmacol* **66:** 1499–1503.

Ramsey DM, Wozniak DJ. (2005). Understanding the control of *Pseudomonas aeruginosa* alginate synthesis and the prospects for management of chronic infections in cystic fibrosis. *Mol Microbiol* **56:** 309–322.

Rao PSS, Yamada Y, Tan YP, Leung KY. (2004). Use of proteomics to identify novel virulence determinants that are required for *Edwardsiella tarda* pathogenesis. *Mol Microbiol* **53:** 573–586.

Refsgaard HHF, Tsai L, Stadtman ER. (2000). Modifications of proteins by polyunsaturated fatty acid peroxidation products. *Proc Natl Acad Sci U S A* **97:** 611–616.

Rodríguez-García A, Barreiro C, Santos-Beneit F, Sola-Landa A, Martín JF. (2007). Genome-wide transcriptomic and proteomic analysis of the primary response to phosphate limitation in *Streptomyces coelicolor* M145 and in a Δ*phoP* mutant. *Proteomics* **7:** 2410–2429.

Rodríguez-Sáinz MC, Hernández-Chico C, Moreno F. (1990). Molecular characterization of *pmbA*, an *Escherichia coli* chromosomal gene required for the production of the antibiotic peptide MccB17. *Mol Microbiol* **4:** 1921–1932.

Santos OCS, Pontes PVML, Santos JFM, Muricy G, Giambiagi-deMarval M, Laport MS. (2010). Isolation, characterization and phylogeny of sponge-associated bacteria with antimicrobial activities from Brazil. *Res Microbiol* **161:** 604–612.

Schmidt A, Kellermann J, Lottspeich F. (2005). A novel strategy for quantitative proteomics using isotope-coded protein labels. *Proteomics* **5:** 4–15.

Sertan-de Guzman AA, Predicala RZ, Bernardo EB, Neilan BA, Elardo SP, Mangalindan GC *et al.* (2007). *Pseudovibrio denitrificans* strain Z143-1, a heptylprodigiosin-producing bacterium isolated from a Philippine tunicate. *FEMS Microbiology Letters* **277:** 188–196.

Slauch JM, Silhavy TJ. (1991). Genetic fusions as experimental tools. In: Miller JH (ed). *Methods in enzymology: bacterial genetic systems*. Academic Press, Inc.: London. pp 213–248.

Smith SGJ, Mahon V, Lambert MA, Fagan RP. (2007). A molecular Swiss army knife: OmpA structure, function and expression. *FEMS Microbiol Lett* **273:** 1–11.

Steinbüchel A, Aerts K, Babel W, Föllner C, Liebergesell M, Madkour MH *et al.* (1995). Considerations on the structure and biochemistry of bacterial polyhydroxyalkanoic acid inclusions. *Can J Microbiol* **41:** 94–105.

Storz G, Imlay JA. (1999). Oxidative stress. *Curr Opin Microbiol* **2:** 188–194.

Taylor MW, Radax R, Steger D, Wagner M. (2007). Sponge-associated microorganisms: evolution, ecology, and biotechnological potential. *Microbiol Mol Biol Rev* **71:** 295–374.

Tetu SG, Brahamsha B, Johnson DA, Tai V, Phillippy K, Palenik B *et al.* (2009). Microarray analysis of phosphate regulation in the marine cyanobacterium *Synechococcus* sp. WH8102. *ISME J* **3:** 835–849.

Tijssen JPF, Beekes HW, Vansteveninck J. (1982). Localization of polyphosphates in *Saccharomyces fragilis*, as revealed by 4',6-diamidino-2-phenylindole fluorescence. *Biochim Biophys Acta* **721:** 394–398.

van der Veen S, van Schalkwijk S, Molenaar D, de Vos WM, Abee T, Wells-Bennik MHJ. (2010). The SOS response of *Listeria monocytogenes* is involved in stress resistance and mutagenesis. *Microbiol-SGM* **156:** 374–384.

Van Mooy BAS, Rocap G, Fredricks HF, Evans CT, Devol AH. (2006). Sulfolipids dramatically decrease phosphorus demand by picocyanobacteria in oligotrophic marine environments. *Proc Natl Acad Sci U S A* **103:** 8607–8612.

Van Mooy BAS, Fredricks HF, Pedler BE, Dyhrman ST, Karl DM, Koblížek M *et al.* (2009). Phytoplankton in the ocean use non-phosphorus lipids in response to phosphorus scarcity. *Nature* **458:** 69–72.

VanBogelen RA, Olson ER, Wanner BL, Neidhardt FC. (1996). Global analysis of proteins synthesized during phosphorus restriction in *Escherichia coli*. *J Bacteriol* **178:** 4344–4366.

Vershinina OA, Znamenskaya LV. (2002). The Pho regulons of bacteria. *Microbiol* **71:** 497–511.

Vining LC. (1992). Secondary metabolism, inventive evolution and biochemical diversity - a review. *Gene* **115:** 135–140.

Vizcaino MI. (2011). The chemical defense of *Pseudopterogorgia americana*: a focus on the antimicrobial potential of a *Pseudovibrio* sp. Ph.D thesis, Medical University of South Carolina, Charleston.

Voigt B, Schweder T, Sibbald MJJB, Albrecht D, Ehrenreich A, Bernhardt J *et al.* (2006). The extracellular proteome of *Bacillus licheniformis* grown in different media and under different nutrient starvation conditions. *Proteomics* **6:** 268–281.

von Krüger WMA, Humphreys S, Ketley JM. (1999). A role for the PhoBR regulatory system homologue in the *Vibrio cholerae* phosphate-limitation response and intestinal colonization. *Microbiol-UK* **145:** 2463–2475.

von Krüger WMA, Lery LMS, Soares MR, de Neves-Manta FS, Silva CMBE, Neves-Ferreira AGD *et al.* (2006). The phosphate-starvation response in *Vibrio cholerae* O1 and *phoB* mutant under proteomic analysis: disclosing functions involved in adaptation, survival and virulence. *Proteomics* **6:** 1495–1511.

Wang Y. (2002). The function of OmpA in *Escherichia coli*. *Biochem Biophys Res Commun* **292:** 396–401.

Wanner BL. (1993). Gene regulation by phosphate in enteric bacteria. *J Cell Biochem* **51:** 47–54.

Widdel F, Pfennig N. (1984). Dissimilatory sulfate- or sulfur-reducing bacteria. In: Krieg NR, Holt JG (eds). *Bergey's manual of systematic bacteriology*. Williams & Wilkins: Baltimore. pp 663–379.

Wilkinson CR, Garrone R, Vacelet J. (1984). Marine sponges discriminate between food bacteria and bacterial symbionts: electron microscope radioautography and *in situ* evidence. *Proc R Soc Lond B Biol Sci* **220:** 519–528.

Young J, Holland IB. (1999). ABC transporters: bacterial exporters-revisited five years on. *BBA-Biomembranes* **1461:** 177–200.

Yu CS, Chen YC, Lu CH, Hwang JK. (2006). Prediction of protein subcellular localization. *Proteins Struct Funct Bioinf* **64:** 643–651.

Zhang J, Du GC, Zhang YP, Liao XY, Wang M, Li Y *et al.* (2010). Glutathione protects *Lactobacillus sanfranciscensis* against freeze-thawing, freeze-drying, and cold treatment. *Appl Environ Microbiol* **76:** 2989–2996.

Supplementary materials

Table S 5.1. Overview of regulated proteins under phosphorus starvation (P_i-surplus (+P_i) compared with P_i-limited (–P_i T_1) conditions). Prediction of transmembrane domains (P t d), signal peptides (P s p), protein localization (P l) and the regulation ratio (R r) are indicated in the respective column. Absence of transmembrane domains or signal peptide in the protein is indicated by an empty cell in the respective column.

Genome locus[a)]	Predicted function of the expressed protein[b)]	P t d[c)]	P s p[d)]	P l[e)]	R r[f)]
	Carbon metabolism				
	Up-regulated under P_i-starvation				
PSE_1257	Phasin			P, C	6.6
PSE_2787	5,10-methylenetetrahydromethanopterin reductase			P	18.2
PSE_3294	Dihydrolipoyllysine-residue acetyltransferase component of pyruvate dehydrogenase complex (E2)			C	2.0
PSE_4002	Pyruvate, phosphate dikinase			C	2.9
PSE_4767	Pyruvate kinase			C	2.7
	Down-regulated under P_i-starvation				
PSE_3391	Citrate synthase			C	–5.7
PSE_4148	Glucose-6-phosphate isomerase			C	–2.8
	Phosphorus metabolism				
	Up-regulated under P_i-starvation				
PSE_1086	Phosphate acetyltransferase (Phosphotransacetylase)			C	13.3
PSE_1087	*Acetate kinase			C	7.4
PSE_2769	Polyphosphate kinase			C	3.9
PSE_4851	*Protein PhnI			C	7.1
PSE_4857	Protein PhnM			C	6.4
PSE_0499	PhoH family protein			C	7.0
PSE_4852	*Protein PhnJ			C	4.2
	Amino acid and nucleotide metabolism				
	Up-regulated under P_i-starvation				
PSE_1095	Acetylglutamate kinase			C	2.1
PSE_0091	L-serine dehydratase 1			C	2.1
PSE_1577	glycine dehydrogenase subunit 1			C	2.0
PSE_1587	AMP nucleosidase			C	13.5
PSE_1775	Histidinol dehydrogenase, prokaryotic-type			C	2.9
PSE_1783	5'-nucleotidase			C	3.6
PSE_2573	bifunctional 2',3'-cyclic nucleotide 2'-phosphodiesterase/3'-nucleotidase			P	8.4
PSE_2796	D-hydantoinase			C, P	4.4
PSE_2943	Ornithine cyclodeaminase			C, P	4.0
PSE_3247	Deoxyguanosinetriphosphate triphosphohydrolase-like protein			C	on[g)]
PSE_3264	beta amino acid--pyruvate transaminase			C	2.4
PSE_3780	dihydroorotase, multifunctional complex type			C	3.6
PSE_4131	serine/threonine dehydratase			C	6.8

Table S 5.1. Continued

Genome locus	Predicted function of the expressed protein	P t d	P s p	P l	R r
PSE_4802	Phenylacetate--CoA ligase			C	6.1
PSE_0557	1-(5-phosphoribosyl)-5-[(5-phosphoribosylamino)methylideneamino] imidazole-4-carboxamide isomerase			C	5.0
PSE_0648	Adenosylhomocysteinase			C	8.9
PSE_4803	*ribonuclease, T2 family			P, C	on[g)]
PSE_2795	*Amidase, hydantoinase/carbamoylase			C	6.3
PSE_1575	*glycine cleavage system T protein			C	2.2
	Down-regulated under P_i-starvation				
PSE_3205	*Sulfate adenylyltransferase subunit 2			C	–2.1
PSE_2994	Vitamin B12-dependent ribonucleotide reductase			C	–3.5
	Protein and peptide metabolism				
	Up-regulated under P_i-starvation				
PSE_1495	Peptidase M16 family protein	1	√	OM, P	2.7
PSE_1533	Protein pmbA homolog			C	2.5
PSE_2484	Serine protease	1	√	C	2.1
PSE_3805	ATP-dependent Clp protease ATP-binding subunit ClpA			C	2.1
PSE_0023	PpiC-type peptidyl-prolyl cis-trans isomerase		√	IM	2.6
PSE_1698	*Hsp33-like chaperonin			C, P	2.6
	Down-regulated under P_i-starvation				
PSE_4759	*Oligoendopeptidase F homolog			C	–2.6
	Transport and secretion				
	Up-regulated under P_i-starvation				
PSE_1679	Spermidine/putrescine-binding periplasmic protein 2		√	P	12.5
PSE_1681	Spermidine/putrescine import ATP-binding protein PotA			C	5.8
PSE_1688	phosphate ABC transporter, periplasmic binding protein PstS		√	P	20.9
PSE_1690	Phosphate transport system permease protein PstA	6		IM	4.5
PSE_1691	Phosphate import ATP-binding protein PstB 1			C	8.5
PSE_2390	Periplasmic oligopeptide-binding protein precursor		√	P	2.6
PSE_3273	Trk system potassium uptake protein TrkA			C	2.0
PSE_3629	ABC transporter, phosphonate, periplasmic substrate-binding protein PhnD	1	√	OM, P, C	10.5
PSE_3630	Phosphonates import ATP-binding protein PhnC			C	66.7
PSE_3720	Type I secretion outer membrane protein, TolC		√	OM	3.7
PSEp_0394	TRAP dicarboxylate transporter, DctM subunit	11	√	IM	3.7
PSE_0472	sn-glycerol-3-phosphate-binding periplasmic protein UgpB		√	P	12.5
PSE_0680	sn-glycerol-3-phosphate-binding periplasmic protein UgpB		√	P	11.2
PSE_0683	sn-glycerol-3-phosphate import ATP-binding protein UgpC			C	4.6
PSE_1692	*Phosphate transport system protein PhoU			C	on[g)]
PSE_4562	*Maltose/maltodextrin import ATP-binding protein MalK			C	7.4
PSE_4505	*extracellular solute-binding protein family 1		√	P	5.0

Table S 5.1. Continued

Genome locus	Predicted function of the expressed protein	P t d	P s p	P l	R r
	Down-regulated under P_i-starvation				
PSE_3436	*NADH dehydrogenase subunit D			C	–2.4
	Fatty acid and lipid metabolism				
	Up-regulated under P_i-starvation				
PSE_2249	Phosphatidic acid phosphatase type 2/haloperoxidase		√	P	4.0
PSE_3595	enoyl-CoA hydratase/isomerase family protein			C	4.5
PSE_0671	*3-oxoacyl-[acyl-carrier-protein] reductase		√	C	2.5
PSE_0406	*enoyl-CoA hydratase/isomerase			C	2.3
	Cell wall and membrane biogenesis				
	Up-regulated under P_i-starvation				
PSE_2526	Phosphomannomutase/phosphoglucomutase			C	2.3
PSE_4236	3-deoxy-manno-octulosonate cytidylyltransferase			C	2.1
PSE_4595	SPFH domain / Band 7 family	2	√	C	2.5
PSE_4678	translocation protein TolB		√	OM	2.3
PSE_3207	UTP--glucose-1-phosphate uridylyltransferase			C	2.5
PSE_3471	penicillin-binding protein, 1A family	1	√	OM	2.0
PSEp_0373	*sulfolipid (UDP-sulfoquinovose) biosynthesis protein			C	22.2
	Down-regulated under P_i-starvation				
PSE_0029	*ErfK/YbiS/YcfS/YnhG family protein			C, P	–2.0
	Translation, transcription and DNA metabolism				
	Up-regulated under P_i-starvation				
PSE_0121	*exodeoxyribonuclease III			C	2.5
PSE_5032	*exodeoxyribonuclease V			C	3.2
PSE_0690	Sigma 54 modulation protein/ribosomal protein S30EA			C	7.6
	Down-regulated under P_i-starvation				
PSE_1499	Isoleucyl-tRNA synthetase	1		C	–2.3
PSE_2716	Ribosomal protein S18			C	–3.0
PSE_2717	Ribosomal protein S6			C	–3.4
PSE_3484	Valyl-tRNA synthetase			C	–2.5
PSE_3854	Ribosomal protein L17			C	–2.2
PSE_3861	Ribosomal protein L30			C	–2.0
PSE_3879	Ribosomal protein L3			C	–2.0
PSE_0409	chromosomal replication initiation protein			C	–3.6
PSE_4740	Ribosomal protein S21	1		C, P	–3.3
PSE_4772	*Ribosomal protein L36			C	–2.6
	Regulation of transcription				
	Up-regulated under P_i-starvation				
PSE_3570	Integration host factor, alpha subunit			C	2.3
PSEp_0002	transcriptional regulator, GntR family protein			C	2.7
PSE_4034	transcriptional regulator, AsnC family protein			C	2.3
PSE_4192	PspA/IM30			C	3.3
PSE_4593	*phage shock protein A, PspA			C	2.1
PSE_4825	Bacterial regulatory protein, MarR			C	on[g)]
PSE_4927	transcriptional regulator, LysR family protein			C	2.1

Table S 5.1. Continued

Genome locus	Predicted function of the expressed protein	P t d	P s p	P l	R r
PSE_0640	two component transcriptional regulator, winged helix family			C	2.2
PSE_2475	*transcriptional regulatory protein PhoP			C	11.1
PSE_1479	*transcriptional regulator, Crp/Fnr family			OM, C	2.2
PSE_0668	*Integration host factor, beta subunit			C	2.0
	Stress response, detoxification and iron metabolism				
	Up-regulated under P_i-starvation				
PSE_1030	Bacterioferritin			C	4.3
PSE_0181	Alkylhydroperoxidase AhpD			C	2.3
PSE_3844	Bacterioferritin			C	4.3
PSE_0381	Glutathione synthetase			C	2.6
	Down-regulated under P_i-starvation				
PSE_1253	Major ferric iron-binding protein			P	–4.6
	Cofactor and vitamin synthesis				
	Up-regulated under P_i-starvation				
PSE_2654	*Glutamine-dependent NAD(+) synthetase			C	2.1
PSE_1410	*3-methyl-2-oxobutanoate hydroxymethyltransferase			C	2.7
	Down-regulated under P_i-starvation				
PSE_0268	*ATP--cobalamin adenosyltransferase			C	–4.4
	Chemotaxis and motility				
	Secondary metabolite production				
	General functional prediction				
	Up-regulated under P_i-starvation				
PSE_0240	*acetyltransferase, GNAT family protein			C	2.6
PSE_1424	GCN5-related N-acetyltransferase			C	12.5
PSE_4878	oxidoreductase domain protein			C	2.1
PSE_0750	*oxidoreductase domain protein			C	5.4
PSE_2236	*amidase family protein			C	on[g)]
PSE_4282	*Xylose isomerase domain protein			C	33.3
PSE_3801	*Histidine triad (HIT) protein			C	2.5
	Down-regulated under P_i-starvation				
PSE_1234	sulfite reductase (NADPH) protein			C	–2.1
PSE_2004	Ferredoxin--NADP reductase			C	–2.5
PSE_2260	*thioesterase superfamily protein			P,C	–2.9
	Unknown function				
	Up-regulated under P_i-starvation				
PSE_2258	conserved hypothetical protein		√	P, C	9.8
PSE_1012	protein containing DUF839, bacterial	1		EC	2.2
PSE_1344	hypothetical protein			C, OM	2.6
PSE_0373	conserved hypothetical protein			C	10.8

Table S 5.1. Continued

Genome locus	Predicted function of the expressed protein	P t d	P s p	P l	R r
PSE_4656	uncharacterised conserved protein		√	OM, EC, IM	4.8
PSE_4666	conserved hypothetical protein	1		P	2.3
PSE_4780	hypothetical protein		√	P	3.2
PSE_4949	protein containing DUF533			P	2.8
PSE_3679	hypothetical protein		√	C	2.0
PSE_3716	*hypothetical protein			EC	2.5

[a)] Localization of the gene encoding the respective protein on the chromosome of *Pseudovibrio* sp. FO-BEG1. A small letter 'p' indicates that the gene is localized on the plasmid.

[b)] Predicted function of the protein according with the annotation of the genome of strain FO-BEG1, available at DDBJ/EMBL/GenBank under the accession number CP003147 for the chromosome and CP003148 for the plasmid

[c)] Number of predicted transmembrane domains according with TMHMM (Krogh *et al.*, 2001)

[d)] Presence of predicted signal peptides according with SignalP (Bendtsen *et al.*, 2004)

[e)] Predicted localization of the protein according with the subCELlular LOcalization predictor (CELLO; (Yu *et al.*, 2006). C = cytoplasmic localization; IM = localization in the inner membrane; P = periplasmic localization; OM = localization in the outer membrane; EC = extracellular localization. Prediction of more than one location for the protein indicates that the prediction is uncertain but most likely in one of the suggested cellular locations

[f)] Regulation ratios of the proteins

[g)] Proteins that were found only in one condition (e.g. only in the ($-P_i$ T_1 but not in +P) cannot be quantified due to missing reference peak intensities and are therefore regarded as turned on or off, respectively

*Proteins quantified only in one replicate

Table S 5.2. Overview of regulated proteins in the late growth phase under phosphate starvation (P_i-limited early growth phase ($-P_i$ T_1) compared with P_i-limited late growth phase ($-P_i$ T_2) conditions). Prediction of transmembrane domains (P t d), signal peptides (P s p), protein localization (P l) and the regulation ratio (R r) are indicated in the respective column. Absence of transmembrane domains or signal peptide in the protein is indicated by an empty cell in the respective column.

Genome locus[a)]	Predicted function of the expressed protein[b)]	P t d[c)]	P s p[d)]	P l[e)]	R r[f)]
	Carbon metabolism				
	Up-regulated in late growth phase of P_i-starvation				
PSE_1257	Phasin			P, C	2.1
PSE_1033	*Methylglyoxal synthase			C	2.2
	Down-regulated in late growth phase of P_i-starvation				
PSE_1872	sugar kinase			P, C	–2.1
PSE_2113	sugar kinase			C	–2.4
PSE_3254	Formate acetyltransferase			C	–3.9
PSE_3295	Pyruvate dehydrogenase E1 component subunit beta			C	–2.2
PSE_3346	glucosamine--fructose-6-phosphate aminotransferase			C	–2.0
PSE_4148	Glucose-6-phosphate isomerase			C	–5.3
PSE_4866	Pyruvate carboxylase			C	–2.7
PSE_0617	2-oxoglutarate dehydrogenase			C	–2.6
	Phosphorus metabolism				
	Up-regulated in late growth phase of P_i-starvation				
PSE_0624	Phospholipase D/Transphosphatidylase			C	2.5
	Amino acid and nucleotide metabolism				
	Down-regulated in late growth phase of P_i-starvation				
PSE_1046	*Adenosine deaminase			C	off[g)]
PSE_1587	AMP nucleosidase			C	–2.2
PSE_2796	D-hydantoinase			C, P	–2.1
PSE_3381	CTP synthetase		√	C	–2.4
PSE_4203	Acetolactate synthase large subunit			C	–2.6
PSE_4214	Ketol-acid reductoisomerase			C	–3.2
PSEp_0397	D-amino acid dehydrogenase small subunit	1	√	P	–2.4
PSE_4753	Adenylosuccinate lyase			C	–2.4
PSE_4789	glutamate synthase [NADPH] large chain			C	–3.1
PSE_0526	chorismate mutase/prephenate dehydratase			C	–2.3
PSE_0557	1-(5-phosphoribosyl)-5-[(5-phosphoribosylamino)methylideneamino] imidazole-4-carboxamide isomerase			C	–2.0
PSE_2517	acetylornithine deacetylase			C	–2.0
PSE_0548	*NAD-specific glutamate dehydrogenase			C	–4.2
	Protein and peptide metabolism				
	Down-regulated in late growth phase of P_i-starvation				
PSE_3446	ATP-dependent protease La			C	–2.5
PSE_3447	ATP-dependent Clp protease ATP-binding subunit clpX			C	–2.0
PSE_3524	Peptidyl-dipeptidase dcp (Dipeptidyl carboxypeptidase)			C	–2.5
PSE_0466	Peptidase M75, Imelysin		√	C, EC	off[g)]

Table S 5.2. Continued

Genome locus	Predicted function of the expressed protein	P t d	P s p	P l	R r
PSE_1491	*10 kDa chaperonin/GroES protein			C	–2.3
PSE_4759	*Oligoendopeptidase F homolog			C	–2.0
	Transport and secretion				
	Up-regulated in late growth phase of P_i-starvation				
PSE_1921	TRAP dicarboxylate transporter, DctP subunit		√	P	2.9
PSEp_0371	*TRAP dicarboxylate transporter, DctP subunit		√	C	2.6
	Down-regulated in late growth phase of P_i-starvation				
PSE_1596	F0F1 ATP synthase subunit B'			C	–2.6
PSE_1988	*Oligopeptide transport ATP-binding protein OppD			C	–2.7
PSE_3273	Trk system potassium uptake protein TrkA			C	–2.7
PSE_3434	*NADH-quinone oxidoreductase subunit F			C	–8.7
PSE_5013	Na(+)-translocating NADH-quinone reductase subunit A			C	–2.3
PSE_0696	NADH dehydrogenase (ubiquinone)			IM	–2.0
PSE_1620	*Electron-transferring-flavoprotein dehydrogenase			P	off[g)]
PSE_3436	*NADH dehydrogenase subunit D			C	off[g)]
	Fatty acid and lipid metabolism				
	Up-regulated in late growth phase of P_i-starvation				
PSE_2249	Phosphatidic acid phosphatase type 2/haloperoxidase		√	P	4.1
	Down-regulated in late growth phase of P_i-starvation				
PSE_2718	acyl-carrier-protein S-malonyltransferase			C	–2.3
PSE_3479	Acetyl-CoA carboxylase/biotin carboxylase			C	–2.5
PSE_0322	3-hydroxydecanoyl-ACP dehydratase			C	–2.4
PSE_3571	3-hydroxydecanoyl-[acyl-carrier-protein] dehydratase			C	–6.1
	Cell wall and membrane biogenesis				
	Translation, transcription and DNA metabolism				
	Down-regulated in late growth phase of P_i-starvation				
PSE_0987	*GTP-binding protein LepA			C	off[g)]
PSE_0077	Ribosomal protein L28			C	–2.4
PSE_2716	Ribosomal protein S18			C	–2.9
PSE_2717	Ribosomal protein S6			C	–2.0
PSE_0293	Leucyl-tRNA synthetase			C	–2.6
PSE_3854	Ribosomal protein L17			C	–2.2
PSE_3856	Ribosomal protein S11			C	–2.2
PSE_3860	Ribosomal protein L15			C	–2.0
PSE_3861	Ribosomal protein L30			C	–4.4
PSE_3862	Ribosomal protein S5			C	–2.1
PSE_3866	Ribosomal protein S14			C, P	–2.1
PSE_3868	Ribosomal protein L24			C, P	–2.7
PSE_3870	Ribosomal protein S17			C	–2.3
PSE_3873	Ribosomal protein S3			C	–2.8
PSE_3875	Ribosomal protein S19			C	–2.1
PSE_3965	Threonyl-tRNA synthetase			C	–2.4
PSE_4255	NAD-dependent DNA ligase			C	–2.2
PSE_4740	Ribosomal protein S21			C, P	–2.0
PSE_0734	Ribosomal protein L27			C	–2.4

Table S 5.2. Continued

Genome locus	Predicted function of the expressed protein	P t d	P s p	P l	R r
PSE_0735	Ribosomal protein L21			C	–2.0
PSE_3411	Ribosomal protein S2			C	–2.0
PSE_3878	Ribosomal protein L4			C	–2.0
PSE_4070	recombinase A			C	–2.0
	Regulation of transcription				
	Down-regulated in late growth phase of P_i-starvation				
PSE_3592	transcriptional regulator protein, MarR family			C	–3.5
PSE_4927	transcriptional regulator, LysR family protein			C	–2.1
PSE_5047	*transcriptional regulator FixK			C	–5.1
PSE_1221	*transcriptional regulator, AraC family			C	–2.7
	Stress response, detoxification and iron metabolism				
	Up-regulated in late growth phase of P_i-starvation				
PSE_1253	Major ferric iron-binding protein		√	P	6.0
PSE_4301	5-oxoprolinase (ATP-hydrolyzing)			C	2.2
PSE_0151	*Hydroxyacylglutathione hydrolase			C	2.1
	Down-regulated in late growth phase of P_i-starvation				
PSEp_0013	*S-formylglutathione hydrolase			C	–2.5
	Cofactor and vitamin synthesis				
	Down-regulated in late growth phase of P_i-starvation				
PSE_4008	*Octaprenyl-diphosphate synthase			C	off[g)]
PSE_0312	*Uroporphyrinogen decarboxylase			C	–2.7
	Chemotaxis and motility				
	Down-regulated in late growth phase of P_i-starvation				
PSE_2607	*flagellar basal body P-ring protein	1	√	OM	–3.6
	Secondary metabolite production				
	Down-regulated in late growth phase of P_i-starvation				
PSEp_0217	Type III polyketide synthase			C	–3.0
	General functional prediction				
	Up-regulated in late growth phase of P_i-starvation				
PSE_3204	bifunctional sulfate adenylyltransferase subunit 1/adenylylsulfate kinase protein			C	3.0
PSE_2260	*thioesterase superfamily protein			P, C	9.3
PSE_2246	*dihydroflavonol 4-reductase/dihydrokaempferol 4-reductase			P, C	2.5
	Down-regulated in late growth phase of P_i-starvation				
PSE_2004	*Ferredoxin--NADP reductase			C	–3.6
	Unknown function				
	Up-regulated in late growth phase of P_i-starvation				
PSE_3679	hypothetical protein		√	C	4.3
PSE_3716	*hypothetical protein			EC	2.7

Table S 5.2. Continued

Genome locus	Predicted function of the expressed protein	P t d	P s p	P l	R r
	Down-regulated in late growth phase of P_i-starvation				
PSE_1746	conserved hypothetical protein			C	–3.4
PSEp_0141	conserved hypothetical protein			C	–2.6
PSE_4656	*uncharacterised conserved protein		√	OM, EC, IM	–3.2
PSE_0949	Hypothetical protein			C, P	–6.8

[a)] Localization of the gene encoding the respective protein on the chromosome of *Pseudovibrio* sp. FO-BEG1. A small letter 'p' indicates that the gene is localized on the plasmid.

[b)] Predicted function of the protein according with the annotation of the genome of strain FO-BEG1, available at DDBJ/EMBL/GenBank under the accession number CP003147 for the chromosome and CP003148 for the plasmid

[c)] Number of predicted transmembrane domains according with TMHMM (Krogh *et al.*, 2001)

[d)] Presence of predicted signal peptides according with SignalP (Bendtsen *et al.*, 2004)

[e)] Predicted localization of the protein according with the subCELlular LOcalization predictor (CELLO; (Yu *et al.*, 2006). C = cytoplasmic localization; IM = localization in the inner membrane; P = periplasmic localization; OM = localization in the outer membrane; EC = extracellular localization. Prediction of more than one location for the protein indicates that the prediction is uncertain but most likely in one of the suggested cellular locations

[f)] Regulation ratios of the proteins

[g)] Proteins that were found only in one condition (e.g. only in the ($-P_i$ T_1 but not in $-P_i$ T_2) cannot be quantified due to missing reference peak intensities and are therefore regarded as turned on or off, respectively

*Proteins quantified only in one replicate

Chapter VI

General conclusions

"Bacteria may be tentatively regarded as biochemical experimenters; owing to their small size and rapid growth, variations must arise very much more frequently than in more differentiated forms of life, and they can in addition afford to occupy more precarious positions in the natural economy than larger organisms with more exacting requirements."

Marjory Stephenson

New aspects of the physiology of *Pseudovibrio* spp.-related strains

The major topic of this work is the physiology of *Pseudovibrio* sp. FO-BEG1. In **Chapter II** and **III**, newly identified metabolic abilities of strain FO-BEG1 based on genomic predictions were described and most of the traits were verified in experimental approaches. The physiological features include the ability to degrade aromatic compounds, the usage of thiosulfate as an alternative electron donor, the utilization of phosphonates as a phosphorus source and the ability to grow under extremely oligotrophic conditions. Especially oligotrophic growth is a surprising ability of *Pseudovibrio* sp. FO-BEG1 since the original isolation location and the isolation strategy are not typical for described oligotrophs. The isolation and identification of oligotrophic bacteria is, in general, focused on nutrient depleted environments and direct isolation using media with ambient concentrations of nutrients (e.g. Schut *et al.*, 1997; Cavicchioli *et al.*, 2003; Giovannoni and Stingl, 2007).

One of the most prominent examples of a prokaryote adapted to ambient concentrations of nutrients in the oceans is the obligate oligotrophic bacterium *Candidatus* Pelagibacter ubique (Rappé *et al.*, 2002). It is a ubiquitous, dominant heterotrophic bacterium in the open oceans belonging to the SAR11 clade, which represents 25 to 50% of the total prokaryotic community in the ocean surface layers (Giovannoni and Stingl, 2007). The average volume of the vibrioid-shaped *Ca.* Pelagibacter ubique cells is about 0.01 μm^3 (Rappé *et al.*, 2002) and the genome consists of 1.3 Mbp (Giovannoni *et al.*, 2005), making it one of the smallest prokaryotes with the smallest genome of all heterotrophs. It has been isolated on sterile coastal water medium, which best represents the environmental nutrient conditions of the organism. It can grow up to cell numbers of 2.5×10^5 cells per milliliter with the addition of 1 µmol l^{-1} of ammonium and 0.1 µmol l^{-1} of phosphate (Rappé *et al.*, 2002). The dissolved organic carbon (DOC) concentrations of the seawater media applied for this approach was ranging between 91.6 and 107.1 µmol l^{-1} (Connon and Giovannoni, 2002). Addition of different carbon sources did not increase the growth of this bacterium and the natural seawater medium remained the only one *Ca.* Pelagibacter ubique was capable of growing in, rendering it an obligate oligotroph (Giovannoni and Stingl, 2007). Another model organism for studying oligotrophic bacteria is *Sphingopyxis alaskensis*, isolated from the Resurrection Bay in Alaska. This bacterium features small, rod-shaped cells with a volume of about 0.05 μm^3 (Cavicchioli *et al.*, 2003 and references therein) and possesses a genome of approximately 3.2 Mbp (Eguchi *et al.*, 2001). However, due to its ability to grow with carbon

concentrations of 0.8 to 800 mg C l^{-1} (0.07 to 66.7 mmol C l^{-1}) (Eguchi *et al.*, 1996) it belongs to the facultative oligotrophs, which are bacteria capable of growing under nutrient deprivation as well as high concentrations of nutrients.

In **Chapter III**, it was demonstrated that both *Pseudovibrio* sp. strain FO-BEG1 and *P. denitrificans*^{T} can grow oligotrophically. However, both strains were isolated from coastal areas, being nutrient rich, compared to the oligotrophic open ocean areas. *Pseudovibrio* sp. FO-BEG1 cells have an average volume of 1.33 (± 0.43) µm^3 (**Chapter V**) and *P. denitrificans*^{T} cells are similar in size, featuring 1.25 µm^3 (Shieh *et al.*, 2004). In this respect both strains do not resemble the extremely small bacteria *Ca.* Pelagibacter ubique and *S. alaskensis*. Additionally, the genome size of almost 6 Mbp of strain FO-BEG1 is above the average genome size of 3.5 to 4.5 Mbp found in other marine bacteria (Moran and Armbrust, 2007; Newton *et al.*, 2010). Despite the fact that both strains do not resemble typical oligotrophs in respect to cell size, isolation location and genome size, both isolates are capable of growing under nutrient limitation, with DOC values among the lowest ever measured for laboratory growth media and at two- to five-fold lower values compared to oligotrophic seawater (Connon and Giovannoni, 2002; Schwedt, 2011). This suggests that bacteria belonging to the genus *Pseudovibrio*, despite their typical eutrophic characteristics, obviously encounter times of nutrient limitation in their environment, leading to the observed adaptations to the oligotrophic conditions.

A comparison of the genome size of *Pseudovibrio* sp. FO-BEG1 and the number of encoded ATP-binding cassette (ABC) transporters (**Figure 6.1**) shows that the number of ABC systems per genome size lies slightly above the average compared to other bacteria with sequenced genomes (Harland *et al.*, 2005). However, the absolute amount of 115 predicted ABC transporters places strain FO-BEG1 among the six bacteria with the highest amount of predicted ABC systems (Harland et al., 2005; please note that for this comparison the ABC transporters were predicted in another way than presented in **Chapter II**, see **Figure 6.1**). Furthermore, the amount of 31 encoded TRAP transporters (**Chapter II**), which are mainly used for dicarboxylic acids import, is one of the highest reported so far (Mulligan *et al.*, 2007; Wagner-Döbler *et al.*, 2010). In comparison with the "typical" oligotrophs *Ca.* Pelagibacter ubique and *S. alaskensis*, which posses 12/2 and 7/0 ABC/TRAP transporters (Williams *et al.*, 2009), the number of 115/31 ABC/TRAP transporters for *Pseudovibrio* sp. FO-BEG1 is astonishingly high suggesting that one of the mechanisms *Pseudovibrio* spp. might use to

cope with nutrient deficiency is the ability to import and utilize a large variety of different substrates, therewith possibly substituting for the relatively large cell size. Also, the enormous physiological variability of strain FO-BEG1, as demonstrated in growth experiments (**Chapter II**), supports this hypothesis. Adaptation to oligotrophic environments can be a strict specialization with an extremely small cell size, inability to move and a restricted substrate spectrum for specific, easily available and degradable nutrients, as exemplified by *Ca.* Pelagibacter ubique. In contrast, *Pseudovibrio* sp. with relatively large, flagellated cells, an immense amount of transporters and a large substrate spectrum can access and degrade a higher variety of complex nutrient-containing molecules. This generalistic life style, which requires a large genome size, seems to be an alternative strategy for growth in low-nutrient environments.

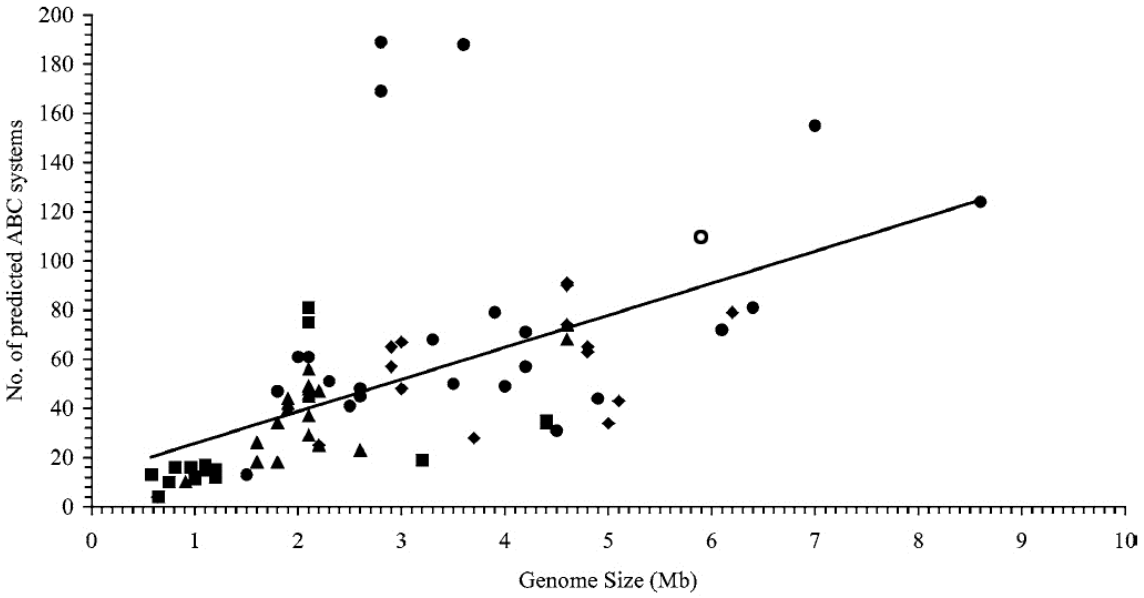

Figure 6.1. Comparison of the predicted ABC systems and the genome size of sequenced bacteria. Squares represent intracellular symbionts; triangles represent extracellular symbionts; diamonds show bacteria with no obvious predominant environment; closed circles show environmental bacteria; the open circle represents *Pseudovibrio* sp. FO-BEG1. Prediction of ABC systems for this graph was performed by summarizing all Pfam (Protein family) domains with a signature for ABC transporters (accession number PF00005). If two domains were in close proximity (distance of 5 genes), one domain was excluded from the analysis, because of the high probability that they were encoding for the same transporter, as described in the publication by Harland *et al.* (2005). In contrast to this approach, the prediction of ABC transporters in **Chapter II** was based only on those types that are required for import of molecules and only if an ABC transporter could be reconstructed completely with all required subunits. Therefore, the number of predicted transporters given in **Chapter II** is lower. Graph modified after Harland *et al.* (2005).

Bacteria adapted to the utilization of many different nutrients have been termed generalists or opportunitrophs (e.g. Moran *et al.*, 2004). This term is often used for the *Roseobacter* clade, a major marine group of ubiquitous and abundant bacteria found in diverse habitats like coastal and open seawaters or associated with particles, marine vertebrates and invertebrates (Buchan *et al.*, 2005 and references therein). Prokaryotes belonging to this clade make up 15 to 20% of the coastal and oceanic bacterioplankton communities and have a versatile metabolism including aerobic anoxygenic photosynthesis, carbon monoxide oxidation, oxidation of inorganic sulfur compounds, as well as degradation of phosphonates, aromatic compounds and dimethylsulfoniopropionate (DMSP) (Moran *et al.*, 2004; Buchan *et al.*, 2005; Newton *et al.*, 2010). The *Roseobacter* clade, together with the genus *Pseudovibrio*, belongs to the family *Rhodobacteraceae*, indicating a close phylogenetic relationship between the two groups. This relationship is likewise represented by a comparable physiology, except for photosynthesis and degradation of DMSP, with the latter not yet tested for the genus *Pseudovibrio*. Both *Roseobacter* and *Pseudovibrio* share the ability to colonize diverse habitats, including symbiotic associations with marine eukaryotes, which are represented in the case of the *Roseobacter* clade mainly by algae (Buchan *et al.*, 2005). Additionally, bacteria from the genus *Marinobacter*, which belongs to the *γ-Proteobacteria*, seem to have similar opportunitrophic properties, as they show a cosmopolitan geographic distribution, can be isolated from very different habitats and are physiologically versatile (Singer *et al.*, 2011).

Characteristics of the *Pseudovibrio* genus identified previously (e.g. Shieh *et al.*, 2004; Enticknap *et al.*, 2006; Sertan-de Guzman *et al.*, 2007) and in the course of this thesis show that these bacteria can be referred to as generalistic bacteria. In accordance with the definition of this group of bacteria, *Pseudovibrio* spp. feature a life style that includes the colonization of diverse habitats and the expression of a versatile metabolism, allowing the bacteria to utilize different substrates and to survive various conditions including anoxia (undergoing fermentation or denitrification) and extreme oligotrophy. Opportunitrophs, however, are regarded as unspecialized bacteria that are mainly adapted to high concentrations of different nutrients, separating them from the oligotrophs, which are specifically adapted to low-nutrient environments (Polz *et al.*, 2006; Azam and Malfatti, 2007; Jiao and Zheng, 2011; Kujawinski, 2011). In the work of Anne Schwedt (2011) as well as in the present thesis we have shown that generalistic bacteria like *Pseudovibrio* and *Marinobacter* species are also capable of multiplying under extreme nutrient limitation. These results imply that a circumscription of

the term opportunitroph to environments with rather high concentrations of nutrients is debatable and that generalistic bacteria should also be regarded as qualified to adapt and multiply in nutrient depleted environments.

Pseudovibrio sp. FO-BEG1: a facultative symbiont of marine invertebrates

In over 50% of all published studies, in which *Pseudovibrio* spp.-related bacteria were identified, they were found associated with sponges (e.g. Hentschel *et al.*, 2001; Webster and Hill, 2001; Enticknap *et al.*, 2006; O'Halloran *et al.*, 2011), indicating a symbiotic connection between Porifera and the genus *Pseudovibrio*. Oftentimes, up to 40% of the sponge mass is comprised of bacteria, which were found to be important and required for sponges (Hentschel *et al.*, 2006; Taylor *et al.*, 2007). However, the mechanisms underlying this symbiotic relationship are not yet well understood (Taylor *et al.*, 2007).

In general, symbionts can be divided into primary or obligate and secondary or facultative symbionts. Obligate symbioses typically form over geological time scales, leading to pronounced coevolutionary adaptations of the prokaryote and the host. Such adaptations include for example a high specialization of the symbiont involving extreme reduction of the genome size down to one Mbp, a decreased G+C content lying only between 16.5 and 33%, and the inability of the symbionts to survive in a free-living stage due to mutations and the reduction of the gene repertoire needed for an autonomous metabolism and synthesis of required molecules (Dale and Moran, 2006; Moran *et al.*, 2008). Owing to the complete dependence on the host and the inability to survive in other environments, obligate symbionts are usually transmitted vertically within the host. In these relationships, it is not surprising that also the host may have developed a strong dependency on certain functions exhibited by the symbiont. These functions include for example a protection mechanism mediated by the synthesis of bioactive compounds or the supply with certain cofactors and nutrients (Dale and Moran, 2006; Moran, 2006). On the other hand, secondary or facultative symbionts, represent interactions between pro- and eukaryotes that started rather recently and show, if at all, a small degree of adaptation of both partners. Such symbioses can be either beneficial or harmful for the host. Also, the symbionts can be transmitted either vertically via the maternal line, or horizontally, whereby it needs to newly infect the host in each generation (Dale and Moran, 2006; Bright and Bulgheresi, 2010). Facultative symbionts are usually not required for host survival and the host-symbiont adaptations are either very small or not existent at all. The effect of these prokaryotes on the host can be diverse, including parasitism or

pathogenesis but may also be beneficial e.g. by protecting the animal against stress and parasites, leading to an increase of the host reproduction rate (Dale and Moran, 2006).

On the basis of the genomic and physiological data shown in **Chapter II**, we proposed that *Pseudovibrio* sp. FO-BEG1 is a facultative symbiont of sponges and other marine invertebrates. With a genome size of almost 6 Mbp and a G+C content of about 50%, no signs of genome reduction or dependency on factors that could not be synthesized by the bacterium itself are detectable. Also, the autonomous growth of this strain on defined media is confirmed by physiological experiments (**Chapter II**). The large genome size and metabolic versatility is indicative for the dual life styles exhibited by *Pseudovibrio* spp.-related species: the genetic repertoire must contain functional genes for prokaryote-eukaryote interactions as well as physiological pathways to successfully compete with marine bacteria outside of the host. It seems that the evolutionary pressure experienced by *Pseudovibrio* at this stage of symbiosis rather leads to a large genome, which can maintain the ability to adapt to different conditions and habitats.

Obligate symbionts typically lack mobile genetic elements (Moran *et al.*, 2008), whereas in the genome of *Pseudovibrio* sp. FO-BEG1, an operon encoding for a gene transfer agent (GTA) as well as several transposase and integrase elements can be detected (**Chapter II**), suggesting that horizontal gene transfer occurs in this strain. It is therefore likely that the genus *Pseudovibrio* represents evolutionary young symbionts of sponges, not yet specifically adapted to the symbiotic host, as already suggested by Enticknap *et al.* (2006) and Muscholl-Silberhorn *et al.* (2007). Enticknap *et al.* (2006) proposed that *Pseudovibrio* spp.-related bacteria can be vertically transmitted within the sponges, however, these bacteria are also found free-living in seawater (Shieh *et al.*, 2004; Agogué *et al.*, 2005; Hosoya and Yokota, 2007). According to the genomic and physiological analyses performed here it can be proposed that *Pseudovibrio* spp.-related bacteria are able to thrive under a variety of different conditions including also symbiotic life strategies. It can be hypothesized that the free-living bacteria were not simply released from a dying sponge but that they could indeed grow autonomously in both nutrient-rich and nutrient-depleted seawater. This possible facultative symbiosis of *Pseudovibrio* spp.-related bacteria and sponges implicates that horizontal transfer, a process of host invasion, is a characteristic expressed by the bacteria. This hypothetical feature of *Pseudovibrio* spp.-related bacteria has never been tested so far, but could be a highly promising subject of study for the investigation of the *de novo* colonization

of sponges, using *Pseudovibrio* sp. as a model organism. Thus, mechanisms of host invasion by sponge-associated bacteria could eventually be studied.

Facultative symbionts have been proposed to apply molecular tools used by pathogenic bacteria for invasion of the host and avoiding its immune system (Dale and Moran, 2006; Moran *et al.*, 2008). The first report of a type III secretion system (T3SS) being involved in a mutualistic animal-bacterium symbiosis was shown by Dale *et al.* (2001) for the insect symbiont *Sodalis glossinidius*. More reports of T3SS in symbionts followed, including *Hamiltonella defensa*, another insect symbiont (Degnan *et al.*, 2009), rhizobia plant symbionts (Deakin and Broughton, 2009), and the endofungal bacterium *Burkholderia rhizoxinica* (Lackner *et al.*, 2011). Likewise, after the discovery of the type VI secretion system (T6SS) in the pathogens *Vibrio cholerae* (Pukatzki *et al.*, 2006) and *Pseudomonas aeruginosa* (Mougous *et al.*, 2006), the involvement of the T6SS in mutualistic symbioses have been proposed (Jani and Cotter, 2010 and references therein). The description of type III and type VI secretion systems in the genome of *Pseudovibrio* sp. FO-BEG1 in **Chapter II** shows for the first time potential mechanisms that could be applied by the bacterium to invade and persist in the respective hosts. The different systems could be required for different stages of the symbiosis. For instance, it has been demonstrated by Dale *et al.* (2005) that one of the two T3SS encoded in the genome of *S. glossinidius* is required for invasion of eukaryotic cells, while the other is expressed after the infection has been established.

Even though *Pseudovibrio* spp.-related bacteria are found mainly in sponges, they also have been identified in tunicates and corals, indicating that the same mechanisms could be applied for interactions with all three phylogenetic groups. In principle, the successful colonization by *Pseudovibrio* spp. depends on the avoidance or deactivation of the immune response of the host. Therefore, the innate immune response of sponges, tunicates and corals might be regarded as the common ground for the infection by *Pseudovibrio* spp.-related bacteria. In most animals, one of the major innate immune response recognition mechanisms of a bacterial invasion is the activity of proteins belonging to the Toll-like receptor (TLR) family, which recognize specific motifs of bacterial cell components (Takeda *et al.*, 2003). The subsequent cascade of phosphorylation reactions, among others, leads to the activation of mitogen-activated protein (MAP) kinases (Akira and Takeda, 2004). Eventually, transcription of genes involved in the immune response is activated (Wang and Liu, 2007), resulting e.g. in the production of anti-microbial peptides, the activation of phagocytic cells and the generation

of toxic oxygen and nitrogen metabolites (Loker *et al.*, 2004). In sponges, proteins belonging to the TLR family as well as MAP kinases were detected (Böhm *et al.*, 2001; Wiens *et al.*, 2005). In ascidians, a genome sequencing approach revealed Toll-like receptors (Dehal *et al.*, 2002), and a proteomic study revealed that a MAP kinase was up-regulated in a diseased species. Also, genetic data suggest that corals possess proteins with the Toll-like receptor (TLR) domain in combination with the Jun N-terminal kinase (JNK) and the p38 MAP kinase, which are key components of the JNK/MAP kinase pathway (Miller *et al.*, 2007). In summary, the three phyla of marine invertebrates that *Pseudovibrio* spp. have been found associated with possess innate immune response factors like Toll-like receptors that recognize bacterial invasion and induce a signaling cascade, demonstrating that common pathways of the innate immune response are present in Porifera, Cnidaria, and Tunicata. In **Chapter II**, the genomic analysis of the investigated *Pseudovibrio* strain FO-BEG1 indicated the presence of effector protein homologues of the type III secretion system, including YpkA. This effector can inhibit the function of MAP kinases, thereby disabling an important pathway of the immune response of the host (Mukherjee *et al.*, 2006). It is therefore conceivable that the molecular "weaponry" of *Pseudovibrio* is specific for certain steps in the innate immune response of the host. According to this specificity the host spectrum is possibly defined.

Phosphate starvation of *Pseudovibrio* sp. FO-BEG1 and implications for the environment

The secretion of organic compounds into the extracellular environment under phosphate starvation by *Pseudovibrio* sp. FO-BEG1 was first observed visually by a yellowish-orange color that intensifies with increasing incubation time and was confirmed on the molecular level via DOC and FT-ICR-MS analyses. The identity and role of the secreted substances are not resolved yet. However, the analyses performed so far allow first speculations on possible roles of the secreted metabolites.

The ICP-OES measurements show an increased uptake of iron in the first 40 hours in the P_i-limited culture compared to P_i-surplus conditions, but after 40 hours increasing amounts of soluble iron can be detected in the supernatant of the P_i-limited medium (**Chapter V, Figure 5.6**). The increase of iron occurs concomitantly with the appearance and intensification of the yellowish-orange color, indicating that one of the secreted molecules could contain iron. If this was the case, the amount of iron taken up by the cells in the early growth phase (0.102 mg l^{-1}) would be similar to the amount of iron released in older cultures

(0.104 mg l^{-1}; **Table 6.1**). The major part of the iron within bacterial cells (up to 94%) is associated with the complexes I to IV in the bacterial respiration chain (Tortell *et al.*, 1999) and thus is required for fundamental metabolic processes. In the case of P_i-limited FO-BEG1 cells, it can be assumed that the majority of the imported iron is stored because within the 40 hours the cells take up about three times more iron than the P_i-surplus cultures (0.102 mg l^{-1} versus 0.036 mg l^{-1}, respectively) after 40 hours in spite of the lower cell numbers.

Table 6.1. Differences in iron concentrations in P_i-surplus and P_i-limited cultures derived from ICP-OES measurements (**Chapter V, Figure 5.6**). Fe in sterile controls at T_0 represents the amount of iron initially added to the cultures. The mean of the iron measured in sterile cultures between T_1 and T_7 represents the soluble and therefore bioavailable amount of iron after the precipitation of iron under both conditions. Iron decrease in sterile controls demonstrates that much more iron precipitates under P_i-surplus conditions compared with P_i-limited conditions. The last column shows how much iron is taken up by *Pseudovibrio* sp. FO-BEG1 after 40 h of growth under P_i-surplus and P_i-starvation.

	Fe in sterile controls at T_0	**Mean Fe value in sterile controls from T_1 to T_7**	**Decrease of Fe in sterile controls**	***Pseudovibrio*-mediated uptake of Fe after 40 h**
P_i-surplus 1.2 mmol l^{-1} phosphate	0.374 mg l^{-1}/ 6.7 µmol l^{-1}	0.107 (±0.009) mg l^{-1}/ 1.92 (±0.16) µmol l^{-1}	0.267 mg l^{-1}/ 4.78 µmol l^{-1}	0.036 mg l^{-1}/ 0.64 µmol l^{-1}
P_i-limitation 0.1 mmol l^{-1} phosphate	0.414 mg l^{-1}/ 7.0 µmol l^{-1}	0.258 (±0.017) mg l^{-1}/ 4.62 (±0.3) µmol l^{-1}	0.156 mg l^{-1}/ 2.38 µmol l^{-1}	0.102 mg l^{-1}/ 1.83 µmol l^{-1}

Generally, the secretion of intracellular iron into the environment can be regarded as a rather uncommon reaction. Therefore, it is assumed that one of the secreted compounds acts as an organic ligand and solubilizes the oxidized Fe^{3+}, which is usually present as aggregated insoluble complexes in the aerobic medium (Wandersman and Delepelaire, 2004). This soluble fraction of iron could then become measurable via ICP-OES, resulting in increased iron values for the respective cultures. Siderophores are organic ligands with low molecular weight and a high affinity for Fe^{3+} that are produced by bacteria during iron starvation in order to solubilize and take up Fe^{3+} (Wandersman and Delepelaire, 2004; Vraspir and Butler, 2009). For instance, Barbeau *et al.* (2002) isolated and structurally identified petrobactin, a siderophore that is produced by the marine bacterium *Marinobacter hydrocarbonoclasticus*

and exhibits a comparable UV-Vis absorption spectrum to the compound secreted by *Pseudovibrio* sp. FO-BEG1 (**Figure 6.2**).

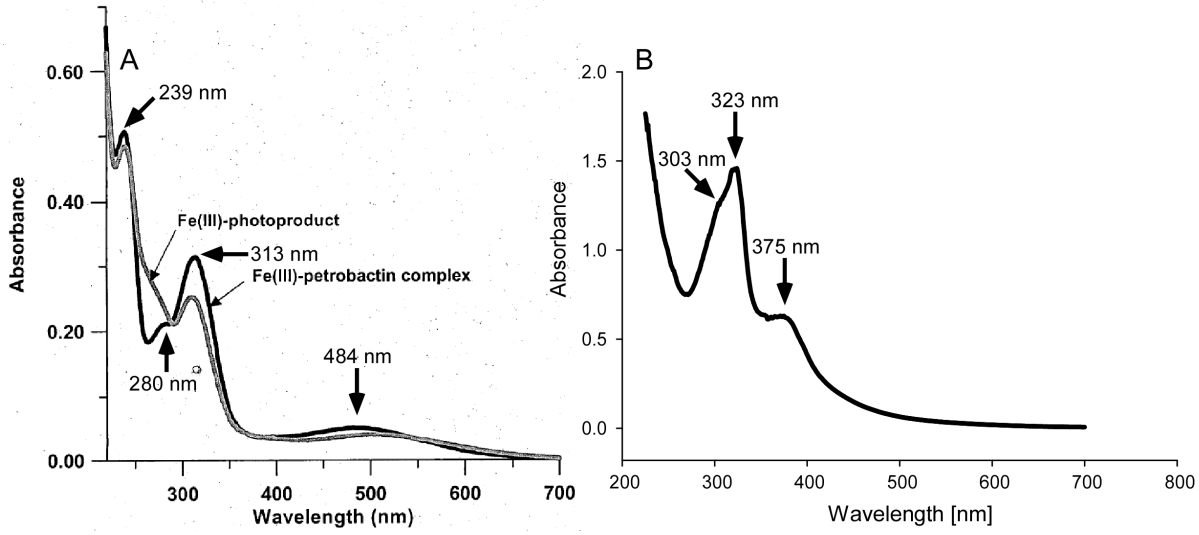

Figure 6.2. Comparison of UV/Vis absorption spectra between the siderophore petrobactin secreted by *Marinobacter hydrocarbonoclasticus* (black line represents the Fe(III)-petrobactin and the gray represents the product of photolysis) (**A**) and the supernatant of a P_i-starved *Pseudovibrio* sp. FO-BEG1 culture (**B**), presumably containing a siderophore. Image (**A**) taken from Barbeau *et al.* (2002).

The production and secretion of a siderophore for the solubilization and uptake of additional iron would also correlate with the increased expression of the iron storage compound bacterioferritin under P_i-starvation in *Pseudovibrio* sp. FO-BEG1, as shown in the proteomic analysis in **Chapter V**. Siderophores are usually secreted during iron starvation, and their synthesis can occasionally be controlled by other metals (Vraspir and Butler, 2009; Braun and Hantke, 2011; Schalk *et al.*, 2011). However, in the here investigated culture the release of the putative siderophore would occur under P_i-limited conditions, which is a phenomenon that, to our knowledge, was never described before. A possible explanation for this circumstance could be that the regulation of siderophore synthesis is not directly induced by phosphate starvation, but either cross-regulated by the PhoB-PhoR regulon or induced by a general stress response to nutrient limitation. Phosphate starvation is known to trigger the general stress response in other bacteria, for instance in *Bacillus* and *Vibrio* as well as in *E. coli* strains (Peterson *et al.*, 2005; Hoi *et al.*, 2006; von Krüger *et al.*, 2006; Lamarche *et al.*, 2008).

Intriguingly, siderophores can promote mutualistic associations between prokaryotes and eukaryotes. It has been proposed by Amin *et al.* (2009) that a *Marinobacter* strain supplies the dinoflagellate *Scrippsiella trochoidea* with iron by the secretion of a photo-labile siderophore that, upon photolysis, releases the solubilized iron, which is taken up by the dinoflagellate. In return, the dinoflagellate supposedly supplies the *Marinobacter* strain with carbon and energy sources by secreting dissolved organic matter (Amin *et al.*, 2009). Interestingly, *Pseudovibrio* spp. has recently been detected on the surface of red algae (Penesyan *et al.*, 2011). Therefore, a function similar to the *Marinobacter* siderophore is conceivable for the putative siderophore released under P_i-starvation by *Pseudovibrio* sp. FO-BEG1. Phototrophic bacteria or algae in the natural environment could rely on the provision of iron by bacteria like strain FO-BEG1, whereas they would supply organic compounds, possibly containing phosphorus. The secretion of e.g. nucleic acids, lipids and proteins by phytoplankton has been reported (Myklestad, 1995 and references therein).

Another possibility is the secretion of siderophores under P_i-limitation in order to promote iron solubilization from Fe-containing precipitates, thereby preventing adhesion of phosphate to the iron or release of phosphate from the precipitates. Iron solubilization from minerals promoted by bacterial siderophores has been demonstrated several times. For instance, the presence of siderophore releasing *Streptomyces* sp. and *Arthrobacter* sp., or just the addition of the purified siderophore desferrioxamine B to a medium containing hornblende, an iron containing mineral, resulted in an up to 20-fold acceleration of Fe release from the mineral (Kalinowski *et al.*, 2000). In another study, *Pseudomonas fluorescens* had significantly higher cell numbers in an iron deficient medium containing ore than in the same medium without the mineral, suggesting that the bacteria were able to extract minerals from the ore, which was proven by the detection of a siderophore-iron complex (Edberg *et al.*, 2010). The ICP-OES data in **Chapter V** show that the sterile controls of P_i-surplus and P_i-limited cultures contain on the average 1.92 (± 0.15) µmol l^{-1} and 4.62 (± 0.3) µmol l^{-1} of soluble iron, respectively, excluding the T_0 time point (**Table 6.1**, see **Chapter V Figure 5.6** for original data). Since the only difference of both media is the phosphate concentration, it can be suggested that iron forms precipitates with phosphates, thereby reducing the amount of soluble iron and phosphate in the medium. Dalton *et al.* (1983) showed that the major components of precipitates formed in a plant tissue culture medium due to unchelated iron was phosphate (51%) and iron (25%). Assuming that iron and phosphate precipitate with similar stoichiometry in the medium used for our experiments, 2.4 µmol l^{-1} of iron would

precipitate with approximately 4.7 µmol l^{-1} of phosphate. In natural environments, the ability to release iron from precipitates, which would liberate bioavailable phosphate, could be an important factor in the phosphate starvation response of *Pseudovibrio* sp. FO-BEG1.

Phosphate starvation can furthermore induce the production of bioactive compounds (Martín, 2004 and references therein), and several *Pseudovibrio* strains have been shown to produce such antimicrobial secondary metabolites (e.g. Sertan-de Guzman *et al.*, 2007; Penesyan *et al.*, 2011; Vizcaino, 2011). Therefore, another assumption about the functionality of the secreted compounds includes antimicrobial bioactive substances. This hypothesis is supported with the proteomic analysis, showing that under P_i-limited conditions a PmbA homologue was up-regulated, which is a chaperone-like molecule involved in the maturation and secretion of microcins. These are gene-encoded, small polypeptides (below 10 kDa) that are highly stabile with respect to heat, high and low pH values, the activity of proteases, and they are typically heavily modified after translation, and are known from enterobacteria where they express antimicrobial activity against closely related strains (Duquesne *et al.*, 2007). Interestingly, certain siderophores, so-called sideromycins, are known to be covalently linked to antibiotics (Braun *et al.*, 2009). Due to the active transport of the sideromycins into the cell, the minimal inhibitory concentration is around 100-fold lower than of those antimicrobial substances that enter the bacterial cells via diffusion (Braun *et al.*, 2009). During the posttranslational modification of some of the microcins, siderophore moieties are added (Miethke and Marahiel, 2007), resulting in a sideromycin-like microcin that acts as an Fe^{3+}-binding molecule with antibiotic activities. Assuming that those antibiotic-containing siderophores could indeed be produced and secreted by *Pseudovibrio* sp. FO-BEG1, it would allow the strain to effectively deploy the antibiotic substance into bacterial cells competing for the same nutrients in the environment. The antimicrobial activity could then lead to death of the competitor, releasing cell components that can be re-utilized by *Pseudovibrio* sp. FO-BEG1. However, experiments performed using the stationary phase supernatant of P_i-limited FO-BEG1 cultures so far did not show any growth inhibition on tested strains (**Chapter V**). It must be noted, however, that those experiments were performed under regular nutritional conditions with iron surplus. It is reasonable to assume that siderophore-linked antibiotics exhibit optimal activity when the targeted cells are iron limited and therefore implement and increase uptake of extracellular siderophores. Especially in natural environments, where iron bioavailability is in general limited for bacteria (Morel and Price, 2003; Vraspir and Butler, 2009), supplying the required nutrient along with an antimicrobial substance could be a

successful strategy to eliminate competitors or to access the released cellular components after cell lysis. Therefore, antimicrobial activity for the compounds secreted by *Pseudovibrio* sp. FO-BEG1 under P_i-limitation cannot be excluded yet.

The PhoR-PhoB regulon is involved in pathogenesis and expression of virulence factors in many bacterial species (Lamarche *et al.*, 2008). For instance, in *Vibrio cholerae* PhoB regulates the expression of an important virulence activator (Pratt *et al.*, 2010), and *phoB* mutants of *Vibrio cholerae* are less efficient than the wild type in colonization of rabbit intestine (von Krüger *et al.*, 1999), suggesting that the PhoB-PhoR regulon plays a role in the virulence of *V. cholerae*. Furthermore, phosphate limitation induces sporulation and endotoxin production in *Clostridium perfringens (*Philippe *et al.,* 2006*)*. In *E. coli*, a protein with a RTX (repeats in toxins) domain, known e.g. from hemolysins and leukotoxins (Lally *et al.*, 1999), along with a type I secretion system, typically utilized for RTX toxin secretion, was proposed to be under the control of PhoB (Yoshida *et al.*, 2010). Furthermore, the Pho regulon controls adhesion expression and thereby the ability of *E. coli* cells to attach to host cells and tissue (Crépin *et al.*, 2011 and references therein). In the genome of the *Pseudovibrio* sp. FO-BEG1, several predicted virulence factors were identified that were described in pathogenic bacteria, which corroborates the hypothesis that this bacterium has the repertoire to initiate a symbiosis with marine invertebrates (**Chapter II**). It is therefore conceivable that the expression of these factors is also controlled by the Pho regulon and is therefore induced during P_i-limitation, as has been described for other bacteria, therefore promoting prokaryote-eukaryote interactions.

In **Chapter II**, we identified a NRPS-PKS cluster in the genome of strain FO-BEG1 with high sequence and architecture similarity to the NRPS-PKS cluster of pathogenic and commensalistic *E. coli* strains, coding for the metabolite colibactin (Nougayrède *et al.*, 2006). In direct cell contact of *E. coli* and the eukaryotic cells, colibactin induces megalocytosis in mammalian cells, resulting in an increased cell and nucleus size and the absence of mitosis (**Figure 6.3**). Due to the presence of colibactin-encoding clusters in many pathogenic *E. coli* it can be regarded as a virulence factor. However, also commensalistic strains posses this NRPS-PKS cluster, questioning the role of colibactin in pathogenesis.

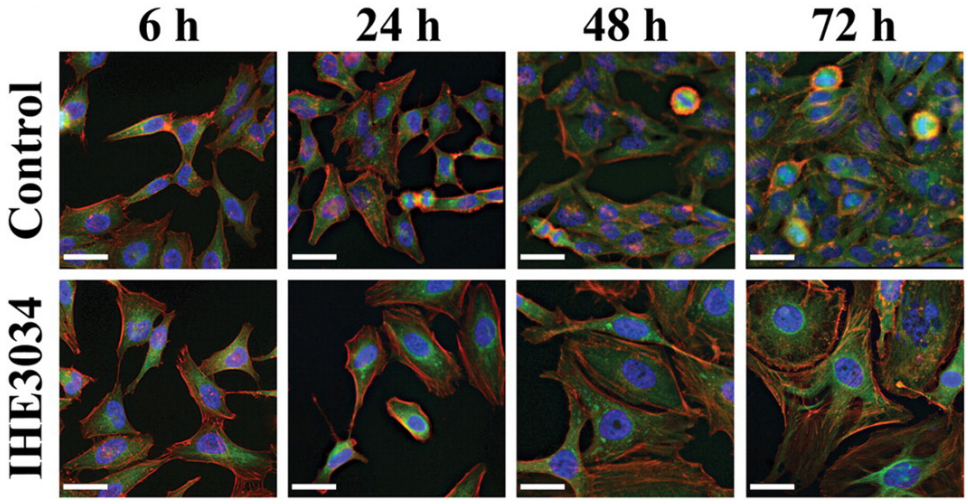

Figure 6.3. Effect of colibactin upon mammalian cells. HeLa cells were incubated for 6 to 72 hours with the pathogenic *E. coli* strain IHE3034 producing colibactin (bottom) or without bacterial cells (top). Cell nuclei are shown in blue, F-actin in red and α-tubulin in green. Scale bars 40 µm. Image modified after Nougayrède *et al.* (2006).

Depending on the amount of colibactin produced and the duration of the exposure to that toxin, colibactin might represent an important factor for colon colonization by slowing down the renewal of the epithelial cells, to which *E. coli* attaches, therefore allowing the bacteria to establish themselves in a stable environment (Hayashi, 2006; Nougayrède *et al.*, 2006). In order to test whether P_i-limitation induces the secretion of the colibactin-related metabolite encoded in the genome of strain FO-BEG1, 15, 50, 70 or 100 µl of the late stationary phase supernatant of phosphate starved cultures was used to inoculate mammalian cell lines, which were monitored at 24 and 48 hours. For this approach, SHS Y5Y (human neuroblastoma cells), B104 (rat neuroblastoma cells), and HeLa (human cervical cancer cells) cell lines were used. However, none of the cell lines showed any response to the treatment, indicating that the tested mammalian cell lines do not react to the secreted compounds induced by phosphate starvation of *Pseudovibrio* sp. FO-BEG1 under tested conditions (results not shown). This demonstrates that, among the secreted metabolites, a colibactin-related substance, which would affect the tested eukaryotic cell lines, is most likely not present. However, further tests are required to verify the ability of *Pseudovibrio* sp. FO-BEG1 to synthesize the colibactin metabolite, especially in direct contact with eukaryotic cells.

Pseudovibrio sp. strains FO-BEG1 and JE062 belong to the *Pseudovibrio denitrificans* species

In **Chapter IV**, the phylogenetic affiliation of *Pseudovibrio* sp. FO-BEG1 with the *Pseudovibrio* type species *P. denitrificans*^{T} (DSM 17465) is discussed. A comparison of metabolic capabilities showed rather insignificant differences, which could be simply a result of different cultivation media used for the maintenance of the two strains. Furthermore, DNA-DNA hybridization (DDH) values (66.3 ±2%) were in a range which does not allow an unambiguous conclusion regarding the phylogenetic affiliation of the two strains. Therefore, strain FO-BEG1 was assigned to the species *Pseudovibrio denitrificans*. Further analyses could be performed to justify this decision. For instance, genomic similarity might be verified by computation of the average nucleotide identity (ANI) between strain FO-BEG1 and *P. denitrificans*^{T}. For this analysis, already a partial genome of about 25% of the total genome size should be sufficient (Richter and Rosselló-Móra, 2009). DDH values in a range between 65 to 75%, whereas 70% represent the border for species circumscription, correspond to 94 to 96% in the ANI value. In general, most of the strains tested by Richter and Rosselló-Móra (2009) show a good correlation between the DDH and ANI value, implying that the ANI value for the comparison of *Pseudovibrio denitrificans*^{T} and strain FO-BEG1 could still fall into the transition zone between 94 and 96%, not clarifying if a species border should be drawn between the analyzed strains without essential differences in the metabolism. However, in some cases a high DDH value was found for two strains with a low ANI value or vice versa (Richter and Rosselló-Móra, 2009). For the time being, according to the low level of divergence on the physiological and genomic level, it was concluded that strain FO-BEG1 is a member of the species *Pseudovibrio denitrificans*.

Based on the genomic analysis of *Pseudovibrio* sp. JE062 in **Chapter II**, this strain was assigned to the same species as strain FO-BEG1, resulting in strains FO-BEG1, JE062, and *P. denitrificans*^{T} forming one species. This is a remarkable result, considering the fact that *P. denitrificans*^{T} was isolated from the coastal waters off Taiwan (Shieh *et al.*, 2004), strain FO-BEG1 was associated with a coral and JE062 with a sponge (Enticknap *et al.*, 2006), both at the coastal area off Florida. This observation further emphasizes the conclusions that were made concerning the life style of *Pseudovibrio* spp. based on genomic and physiological data presented in **Chapter II**. The genus *Pseudovibrio*, in this case specifically *P. denitrificans*, contains extremely versatile bacteria. On the one hand, adaptations to the changing conditions

of the oceanic environment are represented in the ability to use a number of different resources, to grow aerobically as well as anaerobically, and to multiply under extreme nutrient limitation. On the other hand, insights into the genomes of strains FO-BEG1 and JE062 confirm the close association with marine invertebrates with abilities to initiate and sustain a symbiotic relationship.

Perspectives

Pseudovibrio spp.-related strains are found ubiquitously as planktonic bacteria in coastal seawater or in association with marine invertebrates, but their environmental role and significance are yet unexplored. To the best of our knowledge, there are currently 22 published studies, in which *Pseudovibrio* spp.-related strains have been identified by culture-dependent or -independent approaches. The physiological and genomic data presented in **Chapters II**, **III** and **V** demonstrate that *Pseudovibrio* spp.-related species have the potential to influence the major nutrient cycles of carbon, nitrogen, phosphorus, sulfur, and presumably iron and are active even under extreme nutrient deprivation. In order to draw conclusions about their possible impact on carbon, nitrogen, phosphorus and sulfur cycling it is necessary to gain more knowledge about the abundance of these bacteria in different habitats like open oligotrophic ocean regions, coastal seawater or in associations with marine invertebrates. Enticknap *et al.* (2006) reported that *Pseudovibrio* spp.-related clones are underrepresented in 16S rRNA gene libraries, making the method of choice for the abundance studies of the genus *Pseudovibrio* in the environment fluorescent *in situ* hybridization (FISH).

The association of bacterial species related with *Pseudovibrio* and marine invertebrates, specifically sponges, raises the question about the development and the nature of these associations. So far, no *Pseudovibrio* spp. have been identified in diseased sponges, confirming the proposed hypothesis by Webster and Hill (2001) that *Pseudovibrio* spp. do not represent pathogens but are rather mutualistic/commensalistic symbionts of sponges. However, it remains to be demonstrated how *Pseudovibrio* spp. interacts with its partner and how exactly, if at all, the presence of the prokaryote influences the eukaryote and vice versa. Unfortunately, little is known about the interactions between sponges and sponge symbionts (Taylor *et al.*, 2007), especially on the molecular level. As an easily-culturable and versatile bacterium, *Pseudovibrio* sp. FO-BEG1 could contribute significantly to the elucidation of factors required for the establishment and preservation of a symbiosis with sponges, particularly due to the fact that, in general, symbionts are rather difficult to isolate, cultivate

and work with. Another advantage is the fully sequenced genome of strain FO-BEG1 with already identified candidate genes, which could be required for the establishment and the maintenance of a symbiosis, like type III and type VI secretion systems and genes that could be required for adhesion or invasion of host cells (**Chapter II**). A major issue in the research of sponge-symbiont interactions is the absence of established sponge cell lines, which could be used to investigate whether *Pseudovibrio* sp. attaches to or invades host cells or initiates the synthesis of specific molecules (e.g. effectors) required for prokaryote-eukaryote interactions. However, multicellular aggregates from dissociated sponge cell suspensions, known as primmorphs (Sipkema *et al.*, 2005 and references therein), can be obtained and maintained *in vitro* for months, representing a suitable model for the inquiry of bacteria-host interactions. In this context, establishment of a genetic system for *Pseudovibrio* sp. FO-BEG1 will be required, which will allow to mutate or knock out genes and study the resulting phenotype, making *Pseudovibrio* sp. FO-BEG1 an excellent model organism for the study of symbiotic interaction with sponges and other marine invertebrates.

Phosphate starvation induces an intriguing response in *Pseudovibrio* sp. FO-BEG1, resulting in the orange-yellowish coloration of the growth medium (**Chapter V**). The Pho regulon, controlling the response to P_i-limitation in other bacteria and also presumably in strain FO-BEG1, controls a variety of reactions including the synthesis of secondary metabolites and expression of virulence factors in pathogenic bacteria (Martín, 2004; Lamarche *et al.*, 2008). Since the structure and function of the secreted metabolites by strain FO-BEG1 is not known, they could potentially contribute to nutrient acquisition, antimicrobial activity and prokaryote-prokaryote or prokaryote-eukaryote communication. Therefore, further analysis of the P_i-starvation response is required on the cellular, physiological and molecular level. Investigations of the cellular envelope could be performed in order to analyze if the response induces the expression of adhesins or other structures, which might be required for attachment to host cells or biofilm formation. Further analyses of the bioactivity of the secreted substances are required, targeting a higher number of prokaryotic strains, since antimicrobial activity of the secreted molecules can not yet be excluded. Furthermore, the secreted molecules could have beneficial effects on other prokaryotes. In the co-culture of *Beggiatoa* sp. and *Pseudovibrio* sp. FO-BEG1, the sulfide oxidizing bacterium is incapable of growth without strain FO-BEG1, indicating that some kind of interactions between the two prokaryotes must occur. Therefore, it should be investigated whether the secreted metabolites have a beneficial effect on culturability and

growth of other bacteria, as has been shown e.g. for bacterial "helper" strains, which provide other prokaryotes with siderophores, thereby enhancing their proliferation under laboratory conditions (D'Onofrio *et al.*, 2010). Eventually, the role of iron and cobalt in the P_i-starvation response needs to be resolved in order to clarify if these metals are required for physiologic functions or are stored for later usage. Answering these questions will help to interpret the response of *Pseudovibrio* sp. FO-BEG1 to the limitation of an important nutrient, thereby facilitating the understanding of the role of *Pseudovibrio* spp. in the environment.

References

Agogué H, Casamayor EO, Bourrain M, Obernosterer I, Joux F, Herndl GJ *et al.* (2005). A survey on bacteria inhabiting the sea surface microlayer of coastal ecosystems. *FEMS Microbiol Ecol* **54:** 269–280.

Akira S, Takeda K. (2004). Toll-like receptor signalling. *Nat Rev Immunol* **4:** 499–511.

Amin SA, Green DH, Hart MC, Küpper FC, Sunda WG, Carrano CJ. (2009). Photolysis of iron-siderophore chelates promotes bacterial-algal mutualism. *Proc Natl Acad Sci U S A* **106:** 17071–17076.

Azam F, Malfatti F. (2007). Microbial structuring of marine ecosystems. *Nat Rev Microbiol* **5:** 782–791.

Barbeau K, Zhang GP, Live DH, Butler A. (2002). Petrobactin, a photoreactive siderophore produced by the oil-degrading marine bacterium *Marinobacter hydrocarbonoclasticus*. *J Am Chem Soc* **124:** 378–379.

Böhm M, Hentschel U, Friedrich AB, Fieseler L, Steffen R, Gamulin V *et al.* (2001). Molecular response of the sponge *Suberites domuncula* to bacterial infection. *Mar Biol* **139:** 1037–1045.

Braun V, Hantke K. (2011). Recent insights into iron import by bacteria. *Curr Opin Chem Biol* **15:** 328–334.

Braun V, Pramanik A, Gwinner T, Köberle M, Bohn E. (2009). Sideromycins: tools and antibiotics. *Biometals* **22:** 3–13.

Bright M, Bulgheresi S. (2010). A complex journey: transmission of microbial symbionts. *Nat Rev Microbiol* **8:** 218–230.

Buchan A, González JM, Moran MA. (2005). Overview of the marine *Roseobacter* lineage. *Appl Environ Microbiol* **71:** 5665–5677.

Cavicchioli R, Ostrowski M, Fegatella F, Goodchild A, Guixa-Boixereu N. (2003). Life under nutrient limitation in oligotrophic marine environments: an eco/physiological perspective of *Sphingopyxis alaskensis* (formerly *Sphingomonas alaskensis*). *Microb Ecol* **45:** 203–217.

Connon SA, Giovannoni SJ. (2002). High-throughput methods for culturing microorganisms in very-low-nutrient media yield diverse new marine isolates. *Appl Environ Microbiol* **68:** 3878–3885.

Crépin S, Chekabab SM, Le Bihan G, Bertrand N, Dozois CM, Harel J. (2011). The Pho regulon and the pathogenesis of *Escherichia coli*. *Vet Microbiol* **153:** 82–88.

D'Onofrio A, Crawford JM, Stewart EJ, Witt K, Gavrish E, Epstein S *et al.* (2010). Siderophores from neighboring organisms promote the growth of uncultured bacteria. *Chem Biol* **17:** 254–264.

Dale C, Moran NA. (2006). Molecular interactions between bacterial symbionts and their hosts. *Cell* **126:** 453–465.

Dale C, Jones T, Pontes M. (2005). Degenerative evolution and functional diversification of type-III secretion systems in the insect endosymbiont *Sodalis glossinidius*. *Mol Biol Evol* **22:** 758–766.

Dale C, Young SA, Haydon DT, Welburn SC. (2001). The insect endosymbiont *Sodalis glossinidius* utilizes a type III secretion system for cell invasion. *Proc Natl Acad Sci U S A* **98:** 1883–1888.

Dalton CC, Iqbal K, Turner DA. (1983). Iron phosphate precipitation in Murashige and Skoog media. *Physiologia Plantarum* **57:** 472–476.

Deakin WJ, Broughton WJ. (2009). Symbiotic use of pathogenic strategies: rhizobial protein secretion systems. *Nat Rev Microbiol* **7:** 312–320.

Degnan PH, Yu Y, Sisneros N, Wing RA, Moran NA. (2009). *Hamiltonella defensa*, genome evolution of protective bacterial endosymbiont from pathogenic ancestors. *Proc Natl Acad Sci U S A* **106:** 9063–9068.

Dehal P, Satou Y, Campbell RK, Chapman J, Degnan B, De Tomaso A *et al.* (2002). The draft genome of *Ciona intestinalis*: insights into chordate and vertebrate origins. *Science* **298:** 2157–2167.

Duquesne S, DestoumieuxGarzón D, Peduzzi J, Rebuffat S. (2007). Microcins, gene-encoded antibacterial peptides from enterobacteria. *Nat Prod Rep* **24:** 708–734.

Edberg F, Kalinowski BE, Holmström SJM, Holm K. (2010). Mobilization of metals from uranium mine waste: the role of pyoverdines produced by *Pseudomonas fluorescens*. *Geobiology* **8:** 278–292.

Eguchi M, Nishikawa T, MacDonald K, Cavicchioli R, Gottschal JC, Kjelleberg S. (1996). Responses to stress and nutrient availability by the marine ultramicrobacterium *Sphingomona*s sp. strain RB2256. *Appl Environ Microbiol* **62:** 1287–1294.

Eguchi M, Ostrowski M, Fegatella F, Bowman J, Nichols D, Nishino T *et al.* (2001). *Sphingomonas alaskensis* strain AFO1, an abundant oligotrophic ultramicrobacterium from the North Pacific. *Appl Environ Microbiol* **67:** 4945–4954.

Enticknap JJ, Kelly M, Peraud O, Hill RT. (2006). Characterization of a culturable alphaproteobacterial symbiont common to many marine sponges and evidence for vertical transmission via sponge larvae. *Appl Environ Microbiol* **72:** 3724–3732.

Giovannoni S, Stingl U. (2007). The importance of culturing bacterioplankton in the 'omics' age. *Nat Rev Microbiol* **5:** 820–826.

Giovannoni SJ, Tripp HJ, Givan S, Podar M, Vergin KL, Baptista D *et al.* (2005). Genome streamlining in a cosmopolitan oceanic bacterium. *Science* **309:** 1242–1245.

Harland DN, Garmory HS, Brown KA, Titball RW. (2005). An association between ATP binding cassette systems, genome sizes and lifestyles of bacteria. *Res Microbiol* **156:** 434–442.

Hayashi T. (2006). Breaking the barrier between commensalism and pathogenicity. *Science* **313:** 772–773.

Hentschel U, Usher KM, Taylor MW. (2006). Marine sponges as microbial fermenters. *FEMS Microbiol Ecol* **55:** 167–177.

Hentschel U, Schmid M, Wagner M, Fieseler L, Gernert C, Hacker J. (2001). Isolation and phylogenetic analysis of bacteria with antimicrobial activities from the mediterranean sponges *Aplysina aerophoba* and *Aplysina cavernicola*. *FEMS Microbiol Ecol* **35:** 305–312.

Hoi LT, Voigt B, Jürgen B, Ehrenreich A, Gottschalk G, Evers S *et al.* (2006). The phosphate-starvation response of *Bacillus licheniformis*. *Proteomics* **6:** 3582–3601.

Hosoya S, Yokota A. (2007). *Pseudovibrio japonicus* sp. nov., isolated from coastal seawater in Japan. *Int J Syst Evol Microbiol* **57:** 1952–1955.

Jani AJ, Cotter PA. (2010). Type VI secretion: not just for pathogenesis anymore. *Cell Host Microbe* **8:** 2–6.

Jiao NZ, Zheng Q. (2011). The microbial carbon pump: from genes to ecosystems. *Appl Environ Microbiol* **77:** 7439–7444.

Kalinowski BE, Liermann LJ, Givens S, Brantley SL. (2000). Rates of bacteria-promoted solubilization of Fe from minerals: a review of problems and approaches. *Chem Geol* **169:** 357–370.

Kujawinski EB. (2011). The impact of microbial metabolism on marine dissolved organic matter. *Ann Rev Mar Sci* **3:** 567–599.

Lackner G, Moebius N, Hertweck C. (2011). Endofungal bacterium controls its host by an *hrp* type III secretion system. *ISME J* **5:** 252–261.

Lally ET, Hill RB, Kieba LR, Korostoff J. (1999). The interaction between RTX toxins and target cells. *Trends Microbiol* **7:** 356–361.

Lamarche MG, Wanner BL, Crépin S, Harel J. (2008). The phosphate regulon and bacterial virulence: a regulatory network connecting phosphate homeostasis and pathogenesis. *FEMS Microbiol Rev* **32:** 461–473.

Loker ES, Adema CM, Zhang SM, Kepler TB. (2004). Invertebrate immune systems - not homogeneous, not simple, not well understood. *Immunol Rev* **198:** 10–24.

Martín JF. (2004). Phosphate control of the biosynthesis of antibiotics and other secondary metabolites is mediated by the PhoR-PhoP system: an unfinished story. *J Bacteriol* **186:** 5197–5201.

Miethke M, Marahiel MA. (2007). Siderophore-based iron acquisition and pathogen control. *Microbiol Mol Biol Rev* **71:** 413–451.

Miller DJ, Hemmrich G, Ball EE, Hayward DC, Khalturin K, Funayama N *et al.* (2007). The innate immune repertoire in Cnidaria - ancestral complexity and stochastic gene loss. *Genome Biol* **8:** R59.

Moran MA, Armbrust EV. (2007). Genomes of sea microbes. *Oceanography* **20:** 47–55.

Moran MA, Buchan A, González JM, Heidelberg JF, Whitman WB, Kiene RP *et al.* (2004). Genome sequence of *Silicibacter pomeroyi* reveals adaptations to the marine environment. *Nature* **432:** 910–913.

Moran NA. (2006). Symbiosis. *Curr Biol* **16:** R866–R871.

Moran NA, McCutcheon JP, Nakabachi A. (2008). Genomics and evolution of heritable bacterial symbionts. *Annu Rev Genet* **42:** 165–190.

Morel FMM, Price NM. (2003). The biogeochemical cycles of trace metals in the oceans. *Science* **300:** 944–947.

Mougous JD, Cuff ME, Raunser S, Shen A, Zhou M, Gifford CA *et al.* (2006). A virulence locus of *Pseudomonas aeruginosa* encodes a protein secretion apparatus. *Science* **312:** 1526–1530.

Mukherjee S, Keitany G, Li Y, Wang Y, Ball HL, Goldsmith EJ *et al.* (2006). *Yersinia* YopJ acetylates and inhibits kinase activation by blocking phosphorylation. *Science* **312:** 1211–1214.

Mulligan C, Kelly DJ, Thomas GH. (2007). Tripartite ATP-independent periplasmic transporters: application of a relational database for genome-wide analysis of transporter gene frequency and organization. *J Mol Microb Biotech* **12:** 218–226.

Muscholl-Silberhorn A, Thiel V, Imhoff JF. (2007). Abundance and bioactivity of cultured sponge-associated bacteria from the mediterranean sea. *Microb Ecol* **55:** 94–106.

Myklestad SM. (1995). Release of extracellular products by phytoplankton with special emphasis on polysaccharides. *Sci Total Environ* **165:** 155–164.

Newton RJ, Griffin LE, Bowles KM, Meile C, Gifford S, Givens CE *et al.* (2010). Genome characteristics of a generalist marine bacterial lineage. *ISME J* **4:** 784–798.

Nougayrède JP, Homburg S, Taieb F, Boury M, Brzuszkiewicz E, Gottschalk G *et al.* (2006). *Escherichia coli* induces DNA double-strand breaks in eukaryotic cells. *Science* **313:** 848–851.

O'Halloran JA, Barbosa TM, Morrissey JP, Kennedy J, O'Gara F, Dobson ADW. (2011). Diversity and antimicrobial activity of *Pseudovibrio* spp. from Irish marine sponges. *J Appl Micobiol* **110:** 1495–1508.

Penesyan A, Tebben J, Lee M, Thomas T, Kjelleberg S, Harder T *et al.* (2011). Identification of the antibacterial compound produced by the marine epiphytic bacterium *Pseudovibrio* sp. D323 and related sponge-associated bacteria. *Mar Drugs* **9:** 1391–1402.

Peterson CN, Mandel MJ, Silhavy TJ. (2005). *Escherichia coli* starvation diets: essential nutrients weigh in distinctly. *J Bacteriol* **187:** 7549–7553.

Philippe VA, Méndez MB, Huang IH, Orsaria LM, Sarker MR, Grau RR. (2006). Inorganic phosphate induces spore morphogenesis and enterotoxin production in the intestinal pathogen *Clostridium perfringens*. *Infect Immun* **74:** 3651–3656.

Polz MF, Hunt DE, Preheim SP, Weinreich DM. (2006). Patterns and mechanisms of genetic and phenotypic differentiation in marine microbes. *Philos T R Soc B* **361:** 2009–2021.

Pratt JT, Ismail AM, Camilli A. (2010). PhoB regulates both environmental and virulence gene expression in *Vibrio cholerae*. *Mol Microbiol* **77:** 1595–1605.

Pukatzki S, Ma AT, Sturtevant D, Krastins B, Sarracino D, Nelson WC *et al.* (2006). Identification of a conserved bacterial protein secretion system in *Vibrio cholerae* using the *Dictyostelium* host model system. *Proc Natl Acad Sci U S A* **103:** 1528–1533.

Rappé MS, Connon SA, Vergin KL, Giovannoni SJ. (2002). Cultivation of the ubiquitous SAR11 marine bacterioplankton clade. *Nature* **418:** 630–633.

Richter M, Rosselló-Móra R. (2009). Shifting the genomic gold standard for the prokaryotic species definition. *Proc Natl Acad Sci U S A* **106:** 19126–19131.

Schalk IJ, Hannauer M, Braud A. (2011). New roles for bacterial siderophores in metal transport and tolerance. *Environ Microbiol* **13:** 2844–2854.

Schut F, Prins RA, Gottschal JC. (1997). Oligotrophy and pelagic marine bacteria: facts and fiction. *Aquat Microb Ecol* **12:** 177–202.

Schwedt A. (2011). Physiology of a marine *Beggiatoa* strain and the accompanying organism *Pseudovibrio* sp. - a facultatively oligotrophic bacterium. Ph.D thesis, Universität Bremen, Bremen.

Sertan-de Guzman AA, Predicala RZ, Bernardo EB, Neilan BA, Elardo SP, Mangalindan GC *et al.* (2007). *Pseudovibrio denitrificans* strain Z143-1, a heptylprodigiosin-producing bacterium isolated from a Philippine tunicate. *FEMS Microbiol Lett* **277:** 188–196.

Shieh WY, Lin YT, Jean WD. (2004). *Pseudovibrio denitrificans* gen. nov., sp. nov., a marine, facultatively anaerobic, fermentative bacterium capable of denitrification. *Int J Syst Evol Microbiol* **54:** 2307–2312.

Singer E, Webb EA, Nelson WC, Heidelberg JF, Ivanova N, Pati A *et al.* (2011). Genomic potential of *Marinobacter aquaeolei*, a biogeochemical "opportunitroph". *Appl Environ Microbiol* **77:** 2763–2771.

Sipkema D, Osinga R, Schatton W, Mendola D, Tramper J, Wijffels RH. (2005). Large-scale production of pharmaceuticals by marine sponges: sea, cell, or synthesis? *Biotechnol Bioeng* **90:** 201–222.

Takeda K, Kaisho T, Akira S. (2003). Toll-like receptors. *Annu Rev Immunol* **21:** 335–376.

Taylor MW, Radax R, Steger D, Wagner M. (2007). Sponge-associated microorganisms: evolution, ecology, and biotechnological potential. *Microbiol Mol Biol Rev* **71:** 295–374.

Tortell PD, Maldonado MT, Granger J, Price NM. (1999). Marine bacteria and biogeochemical cycling of iron in the oceans. *FEMS Microbiol Ecol* **29:** 1–11.

Vizcaino MI. (2011). The chemical defense of *Pseudopterogorgia americana*: a focus on the antimicrobial potential of a *Pseudovibrio* sp. Ph.D thesis, Medical University of South Carolina, Charleston.

von Krüger WMA, Humphreys S, Ketley JM. (1999). A role for the PhoBR regulatory system homologue in the *Vibrio cholerae* phosphate-limitation response and intestinal colonization. *Microbiol-UK* **145:** 2463–2475.

von Krüger WMA, Lery LMS, Soares MR, de Neves-Manta FS, Silva CMBE, Neves-Ferreira AGD *et al.* (2006). The phosphate-starvation response in *Vibrio cholerae* O1 and *phoB* mutant under proteomic analysis: disclosing functions involved in adaptation, survival and virulence. *Proteomics* **6:** 1495–1511.

Vraspir JM, Butler A. (2009). Chemistry of marine ligands and siderophores. *Ann Rev Mar Sci* **1:** 43–63.

Wagner-Döbler I, Ballhausen B, Berger M, Brinkhoff T, Buchholz I, Bunk B *et al.* (2010). The complete genome sequence of the algal symbiont *Dinoroseobacter shibae*: a hitchhiker's guide to life in the sea. *ISME J* **4:** 61–77.

Wandersman C, Delepelaire P. (2004). Bacterial iron sources: from siderophores to hemophores. *Annu Rev Microbiol* **58:** 611–647.

Wang XX, Liu YS. (2007). Regulation of innate immune response by MAP kinase phosphatase-1. *Cell Signal* **19:** 1372–1382.

Webster NS, Hill RT. (2001). The culturable microbial community of the Great Barrier Reef sponge *Rhopaloeides odorabile* is dominated by an α-proteobacterium. *Mar Biol* **138:** 843–851.

Wiens M, Korzhev M, Krasko A, Thakur NL, Perovic-Ottstadt S, Breter HJ *et al.* (2005). Innate immune defense of the sponge *Suberites domuncula* against bacteria involves a MyD88-dependent signaling pathway: induction of a perforin-like molecule. *J Biol Chem* **280:** 27949–27959.

Williams TJ, Ertan H, Ting L, Cavicchioli R. (2009). Carbon and nitrogen substrate utilization in the marine bacterium *Sphingopyxis alaskensis* strain RB2256. *ISME J* **3:** 1036–1052.

Yoshida Y, Sugiyama S, Oyamada T, Yokoyama K, Makino K. (2010). Identification and characterization of novel phosphate regulon genes, *ecs0540–ecs0544*, in *Escherichia coli* O157:H7. *Mol Genet Genomics* **284:** 197–205.

Acknowledgments

I would like to deeply thank Heide Schulz-Vogt for making it possible for me to write my Ph.D thesis at this wonderful MPI institute. Thank you for your great support and guidance throughout the years and for giving me the chance to find my own way. “Wisdom comes from experience. Experience is often a result of lack of wisdom.” *Terry Pratchett*

Prof. Dr. Ulrich Fischer, I would like to thank you for your agreement to review my thesis, for your patience and for the instructing and interesting discussions we had. I also would like to thank Prof. Dr. Rudolf Amann and Prof. Dr. Jens Harder for joining my thesis committee. Especially Jens I would like to thank for many nice, instructive and fruitful discussions during the last years.

Dr. Thorsten Dittmar, thank you very much for the possibility to measure at the FT-ICR-MS and for your great past and future help with the analysis of the data. Many thanks also to Ina Ulber for help with the DOM extraction and DOC measurements and Katrin Klaproth for the uncountable MS measurements and support with the data evaluation.

Dr. Martin Kölling, thank you for allowing us to measure our samples with the ICP-OES and thank you Silvana Pape, for the performance of the measurements – the data opened even more questions.

Many thanks to Prof. Dr. Jörn Piel for the analysis of the NRPS-PKS cluster and Dr. Mihaela Gurgui for the following *in vitro* analysis of the yellow supernatant.

Dr. Olav Grundmann, I would like to thank you for your interest in the analysis of the secreted compounds and for the hours we spent trying to purify it via the SEC. I also would like to thank Dr. Florin Musat and Gao Chen for sharing their knowledge about the RP-HPCL with me.

Dr. Michael Richter, thank you very much for the constant support during and after the genome annotation and helping with all the questions I had.

Dr. Alexander Galushko I would like to thank for having an open ear for my problems, great advices, for introducing me into the world of ultraviolet-visible spectroscopy and for the bike tours in the Blockland.

As the best librarian in the world, I would like to thank Bernd Stickfort for the constant supply with hard-to-get literature and especially for the enthusiasm for Russian papers and very old works that many people cite but very little read.

I would like thank Martina Meyer and Susanne Menger for their amazing help with the lab work, flow injection and NOx analysis and many, many growth experiments. Many thanks also to Christina Probian and Ramona Appel for their support during HPLC measurements. You all are the most wonderful TAs one could wish for.

Nora Buddruhs welcomed me at the DSMZ and made the sample preparation for Biolog measurements very easy – thank you!

Prof. Dr. Alexey Kamyshny I would like to thank for the quick and detailed introduction into the world of sulfur, the measurements of the tetrathionate samples and for keeping up the Russian spirit at the MPI.

To the most wonderful Ecophysiology research group (Anne, Verena, Sandra, Stefano, Anne-Christin, Artur, Sascha, Martina, Susanne and Christin) I would like to express my gratitude for the great time we had together.

I would especially like to thank Richard, Steffi, Stefano, Verena, Arthur, Anne-Christin and Arne for the nerdy sit-ins trying to save the world. Many, many thanks to Verena and Anne-Christin for their dedicated scientific and private support. Stefano, thank you very much for joining the project, for the many hours of great discussions, for the nifty experiments we came up with and the trouble and fun we had while performing them, and for your friendship.

My past (Jörg Brock, Ulrike Jaekel, Hajo Zech) and present (Dennis Enning, Robert Marmulla and Artur Fink) cohabitants in cell 2133, thank you for great office parties, depressing and manic conversations on and off topic and the moral support you gave me.

I also would like to thank Sandra and Bogdan, and Lini and Andreas for completing my family. Many thanks to Micha, Viktor, Alla, Tanja, and Mishka for not forgetting me, despite the distance.

My dear wife I would like to thank for being there for me, for her laughing and reminding me of all the small things that matter in life. I love you. Thanks also to all my furry roommates, especially Bitterkeit, for not destroying anything of importance.

От всего сердца благодарю своих родителей за постоянную, моральную, физическую и финанциальную поддержку. Спасибо что понимаете, прощаете и помогаете мне во всем. Я вас очень люблю.